

COOPERATIVE AND CONSENSUS-BASED CONTROL FOR
A TEAM OF MULTI-AGENT SYSTEMS

IMAN SABOORI

A THESIS
IN
THE DEPARTMENT
OF
ELECTRICAL AND COMPUTER ENGINEERING

PRESENTED IN PARTIAL FULFILLMENT OF THE REQUIREMENTS
FOR THE DEGREE OF DOCTOR OF PHILOSOPHY
CONCORDIA UNIVERSITY
MONTRÉAL, QUÉBEC, CANADA

MAY 2016

© IMAN SABOORI, 2016

CONCORDIA UNIVERSITY
School of Graduate Studies

This is to certify that the thesis prepared

By: **Mr. Iman Saboori**
Entitled: **Cooperative and Consensus-Based Control for
a Team of Multi-Agent Systems**

and submitted in partial fulfillment of the requirements for the degree of

Doctor of Philosophy (Electrical Engineering)

complies with the regulations of this University and meets the accepted standards with respect to originality and quality.

Signed by the final examining committee:

_____ Chair
Dr. Marius Paraschivoiu
_____ External Examiner
Dr. Mo Jamshidi
_____ Examiner
Dr. Luis Rodrigues
_____ Examiner
Dr. Shahin Hashtrudi Zad
_____ Examiner
Dr. Fariborz Haghighat
_____ Supervisor
Dr. Khashayar Khorasani

Approved by: _____
Dr. Abdel Sebak, Graduate Program Director

Dr. Amir Asif ,Dean
Faculty of Engineering & Computer Science

Abstract

Cooperative and Consensus-Based Control for a Team of Multi-Agent Systems

Iman Saboori, Ph.D.

Concordia University, 2016

Cooperative control has attracted a noticeable interest in control systems community due to its numerous applications in areas such as formation flying of unmanned aerial vehicles, cooperative attitude control of spacecraft, rendezvous of mobile robots, unmanned underwater vehicles, traffic control, data network congestion control and routing. Generally, in any cooperative control of multi-agent systems one can find a set of locally sensed information, a communication network with limited bandwidth, a decision making algorithm, and a distributed computational capability. The ultimate goal of cooperative systems is to achieve consensus or synchronization throughout the team members while meeting all communication and computational constraints. The consensus problem involves convergence of outputs or states of all agents to a common value and it is more challenging when the agents are subjected to disturbances, measurement noise, model uncertainties or they are faulty.

This dissertation deals with the above mentioned challenges and has developed methods to design distributed cooperative control and fault recovery strategies in multi-agent systems. Towards this end, we first proposed a transformation for Linear Time Invariant (LTI) multi-agent systems that facilitates a systematic control design procedure and make it possible to use powerful Lyapunov stability analysis tool to guarantee its consensus achievement. Moreover, Lyapunov stability analysis techniques for switched systems are investigated and a novel method is introduced which is well suited for designing consensus algorithms for switching topology multi-agent systems. This method also makes it possible to deal with disturbances with limited root mean square (RMS) intensities. In order to decrease controller design complexity, a

method is presented which uses algebraic connectivity of the communication network to decouple augmented dynamics of the team into lower dimensional parts, which allows one to design the consensus algorithm based on the solution to an algebraic Riccati equation with the same order as that of agent. Although our proposed decoupling method is a powerful approach to reduce the complexity of the controller design, it is possible to apply classical pole placement methods to the transformed dynamics of the team to develop and obtain controller gains.

The effects of actuator faults in consensus achievement of multi-agent systems is investigated. We proposed a framework to quantitatively study actuator loss-of-effectiveness effects in multi-agent systems. A fault index is defined based on information on fault severities of agents and communication network topology, and sufficient conditions for consensus achievement of the team are derived. It is shown that the stability of the cooperative controller is linked to the fault index. An optimization problem is formulated to minimize the team fault index that leads to improvements in the performance of the team. A numerical optimization algorithm is used to obtain the solutions to the optimal problem and based on the solutions a fault recovery strategy is proposed for both actuator saturation and loss-of-effectiveness fault types.

Finally, to make our proposed methodology more suitable for real life scenarios, the consensus achievement of a multi-agent team in presence of measurement noise and model uncertainties is investigated. Towards this end, first a team of LTI agents with measurement noise is considered and an observer based consensus algorithm is proposed and shown that the team can achieve H_∞ output consensus in presence of both bounded RMS disturbance input and measurement noise. In the next step a multi-agent team with both linear and Lipschitz nonlinearity uncertainties is studied and a cooperative control algorithm is developed. An observer based approach is also developed to tackle consensus achievement problem in presence of both measurement noise and model uncertainties.

Acknowledgments

I would like to express my acknowledgments and gratitude to all of my colleagues, friends and professors who helped me during my Ph.D. studies at Concordia University specially my supervisor Doctor Khorasani who guided me through my Ph.D. thesis.

I would also like to thank my committee members Dr. Haghghat, Dr. Hashtrudi Zad, Dr. Jamshidi and Dr. Rodrigues for their time and guidance through reviewing and evaluating my work.

Finally, I would like to thank my wife, Maryam, for her love, persistent support and belief in me. My deepest gratitude goes to my parents for their unconditional love and prayers throughout my life.

Dedicated to my parents and my wife, with love and gratitude.

Contents

List of Figures	viii
List of Tables	xii
Nomenclature	xiv
1 Introduction	1
1.1 Motivation	1
1.2 Literature Review	4
1.2.1 Consensus Achievement of Healthy Teams	5
1.2.2 Cooperative Fault Tolerant Consensus	13
1.3 General Problem Statement	15
1.4 Thesis Contribution	17
1.5 Thesis Outline	19
2 Background Information	21
2.1 Algebraic Graph Theory	22
2.2 Matrix Analysis of Graphs	30
2.3 Cooperative Control and Consensus Achievement	33
2.4 Kronecker Product and Its Properties	34
2.5 Lyapunov Stability Analysis	36
2.6 Summary	40
3 H_∞ Consensus Achievement of Multi-Agent Systems with Directed and Switching Topology Networks	41
3.1 Background and Preliminary Results	42
3.2 Problem Statement	52

3.3	Main Result	55
3.4	Simulation Results	59
3.5	Summary	61
4	Actuator Fault Accommodation Strategy for a Team of Multi-Agent Systems Subject to Switching Topology	65
4.1	Multi-Agents System Model	67
4.2	Problem Statement and Main Results	71
4.2.1	Weighted Consensus Strategy	72
4.2.2	Consensus Control Reconfiguration Strategy	77
4.2.3	Consensus Achievement of the Multi-agent Team in Presence of Actuator Saturation	79
4.3	Simulation Results	81
4.4	Summary	98
5	Consensus Achievement of Multi-Agent Teams In Presence of Measurement Noise and Model Uncertainties	100
5.1	Consensus Achievement in Presence of Measurement Noise	101
5.1.1	Problem Statement And The Main Result	101
5.1.2	Simulation Results	110
5.2	Consensus Achievement In Presence of Model Uncertainties	118
5.2.1	Problem Statement and Main Result	118
5.2.2	Output Consensus Achievement in Presence of Model Uncertainties and Measurement Noise	124
5.2.3	Simulation Results	127
5.3	Cooperative Adaptive Consensus Achievement of Nonlinear Multi-Agent Systems	133
5.4	Summary	156
6	Conclusions and future work	157
6.1	Future work	158
	Bibliography	161

List of Figures

1.1	Collective behavior of animals groups. [1]	2
2.1	Visual representation of a graph	22
2.2	Spanning tree of a graph.	24
2.3	Spanning tree of a graph.	24
2.4	Union of Gersgorin circles for Laplacian matrix [1].	27
2.5	Various graph topologies [1].	28
3.1	Communication network digraphs for a team of 4 UUVs.	61
3.2	Depth of the agents using the weighted H_∞ method.	62
3.3	Control effort of the agents using the weighted H_∞ method.	62
3.4	Depth of the agents using the H_∞ method.	63
3.5	Control effort of the agents using the H_∞ method.	63
4.1	Clockwise ring topology of the information flow graph.	81
4.2	Norm of the agents states corresponding to the healthy team.	82
4.3	Consensus error of the healthy team.	83
4.4	Control signals of the healthy team	83
4.5	Consensus error of the team in presence of faults (95% estimated accurately by the FDI module) by invoking our proposed consensus scheme without reconfiguration.	84
4.6	Control signals of the team in presence of faults (95% estimated accurately by the FDI module) by invoking our proposed consensus scheme without reconfiguration.	85
4.7	Consensus error of the team in presence of faults (30% estimated accurately by the FDI module) by invoking our proposed consensus scheme without reconfiguration.	86

4.8	Control signals of the team in presence of faults (30% estimated accurately by the FDI module) by invoking our proposed consensus scheme without reconfiguration.	87
4.9	Consensus error of the team in presence of faults (30% estimated accurately by the FDI module) by invoking the reconfiguration strategy.	88
4.10	Norm of the agent states in presence of faults by invoking the reconfiguration strategy.	89
4.11	Control signals of the team in presence of faults (30% estimated accurately by the FDI module) by invoking the reconfiguration strategy.	89
4.12	Consensus error of the team in presence of faults (30% estimated accurately by the FDI module) by invoking the centralized fault recovery approach developed in [44].	90
4.13	Control signals of the team in presence of faults (30% estimated accurately by the FDI module) by invoking the centralized fault recovery approach developed in [44].	91
4.14	Consensus error of the team in presence of faults (30% estimated accurately by the FDI module) by invoking the decentralized fault recovery approach developed in [44].	92
4.15	Control signals of the team in presence of faults (30% estimated accurately by the FDI module) by invoking the decentralized fault recovery approach developed in [44].	93
4.16	Norm of the agents states in presence of actuator saturation faults without using our proposed reconfiguration strategy. . .	94
4.17	Consensus error of the team in presence of actuator saturation faults without using our proposed reconfiguration strategy. . .	96
4.18	Control signals of the agents affected by actuator saturation faults without using our proposed reconfiguration strategy. . .	96
4.19	Norm of the agents states in presence of actuator saturation faults by invoking our proposed reconfiguration strategy. . . .	97
4.20	Consensus error of the team in presence of actuator saturation faults by invoking our proposed reconfiguration strategy. . . .	97

4.21	Control signals of the agents affected by actuator saturation faults by invoking our proposed reconfiguration strategy. . . .	98
5.1	Communication networks digraphs.	111
5.2	Angular velocity of the agents.	112
5.3	Pitch angle of the agents.	112
5.4	Depth (output signal) of the agents.	113
5.5	Control input of the agents.	113
5.6	Observers estimation errors.	114
5.7	Communication network topology [143].	115
5.8	The outputs of the agents by using the method in [143].	116
5.9	The control inputs of the agents by using the method in [143].	116
5.10	The outputs of the agents by using the method in [143].	117
5.11	The control inputs of the agents by using the method in [143].	117
5.12	Angular velocity of the agents.	128
5.13	Pitch angle of the agents.	129
5.14	Depth (output signal) of the agents.	129
5.15	Control inputs of the agents.	130
5.16	Communication network topologies that are used in [94].	131
5.17	Switching signal that is used in [94].	131
5.18	Trajectories of the first states in Example 1 of [94].	132
5.19	Trajectories of the second states in Example 1 of [94].	132
5.20	Trajectories of the first states of the agents using our proposed method.	133
5.21	Trajectories of the second states of the agents using our proposed method.	134
5.22	Communication networks topologies.	142
5.23	Depth of the agents with different nonlinearities and without using a neural network-based control approach.	143
5.24	Pitch angle of the agents with different nonlinearities and by using a neural network-based control approach.	144
5.25	Angular velocity of the agents with different nonlinearities and by using a neural network-based control approach.	144

5.26	Depth of the agents with different nonlinearities and by using a neural network-based control approach.	145
5.27	Consensus error of the team with different nonlinearities and by using a neural network-based control approach.	145
5.28	Control inputs of the agents with different nonlinearities and by using a neural network-based control approach.	146
5.29	Neural network weights of the team with different nonlinearities.	146
5.30	Depth of the agents with identical nonlinearities and without using the cooperative learning term.	148
5.31	Neural network weights of the team with identical nonlinearities and without using the cooperative learning term.	148
5.32	Pitch angle of the agents by using neural network and without employing the cooperative learning term.	149
5.33	Angular velocity of the agents by using neural network and without employing the cooperative learning term.	150
5.34	Depth of the agents without using neural network and without employing the cooperative learning term.	150
5.35	Consensus error of the team by using neural network and without employing the cooperative learning term.	151
5.36	Control inputs of the agents by using neural network and without employing the cooperative learning term.	151
5.37	Neural network weights of the team and without employing the cooperative learning term.	152
5.38	Depth of the agents by using the non-cooperative adaptive method.	153
5.39	Control inputs of the agents by using the non-cooperative adaptive method.	153
5.40	Estimated parameters by using the non-cooperative adaptive method.	154
5.41	Depth of the agents by using the cooperative adaptive method.	154
5.42	Control inputs of the agents by using the cooperative adaptive method.	155
5.43	Estimated parameters by using the cooperative adaptive method.	155

List of Tables

2.1	Eigenvalues of Laplacian matrices of graphs presented in Figure 2.5 [1].	29
3.1	The controller parameters and comparative performance of the resulting two control strategies.	61
3.2	The comparison between our proposed H_∞ method and the method in [58].	64
4.1	The comparison between our proposed method and the methods in [44].	95
4.2	The comparison between consensus performance of the team in presence of actuator saturations	99
5.1	The comparison between our proposed method and the method in [143].	118
5.2	The comparison between our proposed method and the method in [94].	134
5.3	Quantitative comparison results for the team with different nonlinearities with and without using the neural network-based control approach.	147
5.4	The simulation results for the team with identical nonlinearities.	149
5.5	The comparison between cooperative and non-cooperative adaptive methods.	156

Nomenclature

LTI Linear Time Invariant

FDI Fault Detection and Isolation

ARE Algebraic Riccati Equation

LMI Linear Matrix Inequality

UUV Unmanned Underwater Vehicle

Chapter 1

Introduction

1.1 Motivation

In recent years, the number of applications in which interactions between human and agents are not possible has been increased, and it motivated many researchers to solve these types of complicated engineering problems and applications. Towards this end, one can transform the problem into a distributed network of smaller and simpler autonomous subsystems which can operate without humans involvement. The collective behaviors of animal groups in nature, shown that distributed decisions made by each individual for its own position, direction and speed of motion can make the whole group to behave like a single entity, which has its own rules of motion and decision making. Examples of such a collective behavior can be seen in birds formations, flocks of birds, schools of fish and mammal herds, see Figure 1.1. Inspired by these natural collective behaviors of animals in their groups, scientists and engineers are encouraged to network group of systems to let them exchange their information. Afterward, each agent use its locally available information and a cooperative control strategy to react in such a way that the overall team perform required tasks without a need to use external supervisor.

Cooperative control of multi-agent systems covers a wide range of applications such as autonomous underwater vehicles [2–4], unmanned aerial vehicles [5–7], mobile robots [8–10], and satellite clusters [11–13]. However, each of these areas has its own specific difficulties but some common underlying

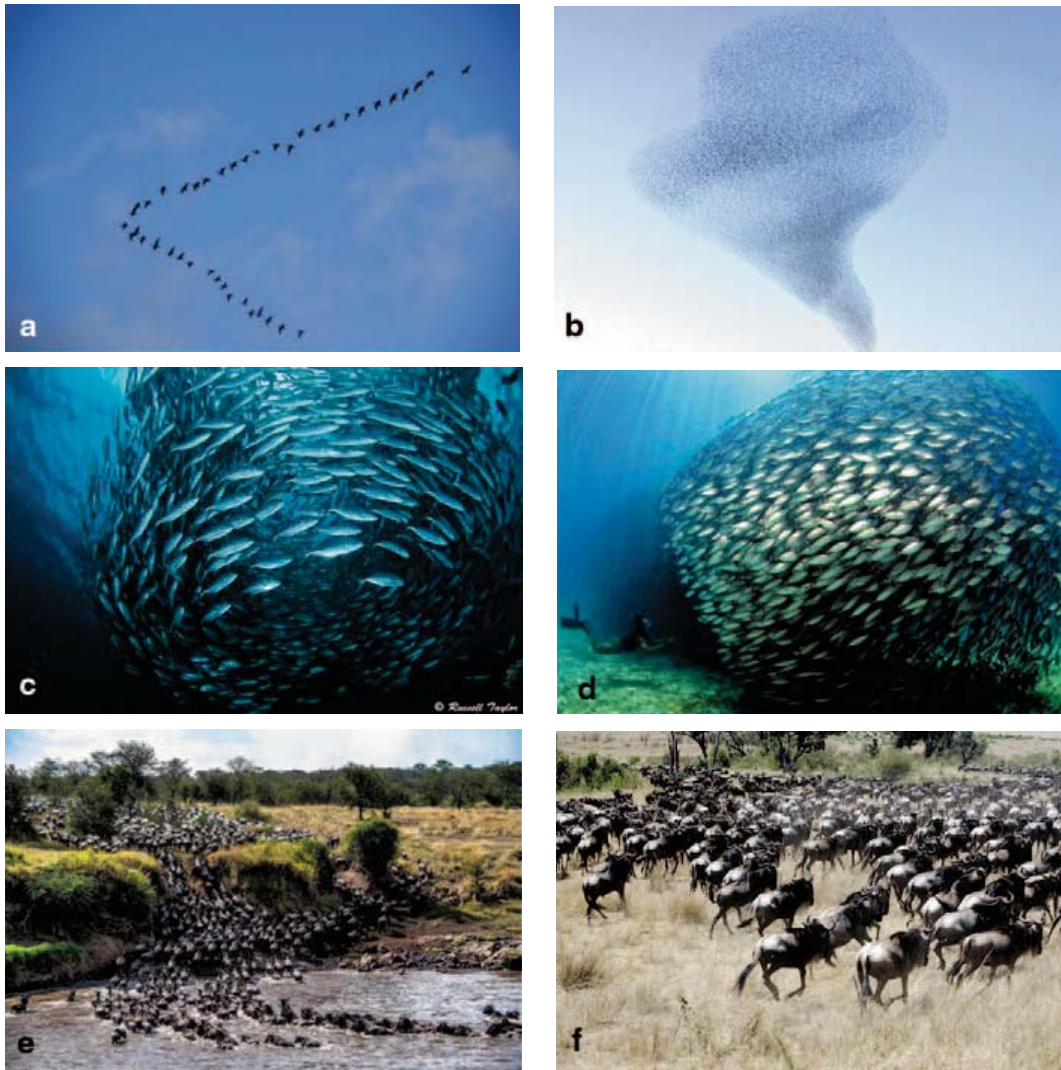


Figure 1.1: Collective behavior of animals groups. [1]

characteristics can be identified. Many practical and theoretical challenges are involved in cooperative control of multi-agent systems. Instead of a single system we have a system of subsystems which need to communicate together while the communication bandwidths are limited. It is a difficult task to determine which agents to communicate at each time and what to communicate. Moreover there is a compromise between individual's goals and the team goal. In multi-agent systems, there are a number of research problems that have resulted in development of many useful tools and theories. Among different problems in the multi-agent systems research area, consensus problem is one of the most favorable, which is to provide a distributed way, with minimal

computation and communication requirement to find the average of a shared quantity in a network of agents or computational units. Here, agents are usually coupled since they are performing the operation without directly influencing each other. Each agent in the team makes its own decisions by using only limited data obtained by its own measurements or communication with neighboring agents.

Despite dedication of a large body of works to study multi-agent networks and cooperative control there are still unsolved problems in this area among them are uncertainties and failure in the agents, limited communication and actuation capability. Most of introduced consensus algorithms are focused on systems with single-integrator or double integrator kinematics agents while practical application usually consist of LTI and nonlinear dynamical systems. Another important issue in control systems is the safety and reliability. In many cases, the loss of performance or stability may cause serious damage, especially in safety critical systems such as robots in hazardous areas, airplanes and spacecraft. To avoid this problem, some methods are developed to design fault tolerant controller for a single system, which maintains its performance and stability in the event of malfunction in the components of systems.

In the case of cooperative systems, the occurrence of faults in any of team members may affect the consensus achievement of the team. Hence, in the same way, it is desirable to develop fault tolerant consensus algorithms. Actuator fault is a common type of fault among different types of faults in systems that can occur and they mainly include loss of effectiveness and saturation faults. Clearly, there are many scenarios that the team consensus could not be maintained in the case of occurrence of actuator faults in some members, but it could be possible to recover the team consensus in some scenarios. Motivated by these short comings the current thesis addresses a distributed consensus algorithms for multi-agent teams in presence of disturbance signals, measurement noise, and model uncertainties including Lipschitz nonlinearity. We are also addressed consensus algorithms that could tolerate different actuators faults.

1.2 Literature Review

Cooperative control of autonomous multi-agent systems has been extensively investigated in the past few years [14, 15] and the works in this field can be categorized in two general areas [16]. The first category is consensus based formation of mobile agents including mobile robots [17], unmanned aerial vehicles (UAVs) [18], satellites [19], aircrafts, autonomous under water vehicles (AUVs) [20] and automated high way systems. The second category is non-consensus based cooperative control algorithms such as task assignment [21], payload transport [22], role assignment [23], air traffic control [24], and search and timing. The consensus problem involves convergence of the outputs or states of all the agents to a common value [25]. It implies that each agent has access to other agents state, known as the neighboring agents by using either a communication network or sensing devices [15], [26]. Depending on the amount of data exchange between systems and the available data of the other systems, centralized or distributed cooperative control strategies can be used [27]. The centralize strategy relies on the assumption that each team member has the access to all the other team members data and in the distributed strategy it is assumed that it has only access to data of some neighboring team members. Usually, it is preferred to use distributed algorithm to achieve consensus. To model the agents communication network, agents are usually represented by nodes in an undirected or directed graph and edges between the two nodes represent the data exchanges between the corresponding agents.

Over the past decade the consensus problem has been studied extensively in the literature due to its applications in numerous areas such as cooperative control of unmanned aerial vehicles [28], formation of mobile robots [29], unmanned undersea vehicles distributed control [30], and sensor networks [31], among others and different aspects of the consensus achievement of multi-agent systems has been investigated including consensus problem of first-order or second-order integrators with fixed and switching graph topologies [32], communication delay [33], graph connectivity preservation [34], reference signals [35]

However, most of the work in this area have considered the agents dynamics as either first-order or second-order integrators [36–39]. Although, in

these works interesting results have been obtained mostly in absence of disturbance signals and actuator faults. However, development and investigation of consensus achievement of multi-agent systems with switching topologies and directed information flow graphs in presence of disturbance signals, model uncertainties, measurement noise, or actuator faults have not been investigated extensively in the literature [40].

In the literature, both fixed [41] and switching [42] communication network topologies are investigated and consensus problem under both directed [43] and undirected [44] are studied. However, problems that consider directed and switching communication networks are more general and more practical. A number of interesting results have been published [45] by assuming that all agents are healthy and no anomalies, faults, or failures are present in the agents.

In following subsections, a detailed literature review on consensus achievement in teams is presented.

1.2.1 Consensus Achievement of Healthy Teams

The consensus of high-order integrator systems with time-delay and switching in the communication network topologies is also addressed in [46].

In [47], the consensus of a leaderless team of high-order integrator agents is investigated and necessary and sufficient conditions for convergence is studied. Although, a large class of LTI systems including the single input systems can be transformed into a collection of high-order integrators, this may not be practical for all LTI systems.

An optimal consensus seeking in a network of multi-agent systems based on the LMI approach is presented in [48] for a team of LTI systems. Although, the agents can be heterogeneous, it is shown that in the proposed optimal design procedure the solution of the Riccati equation does not guarantee the consensus achievement and LMI formulation was used to achieve the consensus seeking requirements.

In [49], a team of LTI agents is designed to accomplish consensus over a common value for the agents' output by using the cooperative game theory and design requirements for the entire team are developed by using the LMI

formulation of the minimization problem.

A semi-decentralized controller is designed in [50] for a team of LTI agents to accomplish cohesive motion with consensus on an agreed upon trajectory in both leaderless and modified leader-follower structures.

The consensus problem of a team of homogeneous LTI agents with a fixed topology directed information flow graph is addressed in [51]. To achieve this goal a set LMIs which are dependent on the eigenvalues of the Laplacian matrix should be solved. Since, the exact values of the Laplacian matrix are depend on the overall structure of information fellow graph, it cannot be computed based on the local and neighboring agents' data and should be pre-determined in a centralized manner. In [52], synchronization control in arrays of identical output-coupled LTI systems is addressed and sufficient conditions for the existence of a synchronizing control input are analyzed. It is shown that for marginally stable systems that are detectable a synchronizing controller exists if the directed information flow graph describing the communication is fixed and connected. Here, the effects of disturbance in agents are not studied.

Consensus problem of homogeneous LTI system is investigated in [53] and an LQR-based consensus algorithm is proposed for fixed topology information flow graph. Again, the effects of disturbance in agents are not studied. The H_∞ consensus problem in a homogeneous team of LTI systems is addressed in [54] for undirected and fixed topology flow graph. To achieve this goal, a set of $n - 1$ LMIs, which are dependent on eigenvalues of the Laplacian matrix should be solved. Here, n is the number of agents in the team. Again, due to dependency of LMIs on eigenvalues of the Laplacian matrix, the controller cannot be designed based on the local and neighboring agents' data and should be pre-determined in centralized manner. In [55], the consensus problem of multi-agent team of LTI systems under fixed topology directed information flow graph is studied. To design the consensus algorithm knowing the exact values of the Laplacian matrix eigenvalues is needed and the effect of disturbances is not taken into account.

In [56], the consensus problem in a team of identical LTI agents with time-delay is investigated and an algorithm is proposed based on the solution of certain LMIs.

In [57], an H_∞ consensus algorithm for a team of homogeneous LTI systems is proposed. The topology of the information flow graph is assumed to be switching and a quadratic Lyapunov function is used to show the convergence of the H_∞ consensus algorithm. Although, the authors investigate consensus in a switching topology of multi-agent systems, the switching strategy cannot be arbitrary and should be pre-assigned.

An $L_2 - L_\infty$ consensus control is proposed in [58] for a team of high-order integrators with directed and switching topology information flow graph. However, in that work the disturbance signal is limited to L_2 signals and for designing the consensus protocol a set of LMIs should be solved for **all** the information flow graph topologies. This implies that details on all the information flow graph topologies should be known *a priori* and before the design of the controllers, which imposes in many cases impractical limitations and constraints on the use of this strategy. Furthermore, the algorithm becomes computationally infeasible if the number of network topologies is large.

In [59] a “practical consensus” protocol for a team of LTI systems with directed information flow graphs is presented. In this work “practical consensus” implies that the consensus error remains bounded in presence of an L_2 or L_∞ disturbance signal, however the communication network topology is assumed to be fixed. The sufficient conditions to design the consensus protocol is presented by a set of LMIs. Although, the disturbance signal could be an L_∞ signal, arbitrary switching in the network topologies are not considered.

H_2 and H_∞ consensus approaches have been investigated in [60] for a team LTI systems. To design the consensus protocol the consensus problem is transformed to design an H_2 or H_∞ controller by stabilizing n different LTI systems that their dynamics depends on the eigenvalues of the network Laplacian matrix. However, the communication network topology is assumed to be undirected and fixed and the disturbance signals are assumed to be L_2 .

H_∞ consensus control for a team of LTI multi-agent systems under undirected information flow graph is addressed in [61], and based on the solutions of two LMIs, a distributed output feedback protocol is proposed.

In [43], the authors solve the H_∞ consensus problem for a team of LTI multi-agent systems with a directed and *fixed* information flow graph topology.

The H_∞ robust control problem of an uncertain linear switched systems with dwell time is presented in [62] and a bounded real lemma is proposed based on the solutions of a set of LMIs. A quadratic Lyapunov function is presented to guarantee the stability and H_∞ performance of the overall closed-loop system.

The algorithm, presented in [63], solves the H_∞ consensus problem of a homogeneous team of LTI systems under an undirected and fixed information flow graph. To obtain the state-feedback gains of the distributed consensus controller, a set of LMIs should be solved.

The disturbance rejection problem in the coordination control of a group of autonomous LTI systems subject to external disturbances is studied in [64] for a class of undirected network topologies, that are said to possess a desired level of disturbance rejection. It is shown that the H_∞ problem of the multi-agent systems can be solved by analyzing the H_∞ control problem of a set of independent systems whose dimensions are equal to that of a single node. The solution also depends on the network topology and certain criteria are derived in terms of LMIs.

The L_2 norm gain computation method for a switched linear system is presented in [65], when the time interval between switchings is sufficiently large and the stabilizing and anti-stabilizing solutions of a set of algebraic Riccati equations for the systems being switched satisfy certain inequalities.

Sufficient conditions for the stability of linear switched system with dwell time in presence of external disturbances is presented in [66]. To achieve this goal, a piecewise quadratic Lyapunov function is considered, which is non-increasing at the switching instants. A set of LMIs are presented to determine this piecewise quadratic Lyapunov function.

In [67], the output consensus problem of a team of heterogeneous LTI single-input single-output systems under a fixed information flow graph is studied and the effects of a class of model uncertainties is investigated. A distributed controller with internal dynamics is proposed which is use only the outputs of the agents.

The output-feedback consensus problem for a homogeneous team of LTI systems in absence of external disturbance is studied in [68].The information

flow graph topology is assumed to be switched fast enough and an averaging approach is used to model the communication network.

In [69], an output-feedback distributed algorithm is presented to solve the consensus problem of a team of identical LTI systems under a fixed topology communication network and in absence of the disturbance. An LMI approach is used to obtain the controller gains.

Beside numerous work in the literature such as [25], [70], [71], [35] addressing consensus algorithms for teams of single and double integrator by using the common assumption that the underlying communication/sensing network is connected for all time, i.e. there exists an expanding tree in the graph associated with the network. In some papers such as [72], [73], [74], the connectivity preservation of the network while it achieves consensus is also considered.

In [34], [75] potential functions are proposed that increase but remains bounded when two connected agents reach the sensing threshold. The main shortcoming of these works is that there is no relationship between the agents actuation capabilities and this bound. The reference [72] addresses the connectedness issue in multi-agent rendezvous and the formation control problems over dynamic interaction graphs by adding appropriate weights to the edges in the graphs. The nonlinear feedback laws that are based on weighted graph Laplacians are introduced and they are shown to be able to solve the rendezvous and formation-control problems while ensuring connectedness. They have also not considered any bound on the control inputs in their works. In [34] a general class of distributed potential-based bounded control laws with connectivity preserving property for single-integrator agents is proposed. The main idea of the proposed approach is to design the potential function such that when two agents are going to lose a connection the gradient of the potential function lies in the direction of that edge in order to shrink it.

In [76] the rendezvous problem with connectivity preservation having double-integrator dynamics using hysteresis functions are presented. A class of bounded potential functions are constructed to guarantee the connectivity, but as in previous works they cannot define a specific bound based on the agents actuation constraints.

In [77] a distributed control framework based on potential fields is presented

for multi-agent flocking problem that simultaneously addresses the desired velocity alignment as well as the connectivity preservation of the underlying network that is necessary for alignment. Double integrator models of agents and design of nearest neighbor control laws are presented.

A distributed H_∞ consensus of multi-agent systems with a class of Lipschitz like nonlinearity the agents dynamics is presented in [78]. The communication network topology is assumed to be undirected and fixed and sufficient conditions to design the consensus algorithm are derived as a set of LMIs.

In [79], the consensus problem for a team of homogeneous third-order nonlinear systems under a fixed undirected flow graph is investigated. It is assumed that the dimension of control input of each agent is three and the nonlinearity function in agent's dynamics satisfies a Lipschitz-like condition. Although, the information flow graph is assumed to be undirected, the proposed consensus algorithm solves the leader-follower consensus problem.

In [80], a consensus algorithm is developed for a team of heterogeneous affine nonlinear systems with a switching topology information flow graph. It is assumed that the dimension of the control input and states of each agent are the same. Moreover, the nonlinear function which maps the control input to the state derivatives in the dynamics of the system is invertible. Therefore, the approach is not general and cannot be applied to a large class of real systems.

Consensus problem of a team of nonlinear systems by using a linear consensus algorithm and feedback linearization technique is presented in [81]. The main idea is that a diffeomorphism transformation exists so that the nonlinear system can be transformed into the form of LTI systems by using feedback linearization technique. Therefore, a consensus algorithm for the LTI systems can then be applied to achieve consensus of the original nonlinear system that is feedback linearized.

The work in [82] studies the decentralized consensus problem of a class of nonlinear multi-agent systems with Lipschitz nonlinearity and undirected communication topologies. To achieve this goal, a consensus algorithm is presented which uses relative states of the neighboring agents to design a controller. A set of $n - 1$ LMIs having the same dimension as that of a single

agent should then be solved where n is the number of agents in the team.

The consensus problem for multi-agent systems having LTI and Lipschitz nonlinear dynamics is addressed in [83]. Distributed relative-state consensus algorithm using an adaptive law to adjust the coupling weights between the neighboring agents are designed for both the LTI and Lipschitz dynamics, under which consensus is achieved for undirected information flow graphs. Since, directed graphs are not supported, an extension to the case with a leader-follower is also presented. It is worth noting that in contrast to the earlier results the proposed consensus algorithm is fully decentralized and there is no need to use any global information.

In [84], the synchronization problem for a team of nonlinear systems is investigated. Here, again the topology of information flow graph is assumed to be fixed and undirected and nonlinear dynamics of agents is Lipschitz and QUAD. The QUAD condition is an assumption on the nonlinear vector function f which satisfies $(x-y)^T[f(x)-f(y)]-(x-y)^T\Delta(x-y)\leq-\omega(x-y)^T(x-y)$ for some arbitrary Δ and ω .

A synchronization method for a class of second-order multi-agent systems with a Lipschitz like nonlinearity is studied in [85]. In their work, the multi-agents team has a leader follower architecture and the proposed controller uses an observer to estimate agents' states based on their output variables and finally by mean of Lyapunov analysis it is shown that the overall team is synchronized in a finite-time.

Containment control of second-order Lipschitz nonlinear multi-agent systems is investigated in [86] and both static distributed controller for teams with directed communication networks and adaptive controller for teams with undirected network topologies are presented and it is analytically proved that all followers will asymptotically converge to the convex hull which spanned by states of the leaders.

In [87] a team of first-order nonlinear systems under both fixed and switching topology communication networks is considered and a consensus controller design is proposed and finally necessary and sufficient conditions are presented. In their work, the nonlinearity can be discontinuous.

A cooperative containment control of a second-order linear multi-agents

system with multiple leaders under directed and fixed topology communication network in presence of unknown disturbance signal is presented in [88].

An adaptive distributed consensus algorithm for a class of multi-agent systems with bounded nonlinearities is proposed in [89]. Agents are modeled as high-order systems, communication network is undirected, and it is assumed that the nonlinearities are non-identical.

In [90] a distributed formation controller based on linear extended observers for a team of second-order nonlinear systems is presented. In their work, it is assumed that the team has a virtual leader and properties of dynamics nonlinearity implies some limitations on acceleration and velocity of the agents.

A first-order nonlinear multi-agents system is studied in [91] and a consensus algorithm based on sampled-data information is presented. To analyze stability of their proposed algorithm first dynamics of sampled-data team is converted to an equivalent nonlinear system with varying time delays and time-delayed systems stability analysis tools are utilized.

A cooperative-learning algorithm for a team of identical nonlinear systems with undirected communication network is presented in [92]. In their work, radial basis function neural network is used to approximate dynamics nonlinearity and it is stated that if the agents exchange their RBFNN information with each other and use it in their learning rules the overall learning performance of the team will improve dramatically.

In [93] a cooperative learning algorithm for updating RBFNN weights for a team of nonlinear systems is presented. In their work, dynamics of the agents are identical but the reference signals are assumed to be different and tracking performance of the agents is guaranteed.

Consensus achievement problem in a leaderless homogeneous team of agents with Lipschitz nonlinearity under directed and switching topology communication network is studied in [94]. In their work, necessary and sufficient conditions for designing a distributed consensus algorithm is presented as a set of LMIs.

1.2.2 Cooperative Fault Tolerant Consensus

Fault diagnosis and isolation (FDI) of single and multi-agent systems have been extensively studied in the literature.

Among different actuator faults types, due to the physical limitation and constraints of practical systems, saturation fault is probably among one of the most common phenomena and its classical examples do include limits in deflections of control surfaces of UAVs, the voltage limits on electrical motors and flow rates of hydraulic actuators [95].

Fault detection and isolation (FDI) of single and multi-agent systems have been extensively studied in the literature [96–103]. In [104], fault detection problem in Markovian jump systems is studied. In [97], an adaptive observer-based technique is used to detect occurrence and estimate the severity of actuator faults in LTI systems.

In [105], Kalman filter is used to diagnose and isolate the faults in the system. To identify faults with very small amplitudes, a statistical local approach is used in [98]. A robust decentralized actuator fault detection and estimation technique based on sliding-mode observers is presented in [106].

Fault detection, isolation, and estimation of networked sensing systems with incomplete measurements is investigated in [107]. In [99], a consensus based overlapping decentralized fault detection and isolation approach is presented. Development, design and analysis of actuator fault detection and isolation for a team of multi-agent systems is presented in [100]. In [102], a decentralized robust fault detection and isolation filter design technique for a non-homogeneous team of multi-agent systems is proposed.

In the area of fault tolerant cooperative control few work are available in the literature.

A multi-agent team with partial information exchange is considered in [50] and based on the solution of a set of LMIs, an optimal output consensus algorithm is proposed for both leader-less and modified leader-follower structures. The effect of the float fault in actuator of some of the agents is also investigated and robustness of the proposed consensus method is demonstrated.

A cooperative hierarchical actuator fault accommodation for formation flying vehicles with absolute measurements is presented in [19]. The agents are

modeled as LTI systems and it is assumed that local fault recovery module can detect the loss-of-effectiveness actuator fault and partially recover the faulty agent. Based on the solution of a set of linear matrix inequalities (LMI), a decentralized formation level fault recovery module is designed to boost the overall performance of the team.

A hierarchical actuator fault accommodation framework for formation flying satellites, which are modeled as double integrators, is proposed in [108].

A modified leader-follower problem for a team of double integrators is studied in [109] and an optimal control-based approach is used to design a semi-decentralized cooperative controller. Furthermore, the performance of the team in presence of actuator float faults in some agents is investigated.

In [18], a multi-agent team of moving vehicles is considered and its performance analysis in presence of actuator faults is investigated. The team structure is assumed to be a modified leader-follower and its goal is to accomplish a cohesive motion. A semi-decentralized cooperative controller is designed and is shown that occurrence of loss-of-effectiveness faults in the actuators does not deteriorate the stability nor the consensus seeking goal of the team.

A connectivity preserving consensus algorithm in presence of actuator saturation is presented in [110].

An output feedback consensus achievement algorithm for a team of LTI system with switching communication topology based on the solution to a set LMIs is presented in [111].

In [44], a hierarchical cooperative actuator fault accommodation in formation flight of unmanned vehicles using relative measurements is addressed for LTI systems and a centralized and decentralized consensus algorithms are proposed.

The developed hierarchical design method in [44] consist of three modules, namely the low-level fault recovery (LLFR), the formation-level fault recovery (FLFR) and the high-level (HL) fault recovery. In the LLFR stage it is assumed that all actuator faults are detected by the FDI module and their severities are estimated exactly. Using these estimates of fault severities, an optimization problem is provided and based on its solution, the gains of

the consensus algorithm are reconfigured. To guarantee the consensus achievement of low-level fault recovered multi-agent team, an LMI approach was used. Since, in practice it is not possible to exactly estimate the fault severities, the performance of the low-level recovered multi-agent team is then monitored by a high-level module and the FLFR module is activated whenever a loss of performance is detected at the low-level. In the FLFR step it is assumed that only one of the estimated fault severities is inaccurate and it is shown that by adjusting the parameters of the optimization problem, the consensus error of the multi-agent team remains within a predefined bound.

A cooperative hierarchical actuator fault accommodation for formation flying vehicles with absolute measurements is also presented in [19, 112] and in [113] using relative measurements. The agents are modeled as LTI systems and it is assumed that local fault recovery module can detect the loss-of-effectiveness actuator faults and partially recover the faulty agent. Based on the solution of LMIs, a decentralized formation-level fault recovery module is designed to enhance the overall performance of the team.

In [114] global consensus problem for second-order multi-agent systems is studied and a cooperative algorithm is proposed which results in consensus achievement of the team in presence of random directional communication link failures.

1.3 General Problem Statement

The main objective of this work is to explore consensus-based cooperative control of multi-agent systems. A multi-agent system is a team of independent autonomous systems that are employing a distributed control algorithm to fulfill a common goal as an entity. Despite dedication of a large body of works to study multi-agent networks and cooperative control there are still unsolved problems and challenges in this area mainly maintaining the safety and reliability of the team while dealing with actuator failures, model uncertainties, measurement noise, and disturbances. In many cases, the loss of performance or stability may cause serious damages, especially in safety critical systems such as robots in hazardous areas, airplanes and spacecraft. To avoid this

problem, some methods are developed to design fault tolerant controller, noise and disturbances rejection methods, and robust controller against model uncertainties for a single system, which maintains its performance and stability in the event of malfunction in the components of system, environmental disturbances, sensor noise and model uncertainties.

In the case of cooperative systems, the effects of these parameters on any of team members may affect the consensus achievement of the entire team. Hence, in the same way, it is desirable to develop consensus algorithm that are tolerant against faults and model uncertainties and also distributed disturbance and noise rejection methods. Actuator fault is a common type of fault among different types of faults that can occur in systems.

Motivated by these shortcomings in this thesis we first study effects of disturbances on consensus achievement of an LTI multi-agent system and our objective is to propose a transformation and a framework which aids us methodically design cooperative controllers in first place and makes it possible to use powerful Lyapunov stability analysis tool to guarantee its consensus achievements in the presence of disturbances while the communication network topology is directed and switching. Next, effects of actuator faults in consensus achievement of a multi-agent team is studied and the goal is to propose a novel consensus algorithm which can deal with actuator saturation and preserves the connectivity of the communication network. The other objective of this thesis is to propose a framework to quantitatively studies the effects of actuator fault in consensus achievement of LTI multi-agent systems which leads us to formulate an optimization problem and design a cooperative fault recovery strategy to improve the performance of the team. The next problem that we tackle in this work is to study consensus achievement of multi-agent systems with measurement noise and uncertainties including Lipschitz nonlinearities in the presence of disturbances with directed switching networks. Finally, a cooperative-adaptive consensus algorithm for a class multi-agent systems with unknown nonlinearity under undirected and switching topology communication network in presence of unknown disturbances is presented.

1.4 Thesis Contribution

The main contributions of this thesis are presented as follows:

1. The main challenge to systematically design consensus algorithm for general LTI multi-agents systems is that the controller should guarantee the stability of overall team but at the same time it should not be asymptotically stable. One of the contributions of this thesis is that we proposed a transformation which lets us map dynamics of the multi-agent system with a directed information flow graph to another LTI system. As a result one can design an state feedback controller that asymptotically stabilizes the transformed LTI system and use it as distributed consensus algorithm. Consequently, it allows us to use classical controller design techniques to perform stability analysis methods such as Lyapunov functions, and there is no need to solve any set of LMIs in the cooperative control design procedure. Although, using our proposed transformation, it is possible to design the controller for transformed LTI system, however dimensions of transformed LTI system for a team consisted of n agents is n times larger than the dimensions of each agent. It could dramatically increase the computational complexity of controller design. One of the contributions of this work is to propose a method to use algebraic connectivity of communication network and decouple dynamics of the transformed system into two parts. This will let one deal with equations with the same dimensions as each agents. It becomes more clear when knowing that the time-complexity of solving an LMI is $O(N^6)$ [115], and time-complexity of solving an algebraic Riccati equation (ARE) is $O(N^4)$ [116], where N is dimension of the equations.
2. Dynamics of multi-agent systems with switching topology communication network even with LTI agents is no longer time invariant. Therefore, design and stability analysis tool for LTI systems may not be useful. It is more challenging when the effects of the disturbances are taken into account. Developing a Lemma which lets us use Lyapunov functions to analyze stability and disturbance attenuation performance of multi-agent teams, is one of the main contributions of this thesis. It is worth noting

that our proposed Lemma lets us design cooperative controllers and perform stability analysis for multi-agent systems with switching topologies in the presence of either L_2 and finite RMS disturbance signals.

3. One of the main contributions of this dissertation is to propose a framework that lets us quantitatively measure effects of actuator faults of the agents on the consensus achievement of multi-agent system. It is shown that convergence of consensus algorithm is guaranteed as long as the overall fault index of the team is within a bound. It will let us deal with concurrent faults in multiple agents and since it also depends on some controller parameters one can develop fault recovery algorithms that force healthy agent to dedicate more control effort and compensate for that of faulty agents. To achieve this goal, we formulate an optimization problem that lets us design aforementioned recovery strategies while consensus achievement of the team is guaranteed.
4. Another contribution of this thesis is in the development of distributed consensus algorithm for teams of multi-agents with bounded RMS measurement noise and model uncertainties including Lipschitz nonlinearity. Here, we presents criterion for observer and controller gains that let us extend our proposed methods for state-feedback cooperative control design and use it to systematically solve the consensus achievement problem of multi-agent teams in presence of noise and uncertainties.
5. Finally, a cooperative-learning method is proposed which can be used for cooperatively online-updating of a general function approximator parameters, including RBF neural networks. It means that, all agents will exchange their learning information among each other and will use information from neighboring agents in their learning rules. In addition, we proposed a consensus algorithm based on aforementioned cooperative-learning method for a team of nonlinear systems.

1.5 Thesis Outline

The remainder of this thesis is organized as follows. In Chapter 2 the background information about topics that are required in later chapters are presented. We start with algebraic graph theory and afterwards we present matrix analysis methods for graphs. It is followed by preliminary definitions in cooperative control and consensus achievement in multi-agents systems. Furthermore, Kronecker product and its properties are presented. Finally this chapter concludes by presenting Lyapunov stability analysis technique.

Chapter 3 the consensus problems with H_∞ and weighted H_∞ bounds for a homogeneous team of Linear Time Invariant (LTI) multi-agent systems with a switching topology and directed communication network graph are studied. It begins with a brief preliminaries on algebraic graph theory and several lemmas that we have developed for this work. The formal problem statement of the chapter is presented afterwards and it is followed by our proposed consensus algorithm design methodology. Numerical simulations that support our proposed theoretical results conclude the chapter.

Next, a cooperative actuator fault accommodation strategy is studied in Chapter 4. The multi-agents system is considered to be a team of LTI multi-agent systems and information flow graph is directed and switching topology. The effects of two types of actuator faults, namely loss-of-effectiveness fault and saturation fault are investigated and it is assumed that the faults can simultaneously occur in more than one agent and the exact estimate of the fault severities are not available.

Chapter 5 studies the disturbance attenuation properties of consensus achievement algorithms for a multi-agent team with output measurement noise and teams of agents with model uncertainties including Lipschitz nonlinearity. The communication network topology is assumed to be switching. The teams are homogeneous and the information flow graph is directed and the effectiveness of the proposed consensus algorithm is illustrated by performing numerical simulations. Furthermore, a cooperative-adaptive consensus algorithm for a team on multi-agent systems with unknown nonlinearity is proposed in this chapter.

Finally, conclusions and suggestions for future work are provided in Chapter 6.

Chapter 2

Background Information

In this thesis, we study consensus-based cooperative control of multi-agent systems which consist of a group of dynamical systems with ability to exchange information among each other. In the cooperative control our goal is to design a distributed control strategy to allow each agent determines its control signal only based on its own local information and limited information provided by others, while the overall multi-agent system as a single entity performs its desired objectives. Towards this end, having knowledge about information flow path and its dynamics is important and graph theory is one of the best ways to model it. Graph theory and algebraic graphs are deeply investigated in the literature [1, 70, 117]. In section 2.1 some important definitions and principal properties of algebraic graphs, which are required in remainder of this thesis, will be presented from [1]. In algebraic graph theory, we associate some matrices to each graph and therefore matrix analysis methods will help us to have better understanding and a tool to integrate graph topology in cooperative control design procedure. This topic is covered in section 2.2 and it is followed by basic definition of cooperative control and consensus achievement of multi-agent systems in section 2.3. Kronecher product of matrices and its properties play an important role in stability analysis of cooperative control strategies using Lyapunov stability analysis. In sections 2.4 and 2.5 these topics are presented.

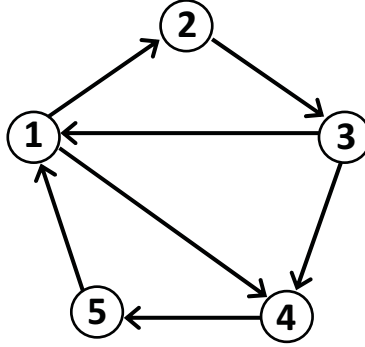


Figure 2.1: Visual representation of a graph

2.1 Algebraic Graph Theory

A graph \mathcal{G} mathematically is defined as a tuple of nodes or vertices set \mathcal{V} and edges or arcs set \mathcal{E} . In our work, \mathcal{V} is set of all agents. Now, let v_i, v_j denote agents which are exchanging information and information flow from v_i to v_j . We say that there is an edge from v_i to v_j and denote it as tuple (v_i, v_j) which is an element of set \mathcal{E} . To visually represent a graph, nodes are drawn as dots, little circles, or numbers and whenever there is an edge from node v_i to v_j it is shown by drawing an arrow v_i to v_j . Figure 2.1 shows visual representation of a graph. In this thesis, we do not consider information flow from an agent to itself and assume that underlying information graph is simple.

Definition 2.1. *Graph G is simple if and only if for any node $v_i \in \mathcal{V}$, $(v_i, v_i) \notin \mathcal{E}$.*

For each edge (v_i, v_j) , node v_i is called parent and v_j is called child, and we say that the edge is an outgoing edge of v_i and an incoming edge of v_j .

Definition 2.2. *The in-degree of a node is defined as number of edges that are incoming with respect to that node and the out-degree is the number of its outgoing edges.*

The neighboring set of node v_i , which is denoted by \mathcal{N}_i is defined as set of all nodes v_j with edges outgoing with respect to v_j and incoming with respect to v_i . Cardinality of neighboring set of a node is equal to its in-degree.

Definition 2.3. *A balanced graph is a graph that in-degree and out-degree of all its nodes are equal.*

A graph is called bidirectional if for a pair of nodes any edge (v_i, v_j) , there exists edge (v_j, v_i) , otherwise it is called directed graph or digraph. A graph is weighted if one assigns a real positive number a_{ij} to any edge (v_i, v_j) . If a graph is bidirectional and for any pair of edges (v_i, v_j) and (v_j, v_i) , the associated weights a_{ij} and a_{ji} be equal, the graph is called to be undirected. A directed path from node v_a to v_b is a sequence of nodes $v_a, v_1, \dots, v_n, v_b$, such that edges $(v_a, v_1), (v_1, v_2), \dots, (v_n, v_b)$ exist, and the number of these edges is equal to the length of the directed path. Node v_i is connected to node v_j if there exists a directed path from node v_i to node v_j and the distance from node v_i to v_j is defined as minimum length of all directed paths from v_i to v_j .

Definition 2.4. *A loop is a directed path from a node to itself.*

A graph is called strongly connected if all of its nodes are connected to each other and it is called connected if it is also bidirectional. A bidirectional graph is a tree if it is connected and only one path exists between any of its two distinct nodes.

Definition 2.5. *A graph is called directed tree if for all nodes except one node, which is called root, has in-degree equal to one.*

In other words, a graph is a (directional) tree if it is (strongly) connected and has no loops. Graph $\mathcal{G} = \{\mathcal{V}, \mathcal{E}\}$ has a spanning tree $\mathcal{G}_{ST} = \{\mathcal{V}, \mathcal{E}_{ST}\}$, if \mathcal{G}_{ST} is a directed tree and $\mathcal{E}_{ST} \subseteq \mathcal{E}$. In this case, there is a directed path from the root node to any other node in the graph. A graph may have more than one spanning tree and therefore more than one root node.

Definition 2.6. *The set of roots of all spanning trees of a graph is called root set or leader set of the graph.*

Any strongly connected graph has a spanning tree and its nodes set is its root set as well. Figure 2.2 and Figure 2.3 show two different spanning trees of our example graph, that is presented in Figure 2.1. As it can be seen in Figure 2.2, node 1 is the root of spanning tree and in Figure 2.3 it is node

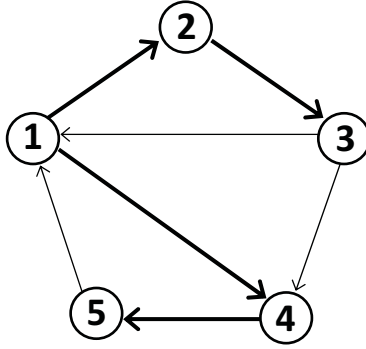


Figure 2.2: Spanning tree of a graph.

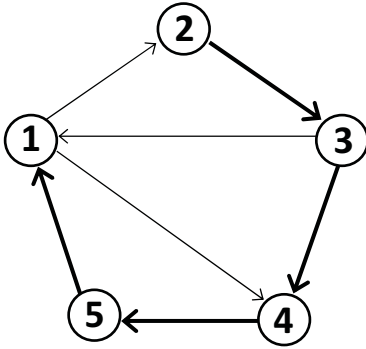


Figure 2.3: Spanning tree of a graph.

2. There are also other spanning trees for this example graph and since it is strongly connected, any of its node can be root of a spanning tree of the graph.

The structure of a weighted graph can be represented by a matrix, which is $\mathcal{A} = [a_{ij}]$ and it is called adjacency or connectivity matrix. Here, a_{ij} denotes the weight of edge (v_i, v_j) . As mentioned earlier, in our work graph is simple and therefore $a_{ii} = 0$. By using algebraic graph theory, one can study all the properties of a graph by only looking at its associated adjacency matrix. Two of these properties are weighted in-degree of node v_i that is defined as follows:

$$deg_{in}(i) = \sum_j a_{ij}$$

and its weighted out-degree which is defined as follows:

$$deg_{out}(i) = \sum_j a_{ij}$$

Graph diameter and in-volume of a graph are other important properties of a graph.

Definition 2.7. *Graph diameter refers to the longest directed path between two of its nodes*

Definition 2.8. *In-volume of a graph is defined as summation of in-degrees of all graph nodes.*

A graph is called weighted balanced if in-degree and out-degree for all of its node are equal and a graph is undirected if its adjacency matrix is symmetric. If non-zero weights of a graph are 1, weighted in-degree and in-degree of a node, weight out-degree and out-degree of a node, and weighted balanced and balanced graphs are equivalent. Another matrix that we may assign to a weighted graph is Laplacian matrix and it is one the most important matrices in studying of multi-agent systems. It is denoted by $\mathcal{L} = \mathcal{D} - \mathcal{A}$, where \mathcal{D} denotes diagonal weighted in-degree matrix. Therefore, summation of all rows of a Laplacian matrix is zero. The adjacency and Laplacian matrices associated with our example graph shown in Figure 2.1 are given as follows:

$$\mathcal{A} = \begin{bmatrix} 0 & 0 & 1 & 0 & 1 \\ 1 & 0 & 0 & 0 & 0 \\ 0 & 1 & 0 & 0 & 0 \\ 1 & 0 & 1 & 0 & 0 \\ 0 & 0 & 0 & 1 & 0 \end{bmatrix}, \quad \mathcal{L} = \begin{bmatrix} 2 & 0 & -1 & 0 & -1 \\ -1 & 1 & 0 & 0 & 0 \\ 0 & -1 & 1 & 0 & 0 \\ -1 & 0 & -1 & 2 & 0 \\ 0 & 0 & 0 & -1 & 1 \end{bmatrix}$$

In order to study important properties of Laplacian matrix and to understand how it can be used in the cooperative control design procedure, let us transform Laplacian matrix into its normal Jordan form $\mathcal{L} = \mathcal{M}\mathcal{J}\mathcal{M}^{-1}$, where \mathcal{M} denotes the transformation matrix. The main diagonal elements of matrix \mathcal{J} are eigenvalues of Laplacian matrix and columns of the transformation matrix are their associated right eigenvectors [118]. If a Laplacian matrix has a repeated eigenvalue λ_i , the size of its corresponding Jordan block is called geometric multiplicity of eigenvalue λ_i and the summation of size of all its Jordan block is said to be its algebraic multiplicity.

Definition 2.9. *An eigenvalue is called simple if its geometric and algebraic multiplicity is equal to 1.*

Without loss of generality, let us assume all eigenvalues of a Laplacian matrix are ordered such that $|\lambda_1| \leq |\lambda_2| \leq \dots \leq |\lambda_N|$. For undirected graphs, since Laplacian matrix is symmetric, all the eigenvalues are real number and can be ordered as $\lambda_1 \leq \lambda_2 \leq \dots \leq \lambda_N$.

One of the key properties of Laplacian matrix is that 0 is one of its eigenvalues and vector $\mathbf{1} = [1, 1, \dots, 1]^T$ is its associated eigenvector and it can be proven by using the fact that summation of all rows of Laplacian matrix is equal to zero. Therefore, Laplacian matrix cannot be full rank and at the best it can be $N - 1$. In fact rank of a Laplacian matrix is $N - 1$ if and only if its associated graph has a spanning tree [25, 119]. Considering the fact that main diagonal elements of a Laplacian matrix are not negative and using Gersgorin circle criterion, one can obtain more information about its eigenvalues. Gersgorin circle criterion explains that eigenvalues of a matrix $M = [m_{ij}] \in \mathbb{R}^{N \times N}$ in complex plane are located in union of following circles [120]

$$\left\{ Z \in \mathbb{C} : |Z - m_{ii}| \leq \sum_{i \neq j} |m_{ij}| \right\}$$

In Laplacian matrix $\ell_{ii} = \sum_{i \neq j} \ell_{ij}$ and therefore the union of its Gersgorin circles is a circle with radius Δ and its center is located on real number axis at Δ , where Δ denotes maximum in-degree of associated graph nodes. Figure 2.4 depicts these circle in a complex plane. If we normalize adjacency matrix of a graph, which means summation of all rows are equal to 1, eigenvalues of Laplacian matrix are within a circle centered at 1 with radius of 1. In this way it will be easier to compare eigenvalues of two different graph and study effects of their topology on their eigenvalues.

As it can be seen in Figure 2.4 real part of all eigenvalues of Laplacian matrix are not negative and therefore $\lambda_1 = 0$ and $\lambda_2 \neq 0$ if and only if its associated graph has a spanning tree. In fact λ_2 is the most important eigenvalue of this Laplacian matrix in designing cooperative control algorithm and determine their performance and convergence rate. The larger value of λ_2 , the faster convergence rate of the algorithm is.

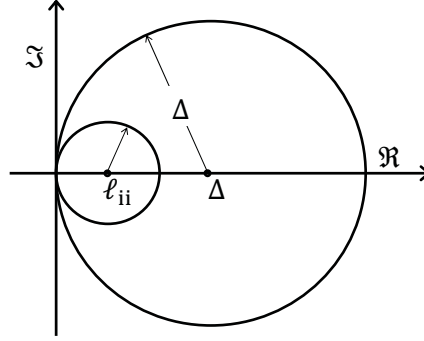


Figure 2.4: Union of Gersgorin circles for Laplacian matrix [1].

Definition 2.10. *The second eigenvalue λ_2 , is called Fiedler eigenvalue of Laplacian matrix and has an intrinsic relation with the graph topology and its connectivity.*

It is also known as algebraic connectivity of the graph [121]. There are some upper and lower bounds of Fiedler eigenvalue for undirected graphs in the literature [122–124]. Definition of some of aforementioned lower and upper bounds are listed below:

$$\lambda_2 \leq \frac{N}{N-1} d_{\min} \quad (2.1)$$

$$\lambda_2 \geq \frac{1}{\text{Diam}(\mathcal{G})\text{Vol}(\mathcal{G})} \quad (2.2)$$

where d_{\min} denotes minimum in-degree of graph nodes, $\text{Diam}(\mathcal{G})$ denotes diameter of graph \mathcal{G} and $\text{Vol}(\mathcal{G})$ denote in-volume of the graph.

There are also some useful inequalities Fiedler eigenvalue in case of directed graphs, but those are more complicated [125, 126]. To show intrinsic relation between eigenvalues of Laplacian matrix and its associated graph topology and give a feeling about it a set of various types of graphs which are usually appear in cooperative systems are presented in Figure 2.5 [1].

If the weight of existing edges of graphs shown in Figure 2.5 are set to 1, the eigenvalues of resulting Laplacian matrices are presented in Table 2.1. As it can be seen in Table 2.1

- for all of the graphs $\lambda_1 = 0$,

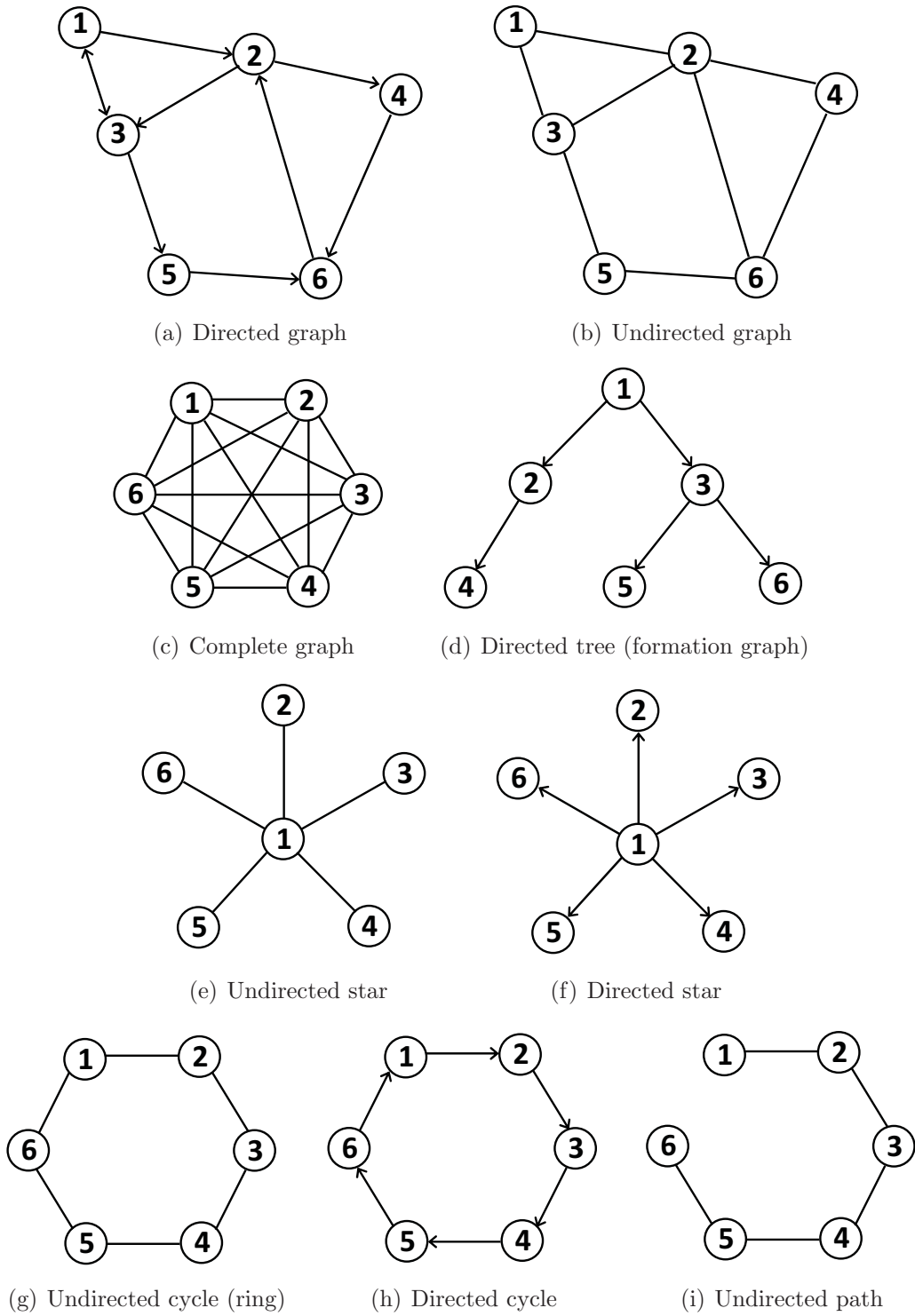


Figure 2.5: Various graph topologies [1].

Table 2.1: Eigenvalues of Laplacian matrices of graphs presented in Figure 2.5 [1].

	λ_1	λ_2	λ_3	λ_4	λ_5	λ_6
Directed graph	0	0.7793	1	$2.2481 + 1.0340i$	$2.2481 - 1.0340i$	2.7245
Undirected graph	0	1.382	1.6972	3.618	4	5.3028
Complete graph	0	6	6	6	6	6
Directed tree	0	1	1	1	1	1
Undirected star	0	1	1	1	1	6
Directed star	0	1	1	1	1	1
Undirected cycle	0	1	1	3	3	4
Directed cycle	0	$0.5 + 0.866i$	$0.5 - 0.866i$	$1.5 + 0.866i$	$1.5 - 0.866i$	2
Undirected path	0	0.2679	1	2	3	3.7321

- all eigenvalues of undirected graphs are non-negative real numbers. However, it is possible to have a directed graph with all real eigenvalues,
- all non-zero eigenvalues of fully connected or complete graph with N node are equal and are N [127]. It is easy to verify from inequality (2.1) that the most connected graph has the maximum possible value of $\lambda_2 = N$,
- Non-zero eigenvalues of directed trees are equal to 1 [128]. Since, directed start is directed tree all of its eigenvalues are equal to 1 as well,
- Undirected start has an eigenvalue equal to N all other non-zero eigenvalues are equal to 1 [128],
- Eigenvalues of directed cycle are located evenly on a circle with radius of 1 and center at 1 in complex plane.

2.2 Matrix Analysis of Graphs

As it is seen in previous section there is deep connection between graphs and matrices and matrix analysis techniques are helpful to reveal different properties of graphs and their topology.

Definition 2.11. *A row/column permutation matrix T , is a matrix square matrix which has exactly one element equal to 1 in each row and column and all other elements are equal to 0 [129].*

Definition 2.12. *Square matrix A is said to be reducible if there exist a row/column permutation matrix T such that TAT^T be a lower block triangular matrix. A matrix is called irreducible if it is not reducible.*

Theorem 2.1. *Graph \mathcal{G} with adjacency matrix A is strongly connected if and only if A is irreducible [130].*

Definition 2.13. *Matrix A is called nonnegative and it is denoted by $A \succeq 0$ if all of its elements are nonnegative, and it is said to be positive if all of its elements are positive. Positive matrices are denoted by $A \succ 0$.*

Note that a positive matrix is not necessarily positive-definite matrix and it is not required to be even be a square matrix.

Definition 2.14. *A nonnegative matrix is a row stochastic matrix if all row summation of its elements are equal to 1 and it is doubly stochastic if both itself and its transpose are stochastic matrices.*

Theorem 2.2. *A nonnegative matrix is row stochastic if and only if it has an eigenvalue equal to 1 and vector $\mathbf{1} = [1, 1, \dots, 1]^T$ be its associated eigenvector [1].*

Theorem 2.3. *Stochastic matrix $A \in \mathbb{R}^{n \times n}$ has following properties [131]:*

- $\rho(A) = 1$, where $\rho(A)$ is spectral radius of the matrix.
- If A is adjacency matrix \mathcal{G} , then $\text{rank}(A) = n - 1$ if and only if matrix G has a spanning tree.
- If A is adjacency matrix \mathcal{G} , then $\lambda_1 = \rho(A) = 1$ is the only eigenvalue of A with magnitude equal to 1, if graph G has a spanning tree and $a_{ii} > 0$ for all i .

Definition 2.15. *A minor of matrix $A \in \mathbb{R}^{m \times n}$ is a the determinant of a $k \times k$ matrix which is resulted by eliminating $m - k$ rows and $n - k$ columns of A , and is denoted by $[A]_{\mathcal{I}, \mathcal{J}}$ where $\mathcal{I} \subset \{1, 2, \dots, m\}$ and $\mathcal{J} \subset \{1, 2, \dots, n\}$ are sets of remaining rows and columns. $[A]_{\mathcal{I}, \mathcal{J}}$ is called a principal minor of matrix A if sets \mathcal{I} and \mathcal{J} are equal [130].*

Definition 2.16. *A leading principal minor of a matrix A , is a principal minor of A associated to a square upper-left sub-matrix of A .*

Definition 2.17. *Square matrix $A \in \mathbb{R}^{n \times n}$ is called an Z-matrix if all its off-diagonal elements are nonpositive.*

Definition 2.18. *Square matrix $M \in \mathbb{R}^{n \times n}$ is called an M-matrix if it is a Z-matrix and all its principal minors are non-negative and it is a non-singular M-matrix if all its principal minors are positive.*

Theorem 2.4. *Consider Z-matrix $M \in \mathbb{R}^{n \times n}$, following statements are equivalent [130]:*

- M is a non-singular M -matrix.
- All leading principal minors of M are positive.
- Real part of all eigenvalues of M are positive.
- Matrix M is invertible and all elements of M^{-1} are nonnegative.
- There exist vectors v and w with all positive element such that all elements of vectors Mv and $M^T w$ be positive.
- There is a diagonal positive definite matrix S such that $MS + SM^T$ is positive definite.

Theorem 2.5. Consider Z -matrix $M \in \mathfrak{R}^{n \times n}$, following statements are equivalent [130]:

- M is a singular M -matrix.
- All leading principal minors of M are nonnegative.
- Real part of all eigenvalues of M are nonnegative.
- For any diagonal positive definite matrix B , matrix $B + M$ is invertible and all elements of $(B + M)^{-1}$ are nonnegative.
- There exist vectors v and w with all positive element such that all elements of vectors Mv and $M^T w$ be nonnegative.
- There is a diagonal matrix S , which has all nonnegative elements, such that $MS + SM^T$ is positive semidefinite.

Theorem 2.6. Irreducible M -matrix $A \in \mathfrak{R}^{n \times n}$ satisfies following statements [130]:

- $\text{rank}(A) = n - 1$
- There exist a vector with all positive elements v such that $Av = 0$

Theorem 2.7. For any singular but irreducible M -matrix A and positive constant ϵ matrix $A - \text{diag}\{0, 0, \dots, \epsilon\}$ is a nonsingular M -matrix [132].

Corollary 2.1. *Consider singular and irreducible M-matrix $A \in \mathbb{R}^{n \times n}$ and nonnegative constants ϵ_i , for $i = 1, \dots, n$, where at least one of $\epsilon_i > 0$, then matrix $A - \text{diag}\{\epsilon_1, \epsilon_2, \dots, \epsilon_n\}$ is a nonsingular M-matrix [132].*

2.3 Cooperative Control and Consensus Achievement

In this section the correlation between algebraic graph theory and cooperative control of multi-agent is presented. To introduce multi-agent system we first need to define agents.

Definition 2.19. *An agent is a dynamical system with a state vector which evolves through time based on its past value and a control input vector. Here, the state of the agents is not dependent on any other agent, but control input is a function of the agent and some other agents state vectors.*

Since the state vector of agents are decoupled and the interaction between agents are through their control inputs, basically without a common control strategy and information exchange among different agents, they are completely independent systems.

Definition 2.20. *A multi-agent system is a set of agents that are exchange information and collaborate to each other based on a common control strategy to achieve a goal as a single entity which cannot be done by each agent alone.*

The connection between multi-agent systems and algebraic graph theory is their necessity to exchange information which can be best modeled by an information flow graph \mathcal{G} . Let label each agent with a number and let each node in graph \mathcal{G} represents an agent and each edge from node v_i to node v_j shows information flow from agent i to agent j . Note that the exchanged information can be whole state vector of agents (agent state) or a function of that (agent output).

Definition 2.21. *A multi-agent system is called homogenous multi-agent systems if the dynamics and the exchanged information of all agents are the same, otherwise it is called heterogeneous multi-agent system.*

Definition 2.22. *It is said that a multi-agent system follows a distributed control strategy with topology \mathcal{G} if the control input of each agent be a function of its own state (or output) and states (or outputs) of other agents that are in in-neighbor set of the agent in the graph.*

In this thesis, distributed control strategy some times is also called cooperative control or multi-agent controller. It is also worth noting, the multi-agent systems and notations here are mainly used in control systems community [133, 134] and is different from those used by computer science community [135]. In this sense the main concern of cooperative control strategies is to solve consensus problem.

Definition 2.23. *Consensus problem in multi-agent system is to find a distributed control strategy that cause all agents to agree on a common value for a variable of interest. This value is usually called the consensus value and can be state, output, etc of agents.*

2.4 Kronecker Product and Its Properties

The Kronecker product of two matrices, namely $A = [a_{ij}] \in \mathfrak{R}^{m \times n}$ and $B = [b_{ij}] \in \mathfrak{R}^{p \times q}$ is a $mp \times nq$ matrix, that is denoted by $A \otimes B$ and is defined as

follows [136]:

$$A \otimes B = \begin{bmatrix} a_{11}b_{11} & a_{11}b_{12} & \cdots & a_{11}b_{1q} & \cdots & \cdots & a_{1n}b_{11} & a_{1n}b_{12} & \cdots & a_{1n}b_{1q} \\ a_{11}b_{21} & a_{11}b_{22} & \cdots & a_{11}b_{2q} & \cdots & \cdots & a_{1n}b_{21} & a_{1n}b_{22} & \cdots & a_{1n}b_{2q} \\ \vdots & \vdots & \ddots & \vdots & & & \vdots & \vdots & \ddots & \vdots \\ a_{11}b_{p1} & a_{11}b_{p2} & \cdots & a_{11}b_{pq} & \cdots & \cdots & a_{1n}b_{p1} & a_{1n}b_{p2} & \cdots & a_{1n}b_{pq} \\ a_{21}b_{11} & a_{21}b_{12} & \cdots & a_{21}b_{1q} & \cdots & \cdots & a_{2n}b_{11} & a_{2n}b_{12} & \cdots & a_{2n}b_{1q} \\ a_{21}b_{21} & a_{21}b_{22} & \cdots & a_{21}b_{2q} & \cdots & \cdots & a_{2n}b_{21} & a_{2n}b_{22} & \cdots & a_{2n}b_{2q} \\ \vdots & \vdots & \ddots & \vdots & & & \vdots & \vdots & \ddots & \vdots \\ a_{21}b_{p1} & a_{21}b_{p2} & \cdots & a_{21}b_{pq} & \cdots & \cdots & a_{2n}b_{p1} & a_{2n}b_{p2} & \cdots & a_{2n}b_{pq} \\ \vdots & \vdots & \ddots & \vdots & \ddots & & \vdots & \vdots & \ddots & \vdots \\ \vdots & \vdots & \ddots & \vdots & & \ddots & \vdots & \vdots & \ddots & \vdots \\ a_{m1}b_{11} & a_{m1}b_{12} & \cdots & a_{m1}b_{1q} & \cdots & \cdots & a_{mn}b_{11} & a_{mn}b_{12} & \cdots & a_{mn}b_{1q} \\ a_{m1}b_{21} & a_{m1}b_{22} & \cdots & a_{m1}b_{2q} & \cdots & \cdots & a_{mn}b_{21} & a_{mn}b_{22} & \cdots & a_{mn}b_{2q} \\ \vdots & \vdots & \ddots & \vdots & & & \vdots & \vdots & \ddots & \vdots \\ a_{m1}b_{p1} & a_{m1}b_{p2} & \cdots & a_{m1}b_{pq} & \cdots & \cdots & a_{mn}b_{p1} & a_{mn}b_{p2} & \cdots & a_{mn}b_{pq} \end{bmatrix}$$

Some times for simplicity following notation is used to define Kronecker product of two matrices:

$$A \otimes B = \begin{bmatrix} a_{11}B & a_{12}B & \cdots & a_{1n}B \\ a_{21}B & a_{22}B & \cdots & a_{2n}B \\ \vdots & \vdots & \ddots & \vdots \\ a_{m1}B & a_{m2}B & \cdots & a_{mn}B \end{bmatrix} \quad (2.3)$$

The Kronecker product has some interesting properties that are used in this thesis, including [120]:

$$A \otimes (B + C) = A \otimes B + A \otimes C \quad (2.4)$$

$$(A + B) \otimes C = A \otimes C + B \otimes C$$

$$(\alpha A) \otimes B = A \otimes (\alpha B) = \alpha A \otimes B \quad (2.5)$$

$$(A \otimes B) \otimes C = A \otimes (B \otimes C) \quad (2.6)$$

$$(A \otimes B)^T = A^T \otimes B^T \quad (2.7)$$

$$(A \otimes B) \otimes (C \otimes D) = AC \otimes BD \quad (2.8)$$

And also if A and B are (semi-)positive definite matrices, then $A \otimes B$ is a (semi-)positive definite matrix.

2.5 Lyapunov Stability Analysis

In this section essential definitions and theorems on Lyapunov stability analysis method, that will be used frequently in the remainder of the thesis, are provided from [137].

Definition 2.24. *Consider following autonomous system*

$$\dot{x} = f(x) \quad (2.9)$$

where $x \in \mathbb{R}^n$ is the state vector of the systems and $f : D \rightarrow \mathbb{R}^n$ is locally Lipschitz map from domain $D \subset \mathbb{R}^n$ into \mathbb{R}^n . $\bar{x} \in D$ is called an equilibrium point of autonomous system (2.9), if $f(\bar{x}) = 0$.

In this section it is assumed that $f(0) = 0$ and therefore, origin is an equilibrium point of above autonomous system.

Definition 2.25. *The origin is called a stable equilibrium point of system (2.9), if for any $\epsilon > 0$, there exist a $\delta = \delta(\epsilon) > 0$ such that*

$$\|x(0)\| < \delta \Rightarrow \|x(t)\| < \epsilon, \forall t \geq 0$$

Definition 2.26. *An equilibrium point is called unstable if it is not stable.*

Definition 2.27. *An equilibrium point is said to be asymptotically stable if it is stable and there exist a $\delta > 0$ such that*

$$\|x(0)\| < \delta \Rightarrow \lim_{t \rightarrow \infty} x(t) = 0$$

Theorem 2.8. *Origin is a stable equilibrium point of autonomous system (2.9) if there exist a continuously differentiable function $V : D \rightarrow \mathbb{R}$, which is called Lyapunov function, such that*

- $V(0) = 0$ and $V(x) > 0$ for all $x \in D - \{0\}$,
- $\dot{V}(x) \leq 0$ for all $x \in D$.

Theorem 2.9. *Origin is an asymptotically stable equilibrium point of autonomous system (2.9) if there exist a Lyapunov function $V(x)$, such that*

- $V(0) = 0$ and $V(x) > 0$ for all $x \in D - \{0\}$,
- $\dot{V}(x) < 0$ for all $x \in D - \{0\}$.

Theorem 2.10. *Origin is an asymptotically stable equilibrium point of linear system*

$$\dot{x} = Ax$$

if and only if real part of all eigenvalues of matrix A are negative. In that case matrix A is said to be a Hurwitz matrix.

Theorem 2.11. *Matrix A is a Hurwitz matrix if and only if for any symmetric positive definite matrix Q there exist a symmetric positive definite matrix P that satisfies the following equation, which is called Lyapunov equation.*

$$PA + A^T P = -Q$$

Definition 2.28. *Consider continuous function $\alpha : [0, a) \rightarrow [0, \infty)$. It is called a class \mathcal{K} function if it is strictly increasing function and $\alpha(0) = 0$. If $a = \infty$ and $\lim_{r \rightarrow \infty} \alpha(r) = \infty$ then function α is said to belong to class \mathcal{K}_∞ functions.*

Definition 2.29. *Continuous function $\beta : [0, a) \times [0, \infty) \rightarrow [0, \infty)$ is called a class \mathcal{KL} function if*

- for each $s \geq 0$, function $\beta(r, s)$ is a class \mathcal{K} function with respect to r ,
- for each $r \in [0, a)$ function $\beta(r, s)$ is decreasing with respect to s , and $\lim_{s \rightarrow \infty} \beta(r, s) = 0$

Definition 2.30. *Origin is an equilibrium point of nonautonomous system (2.10) at $t = 0$*

$$\dot{x} = f(t, x) \tag{2.10}$$

if, for any $t \geq 0$, $f(t, 0) = 0$, where function $f : [0, \infty) \times D \rightarrow \mathbb{R}^n$ is a piecewise continuous in t and locally Lipschitz in x on $[0, \infty) \times D$, $D \in \mathbb{R}^n$, and $0 \in D$.

Definition 2.31. Consider equilibrium point of nonautonomous systems (2.10) at $x = 0$. it is called a

- stable equilibrium point of the system if, for each $\epsilon > 0$ there exist a $t_0 \geq 0$ and $\delta = \delta(\epsilon, t_0)$ such that

$$\|x(t_0)\| < \delta \Rightarrow \|x(t)\| < \epsilon, \quad \forall t \geq t_0$$

- unstable equilibrium point of the system if it is not stable,
- uniformly stable equilibrium point of the system if for any $t_0 \geq 0$ it is stable,
- asymptotically stable equilibrium point of the system if it is stable and there exist $c = c(t_0) > 0$, such that for all $\|x(t_0)\| < c$

$$\lim_{t \rightarrow \infty} \|x(t)\| = 0$$

- uniformly asymptotically stable equilibrium point of the system if it is uniformly stable and there exist $c > 0$, independent of t_0 , such that for all $\|x(t_0)\| < c$ and for any $\eta > 0$

$$\exists T = T(\eta) > 0 \quad \text{s.t.} \quad \|x(t)\| < \eta, \quad \forall t \geq t_0 + T(\eta)$$

- globally uniformly asymptotically stable equilibrium point of the system if it is uniformly stable, $\delta(\epsilon)$ can be chosen such that

$$\lim_{\epsilon \rightarrow \infty} \delta(\epsilon) = \infty$$

, and for any $c, \eta > 0$

$$\exists T = T(c, \eta) > 0 \quad \text{s.t.} \quad \|x(t)\| < \eta, \quad \forall t \geq t_0 + T(c, \eta)$$

Throughout this thesis whenever origin is a uniformly stable or uniformly asymptotically stable equilibrium point of a nonautonomous system for simplicity we said that system is stable or asymptotically stable.

Theorem 2.12. *Consider nonautonomous systems (2.10). Its equilibrium at origin is*

- *uniformly stable if and only if there exist a class \mathcal{K} function α and $c > 0$ such that for any $t_0 \geq 0$ and $\|x(t_0)\| < c$*

$$\|x(t)\| \leq \alpha(\|x(t_0)\|), \quad \forall t \geq t_0$$

- *uniformly asymptotically stable if and only if there exist a class \mathcal{KL} function β and $c > 0$ such that for any $t_0 \geq 0$ and $\|x(t_0)\| < c$*

$$\|x(t)\| \leq \beta(\|x(t_0)\|, t - t_0), \quad \forall t \geq t_0$$

- *globally uniformly asymptotically stable if and only if for any $x(t_0)$ the above inequality holds.*

A special case of asymptotic stability that is used in this thesis is exponential stability concept.

Definition 2.32. *Origin is an exponentially stable equilibrium of nonautonomous system (2.10) if there exist c, k , and $\lambda > 0$ such that for all $\|x(t_0)\| < c$ following inequality holds:*

$$\|x(t)\| \leq k \|x(t_0)\| e^{-\lambda(t-t_0)}$$

Furthermore, if it holds for any $x(t_0)$, the origin is globally exponentially stable.

Theorem 2.13. *Consider nonautonomous system (2.10), its equilibrium point at origin is*

- *uniformly stable if there exist a continuously differentiable function $V : [0, \infty) \times D \rightarrow \mathfrak{R}$, which is called a Lyapunov function, such that for any $t \geq 0$ and any $x \in D$ the following inequalities are satisfied:*

$$W_1(x) \leq V(t, x) \leq W_2(x) \tag{2.11}$$

$$\frac{\partial V}{\partial t} + \frac{\partial V}{\partial x} f(t, x) \leq 0 \quad (2.12)$$

where $W_1(x)$ and $W_2(x)$ are continuous positive definite function on D .

- uniformly asymptotically stable if there exist a Lyapunov function that satisfies above mentioned assumptions, inequality (2.11) holds, and there exist a continuous positive definite function $W_3(x)$ on D such that

$$\frac{\partial V}{\partial t} + \frac{\partial V}{\partial x} f(t, x) \leq -W_3(x)$$

- exponentially stable if there exist a Lyapunov function that satisfies above mentioned assumptions, and positive constants k_1, k_2, k_3 and a such that the following inequalities hold

$$k_1 \|x\|^a \leq V(t, x) \leq k_2 \|x\|^a$$

$$\frac{\partial V}{\partial t} + \frac{\partial V}{\partial x} f(t, x) \leq k_3 \|x\|^a$$

2.6 Summary

This chapter summarized some basic definitions and theorem that are required in remainder of thesis. First, some useful definitions and properties of graphs and algebraic graph theory was presented. It was followed by matrix analysis and cooperative control of multi-agents systems, and finally stability analysis methodology was presented.

In the next chapter we study the consensus problems with H_∞ and weighted H_∞ bounds for a homogeneous team of LTI multi-agent systems with a switching topology and directed communication network graphs.

Chapter 3

H_∞ Consensus Achievement of Multi-Agent Systems with Directed and Switching Topology Networks

In this chapter the consensus problem with H_∞ and weighted H_∞ bounds for a homogeneous team of LTI multi-agent systems with a switching topology and directed communication network graph are studied. Sufficient conditions to design distributed controllers are proposed based on state feedback corresponding to bounded L_2 gain and RMS bounded disturbances. Based on the solution of an algebraic Riccati equation that circumvents the need to solve Linear Matrix Inequalities (LMIs), a design methodology is proposed to properly select the controller gains. The stability properties of the proposed controllers are then investigated based on Lyapunov stability analysis. The effectiveness of our proposed consensus algorithms are then illustrated by performing simulations for diving consensus of a team of Unmanned Underwater Vehicles (UUVs).

Towards this end, based on two quantitative measures of the Laplacian matrices, a transformation is introduced and a novel method is proposed to guarantee the H_∞ performance of the overall system in presence of bounded RMS disturbance signals. In our approach, a piecewise quadratic Lyapunov

function is used which is determined by solving a set of algebraic Lyapunov equations and an Algebraic Riccati Equation (ARE).

The main contributions of our work in the context of the mentioned in the literature are as follows: (a) the communication network topology is directed and can switch arbitrarily, (b) the proposed algorithms can solve the H_∞ and the weighted H_∞ consensus problems for disturbance signals that have bounded RMS and are not limited to only L_2 signals, (c) the existence of the consensus algorithms are guaranteed if an LTI system can be state feedback stabilized with a bounded L_2 norm gain, and finally (d) there is no need to solve any set of LMIs and instead the controllers can be designed by solving an ARE. It is worth noting that the time complexity of solving an LMI is $O(n^2p^4)$ [115], where n is the number of agents in the team and p is the number of states of each agent, therefore it is not always computationally feasible to design a consensus algorithm for teams with large number of agents or agents with large number of states by using these techniques. However, ARE can be solved with time complexity of $O(p^4)$ [116] and the existence of a solution can be guaranteed.

The remainder of the chapter is organized as follows. In Section 3.1, brief preliminaries on algebraic graph theory and several lemmas that we have developed for this work are presented. The problem statement is provided in Section 3.1 and the consensus algorithm design methodology is proposed in Section 3.3. Section 3.4 provides numerical simulations that support our proposed theoretical results, and finally Section 3.5 concludes the chapter.

3.1 Background and Preliminary Results

In this section, first we present some basic concepts and notations of algebraic graph theory and switching systems which will be used for stability analysis of our proposed consensus algorithms. More information on algebraic graph theory is available in [70]. We then present some relevant preliminary results of ours that will be used in development of the main result of this chapter in Section 3.1.

Definition 3.1. *The information flow digraph (directed graph) $\mathcal{G}(t)$ is defined*

as set $\mathcal{G}(t) = \{\mathcal{V}, \mathcal{E}_{\mathcal{G}}(t)\}$ with the node set $\mathcal{V} = \{1, 2, \dots, n\}$ and the edge set $\mathcal{E}_{\mathcal{G}}(t) = \{(i, j) | i, j \in \mathcal{V}\}$.

Here, any $i \in \mathcal{V}$ is called a node of graph $\mathcal{G}(t)$ and any 2-tuple (i, j) , where i and j are nodes of graph $\mathcal{G}(t)$, is called an edge of the graph between nodes i and j if $(i, j) \in \mathcal{E}_{\mathcal{G}}(t)$.

Definition 3.2. The digraph $\mathcal{G}(t)$ is called strongly connected if and only if for any there is a path between any two distinct nodes of the graph.

Definition 3.3. The edge between nodes i and j is undirected if and only if for any $i, j \in \mathcal{V}$ where $i \neq j$ and $(i, j) \in \mathcal{E}_{\mathcal{G}}(t)$ then $(j, i) \in \mathcal{E}_{\mathcal{G}}(t)$, otherwise it is called a directed edge.

Definition 3.4. The sequence of 2-tuples $(i, k_1), (k_1, k_2), \dots, (k_p, j)$, where $i, k_1, k_2, \dots, k_p, j$ are nodes of graph $\mathcal{G}(t)$ is called a path from node i to node j if all of 2-tuples in the sequence are edges of the graph.

Definition 3.5. The digraph $\mathcal{G}(t)$ is an undirected graph if and only if all its edges are undirected.

Assumption 3.1. Throughout this chapter, it is assumed that there is no edge from a node to itself.

Definition 3.6. The communicating/sensing matrix of graph $\mathcal{G}(t)$, which is denoted by $\mathcal{S}(\mathcal{G}(t))$, is defined as $\mathcal{S}(\mathcal{G}(t)) = [s_{ij}(t)] \in \mathbb{R}^{n \times n}$, where:

$$s_{ij}(t) = \begin{cases} 1 & i \neq j \text{ and } (i, j) \in \mathcal{E}_{\mathcal{G}}(t) \\ 0 & i = j \text{ or } (i, j) \notin \mathcal{E}_{\mathcal{G}}(t) \end{cases}$$

Definition 3.7. The set of neighbors of the node i of graph $\mathcal{G}(t)$ is denoted by $\mathcal{N}_i(\mathcal{G}(t))$ and is defined as follows

$$\mathcal{N}_i(\mathcal{G}(t)) = \{j | (i, j) \in \mathcal{E}_{\mathcal{G}}(t)\}$$

Definition 3.8. The Laplacian matrix of graph $\mathcal{G}(t)$ is denoted by $\mathcal{L}(\mathcal{G}(t))$

and is defined as $\mathcal{L}(\mathcal{G}(t)) = [\ell_{ij}(t)] \in \mathfrak{R}^{n \times n}$, where

$$\ell_{ij}(t) = \begin{cases} \kappa_i(t) & i = j \\ -\frac{\kappa_i(t)}{|\mathcal{N}_i(\mathcal{G}(t))|} & i \neq j \text{ and } j \in \mathcal{N}_i(\mathcal{G}(t)) \\ 0 & i \neq j \text{ and } j \notin \mathcal{N}_i(\mathcal{G}(t)) \end{cases} \quad (3.1)$$

and $|\mathcal{N}_i(\mathcal{G}(t))|$ is the cardinality of $\mathcal{N}_i(\mathcal{G}(t))$ and $\kappa_i(t)$ is the degree of the i^{th} node.

Remark 3.1. In this chapter, we set $\kappa_i(t) = |\mathcal{N}_i(\mathcal{G}(t))|$.

Lemma 3.1. Since the row sum of the matrix $\mathcal{L}(\mathcal{G}(t))$ is zero, it has an eigenvalue at $\lambda_1 = 0$ and its associated right eigenvector is $\mathbf{1} = [1, 1, \dots, 1]^T \in \mathfrak{R}^n$.

Let us define the set Γ as the collection of all digraphs with the node set \mathcal{V} . Since the number of all possible digraphs with the node set \mathcal{V} is $n(n-1)$, therefore let us define the set

$$\mathcal{I}_{\mathcal{N}} = \{1, 2, \dots, n(n-1)\}$$

and the injective mapping function

$$\mathcal{F}(i) : \mathcal{I}_{\mathcal{N}} \rightarrow \Gamma$$

Definition 3.9. The piecewise constant switching signal $\sigma(t)$ is defined as the following function

$$\sigma(t) : [0, \infty) \rightarrow \mathcal{I}_{\sigma},$$

where the set $\mathcal{I}_{\sigma} \subset \mathcal{I}_{\mathcal{N}}$.

Definition 3.10. Throughout this thesis, $\mathcal{G}_{\sigma(t)}$ is defined as $\mathcal{G}_{\sigma(t)} = \mathcal{F}(\sigma(t))$, where $\sigma(t)$ is a piecewise constant switching signal.

Remark 3.2. In the remainder of the chapter and for brevity, \mathcal{G}_{σ} denotes $\mathcal{G}_{\sigma(t)}$ and L_{σ} denotes $\mathcal{L}(\mathcal{G}_{\sigma})$.

Definition 3.11. The instant $\mathbf{t} \geq 0$ is a switching instant of piecewise constant switching signal $\sigma(t)$ if it is not continuous at $t = \mathbf{t}$.

Definition 3.12. The dwell times τ_1, τ_2, \dots of piecewise constant switching signal $\sigma(t)$ are defined as $\tau_k = t_k - t_{k-1}$ where $t_0 = 0 < t_1 < t_2 < \dots$ denote the switching instants of $\sigma(t)$. The dwell times are periods of time when the multi-agent team uses the information flow graph.

Definition 3.13. Function $N_\sigma(T_1, T_2)$ indicates the number of switching instances of $\sigma(t)$ in the interval (T_1, T_2) and function $N_\sigma(t)$ is defined as $N_\sigma(t) = N_\sigma(0, t)$.

Definition 3.14. [138] Consider piecewise constant switching signal $\sigma(t)$, $\tau_a > 0$ and $N_0 \geq 0$. If for any $T_2 > T_1 \geq 0$, the following inequality holds

$$N_\sigma(T_1, T_2) \leq N_0 + \frac{T_2 - T_1}{\tau_a}$$

then τ_a is called the average dwell time of switching signal $\sigma(t)$. In this thesis we set $N_0 = 0$.

Below, we introduce and present several of our lemmas that will be used in the remainder of the chapter for stability analysis of our proposed consensus algorithms.

Lemma 3.2. Given any vectors $\mathbf{x}_1, \dots, \mathbf{x}_n \in \mathbb{R}^p$ and corresponding to the Laplacian matrix L defined in (3.1) the following equation holds:

$$\sum_{j=1}^n \ell_{ij} \mathbf{x}_j - \sum_{j=1}^n \ell_{nj} \mathbf{x}_j = \sum_{j=1}^{n-1} h_{ij} (\mathbf{x}_j - \mathbf{x}_n) \quad (3.2)$$

where $h_{ij} = \ell_{ij} - \ell_{nj}$ and $i, j = 1, \dots, n-1$.

Proof. Knowing that for $i \in \mathcal{V}$ we have:

$$\sum_{j=1}^n \ell_{ij} = 0$$

one can conclude that:

$$\begin{aligned}
\sum_{j=1}^n \ell_{ij} \mathbf{x}_i - \sum_{j=1}^n \ell_{nj} \mathbf{x}_i &= \sum_{j=1}^{n-1} \ell_{ij} (\mathbf{x}_i - \mathbf{x}_n) + \mathbf{x}_n \sum_{j=1}^n \ell_{ij} - \sum_{j=1}^{n-1} \ell_{nj} (\mathbf{x}_i - \mathbf{x}_n) - \mathbf{x}_n \sum_{j=1}^n \ell_{nj} \\
&= \sum_{j=1}^{n-1} (\ell_{ij} - \ell_{nj}) (\mathbf{x}_i - \mathbf{x}_n)
\end{aligned}$$

■

Lemma 3.3. *Consider the matrix H which is defined as:*

$$H = \mathcal{H}(\mathcal{G}) = [h_{ij}] \in \mathfrak{R}^{(n-1) \times (n-1)},$$

where $h_{ij} = \ell_{ij} - \ell_{nj}$ as defined in Lemma 3.2. If the graph \mathcal{G} has a directed spanning tree, the real parts of all the eigenvalues of the matrix H are positive.

Proof. Knowing that L has zero row sums, 0 is an eigenvalue of L and since it is diagonally dominant and has non-negative diagonal elements, it follows from Greshgorin's disc theorem that all the non-negative eigenvalues of L have positive real parts. Furthermore, using Remark 1 in [15] and the fact that \mathcal{G} has a directed spanning tree, 0 is a simple eigenvalue [25]. Therefore L has $n - 1$ nonzero eigenvectors with positive real parts and to complete the proof, it is sufficient to show that all the nonzero eigenvalues of L are eigenvalues of H .

Consider $\lambda \in \mathbb{C}$ as a nonzero eigenvalue of L and the vector $y = [y_1, \dots, y_n]^T \in \mathbb{C}^n$ as its associated eigenvector. Let us define $y^* = [y_1 - y_n, \dots, y_{n-1} - y_n]^T \in \mathbb{C}^{n-1}$. Since λ is a nonzero eigenvalue, therefore $y^* \neq 0$. Consider $w = [w_1, \dots, w_{n-1}]^T \in \mathbb{C}^{n-1}$ and let $w = Hy^*$. We have to show that $w = \lambda y^*$,

that is

$$\begin{aligned}
w_i &= \sum_{j=1}^{n-1} h_{ij} y_j^* = \sum_{j=1}^{n-1} \ell_{ij} y_j^* - \sum_{j=1}^{n-1} \ell_{nj} y_j^* \\
&= \sum_{j=1}^{n-1} \ell_{ij} y_j - \sum_{j=1}^{n-1} \ell_{ij} y_n - \sum_{j=1}^{n-1} \ell_{nj} y_j + \sum_{j=1}^{n-1} \ell_{nj} y_n \\
&= \sum_{j=1}^n \ell_{ij} y_j - y_n \sum_{j=1}^n \ell_{ij} - \sum_{j=1}^n \ell_{nj} y_j + \ell_{nj} y_n \sum_{j=1}^n \ell_{nj} \\
&= \sum_{j=1}^n \ell_{ij} y_j - \sum_{j=1}^n \ell_{nj} y_j = \lambda y_i - \lambda y_n = \lambda y_i^*
\end{aligned}$$

This completes the proof of the lemma. ■

Lemma 3.4. *Consider the matrices $H_\sigma = \mathcal{H}(\mathcal{G}_\sigma)$ as defined in Lemma 3.3. If all the graphs \mathcal{G}_σ for all $\sigma \in \mathcal{I}_\sigma$ have directed spanning trees, then for any positive constant ϵ which satisfies the following inequality*

$$0 < \epsilon < 2 \min_{\sigma \in \mathcal{I}_\sigma} \{ \text{Re}(\lambda(H_\sigma)) \}, \quad (3.3)$$

there exist symmetric positive definite matrices $P_{H_\sigma}, Q_{H_\sigma} \in \mathfrak{R}^{n-1 \times n-1}$ such that

$$P_{H_\sigma} H_\sigma + H_\sigma^T P_{H_\sigma} - \epsilon P_{H_\sigma} = Q_{H_\sigma} > 0 \quad (3.4)$$

Proof. From Lemma 3.3, it follows that the real part of all the eigenvalues of H are positive. Let us select real constant ϵ such that satisfies the following inequality (3.3). Therefore, the real part of all the eigenvalues of the matrix $H_\sigma - \frac{1}{2}\epsilon I$ are positive and it concludes the lemma [137]. ■

Remark 3.3. *In an undirected graph the term $\text{Re}(\lambda_{\min}(H_\sigma))$ is equal to and in a directed graph is larger than or equal to the algebraic connectivity of the graph [125]. In other words, ϵ is a measure of the minimum connectivity of all the information flow graphs of the agents in the team and the smaller ϵ implies that the graphs are less connected.*

Lemma 3.5. *Consider a piecewise constant switching signal $\sigma(t)$ with an average dwell time τ_a . For any time $T > 0$, let us define $N = N_\sigma(T)$, $t_0 = 0$,*

$t_{N+1} = T$ and let $0 < t_1 < t_2 < \dots < t_N$ denote the switching instances of $\sigma(t)$. Consider a set of continuous, differentiable and positive definite functions $\{V_i(x) | i \in \mathcal{I}_\sigma\}$, and assume there exists $\mu > 1$ such that for any $i, j \in \mathcal{I}_\sigma$

$$V_i(x) \leq \mu V_j(x)$$

Let the function $\xi(t)$ be defined as follows

$$\xi(t) = e^{\delta_k(t-t_k)}$$

where $k = N_\sigma(t)$ and $\delta_k = \frac{\ln(\mu)}{t_{k+1}-t_k}$. Given the function $V_i(x)$, let us now define a piecewise continuous function $V_\sigma = V_{\sigma(t)}(x)$. We can guarantee that:

part a) The following inequality holds for any $\bar{\delta} \geq \frac{\ln(\mu)}{\tau_a}$:

$$\frac{1}{T} \int_0^T \xi(t) \left(\dot{V}_\sigma + \bar{\delta} V_\sigma \right) dt + \frac{1}{T} V_{\sigma(0)}(x(0)) \geq 0$$

part b) The following inequality holds:

$$\frac{1}{T} \int_0^T \mu^{-N_\sigma(t)} \dot{V}_\sigma(x, t) dt + \frac{1}{T} V_{\sigma(0)}(x(0)) \geq 0$$

Proof. **part a)** From the definition of $\xi(t)$ it is easy to verify that

$$1 \leq \xi(t) < \mu$$

and

$$\lim_{t \rightarrow t_{k+1}^-} \xi(t) = \mu$$

for any $k = 0, \dots, N$. Let us define

$$\frac{1}{T} \int_{t_k}^{t_{k+1}^-} \xi(t) \left(\dot{V}_\sigma + \bar{\delta} V_\sigma \right) dt = \lim_{\tau \rightarrow t_{k+1}^-} \frac{1}{T} \int_{t_k}^{\tau} \xi(t) \left(\dot{V}_\sigma + \bar{\delta} V_\sigma \right) dt$$

Since for any time $t \in [t_k, t_{k+1})$, $k = 1, \dots, N$, the switching signal is $\sigma(t) = \sigma(t_k)$, we have $V_\sigma(\cdot) = V_{\sigma(t_k)}(\cdot)$. In addition, in the time interval $[t_k, t_{k+1}]$ the topology of the information flow graph changes once. By considering that

$N_0 = 0$ and using Definition 3.14 one can conclude that $\tau_a \leq t_{k+1} - t_k$. Given that $\mu > 1$, we have

$$\bar{\delta} \geq \frac{\ln(\mu)}{\tau_a} \geq \frac{\ln(\mu)}{t_{k+1} - t_k} = \delta_k.$$

Therefore, by replacing $\xi(t)$ from its definition into the above equation we obtain:

$$\begin{aligned} & \frac{1}{T} \int_{t_k}^{t_{k+1}^-} \xi(t) \left(\dot{V}_\sigma + \bar{\delta} V_\sigma \right) dt \\ &= \frac{1}{T} \int_{t_k}^{t_{k+1}^-} \xi(t) \left(\dot{V}_{\sigma(t_k)} + \delta_k V_{\sigma(t_k)} \right) dt + \frac{1}{T} \int_{t_k}^{t_{k+1}^-} \xi(t) (\bar{\delta} - \delta_k) V_{\sigma(t_k)} dt \\ &\geq \frac{1}{T} \int_{t_k}^{t_{k+1}^-} e^{\delta_k(t-t_k)} \left(\dot{V}_{\sigma(t_k)} + \delta_k V_{\sigma(t_k)} \right) dt \\ &= \frac{1}{T} e^{-\delta_k t_k} \int_{t_k}^{t_{k+1}^-} \frac{d}{dt} \left(e^{\delta_k t} V_{\sigma(t_k)} \right) dt \\ &= \lim_{\tau \rightarrow t_{k+1}^-} e^{\delta_k(t-t_k)} \frac{1}{T} V_{\sigma(t_k)}(x(t)) \Big|_{t_k}^\tau \\ &= \frac{1}{T} \left(\mu V_{\sigma(t_k)}(x(t_{k+1})) - V_{\sigma(t_k)}(x(t_k)) \right) \end{aligned} \tag{3.5}$$

Now, by using the above inequality, one obtains:

$$\begin{aligned} & \frac{1}{T} \int_0^T \xi(t) \left(\dot{V}_\sigma + \bar{\delta} V_\sigma \right) dt \\ &= \frac{1}{T} \sum_{k=0}^N \int_{t_k}^{t_{k+1}^-} \xi(t) \left(\dot{V}_\sigma + \bar{\delta} V_\sigma \right) dt \\ &\geq \frac{1}{T} \sum_{k=0}^N \left(\mu V_{\sigma(t_k)}(x(t_{k+1})) - V_{\sigma(t_k)}(x(t_k)) \right) \\ &= -\frac{1}{T} V_{\sigma(t_0)}(x(t_0)) + \frac{1}{T} \sum_{k=1}^N \left(\mu V_{\sigma(t_{k-1})}(x(t_k)) - V_{\sigma(t_k)}(x(t_k)) \right) \\ &\quad + \mu \frac{1}{T} V_{\sigma(t_N)}(x(t_{N+1})) \\ &\geq \frac{1}{T} \left(\mu V_{\sigma(t_N)}(x(T)) - V_{\sigma(0)}(x(0)) \right) \end{aligned}$$

Since $V_{\sigma(t_N)}(x(T)) \geq 0$, this concludes the proof of part a).

part b) For any $k = 0, \dots, N$, let us define

$$\frac{1}{T} \int_{t_k}^{t_{k+1}^-} \mu^{-N_\sigma(t)} \dot{V}_\sigma dt = \lim_{\tau \rightarrow t_{k+1}^-} \frac{1}{T} \int_{t_k}^{\tau} \mu^{-N_\sigma(t)} \dot{V}_\sigma dt$$

We have:

$$\begin{aligned} & \frac{1}{T} \int_0^T \mu^{-N_\sigma(t)} \dot{V}_\sigma dt \\ &= \frac{1}{T} \sum_{k=0}^N \int_{t_k}^{t_{k+1}^-} \mu^{-k} \dot{V}_\sigma dt \\ &= \frac{1}{T} \sum_{k=0}^N \mu^{-k} (V_{\sigma(t_k)}(x(t_{k+1})) - V_{\sigma(t_k)}(x(t_k))) \\ &\geq \frac{1}{T} \mu^{-(N+1)} V_{\sigma(t_N)}(x(T)) - \frac{1}{T} V_{\sigma(0)}(x(0)) \end{aligned}$$

Since $V_{\sigma(t_N)}(x(T)) \geq 0$, this concludes the proof of part b). ■

Lemma 3.6. Consider a set of vectors $\omega_1, \dots, \omega_n \in \mathfrak{R}^a$, then the following inequality holds:

$$\sum_{i=1}^{n-1} \|\omega_i - \omega_n\|^2 \leq n \sum_{i=1}^n \|\omega_i\|^2$$

Proof. It is straightforward to see that we have

$$-\omega_i^T \omega_n - \omega_n^T \omega_i \leq (n-1) \omega_i^T \omega_i + \frac{1}{n-1} \omega_n^T \omega_n \quad (3.6)$$

By adding $\omega_i^T \omega_i + \omega_n^T \omega_n$ to both sides of the inequality (3.6), one obtains:

$$\|\omega_i - \omega_n\|^2 \leq n \omega_i^T \omega_i + \frac{n}{n-1} \omega_n^T \omega_n$$

Therefore, we have:

$$\sum_{i=1}^{n-1} \|\omega_i - \omega_n\|^2 \leq n \sum_{i=1}^{n-1} \|\omega_i\|^2 + n \|\omega_n\|^2$$

which concludes the proof of the lemma. ■

Lemma 3.7. Consider a piecewise constant switching signal $\sigma(t)$ with an average dwell time τ_a a set of continuous, differentiable and positive definite

functions $\{V_i(x(t), t) | i \in \mathcal{I}_\sigma\}$, where $x(t) \in \mathbb{R}^p$ is the state of the following system

$$\dot{x}(t) = f(x(t), t) \quad (3.7)$$

Assume that the following conditions are satisfied

1. There exists real constant $\delta > 0$ such that for any $t > 0$ we have

$$\dot{V}_{\sigma(t)}(x(t), t) \leq -\delta V_{\sigma(t)}(x(t), t),$$

2. There exist real constants $\alpha_1 > 0$ and $\alpha_2 > 0$ such that for any $t > 0$ we have

$$\alpha_1 \|x(t)\|^2 \leq V_{\sigma(t)}(x(t), t) \leq \alpha_2 \|x(t)\|^2,$$

3. There exists real constant $\mu > 0$ such that for any $t_1 > 0$ and $t_2 > 0$ we have

$$V_{\sigma(t_1)}(x(t_1), t_1) \leq \mu V_{\sigma(t_2)}(x(t_2), t_2),$$

If the average dwell time $\tau_a \geq \frac{\ln(\mu)}{\delta}$, then system (3.7) is exponentially stable.

Proof. For any given $t > 0$, we let $N = N_\sigma(t)$, which is defined in Definition 3.13, $t_0 = 0$ and $0 < t_1 < t_2 < \dots < t_N$ represent the switching instants of $\sigma(t)$ over the interval $(0, t)$, as per Definition 3.12. During the time interval $[t_k, t_k + 1)$, where $0 \leq k \leq N$, the Lyapunov function V_σ is continuous. Therefore, for any $\zeta \in [t_k, t_k + 1)$, by using condition 1 one can conclude that

$$V_\sigma(x(\zeta), \zeta) \leq e^{-\delta(\zeta - t_k)} V_\sigma(x(t_k), t_k) \quad (3.8)$$

Now, let us define $V_{\sigma(t_k)}(t_{k+1}^-)$ as follows

$$V_{\sigma(t_k)}(x(t_{k+1}^-), t_{k+1}^-) = \lim_{t \rightarrow t_{k+1}^-} V_{\sigma(t_k)}(x(t), t)$$

Therefore, from condition 3 one can conclude that the following inequality holds for any $0 \leq k < N$

$$V_{\sigma(t_{k+1})}(x(t_{k+1}), t_{k+1}) \leq \mu V_{\sigma(t_k)}(x(t_{k+1}^-), t_{k+1}^-) \quad (3.9)$$

By using induction the following inequality is obtained from inequalities (3.8) and (3.9)

$$V_{\sigma(t)}(x(t), t) \leq \mu^N e^{-\delta t} V_{\sigma(0)}(x(0), 0) = e^{-\delta t + \ln(\mu)N} V_{\sigma(0)}(x(0), 0).$$

Now, from condition 2 we know that $\alpha_1 \|x(t)\|^2 \leq V_{\sigma(t)}(x(t), t)$ and $V_{\sigma(0)}(x(0), 0) \leq \alpha_2 \|x(0)\|^2$, one can conclude that the following inequality holds

$$\|x(t)\|^2 \leq \frac{\alpha_2}{\alpha_1} e^{-\delta T + \ln(\mu)N} \|x(0)\|^2 \quad (3.10)$$

To show the exponential stability of system (3.7), we need to show that there exist $M^*, m^* > 0$ such that for any $t > 0$, the following inequality holds [137]

$$\|x(t)\| \leq M^* e^{-m^* t} \|x(0)\|$$

From Definition 3.13 one can conclude that $N = N_{\sigma}(t) \leq \frac{T}{\tau_a}$. Therefore, by using the fact that $\tau_a > \frac{\ln(\mu)}{\delta}$, it can be concluded that there exists $\delta^* > 0$ such that for any $t > 0$ we have

$$\delta^* \leq \delta - \ln(\mu)N$$

Therefore, inequality (3.10) results in:

$$\|z(T)\| \leq \sqrt{\frac{\alpha_2}{\alpha_1}} e^{-\frac{1}{2}\delta^* T} \|z(0)\|$$

and this guarantees the exponential stability of the system (3.7) and concludes the proof of the lemma. ■

Now we are in a position to present the problem statement and main result of the chapter.

3.2 Problem Statement

Consider a team of n homogeneous agents modeled as

$$\dot{x}_i = Ax_i + Bu_i + B_{\omega}\omega_i \quad i \in \mathcal{V} \quad (3.11)$$

where $x_i \in \mathbb{R}^p$ is the state of the i^{th} agent, $A \in \mathbb{R}^{p \times p}$, $B \in \mathbb{R}^{p \times m}$, $B_\omega \in \mathbb{R}^{p \times q}$, $\omega_i \in \mathbb{R}^q$ is the external disturbance, $u_i \in \mathbb{R}^m$ is the control input to the i^{th} agent, and the matrix A is not Hurwitz (See Remark 3.5 below).

Assumption 3.2. *The quantity $RMS(\omega_i)$ corresponding to the disturbance ω_i that is defined below exists for all the agents and is finite, that is*

$$RMS(\omega_i) = \sqrt{\lim_{T \rightarrow \infty} \left(\frac{1}{T} \int_0^T \|\omega_i^2\| dt \right)} < \infty \quad i \in \mathcal{V}$$

Definition 3.15. *The control u_i is said to solve the consensus problem if*

$$z_i = x_i - x_n \rightarrow 0 \text{ as } t \rightarrow \infty, \forall i \in \{1, \dots, n-1\} \quad (3.12)$$

Remark 3.4. *It should be emphasized that z_i in the above definition will not be used subsequently in the consensus design and there is no restriction in specifically selecting and labeling the n^{th} agent as the reference state. In other words, z_i will only be used subsequently as a tool for analysis and as a metric representing the consensus error indication.*

Remark 3.5. *Note that the team reaches the trivial consensus solution $x_i = 0$ in case the matrix A is Hurwitz. In this chapter, it is assumed that at least one of the agent's eigenvalues is on the imaginary axis and the team could then achieve a non-trivial consensus solution. In multi-agent system applications such as teams of deep-space spacecraft, unmanned aerial vehicles, unmanned underwater vehicles and mobile robots, this assumption is valid in practice.*

Definition 3.16. *The control u_i solves the consensus problem with an H_∞ norm bound γ_ρ if i) The control u_i solves the consensus problem for $\omega_i \equiv 0$ for $i = 1, \dots, n$, and ii) If $z_i(0) = 0$ for $i = 1, \dots, n-1$, then for any $T > 0$*

$$\frac{1}{T} \sum_{i=1}^{n-1} \int_0^T \|z_i\|^2 dt < \gamma_\rho^2 \frac{1}{T} \sum_{i=1}^n \int_0^T \|\omega_i\|^2 dt \quad (3.13)$$

Definition 3.17. *The control u_i solves the consensus problem with a weighted H_∞ norm bound γ_ρ and rate α if*

- i) *The control u_i solves the consensus problem for $\omega_i \equiv 0$ for $i = 1, \dots, n$, and*

- *ii) If $z_i(0) = 0$ for $i = 1, \dots, n - 1$, then for any $T > 0$*

$$\frac{1}{T} \sum_{i=1}^{n-1} \int_0^T e^{-\alpha t} \|z_i\|^2 dt < \gamma_\rho^2 \frac{1}{T} \sum_{i=1}^n \int_0^T \|\omega_i\|^2 dt \quad (3.14)$$

Let us define the control signal u_i as

$$u_i = - \sum_{j \in \mathcal{N}_i} K(x_i - x_j) \quad (3.15)$$

where $K \in \mathfrak{R}^{m \times p}$ is the *relative state control gain* matrix that is to be selected to achieve the given design specifications.

Consider the piecewise constant switching signal $\sigma(t) : [0, \infty) \rightarrow \mathcal{I}_\sigma$ and the switching topology information flow digraph \mathcal{G}_σ . Let us define $H_\sigma = \mathcal{H}(\mathcal{G}_\sigma)$. Assume that $\forall t > 0$, the digraphs \mathcal{G}_σ have directed spanning trees. From Lemma 3.4, it follows that for any real positive constant ϵ ,

$$0 < \epsilon < 2 \min_{\sigma \in \mathcal{I}_\sigma} \{Re(\lambda(H_\sigma))\} \quad (3.16)$$

there exist symmetric positive definite matrices $P_{H_\sigma}, Q_{H_\sigma} \in \mathfrak{R}^{n-1 \times n-1}$ such that

$$P_{H_\sigma} H_\sigma + H_\sigma^T P_{H_\sigma} - \epsilon I = Q_{H_\sigma} > 0.$$

Let us now define β_1, β_2 and μ as follows

$$\begin{aligned} \beta_1 &= \min_{i \in \mathcal{I}_\sigma} \lambda_{\min}(P_{H_i}), \\ \beta_2 &= \max_{i \in \mathcal{I}_\sigma} \lambda_{\max}(P_{H_i}), \\ \mu &= \frac{\beta_2}{\beta_1} \end{aligned} \quad (3.17)$$

To summarize, above we have defined all the parameters and matrices that are associated with the multi-agent team and their fundamental properties will now be used in the next section where our proposed consensus algorithm is presented.

3.3 Main Result

In this section, a design procedure for the consensus strategy of a multi-agent team based on solution of an algebraic Riccati equation is proposed and the main result of the chapter is presented as a theorem.

Theorem 3.1. *Consider a team of n homogeneous agents where the dynamics of each agent is governed by (3.11), and let the pair (A, B) be stabilizable and consider a piecewise constant switching signal $\sigma(t)$ with an average dwell time τ_a . Assume all the graphs \mathcal{G}_σ have directed spanning trees for $\sigma \in \mathcal{I}_\sigma$ and let ϵ and μ be defined as in equations (3.16) and (3.17), respectively, and let γ_ρ be a positive constant. If there exists positive constant γ such that the following linear system is state feedback stabilizable with L_2 gain bounded by γ*

$$\dot{x}_i = Ax_i + Bu_i + B_\omega \omega_i, \quad x_i(0) = 0$$

implying that

$$\int_0^\infty \|x_i\|^2 dt < \gamma^2 \int_0^\infty \|\omega_i\|^2 dt$$

then there exist symmetric matrices $R_A > 0$ and $Q_A > I$ such that the following algebraic Riccati equation has a symmetric positive definite solution to P_A [139]:

$$P_A A + A^T P_A - P_A B R_A^{-1} B^T P_A + \gamma^{-2} P_A B_\omega B_\omega^T P_A = -Q_A$$

By selecting the relative state cooperative control gain K as:

$$K = \frac{1}{\epsilon} R_A^{-1} B^T P_A \quad (3.18)$$

then the distributed control law (3.15):

part a) solves the H_∞ consensus problem for system (3.11) with a bound

$$\gamma_\rho = \gamma \sqrt{\frac{n\mu^2}{1 - k_\delta}}$$

for $\tau_a > \frac{\ln(\mu)}{k_\delta \delta}$, where $0 < k_\delta < 1$ and $\delta = \frac{\lambda_{\min}(Q_A)}{\lambda_{\max}(P_A)}$, and

part b) solves the weighted H_∞ consensus problem for system (3.11) with a

bound $\gamma_\rho = \gamma\sqrt{n\mu}$ and rate $\alpha = \frac{\ln(\mu)}{\tau_a}$ for $\tau_a > \frac{\ln(\mu)}{\delta}$, where $\delta = \frac{\lambda_{\min}(Q_A)}{\lambda_{\max}(P_A)}$.

Proof. Let us define the augmented team state vector as $\mathbf{x} = [x_1^T, x_2^T, \dots, x_n^T]^T$, so that the model corresponding to the agents governed by (3.11) concatenated together can now be rewritten in the following form:

$$\dot{\mathbf{x}} = I \otimes A\mathbf{x} - L \otimes BK\mathbf{x} + I \otimes B_\omega\omega \quad (3.19)$$

Let $z_i = x_i - x_n$ and $\tilde{\omega}_i = \omega_i - \omega_n$ for $i = 1, \dots, n-1$, and define the vectors $\mathbf{z} = [z_1^T, \dots, z_{n-1}^T]^T$ and $\tilde{\omega} = [\tilde{\omega}_1^T, \dots, \tilde{\omega}_{n-1}^T]^T \in \mathfrak{R}^{p(n-1)}$. Using Lemma 3.2 we have:

$$\dot{\mathbf{z}} = I \otimes A\mathbf{z} - H \otimes BK\mathbf{z} + I \otimes B_\omega\tilde{\omega} \quad (3.20)$$

and

$$\dot{x}_n = Ax_n - B \sum_{j=1}^{n-1} \ell_{nj}Kz_j + B_\omega\tilde{\omega}_n \quad (3.21)$$

Now, by adding and subtracting $I \otimes \frac{1}{2}\epsilon BK\mathbf{z}$ to the right hand side of equation (3.20), it can be rewritten as

$$\dot{\mathbf{z}} = I \otimes \left(A - \frac{1}{2}\epsilon BK\right)\mathbf{z} - (H_\sigma - \frac{1}{2}\epsilon I) \otimes BK\mathbf{z} + I \otimes B_\omega\tilde{\omega} \quad (3.22)$$

Now, consider the following piecewise quadratic Lyapunov function

$$V_\sigma = V_{\sigma(t)}(\mathbf{z}) = \mathbf{z}^T P_{H_\sigma} \otimes P_A \mathbf{z} \quad (3.23)$$

The time derivative of V_σ along the trajectories of the system (3.22) is given by

$$\begin{aligned} \dot{V}_\sigma &= \mathbf{z}^T P_{H_\sigma} \otimes (P_A A + A^T P_A) \mathbf{z} - \mathbf{z}^T P_{H_\sigma} \otimes P_A B R_A^{-1} B^T P_A \mathbf{z} \\ &\quad + \mathbf{z}^T P_{H_\sigma} \otimes P_A B_\omega \tilde{\omega} + \tilde{\omega}^T P_{H_\sigma} \otimes B_\omega^T P_A \mathbf{z} - \frac{1}{\epsilon} \mathbf{z}^T Q_{H_\sigma} \otimes (P_A B R_A^{-1} B^T P_A) \mathbf{z} \end{aligned}$$

It is easy to verify that the following inequality holds:

$$\mathbf{z}^T P_{H_\sigma} \otimes P_A B_\omega \tilde{\omega} + \tilde{\omega}^T P_{H_\sigma} \otimes B_\omega^T P_A \mathbf{z} \leq \gamma^{-2} \mathbf{z}^T P_{H_\sigma} \otimes P_A B B^T P_A \mathbf{z} + \gamma^2 \tilde{\omega}^T P_{H_\sigma} \otimes I \tilde{\omega} \quad (3.24)$$

Since $Q_{H_\sigma} > 0$ and $P_A B R_A^{-1} B^T P_A \geq 0$, using the above inequality we obtain:

$$\dot{V}_\sigma \leq -\mathbf{z}^T P_{H_\sigma} \otimes Q_A \mathbf{z} + \gamma^2 \tilde{\omega}^T P_{H_\sigma} \otimes I \tilde{\omega}$$

Therefore, for $\omega \equiv 0$, we have:

$$\dot{V}_\sigma \leq -\mathbf{z}^T P_{H_\sigma} \otimes Q_A \mathbf{z} \quad (3.25)$$

Knowing that $-Q_A \leq -\lambda_{\min}(Q_A)I = -\delta\lambda_{\max}(P_A)I \leq -\delta P_A$, and

$$\delta = \frac{\lambda_{\min}(Q_A)}{\lambda_{\max}(P_A)},$$

we have:

$$\dot{V}_\sigma \leq -\delta \mathbf{z}^T P_{H_\sigma} \otimes P_A \mathbf{z} \leq -\delta V_\sigma \quad (3.26)$$

It is easy to check that the following properties are satisfied:

1. $\dot{V}_\sigma(t) \leq -\delta V_\sigma(t)$ for all $t > 0$ as per equation (3.26)
2. $\alpha_1 \|z\|^2 \leq V_\sigma(t) \leq \alpha_2 \|z\|^2$ for all $t > 0$, where $\alpha_1 = \beta_1 \lambda_{\min}(P_A)$ and $\alpha_2 = \beta_2 \lambda_{\max}(P_A)$ as per equation (3.23)
3. $V_\sigma(\hat{t}_1) \leq \mu V_\sigma(\hat{t}_2)$ for all $\hat{t}_1, \hat{t}_2 > 0$ as per Lemma 3.5.

Based on the above conditions and knowing the fact that $\tau_a > \frac{\ln(\mu)}{k_\delta \delta} \geq \frac{\ln(\mu)}{\delta}$ from Lemma 3.7 one can conclude the exponential convergence of $\mathbf{z} \rightarrow 0$ as $t \rightarrow \infty$. Therefore, the control law (3.15) can solve the consensus problem for the multi-agent system (3.11) in absence of the disturbances.

part a) To show that the proposed algorithm solves the H_∞ consensus problem, based on Definition 3.16, we have to prove that it can solve the consensus problem in absence of disturbances, as done above, and show that in presence of the disturbance signals ω_i the inequality (3.13) holds for any $T > 0$ if $z_i(0) = 0$, $i = 1, \dots, n$. Towards this end, let us define $t_{N+1} = T$ and the function $\xi(t)$ as $\xi(t) = e^{\delta_k(t-t_k)}$, where $k = N_\sigma(t)$ and $\delta_k = \frac{\ln(\mu)}{t_{k+1}-t_k}$. We now need to show that:

$$\mathbf{z}^T \mathbf{z} - n^{-1} \mu^{-1} \gamma_\rho^2 \tilde{\omega}^T \tilde{\omega} + \frac{\gamma_\rho^2}{n \mu \beta_2 \gamma^2} \left(\dot{V}_\sigma + \delta V_\sigma \right) < 0 \quad (3.27)$$

By using the results in part a) of Lemma 3.5, the following inequality is obtained:

$$\begin{aligned} & \frac{1}{T} \int_0^T \xi(t) \mathbf{z}^T \mathbf{z} dt - \xi(t) n^{-1} \mu^{-1} \gamma_\rho^2 \tilde{\omega}^T \tilde{\omega} dt \\ & \leq \frac{1}{T} \int_0^T \xi(t) \left(\mathbf{z}^T \mathbf{z} - \frac{\gamma_\rho^2}{n\mu} \tilde{\omega}^T \tilde{\omega} + \frac{\gamma_\rho^2}{n\mu\beta_2\gamma^2} (\dot{V}_\sigma + \bar{\delta}V_\sigma) \right) dt < 0 \end{aligned}$$

By invoking Lemma 3.6, and knowing that $1 \leq \xi(t) < \mu$, and using the above inequality one obtains:

$$\begin{aligned} \frac{1}{T} \int_0^T \|\mathbf{z}_i\|^2 dt & \leq \frac{1}{T} \int_0^T \xi(t) \|\mathbf{z}_i\|^2 dt \\ & \leq \frac{\mu^{-1}}{nT} \int_0^T \xi(t) \|\tilde{\omega}_i\|^2 dt \leq \frac{\mu^{-1}}{T} \int_0^T \xi(t) \|\omega_i\|^2 dt < \frac{1}{T} \int_0^T \|\omega_i\|^2 dt \end{aligned}$$

Therefore, the inequality (3.13) is satisfied. Now, by substituting \dot{V}_σ and V_σ into the inequality (3.27), multiplying its left-hand side by $\frac{n\mu\beta_2\gamma^2}{\gamma_\rho^2}$ and noting that $\bar{\delta}P_A = k_\delta\delta P_A \leq k_\delta\lambda_{\min}(Q_A)I \leq k_\delta Q_A$, one obtains:

$$\begin{aligned} & \frac{n\mu\beta_2\gamma^2}{\gamma_\rho^2} \mathbf{z}^T \mathbf{z} - \beta_2\gamma^2 \tilde{\omega}^T \tilde{\omega} + \dot{V}_\sigma + \bar{\delta}V_\sigma \\ & \leq n\mu^2 \frac{\gamma^2}{\gamma_\rho^2} \mathbf{z}^T P_{H_\sigma} \otimes I \mathbf{z} - \gamma^2 \tilde{\omega}^T P_{H_\sigma} \otimes I \tilde{\omega} + \dot{V}_\sigma + k_\delta\delta V_\sigma \\ & \leq \mathbf{z}^T P_{H_\sigma} \otimes \left(-Q_A + n\mu^2 \frac{\gamma^2}{\gamma_\rho^2} I + k_\delta\delta P_A \right) \mathbf{z} \\ & \leq \mathbf{z}^T P_{H_\sigma} \otimes \left(-(1 - k_\delta)Q_A + n\mu^2 \frac{\gamma^2}{\gamma_\rho^2} I \right) \mathbf{z} \\ & \leq (1 - k_\delta) \mathbf{z}^T P_{H_\sigma} \otimes \left(-Q_A + n\mu^2 \frac{\gamma^2}{(1 - k_\delta)\gamma_\rho^2} I \right) \mathbf{z} \end{aligned}$$

Therefore, since $\gamma_\rho = \gamma\sqrt{\frac{n\mu^2}{1-k_\delta}}$ and $Q_A > I$, the inequality (3.27) is satisfied and this concludes the proof of part a).

part b) Based on Definition 3.17 and noting that the control law (3.15) solves the consensus problem in absence of disturbance signals, one needs to show that the inequality (3.14) holds for any $T > 0$ and $z_i(0) = 0$, $i = 1, \dots, n$ to prove that the algorithm solves the weighted H_∞ consensus problem. We

now need to show the validity of the following inequality:

$$\|\mathbf{z}\|^2 - \frac{\gamma_\rho^2}{n} \|\tilde{\omega}\|^2 + \frac{\gamma_\rho^2}{n\beta_2\gamma^2} \dot{V}_\sigma < 0 \quad (3.28)$$

By using the results in part b) of Lemma 3.5, one obtains:

$$\begin{aligned} & \frac{1}{T} \int_0^T \mu^{-N_\sigma(t)} \left(\|\mathbf{z}\|^2 - \frac{\gamma_\rho^2}{n} \|\tilde{\omega}\|^2 \right) dt \\ & \leq \frac{1}{T} \int_0^T \mu^{-N_\sigma(t)} \left(\|\mathbf{z}\|^2 - \frac{\gamma_\rho^2}{n} \|\tilde{\omega}\|^2 + \frac{\gamma_\rho^2}{n\beta_2\gamma^2} \dot{V}_\sigma \right) dt < 0 \end{aligned}$$

Since $N_\sigma(t) \leq \frac{t}{\tau_a}$ and $\alpha \geq \frac{\ln(\mu)}{\tau_a}$, we have $e^{-\alpha t} \leq e^{-\frac{\ln(\mu)}{\tau_a} t} \leq \mu^{-N_\sigma(t)}$ and by invoking Lemma 3.6, one obtains:

$$\begin{aligned} \frac{1}{T} \int_0^T e^{-\alpha t} \|\mathbf{z}\|^2 dt & \leq \frac{1}{T} \int_0^T \mu^{-N_\sigma(t)} \|\mathbf{z}\|^2 dt \\ & < \frac{1}{T} \int_0^T \frac{\gamma_\rho^2}{n} \|\tilde{\omega}\|^2 dt \leq \frac{1}{T} \int_0^T \gamma_\rho^2 \|\omega\|^2 dt \end{aligned}$$

which implies that the inequality (3.14) is satisfied. By substituting \dot{V}_σ into the inequality (3.28) and multiplying its left-hand side by $\frac{n\beta_2\gamma^2}{\gamma_\rho^2}$, one obtains:

$$\begin{aligned} & \frac{n\beta_2\gamma^2}{\gamma_\rho^2} \mathbf{z}^T \mathbf{z} - \beta_2\gamma^2 \tilde{\omega}^T \tilde{\omega} + \dot{V}_\sigma \\ & \leq n\mu \frac{\gamma^2}{\gamma_\rho^2} \mathbf{z}^T P_{H_\sigma} \otimes I \mathbf{z} - \gamma^2 \tilde{\omega}^T P_{H_\sigma} \otimes I \tilde{\omega} + \dot{V}_\sigma \\ & \leq \mathbf{z}^T P_{H_\sigma} \otimes \left(-Q_A + n\mu \frac{\gamma^2}{\gamma_\rho^2} I \right) \mathbf{z} < 0 \end{aligned}$$

Therefore, since $\gamma_\rho = \gamma\sqrt{n\mu}$ and $Q_A > I$, the inequality (3.14) is satisfied and this concludes the proof of part b). \blacksquare

3.4 Simulation Results

The effectiveness and performance capabilities of our proposed consensus design methodologies are now demonstrated through the following numerical simulations. Towards this end, first the *diving consensus* problem of a team

of four unmanned underwater vehicles (UUVs) is considered. These UUVs are 5.3 meters long and weigh 5.4 tons and their linearized diving dynamics can be represented as $\dot{x}_i = Ax_i + Bu_i + B_\omega\omega_i, i = 1, \dots, 4$ [140], where:

$$A = \begin{bmatrix} -0.7 & -0.3 & 0 \\ 1 & 0 & 0 \\ 0 & -\nu_0 & 0 \end{bmatrix}, B = \begin{bmatrix} 0.035 \\ 0 \\ 0 \end{bmatrix}, B_\omega = \begin{bmatrix} 0 \\ 0.1 \\ 0 \end{bmatrix}$$

and where $x_i = [q_i, \theta_i, d_i]^T$, d_i denotes the depth, θ_i denotes the pitch angle, q_i denotes the pitch angular velocity, and ν_0 denotes the nominal value of the surge linear velocity and for simulations is set to $0.3m/s$. The control u_i denotes the deflection of the control surface from the stern plane and ω_i denotes the external disturbances. The three digraphs associated with the switching communication network of the team are shown in Fig. 3.1, where the switching signal is changing every 20 seconds. The value of the constant ϵ in Lemma 3.4 is set to $\min_{\sigma \in I_\sigma} \{Re(\lambda(H_\sigma))\} = 1.382$ and is computed based on the network topologies shown in Fig. 3.1. Furthermore, the other design parameters are selected as $Q_{H_\sigma} = Q_A = I$, $\gamma_\rho = 10$, $\beta_1 = 0.1577$, $\beta_2 = 1.2633$ and $RMS(\omega_i) = 1$.

The depth and the control effort of the agents are depicted in Figures 3.2 and 3.3 for the weighted H_∞ scheme and in Figures 3.4 and 3.5 for the H_∞ scheme. Quantitative comparisons between the two control strategies are shown in Table 3.1. It follows that the weighted H_∞ design approach can achieve the same minimum dwell time constraint by utilizing less control effort, however the H_∞ design approach has a faster settling time. It is worth noting, the consensus error in Table 3.1 is dimensionless.

Second, to compare our proposed H_∞ schemes with another work in the literature, the method presented in [58] is chosen for comparison which can be applied to multi-agent teams with directed and switching information flow graphs. However, the method in [58] can only be applied to a multi-agent of high-order integrators. Therefore, we consider a new team that consists of 3^{rd} order integrator agents. For such a team we take for each agent $B = B_\omega = [0, 0, 1]^T$ with the same communication network topologies as depicted in Fig. 3.1. Moreover, the same feedback gain $K = [2.2905, 4.5878, 3.4494]$ is used

Table 3.1: The controller parameters and comparative performance of the resulting two control strategies.

	H_∞ Performance	Weighted H_∞ Performance
R_A	0.001	0.005
γ	0.2791	2.0397
k_δ	0.85	-
δ	0.1356	0.1108
τ_a	18.05	18.78
K	34.9664 37.7672 -30.1026	13.7931 11.6912 -10.3274
Control effort (max)	17.64 deg	5.22 deg
Control effort (L_2 norm)	90	22.29
Consensus error (RMS)	3×10^{-4}	3.5×10^{-4}
Settling time	11 sec	13 sec

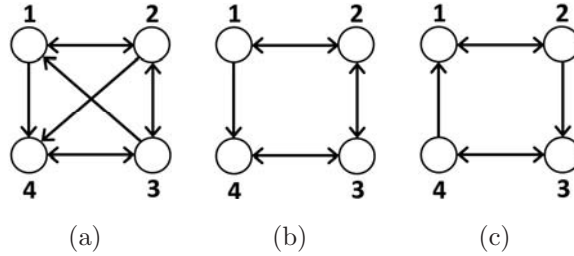


Figure 3.1: Communication network digraphs for a team of 4 UUVs.

for the method in [58] and the one proposed in our work. The quantitative comparison between the two methods is now provided in Table 3.2. This table shows that the method proposed in [58] does lead to a less conservative γ_ρ but at the expense of significant increase in the computational time even for a small team of 4 multi-agents in comparison to our proposed method. This performance is as expected as we have stated in the Introduction section.

3.5 Summary

In this chapter, H_∞ and weighted H_∞ consensus problems for a team of homogenous LTI multi-agent systems are investigated subject to switching topology and directed communication network graphs. A novel design procedure is

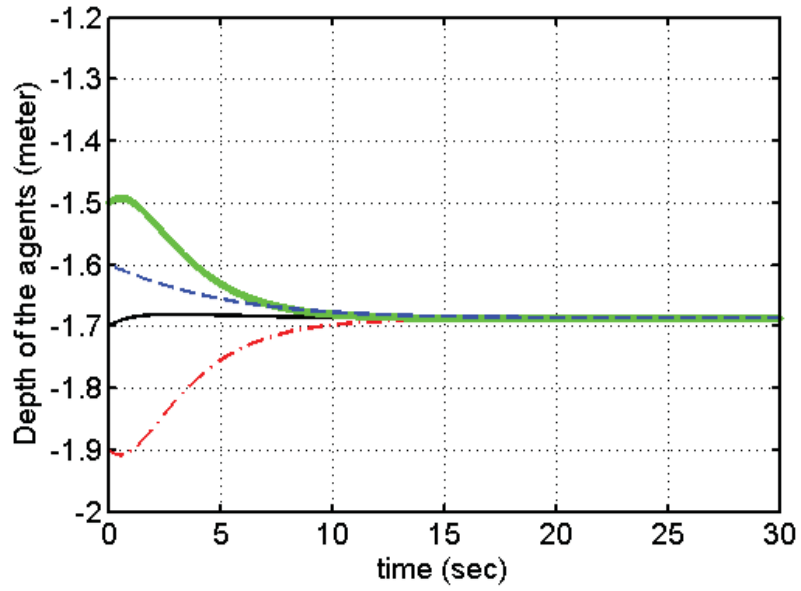


Figure 3.2: Depth of the agents using the weighted H_∞ method.

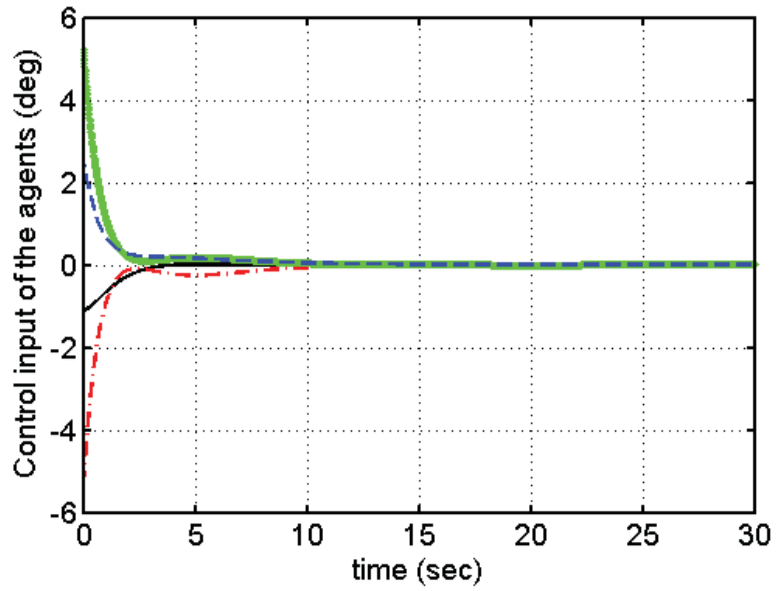


Figure 3.3: Control effort of the agents using the weighted H_∞ method.

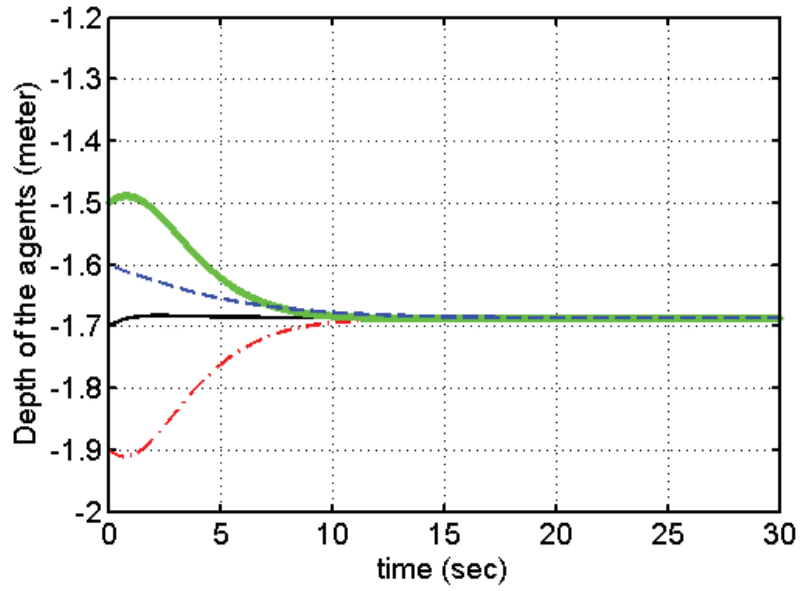


Figure 3.4: Depth of the agents using the H_∞ method.

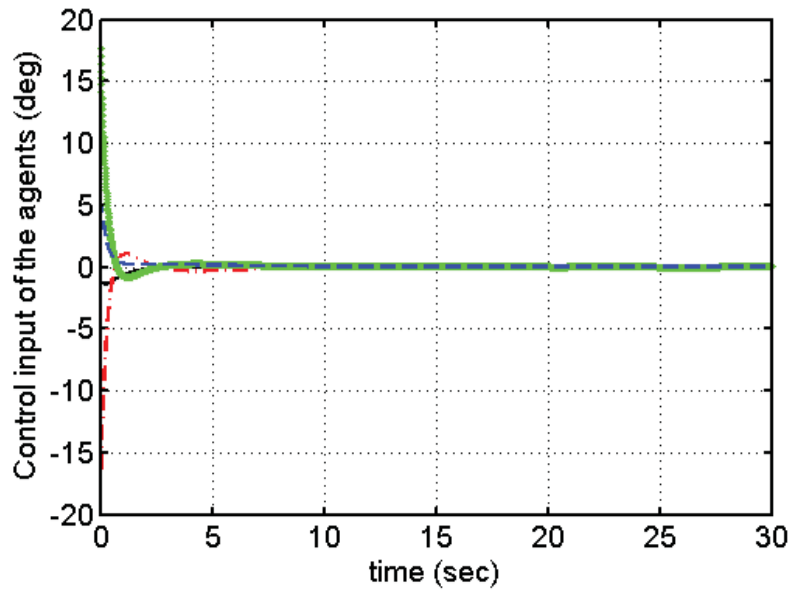


Figure 3.5: Control effort of the agents using the H_∞ method.

Table 3.2: The comparison between our proposed H_∞ method and the method in [58].

	Our H_∞ Performance	Method in [58]
γ_ρ	7.1818	5.6664
Computational time (best case)	0.0014 sec	1.0462 sec
Computational time (worst case)	0.0076 sec	1.0748 sec
Computational time (average)	0.0018 sec	1.0532 sec

proposed based on the solution of an algebraic Riccati equation and sufficient conditions are presented based on state feedback stabilizability of an LTI system with a bounded L_2 gain. The stability of the overall closed-loop switched system is shown based on Lyapunov analysis. Finally, the effectiveness of our proposed two consensus schemes are illustrated through simulations that are applied to a switching network of four unmanned underwater vehicles as well as a team of four 3^{rd} order integrator multi-agent systems. The simulation results also demonstrate that our proposed consensus algorithm design methodology is quite computationally feasible in comparison to the methods proposed in the literature.

In the next chapter we address cooperative actuator fault accommodation strategy for a team of LTI multi-agent systems assuming the information flow graph is directed and switching.

Chapter 4

Actuator Fault Accommodation Strategy for a Team of Multi-Agent Systems Subject to Switching Topology

In this chapter a cooperative actuator fault accommodation strategy is studied. The multi-agents systems is considered to be a team of LTI multi-agent systems and information flow graph is directed and switching topology. The effects of two actuator fault types, namely loss-of-effectiveness fault and saturation fault are investigated and it is assumed that the faults can simultaneously occur in more than one agent and the exact estimate of the fault severities are not available. However, the faults can be detected and isolated by an Fault Detection and Isolation (FDI) module and it also can provide an inaccurate estimate of the fault severities.

Our proposed fault accommodation strategy is based on a weighted consensus algorithm in which the level of control effort that each agent contributes to the consensus achievement of the team is proportional to its weight. In the proposed weighted consensus algorithm, the agents control gains are selected based on the solution of an algebraic Riccati equation (ARE) and whenever, a fault is detected by an FDI module these control gains in our proposed weighted consensus algorithm are modified based on inaccurate estimates of

fault severities.

Due to the fact that in practice an FDI module cannot exactly estimate the fault severities, the faulty agents could not contribute as much as the healthy agents to the consensus achievement of the team. This consequently could affect the overall team performance and mission reliability. To overcome this drawback, the agents weights in our proposed consensus algorithm are reconfigured to compensate for the lack of control effort in the faulty agents by increasing the weight of healthy agents to allocate higher control efforts. Towards this end, a non-convex optimization problem is formulated and a steepest descent gradient algorithm is used to obtain a sub-optimal solution. Based on this solution the agents weights are then reconfigured. Furthermore, a method is also proposed to implement our recovery strategy for dealing with actuator saturation.

In comparison to the work in the literature in our fault accommodation strategy the dynamics of the agents is considered to belong to general LTI systems, the faults in agents can occur simultaneously and in more than one agent, and an accurate estimate of fault severity is not required. Furthermore, in our proposed solution, the communication network is directed, the network topology can switch arbitrarily, and the proposed recovery strategy can be implemented even if the fault severity estimate of more than one agent is inaccurate.

The remainder of the chapter is organized as follows. The model of multi-agent systems and the information flow graph are presented in Section 4.1. The problem statement and our proposed fault recovery strategy are developed and presented in Section 4.2. Section 4.3 provides numerical simulation results that support our proposed theoretical results and compares the performance of our proposed solution with the centralized and decentralized fault recovery approaches that are available in the literature. Finally, the chapter is concluded by a conclusions in Section 4.4.

4.1 Multi-Agents System Model

Consider a team of n homogeneous multi-agent systems where each agent is modeled as follows

$$\dot{x}_i = Ax_i + Bu_i \quad i \in \mathcal{V} = \{1, 2, \dots, n\} \quad (4.1)$$

where $x_i \in \mathbb{R}^p$ denotes the state of the i^{th} agent, $A \in \mathbb{R}^{p \times p}$, $B \in \mathbb{R}^{p \times m}$ and $u_i \in \mathbb{R}^m$ denotes the control input of the i^{th} agent.

Assumption 4.1. *The pair (A, B) is controllable.*

Throughout the chapter it is assumed that actuators may not function ideally and their desired output value and actual control efforts supplied by them may be different. Let us denote the desired output of the actuator of the i^{th} agent by u_i^* and its actual value by u_i . In a healthy agent the real actuator output is the same as its desired value, but in a faulty agent these quantities are not the same and it can be represented as follows:

$$u_i = u_i^h + u_i^f$$

where u_i^h denotes amount of the control effort of the agent if it was healthy and u_i^f denotes the difference between u_i and u_i^h . Now, let us rewrite the dynamical model of the multi-agent team as follows:

$$\dot{x}_i = Ax_i + Bu_i^h + Bu_i^f, \quad i \in \mathcal{V} \quad (4.2)$$

In this chapter, the type of actuator faults that we consider belong to the loss-of-effectiveness (LOE) and actuator saturation faults. The LOE fault can be formally formulated as

$$u_i = (I - \mathcal{F}_i)u_i^* \quad (4.3)$$

where \mathcal{F}_i is a diagonal matrix representing the unknown fault severity of the actuators. In this chapter it is assumed that none of the actuators is fully nonfunctional and therefore $I - \mathcal{F}_i > 0$. To formally represent the actuator

saturation fault let us define a diagonal matrix U_i as:

$$U_i = [U_{i1}, U_{i2}, \dots, U_{im}]^T$$

where $U_{i1}, U_{i2}, \dots, U_{im} > 0$ correspond to the positive saturation bound of the i^{th} agent actuator and m is the dimension of control input. Moreover, let us denote $u_i = [u_{i1}, u_{i2}, \dots, u_{im}]^T$ and $u_i^* = [u_{i1}^*, u_{i2}^*, \dots, u_{im}^*]^T$. For $j = 1, \dots, m$ the relationship between u_{ij} and u_{ij}^* is now represented by:

$$u_{ij} = \begin{cases} U_{ij} & \text{if } u_{ij}^* > U_{ij} \\ u_{ij}^* & \text{if } -U_{ij} \leq u_{ij}^* \leq U_{ij} \\ -U_{ij} & \text{if } u_{ij}^* < -U_{ij} \end{cases} \quad (4.4)$$

Remark 4.1. *In this chapter, it is assumed that an actuator fault is detected and isolated by using an FDI module according to standard results in the literature [100]- [103] and only an approximate and inaccurate estimate of the fault severity is available.*

The agents have only access to measurements that are relative to their neighboring agents for designing their distributed control strategies to achieve consensus. In the case that the actual states of the agent can be measured, one can construct the relative states. A formal definition of the consensus achievement is presented next.

Definition 4.1. *The control input u_i solves the consensus problem if*

$$\|x_i - x_j\| \rightarrow 0 \text{ as } t \rightarrow \infty, \forall i, j \in \{1, \dots, n\} \quad (4.5)$$

Remark 4.2. *Consider the multi-agent system (4.2). Note that for any vector signal $\bar{x}(t)$, one can write*

$$\|x_i - x_j\| = \|x_i - \bar{x} - x_j + \bar{x}\| = \|z_i - z_j\| \leq \|z_i\| + \|z_j\|$$

where

$$\|z_i\| = \|x_i - \bar{x}\|.$$

Therefore, if $\|z_i\| \rightarrow 0$ as $t \rightarrow \infty, \forall i \in \{1, \dots, n\}$ then the multi-agent system

(4.1) achieves consensus.

To describe the set of neighboring agents and the information exchange protocol of the team, let us define the information flow digraph (directed graph) as $\mathcal{G}(t)$, the node set \mathcal{V} and the edge set $\mathcal{E}_{\mathcal{G}}(t)$ as per Definition 3.1. In this chapter, it is assumed that there is no node with an edge to itself. The set of neighbors of an agent i is denoted by $\mathcal{N}_i(\mathcal{G}(t))$ as per Definition 3.7. The Laplacian matrix $\mathcal{L}(\mathcal{G}(t))$ and the node degree κ_i defined as per Definition 3.8 and $|\mathcal{N}_i(\mathcal{G}(t))|$ denotes the cardinality of $\mathcal{N}_i(\mathcal{G}(t))$.

Assumption 4.2. *Throughout this chapter, it is assumed that the digraph $\mathcal{G}(t)$ is always strongly connected. This implies that at any time any node can be reached from any other node by a directed path in the graph.*

Definition 4.2. *We denote $\alpha(\mathcal{G}(t))$ by*

$$\alpha(\mathcal{G}(t)) = \min \{ \text{real}(\lambda(\mathcal{L}(t))) \mid \lambda(\mathcal{L}(t)) \neq 0 \}. \quad (4.6)$$

The quantity $\alpha(\mathcal{G}(t))$ in undirected graphs is equal to and in directed graphs is larger than or equal to the algebraic connectivity of the graph [125]. In other words, the smaller $\alpha(\mathcal{G}(t))$ then the less connected is the graph.

Since the information flow graph $\mathcal{G}(t)$ is always strongly connected, the agents can reconstruct the Laplacian matrix of the communication graph on-line by using distributed algorithms such as the one proposed in the Proposition 3.1 in [77]. Therefore, $\alpha(\mathcal{G}(t))$ can be computed and constructed on-line and there is no need to determine it in advance and off-line.

Consider piece wise continuous signal $\sigma(t)$ as per Definition 3.9 and function $N_\sigma(T_1, T_2)$ as per Definition 3.13 and let τ_a be the average dwell time of switching signal $\sigma(t)$ as per Definition 3.14.

In the remainder of the chapter and for brevity, \mathcal{G}_σ denotes $\mathcal{G}_{\sigma(t)}$ as per Definition 3.10, $L_\sigma = \mathcal{L}(\mathcal{G}_{\sigma(t)})$, $\alpha_\sigma = \alpha(\mathcal{G}_{\sigma(t)})$ and $\mathcal{N}_i(t) = \mathcal{N}_i(\mathcal{G}_{\sigma(t)})$.

Let us define the matrix H_σ , which in the remainder of the chapter will be utilized for the stability analysis of our proposed algorithm, as:

$$H_\sigma = L_\sigma + 2 \frac{\Delta_\sigma}{n} \mathbf{1}\mathbf{1}^T \quad (4.7)$$

where $\mathbf{1} = [1, 1, \dots, 1]^T \in \mathbb{R}^n$ and Δ_σ denotes the maximum in-degree of all the graph nodes over time. We are now in a position to state our first result.

Lemma 4.1. *If the digraph \mathcal{G}_σ is strongly connected, then the real parts of all eigenvalues of the matrix H_σ which is defined by equation (4.7) are positive and greater than or equal to $\alpha(\mathcal{G}(t))$.*

Proof. Let \mathcal{G}_σ^* be a graph that its corresponding Laplacian matrix L_σ^* is equal to

$$L_\sigma^* = \begin{bmatrix} L_\sigma & 0 \\ -\frac{2}{n}\Delta_\sigma\mathbf{1}^T & 2\Delta_\sigma \end{bmatrix}$$

Since the graph \mathcal{G}_σ is strongly connected, the graph \mathcal{G}_σ^* has a directed spanning tree. Using Remark 1 in [15], one can conclude that the real parts of all nonzero eigenvalues of the matrix L_σ^* are positive, and $\lambda = 0$ is a simple eigenvalue of L_σ^* .

It can be observed that $\lambda = 2\Delta_\sigma$ is an eigenvalue of L_σ^* and its eigenvector is $[0_n^T \ 1]^T$. Now assume that $\lambda \neq 2\Delta_\sigma \in \mathbb{C}$ is an eigenvalue of L_σ^* , and the vector $[\mathbf{v}_1^T \ \mathbf{v}_2^T]^T$ is its corresponding eigenvector, where $\mathbf{v}_1 \in \mathbb{C}^n$ and $\mathbf{v}_2 \in \mathbb{C}$. Since $\lambda \neq 2\Delta_\sigma$, therefore $\mathbf{v}_1 \neq 0$, and since

$$L_\sigma^* \begin{bmatrix} \mathbf{v}_1 \\ \mathbf{v}_2 \end{bmatrix} = \begin{bmatrix} L_\sigma \mathbf{v}_1 \\ -\frac{2}{n}\Delta_\sigma\mathbf{1}^T \mathbf{v}_1 + 2\Delta_\sigma \mathbf{v}_2 \end{bmatrix} = \begin{bmatrix} \lambda \mathbf{v}_1 \\ \lambda \mathbf{v}_2 \end{bmatrix}$$

one can conclude that λ is also an eigenvalue of the matrix L_σ .

On the other hand, assume that $\lambda \in \mathbb{C}$ and $\mathbf{v}_1 \in \mathbb{C}^n$ is the eigenvalue and the corresponding eigenvector of L_σ , respectively. According to Theorem 2 in [141], $real(\lambda) < 2\Delta_\sigma$ where it is always possible to define \mathbf{v}_2 as follows:

$$\mathbf{v}_2 = \frac{2}{n(2\Delta_\sigma - \lambda)} \mathbf{1}^T \mathbf{v}_1$$

Therefore, λ is an eigenvalue of L_σ^* and $[\mathbf{v}_1^T \ \mathbf{v}_2^T]^T$ is its associated eigenvector. By applying Lemma 3.3 to L_σ^* one can now conclude proof of the lemma. ■

Using Lemma 4.1, it follows that all eigenvalues of the matrix $H_\sigma - \eta\alpha_\sigma I$ are in the right-half plane, where $\eta < 1$ is a positive constant. Therefore, there

exist symmetric positive definite matrices $P_{H_\sigma}, Q_{H_\sigma} \in \mathbb{R}^{n \times n}$ such that

$$P_{H_\sigma} H_\sigma + H_\sigma^T P_{H_\sigma} - 2\eta\alpha P_{H_\sigma} = Q_{H_\sigma} > 0 \quad (4.8)$$

We now define the parameters $\beta_{\sigma 1}$, $\beta_{\sigma 2}$ and μ_σ as follows:

$$\begin{aligned} \beta_{\sigma 1} &= \lambda_{\min}(P_{H_\sigma}), \\ \beta_{\sigma 2} &= \lambda_{\max}(P_{H_\sigma}), \\ \mu_\sigma &= \frac{\beta_{\sigma 2}}{\beta_{\sigma 1}} \end{aligned} \quad (4.9)$$

We are now in a position to define all the parameters and matrices that are associated with the information flow graph. Their fundamental properties will be used in the next section where our proposed consensus algorithm and fault recovery strategies are presented.

4.2 Problem Statement and Main Results

In this section, first a weighted consensus algorithm is proposed for consensus achievement of the multi-agent team (4.2) in presence of LOE actuator faults and switching network topology. The proposed consensus algorithm is based on the assumption that is presented in Remark 4.1 and uses inaccurate estimates of the fault severities for implementing the desired control laws to the actuators. To make our proposed algorithm more useful in real-world applications, the actuator faults could indeed occur in some agents simultaneously. However, depending on how inaccurate the faults severities estimations are, the consensus achievement of the multi-agent team could be affected. A fault index is therefore defined here to quantitatively measure the effects of inaccurate estimations. Subsequently, based on this fault index an optimization problem and an algorithm to reconfigure the weights of the agents in the consensus algorithm are proposed. Finally, below it is also shown how our active fault recovery scheme can also be used to improve the consensus achievement performance of multi-agent team in presence of actuator saturation.

4.2.1 Weighted Consensus Strategy

Consider the multi-agent system (4.2) and let $\hat{\mathcal{F}}_i$ denote the estimate of the fault severity of the i^{th} agent and $\tilde{\mathcal{F}}_i = \mathcal{F}_i - \hat{\mathcal{F}}_i$ denote the FD estimation error. The objective of our proposed weighted consensus algorithm is to design the desired control signal u_i^* for the i^{th} agent such that the actual actuator output u_i is the same as u_i^h , that is

$$u_i^* = (I - \hat{\mathcal{F}}_i)^{-1}u_i^h \quad (4.10)$$

For a healthy agent or when the fault severity is estimated accurately $u_i = u_i^h$.

Remark 4.3. *In this chapter, it is assumed that none of the actuators is fully non-functional and FDI module uses this fact, therefore all the matrices $I - \hat{\mathcal{F}}_i$ are invertible. Unsurprisingly large values of fault severity estimations in some actuators due to either high degrees of fault severities or estimation error, will result in ill-conditioned matrices and makes recovery procedure ineffective.*

However, in case of an inaccurate fault severity estimation that is of our main interest here there is an error between u_i and u_i^h as given by u_i^f according to:

$$u_i^f = -\tilde{\mathcal{F}}_i(I - \hat{\mathcal{F}}_i)^{-1}u_i^h$$

Let us also define a fault factor matrix F_i as given by

$$F_i = \text{diag}[f_{i1}, \dots, f_{im}] = -\tilde{\mathcal{F}}_i(I - \hat{\mathcal{F}}_i)^{-1} \quad (4.11)$$

Now we specify our proposed weighted consensus achievement algorithm as follows:

$$u_i^h = -G_i \sum_{j \in \mathcal{N}_i} K(x_i - x_j) \quad (4.12)$$

where $K \in \mathfrak{R}^{m \times p}$ is the relative state control gain matrix and

$$G_i = \frac{\kappa_i}{2\eta\alpha_\sigma|\mathcal{N}_i(t)|} \quad (4.13)$$

is the weight associated with the i^{th} agent and κ_i is the in-degree of the i^{th} node of the information flow graph. The value of κ_i is set to 1 for the healthy

agents. Subsequently, we will propose a reconfiguration strategy in order to adjust these values when the FDI module detects a fault in the team.

Definition 4.3. *Associated with the faulty multi-agent team (4.2) we define the team fault estimation error index as follows:*

$$F_{indx} = \sum_{i=1}^n \|F_i\|_{\max} \frac{\kappa_i \sqrt{\mu_\sigma}}{\eta \alpha_\sigma} \sqrt{1 + \frac{1}{|\mathcal{N}_i(t)|}} \quad (4.14)$$

Now, we are in a position to present the main result of this section.

Theorem 4.1. *Let the faulty multi-agent system (4.2) satisfies Assumption 4.1, and a piecewise constant switching signal $\sigma(t)$ and the information flow graph \mathcal{G}_σ satisfy Assumption 4.2. Let α_σ be defined as in equation (4.6) and the team fault estimation error index F_{indx} be defined as in equation (4.14). Consider the positive definite matrix Q_A and let P_A be the symmetric positive definite solution of the following algebraic Riccati equation:*

$$P_A A + A^T P_A - P_A B B^T P_A + Q_A = 0 \quad (4.15)$$

Let the relative state cooperative control gain K in equation (4.12) be selected as

$$K = B^T P_A \quad (4.16)$$

Then there exist $F_{\max} > 0$ and $\tau_a > 0$, such that if the team fault estimation error index F_{indx} satisfies $F_{indx} < F_{\max}$ and the average dwell time of $\sigma(t)$ is τ_a , the multi-agent system (4.2) achieves consensus.

Proof. Consider the augmented vectors $\mathbf{x} = [x_1^T, \dots, x_n^T]^T$, $\mathbf{u}_f = [u_1^{fT}, \dots, u_n^{fT}]^T$ and the block-diagonal matrix $F = \text{diag}[F_1, \dots, F_n]$. The multi-agent system (4.2) model can be rewritten as follows:

$$\dot{\mathbf{x}} = I \otimes A \mathbf{x} - \frac{1}{2\eta\alpha_\sigma} L_\sigma \otimes B K \mathbf{x} + I \otimes B \mathbf{u}_f \quad (4.17)$$

Let us define $z_i = x_i - \bar{x}$ for $i = 1, \dots, n$, where the state vector \bar{x} is governed

by the following dynamical equation

$$\dot{\bar{x}} = A\bar{x} - \frac{\Delta_\sigma}{n\eta\alpha_\sigma} B \sum_{j=1}^n K(\bar{x} - x_j), \quad \bar{x}(0) = \frac{\sum_{j=1}^n x_j(0)}{n} \quad (4.18)$$

Consider the augmented vector \mathbf{z} which is defined as follows:

$$\mathbf{z} = [z_1^T, \dots, z_n^T]^T = \mathbf{x} - \mathbf{1} \otimes \bar{x}$$

. Since $(L_\sigma \otimes BK_R)\mathbf{x} = (L_\sigma \otimes BK_R)\mathbf{z} + (L_\sigma \otimes BK_R)(\mathbf{1} \otimes \bar{x}) = (L_\sigma \otimes BK_R)\mathbf{z}$, from equation (4.17) one can obtain:

$$\begin{aligned} \dot{\mathbf{z}} &= \dot{\mathbf{x}} - (\mathbf{1} \otimes \dot{\bar{x}}) = (I \otimes A)\mathbf{x} - \frac{1}{2\eta\alpha_\sigma} (L_\sigma \otimes BK_R)\mathbf{z} + I \otimes B\mathbf{u}_f \\ &\quad - (I \otimes A)(\mathbf{1} \otimes \bar{x}) - \frac{\Delta_\sigma}{n\eta\alpha_\sigma} (\mathbf{1}\mathbf{1}^T \otimes BK_R)\mathbf{z} \\ &= (I \otimes A)\mathbf{z} - \frac{1}{2\eta\alpha_\sigma} \left((L_\sigma + 2\frac{\Delta_\sigma}{n} \mathbf{1}\mathbf{1}^T) \otimes BK_R \right) \mathbf{z} + I \otimes B\mathbf{u}_f \end{aligned}$$

Now, by adding and subtracting $\frac{1}{2}I \otimes BK\mathbf{z}$ to the right-hand side of equation (4.19), one obtains

$$\dot{\mathbf{z}} = I \otimes (A - \frac{1}{2}BK)\mathbf{z} - \frac{1}{2\eta\alpha_\sigma} (H_\sigma - \eta\alpha_\sigma I) \otimes BK\mathbf{z} + I \otimes B\mathbf{u}_f \quad (4.19)$$

Now, consider the following piecewise quadratic Lyapunov function candidate

$$V_\sigma = V_{\sigma(t)}(\mathbf{z}) = \mathbf{z}^T P_{H_\sigma} \otimes P_A \mathbf{z} \quad (4.20)$$

Taking time derivative of V_σ along the trajectories of the system (4.19) and using the equations (4.16) and (4.8), one can obtain:

$$\begin{aligned} \dot{V}_\sigma &= \mathbf{z}^T \left(P_{H_\sigma} \otimes \left(P_A(A - \frac{1}{2}BK_R) + (A - \frac{1}{2}BK_R)^T P_A \right) \right) \mathbf{z} \\ &\quad - \frac{\mathbf{z}^T}{2\eta\alpha_\sigma} \left((P_{H_\sigma}(H_\sigma - \eta\alpha_\sigma I) + (H_\sigma - \eta\alpha_\sigma I)^T P_{H_\sigma}) \otimes BK_R \right) \mathbf{z} \\ &\quad + \mathbf{z}^T (P_{H_\sigma} \otimes P_A B) \mathbf{u}_f + \mathbf{u}_f^T (P_{H_\sigma} \otimes B^T P_A) \mathbf{z} \\ &= \mathbf{z}^T (P_{H_\sigma} \otimes (P_A A + A^T P_A - P_A B B^T P_A)) \mathbf{z} \end{aligned} \quad (4.21)$$

$$+2\mathbf{z}^T (P_{H_\sigma} \otimes P_{AB}) \mathbf{u}_f - \frac{\mathbf{z}^T}{2\eta\alpha_\sigma} (Q_{H_\sigma} \otimes (P_A B B^T P_A)) \mathbf{z}$$

Let us define diagonal matrix $\Gamma_\sigma = \text{diag}[\gamma_{11}, \dots, \gamma_{ik}, \dots, \gamma_{nm}]$, where $\gamma_{ik} = \frac{\sqrt{|\mathcal{N}_i(t)|+1}}{2\eta\alpha_\sigma\sqrt{\beta_{\sigma 1}\beta_{\sigma 2}|\mathcal{N}_i(t)|}}\kappa_i$. Noting that

$$\mathbf{u}_f = \frac{1}{2\eta\alpha_\sigma} (L_\sigma \otimes B^T P_A) \mathbf{z}$$

it is easy to verify that the following inequality holds:

$$\begin{aligned} 2\mathbf{z}^T (P_{H_\sigma} \otimes P_{AB}) \mathbf{u}_f &\leq \mathbf{z}^T (P_{H_\sigma} \otimes P_{AB}) F^{\frac{1}{2}} \Gamma_\sigma F^{\frac{1}{2}} (P_{H_\sigma} \otimes B^T P_A) \mathbf{z} \\ &+ \frac{1}{4\eta^2\alpha_\sigma^2} \mathbf{z}^T (L_\sigma^T \otimes P_{AB}) F^{\frac{1}{2}} \Gamma_\sigma^{-1} F^{\frac{1}{2}} (L_\sigma \otimes B^T P_A) \mathbf{z} \end{aligned}$$

Knowing the fact that for any two matrices $\mathcal{A} \in \mathfrak{R}^{m \times n}$ and $\mathcal{B} \in \mathfrak{R}^{n \times p}$ we have $\mathcal{A}\mathcal{B} = \sum_{i=1}^n \text{col}_i(\mathcal{A})\text{row}_i(\mathcal{B})$, one can obtain:

$$\begin{aligned} &(P_{H_\sigma} \otimes P_{AB}) F^{\frac{1}{2}} \Gamma_\sigma F^{\frac{1}{2}} (P_{H_\sigma} \otimes B^T P_A) \\ &= \sum_{i=1}^n \sum_{k=1}^m \gamma_{ik} f_{ik} (\text{row}_i^T(P_{H_\sigma}) \otimes \text{row}_k^T(B^T P_A)) \\ &\quad (\text{row}_i(P_{H_\sigma}) \otimes \text{row}_k(B^T P_A)) \\ &= \sum_{i=1}^n \sum_{k=1}^m \gamma_{ik} f_{ik} (\text{row}_i^T(P_{H_\sigma}) \text{row}_i(P_{H_\sigma})) \\ &\quad \otimes (\text{row}_k^T(B^T P_A) \text{row}_k(B^T P_A)) \\ &\leq \sum_{i=1}^n \frac{\|F_i\|_{\max} \kappa_i \sqrt{|\mathcal{N}_i(t)|+1}}{2\eta\alpha_\sigma \sqrt{\beta_{\sigma 1}\beta_{\sigma 2}|\mathcal{N}_i(t)|}} (\text{row}_i^T(P_{H_\sigma}) \text{row}_i(P_{H_\sigma})) \\ &\quad \otimes P_A B B^T P_A \\ &\leq \sum_{i=1}^n \frac{F_{\text{indx}}}{2\beta_{\sigma 2}} (\text{row}_i^T(P_{H_\sigma}) \text{row}_i(P_{H_\sigma})) \otimes P_A B B^T P_A \\ &= \frac{F_{\text{indx}}}{2\beta_{\sigma 2}} P_{H_\sigma}^2 \otimes P_A B B^T P_A \leq \frac{1}{2} F_{\text{indx}} P_{H_\sigma} \otimes P_A B B^T P_A \end{aligned}$$

and

$$\frac{1}{4\eta^2\alpha_\sigma^2} (L_\sigma^T \otimes P_{AB}) F^{\frac{1}{2}} \Gamma_\sigma^{-1} F^{\frac{1}{2}} (L_\sigma \otimes B^T P_A)$$

$$\begin{aligned}
&= \frac{1}{4\eta^2\alpha_\sigma^2} \sum_{i=1}^n \sum_{k=1}^m \gamma_{ik}^{-1} f_{ik} (\text{row}_i^T(L_\sigma) \otimes \text{row}_k^T(B^T P_A)) \\
&\quad (\text{row}_i(L_\sigma) \otimes \text{row}_k(B^T P_A)) \\
&\leq \sum_{i=1}^n \frac{\|F_i\|_{\max} \sqrt{\beta_{\sigma 1} \beta_{\sigma 2} |\mathcal{N}_i(t)|}}{2\eta\alpha_\sigma \kappa_i \sqrt{|\mathcal{N}_i(t)| + 1}} (\text{row}_i^T(L_\sigma) \text{row}_i(L_\sigma)) \\
&\quad \otimes (P_A B B^T P_A)
\end{aligned}$$

Using the fact that:

$$\|\text{row}_i(L_\sigma)\| = \kappa_i \sqrt{1 + \frac{1}{|\mathcal{N}_i(t)|}}$$

The following inequality holds:

$$\begin{aligned}
&\leq \frac{\sqrt{\beta_{\sigma 1} \beta_{\sigma 2}}}{2} \sum_{i=1}^n \left(\frac{\|F_i\|_{\max} \kappa_i}{\eta\alpha_\sigma} \sqrt{\frac{|\mathcal{N}_i(t)| + 1}{|\mathcal{N}_i(t)|}} \right) I \otimes (P_A B B^T P_A) \\
&= \frac{\beta_{\sigma 1}}{2} F_{\text{indx}} I \otimes (P_A B B^T P_A) \leq \frac{1}{2} F_{\text{indx}} P_{H_\sigma} \otimes P_A B B^T P_A
\end{aligned}$$

Now, by substituting the above inequality into equation (4.21) we have:

$$\begin{aligned}
\dot{V}_\sigma &\leq -\mathbf{z}^T \left((P_{H_\sigma} \otimes Q_A) + \frac{1}{2\eta\alpha_\sigma} (Q_{H_\sigma} \otimes P_A B B^T P_A) \right) \mathbf{z} \\
&\quad + F_{\text{indx}} \mathbf{z}^T (P_{H_\sigma} \otimes P_A B B^T P_A) \mathbf{z} \\
&\leq -\mathbf{z}^T (P_{H_\sigma} \otimes (Q_A - F_{\text{indx}} P_A B B^T P_A)) \mathbf{z}
\end{aligned} \tag{4.22}$$

Since matrix $P_A B B^T P_A$ is positive semi-definite, then there exists a $F_{\max} > 0$ such that:

$$Q_A - F_{\max} P_A B B^T P_A \geq Q > 0$$

where Q is a positive definite matrix. Now, let us define

$$\delta = \min \frac{\lambda_{\min}(Q)}{\lambda_{\max}(P_A)}$$

Given that

$$\begin{aligned}
-(P_{H_\sigma} \otimes Q) &\leq -\lambda_{\min}(Q)(P_{H_\sigma} \otimes I) \leq \\
&\quad -\delta \lambda_{\max}(P_A)(P_{H_\sigma} \otimes I) \leq -\delta P_{H_\sigma} \otimes P_A
\end{aligned}$$

we have:

$$\dot{V}_\sigma \leq -\delta \mathbf{z}^T P_{H_\sigma} \otimes P_A \mathbf{z} \leq -\delta V_\sigma \quad (4.23)$$

It is easy to verify that the following properties are satisfied:

1. $\dot{V}_\sigma(t) \leq -\delta V_\sigma(t)$ for all $t > 0$,
2. $\beta_1 \|z\|^2 \leq V_\sigma(t) \leq \beta_2 \|z\|^2$ for all $t > 0$, where $\beta_1 = \beta_{\sigma 1} \lambda_{\min}(P_A)$ and $\beta_2 = \beta_{\sigma 2} \lambda_{\max}(P_A)$, and
3. $V_\sigma(\hat{t}_1) \leq \mu V_\sigma(\hat{t}_2)$ for any $\hat{t}_1, \hat{t}_2 > 0$, where $\mu = \frac{\beta_2}{\beta_1}$.

By selecting $\tau_a > \frac{\ln(\mu)}{\delta}$ and given that $N = N_\sigma(T) \leq \frac{T}{\tau_a}$, one can verify that $\delta^* T \leq \delta T - \ln(\mu)N$ holds for any $T > 0$, where δ^* is a positive constant equal to $\delta - \frac{\ln(\mu)}{\tau_a}$. Therefore, we have:

$$\|z(T)\| \leq \sqrt{\frac{\beta_2}{\beta_1}} e^{-\frac{1}{2}\delta^* T} \|z(0)\| \quad (4.24)$$

and this guarantees the exponential convergence of $\mathbf{z} \rightarrow 0$ as $t \rightarrow \infty$. Using Remark 4.2, one can now conclude that the proof of the theorem is complete. ■

4.2.2 Consensus Control Reconfiguration Strategy

To improve the reliability of the team with respect to fault severity estimation errors that are provided by the FDI module, a consensus control reconfiguration strategy is now proposed. Inspired by the team fault estimation error index as stated in Definition 4.3, in this section our objective is to minimize κ_i for the faulty agents while maximizing α_σ . In other words, our goal is to increase the connectivity of the information flow graph while decrease the role of the faulty agents.

To formally present our proposed reconfiguration strategy, let us define the vector $\mathcal{K} = [\kappa_1, \dots, \kappa_n]^T$ and define $L(\mathcal{K}) = [\ell_{ij}(\kappa_i)]$, where $\ell_{ij}(\kappa_i)$ defined as in equation (3.1). Also, let $\alpha_{\mathcal{K}} = \alpha(L(\mathcal{K}))$, $H_{\mathcal{K}} = L_{\mathcal{K}} + 2\frac{\Delta_{\mathcal{K}}}{n}\mathbf{1}\mathbf{1}^T$, where $\Delta_{\mathcal{K}}$ denotes maximum in-degree of all nodes of a graph with a Laplacian matrix equal to $L_{\mathcal{K}}$. Consider $c_{\kappa_i} = \mathcal{C}(\|\hat{\mathcal{F}}_i\|)$, where $\mathcal{C}(\|\hat{\mathcal{F}}_i\|)$ is a positive and increasing function of the fault estimate of the i^{th} agent.

In our proposed reconfiguration strategy we need to obtain a solution to the following optimization problem:

$$\underset{\mathcal{K}}{\text{Minimize}} \quad \sqrt{\mu_{\mathcal{K}}} \frac{C^T \mathcal{K}}{\alpha_{\mathcal{K}}} \quad (4.25)$$

where $C = [c_{\kappa_1}, c_{\kappa_2}, \dots, c_{\kappa_n}]^T$, $\mu_{\mathcal{K}} = \frac{\lambda_{\max}(P_{\mathcal{K}})}{\lambda_{\min}(P_{\mathcal{K}})}$, and $P_{\mathcal{K}}$ is the solution to $P_{\mathcal{K}}H_{\mathcal{K}} + H_{\mathcal{K}}^T P_{\mathcal{K}} - 2\eta\alpha_{\mathcal{K}} = Q_{H_{\sigma}}$. In general, the above optimization problem has no analytical solution and should be solved by numerical methods. Furthermore, since it is a non-convex optimization problem, in general it cannot be guaranteed that the resulting numerical solution is the global one. However, even sub-optimal solutions can improve the fault recovery performance of the team.

There are various numerical methods available to solve the above optimization problem. In this chapter, Nelder–Mead simplex method presented in [142] is used to obtain find sub-optimal solutions to problem (4.25). In other words, a set of sub-optimal values for κ_i is obtained that can be used to reconfigure the weights of agents in the consensus control algorithm that is defined in equation (4.13). In the reconfigured consensus algorithm the healthy agents are allocating higher control efforts and the consensus achievement of the team is less dependent on the control efforts of the faulty agents and therefore, it leads to improving the fault recovery performance of the team.

Since the new set of agent weights are the solution of an optimization problem, it can be argued that the fault recovery performance of the team has been enhanced by using the reconfiguration strategy, however the amount of quantitative improvement is dependent on the information flow graph structure and can be determined only after solving the optimization problem (4.25).

Remark 4.4. *To select c_{κ_i} in the optimization problem (4.25) without considering the severity of faults, it is possible to set it to 1 for faulty agents and set it to 0 for healthy agents.*

4.2.3 Consensus Achievement of the Multi-agent Team in Presence of Actuator Saturation

Our proposed reconfiguration strategy in the previous subsection can also be used to improve the consensus achievement performance of the multi-agent team due to presence of actuator saturations faults. Towards this end, consider that the agents actuators are subject to saturation faults, which is formally presented in equation (4.4) and let us define \mathfrak{U}_i as minimum of the elements of U_i for each agent. Now, we implement the consensus algorithm (4.12) and set $u_i^* = u_i^h$. By following along the same lines as in the proof of Theorem 4.1 one can verify that the following inequality holds.

$$\|u_i^h\| \leq \frac{\kappa_i}{2\eta\alpha_\sigma} \|K\| \sqrt{1 + \frac{1}{|\mathcal{N}_i(t)|}} \|\mathbf{z}\|$$

Therefore, if one can guarantee that the inequality below holds

$$\frac{C^T \mathcal{K}}{\alpha_\sigma} \|\mathbf{z}\| \leq 1 \quad (4.26)$$

where C is set to

$$C = \left[\frac{\|K_R\|}{2\eta\mathfrak{U}_1} \sqrt{1 + \frac{1}{|\mathcal{N}_1(t)|}}, \dots, \frac{\|K_R\|}{2\eta\mathfrak{U}_n} \sqrt{1 + \frac{1}{|\mathcal{N}_n(t)|}} \right]^T \quad (4.27)$$

and $\mathcal{K} = [\kappa_1, \dots, \kappa_n]^T$, is satisfied for $i = 1, \dots, n$ then one can conclude that all actuators in all agents are in their linear operation region and are not saturated.

The above results are now summarized in the following lemma.

Lemma 4.2. *Consider the multi-agent team (4.2) that satisfies Assumption 4.1 and its actuators are subject to saturation faults as defined in (4.4). Consider a piecewise constant switching signal $\sigma(t)$ and let the information flow graph \mathcal{G}_σ satisfies Assumption 4.2. Let α_σ be defined as in equation (4.6) and consider the vector $\mathcal{K} = [\kappa_1, \dots, \kappa_n]^T$ and positive definite matrix Q_A , and let P_A be the solution of the algebraic Riccati equation (4.15) and the relative state*

cooperative control gain K is defined as in equation (4.16). Assume that the initial conditions of the multi-agent team satisfy

$$\|z(0)\| \leq \left(\frac{C^T \mathcal{K}}{\alpha_\sigma} \sqrt{\mu_\sigma \frac{\lambda_{\max}(P_A)}{\lambda_{\min}(P_A)}} \right)^{-1} \quad (4.28)$$

where C is defined as in equation (4.27), and let the control signal u_i^h defined in equation (4.12) be used as the desired control signal for the agent. Then there exists $\tau_a > 0$, such that if the average dwell time of $\sigma(t)$ is τ_a , the multi-agent system (4.2) achieves consensus.

Proof. From equation (4.9) it follows that $\sqrt{\mu_\sigma \frac{\lambda_{\max}(P_A)}{\lambda_{\min}(P_A)}} = \sqrt{\frac{\beta_2}{\beta_1}} \geq 1$ and therefore from condition (4.28) one can verify that the inequality (4.26) holds. This implies that at $t = 0$, none of the actuators are saturated. Thus, following along the same lines as in the proof of Theorem 4.1 and using the same Lyapunov function and noting that all the actuators are in their linear operating region at the initial conditions, one can verify that the inequality (4.24) holds. Using condition (4.28) and the inequality (4.24), for any $t > 0$ we have:

$$\|z(t)\| \leq \left(\frac{C^T \mathcal{K}}{\alpha_\sigma} \right)^{-1}$$

and from the above inequality one can conclude that the inequality (4.26) is always satisfied and none of the actuators are saturated. Therefore, the multi-agent team achieves consensus. ■

It should be pointed out that improving the tolerance of the multi-agent system and extending the acceptable initial condition boundary is an important issue. The idea here is to adjust the agent gains in our proposed weighted consensus algorithm such that agents with larger saturation bounds contribute more control effort towards the consensus achievement of the multi-agent team. As can be seen in the condition (4.28), the acceptable boundary for the initial conditions is proportional to the inverse of $\sqrt{\mu_\sigma \frac{C^T \mathcal{K}}{\alpha_\sigma}}$, and therefore our proposed solution to the optimization problem (4.25) can maximize this bound.

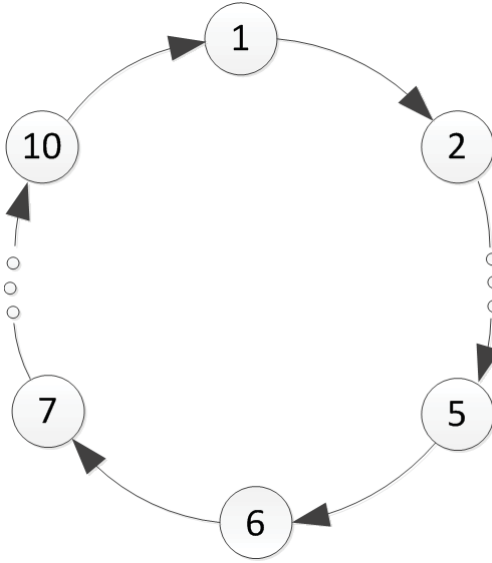


Figure 4.1: Clockwise ring topology of the information flow graph.

4.3 Simulation Results

To show the effectiveness of our proposed fault accommodation method, a multi-agent team of LTI systems consisting of 10 agents having the following representation is considered

$$A = \begin{bmatrix} 0 & 1 & 0 & 0 \\ -1 & 0 & 10 & 10 \\ 0 & 0 & 0 & 0 \\ 0 & 0 & 0 & 0 \end{bmatrix}, \quad B = \begin{bmatrix} 0 & 0 \\ 0 & 0 \\ 1 & 0 \\ 0 & 1 \end{bmatrix}$$

Due to the term $\sqrt{1 + \frac{1}{|\mathcal{N}_i(t)|}}$ in equation (4.14), the worst case scenario to consider is when $|\mathcal{N}_i(t)| = 1$. Therefore, to demonstrate the performance capabilities of our proposed fault recovery strategy, the information flow graph topology is selected to be clockwise or counter-clockwise ring topologies that switches every 10 seconds between them. Figure 4.1 shows the clockwise ring topology.

The design parameter η is set to 0.95, $Q_H = I$ and $Q_A = 10I$. The relative state cooperative control gain is then computed and the resulting matrix is given by:

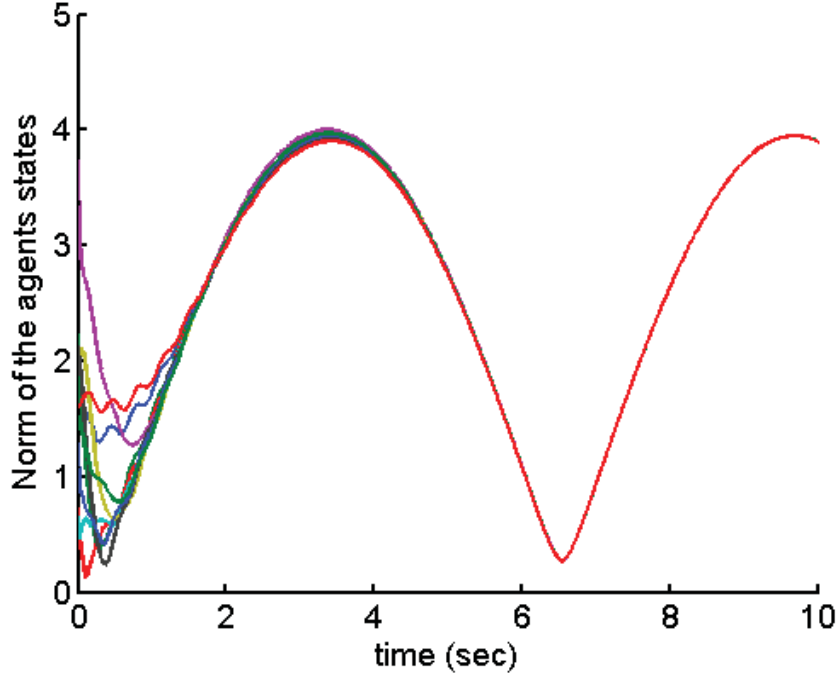


Figure 4.2: Norm of the agents states corresponding to the healthy team.

$$K = \begin{bmatrix} 1.7017 & 2.6654 & 6.9806 & 3.8183 \\ 1.7017 & 2.6654 & 3.8183 & 6.9806 \end{bmatrix}$$

and $G_i = 2.7558$ for $i = 1, \dots, 10$. The initial states of the agents are chosen randomly in the interval $[-2, 2]$. Figure 4.2 shows $\|x_i\|$ corresponding to all agents and Figure 4.3 shows the consensus error of the team, which is defined as follows

$$\sum_{i=1}^n \sum_{j=i+1}^n \|x_i - x_j\|$$

and finally Figure 4.4 illustrates the control signals of the agents. It follows that the team reaches consensus and $\|x_i\|$ remains bounded for all agents and the average consensus team error over 50sec is 1.566.

Now assume that at $t = 1sec$ the 1st, 3rd, 5th, 7th and 9th agents simultaneously face actuator faults with severities of 50% and let the FDI module detects the faults and estimates their severity as 95% of the actual fault severities. Figure 4.5 shows the team consensus error when only our proposed consensus algorithm without reconfiguration strategy is used to accommodate

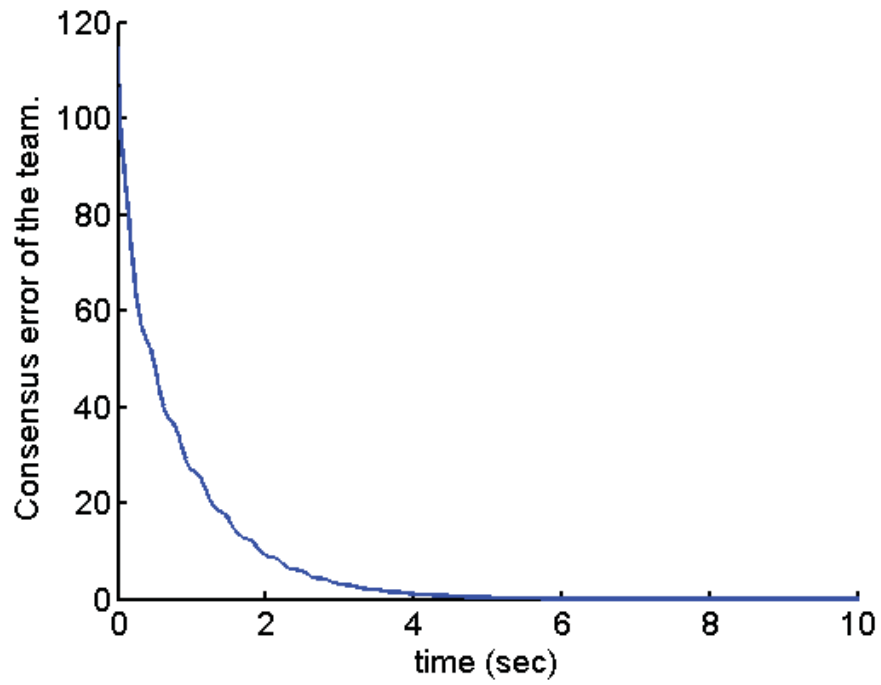


Figure 4.3: Consensus error of the healthy team.

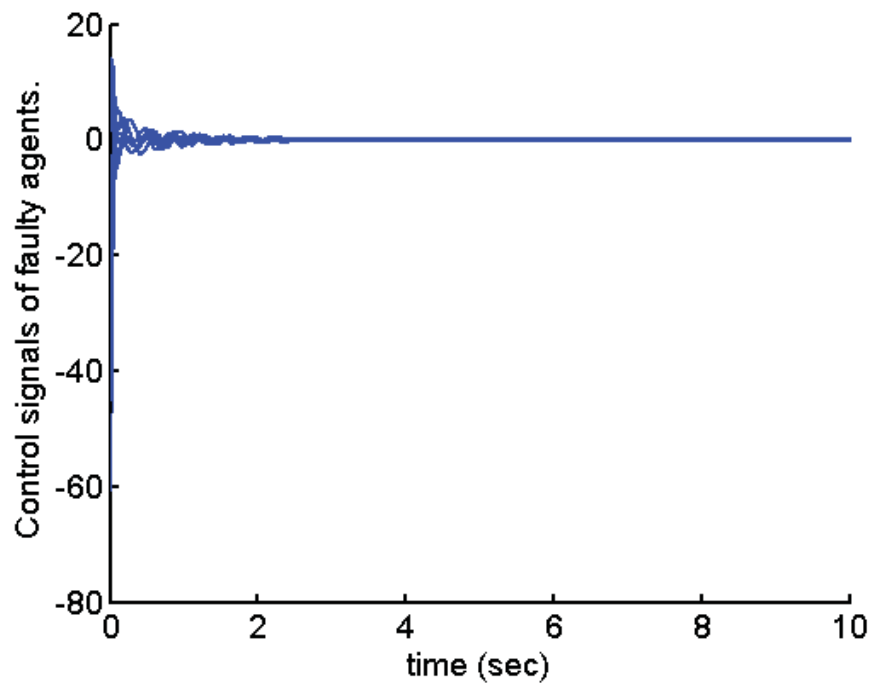


Figure 4.4: Control signals of the healthy team

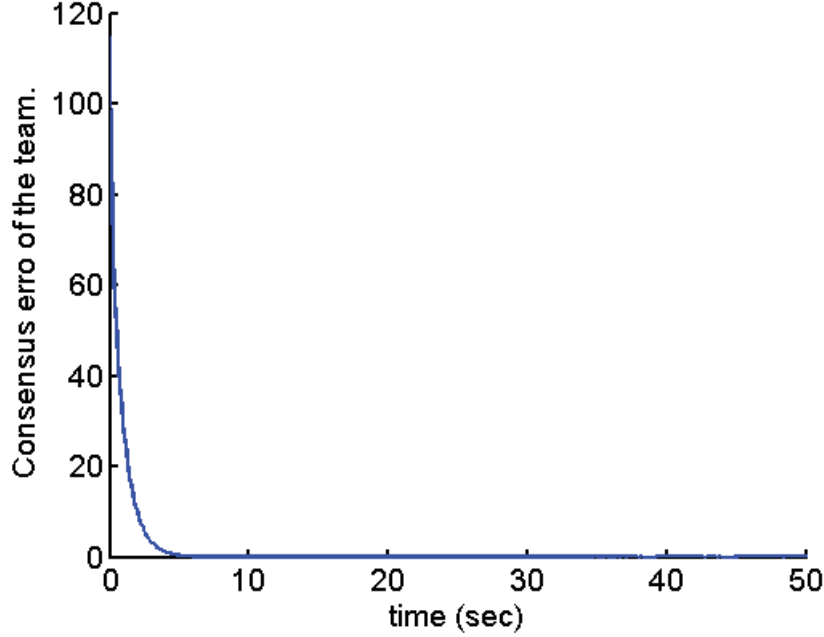


Figure 4.5: Consensus error of the team in presence of faults (95% estimated accurately by the FDI module) by invoking our proposed consensus scheme without reconfiguration.

the faults and Figure 4.6 shows the control signals.

Now consider that the estimate of fault severity is less accurate and it is estimated to within 30% of the actual fault severities. It follows from Figure 4.7 that the team now cannot achieve consensus without using the reconfiguration strategy. Figure 4.8 shows the control signals of the agents.

To implement the reconfiguration strategy, C is selected as stated in Section 4.2.2 according to:

$$\mathcal{C}(\|\hat{\mathcal{F}}_i\|) = \frac{1}{1 - \|\hat{\mathcal{F}}_i\|^2} - 1$$

and the step size \mathfrak{s}_n is set to 0.95. The weights of the agents as defined in equation (4.13) are obtained based on the solutions to the optimization problem (4.25) associated with the clockwise and counter-clockwise ring topologies. By applying Matlab *fminsearch* function as implementation of optimization method presented in [142], the resulting values for the agent weights are obtained as 1.67, 3.84, 1.72, 3.73, 1.82, 3.86, 1.86, 3.86, 1.75, 3.86 for first to 10th

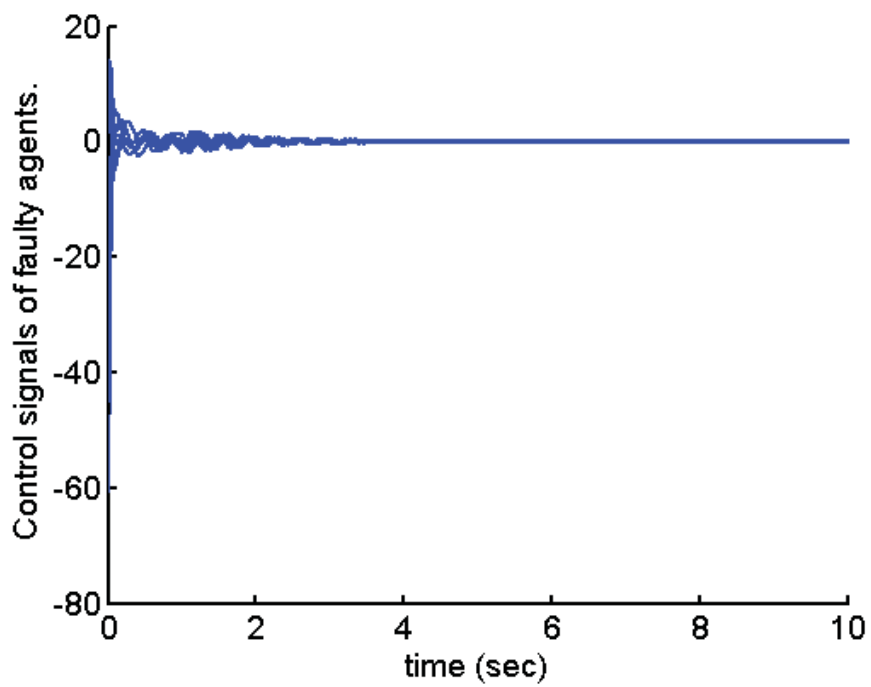


Figure 4.6: Control signals of the team in presence of faults (95% estimated accurately by the FDI module) by invoking our proposed consensus scheme without reconfiguration.

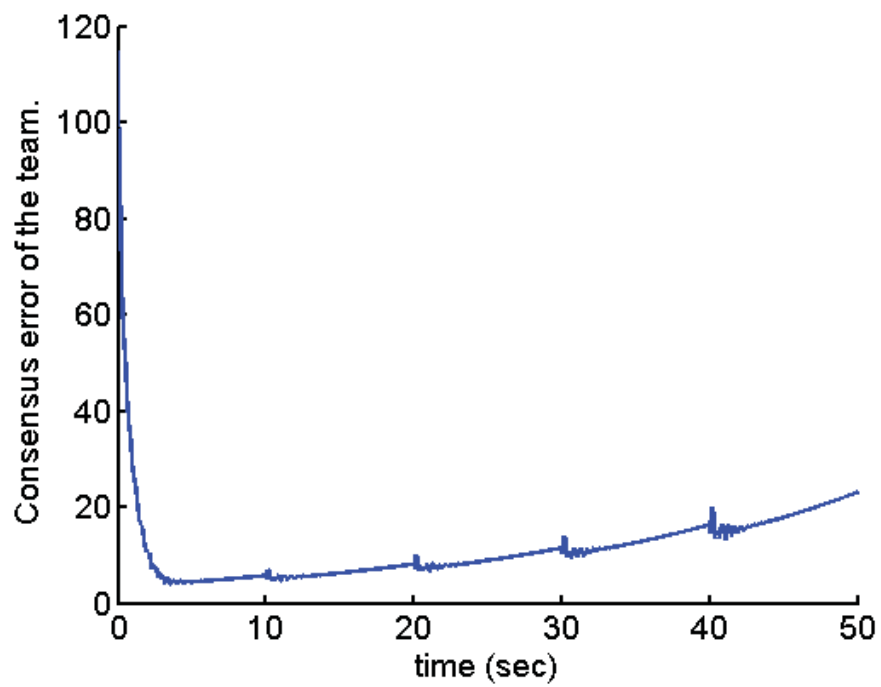


Figure 4.7: Consensus error of the team in presence of faults (30% estimated accurately by the FDI module) by invoking our proposed consensus scheme without reconfiguration.

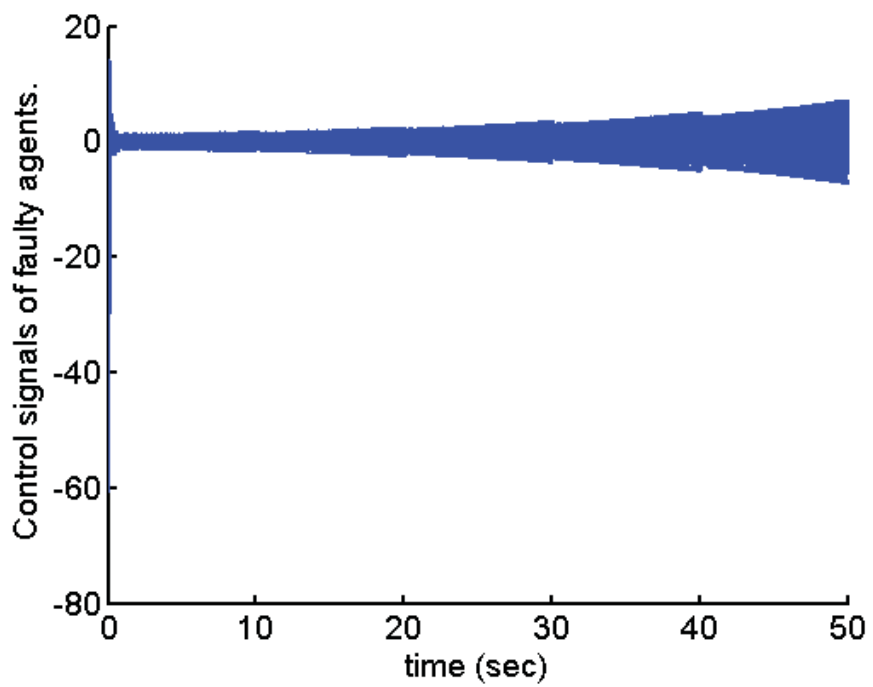


Figure 4.8: Control signals of the team in presence of faults (30% estimated accurately by the FDI module) by invoking our proposed consensus scheme without reconfiguration.

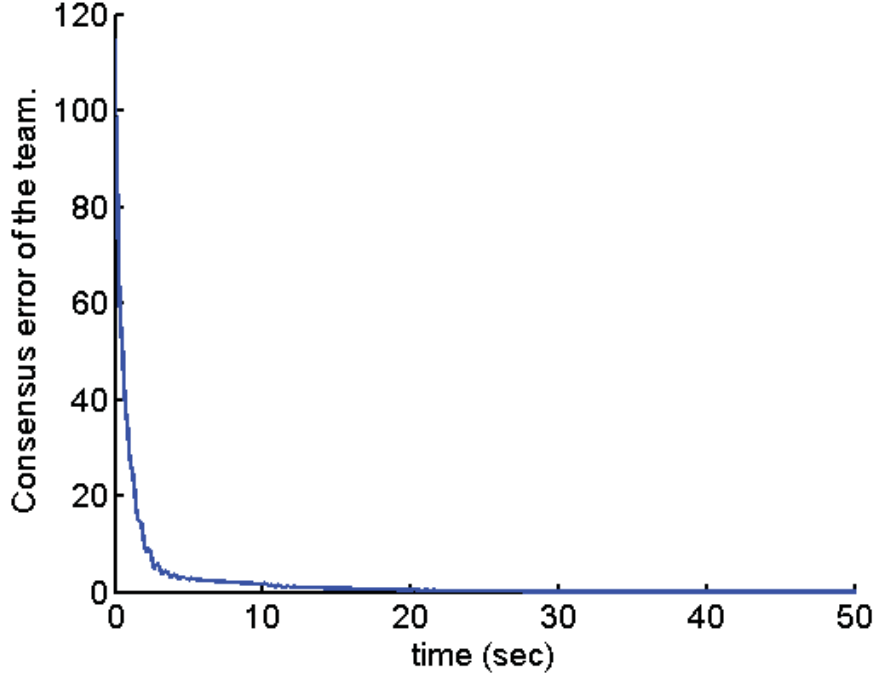


Figure 4.9: Consensus error of the team in presence of faults (30% estimated accurately by the FDI module) by invoking the reconfiguration strategy.

agent, respectively. As stated in Section 4.2, the optimization problem is non-convex and therefore one cannot generally guarantee that the above solution is the global minimum of the optimization problem (4.25). However, it can be shown that the fault tolerant performance of the multi-agent team is significantly improved. Figures 4.9, 4.10 and 4.11 depict the consensus errors of the team, the norms of agent states and control signals after applying the reconfiguration strategy, respectively. In this case, the average of the team consensus error over $50sec$ is 1.966.

It can be observed that the consensus error converges to zero and the norm of agents states remain bounded despite a large amount of uncertainty in the estimation of the fault severities.

Next we compare our proposed algorithm with the work in the literature on centralized and decentralized fault recovery methods as presented in [44]. It is worth noting that in both fault recovery strategies in [44] the communication network topology should be fixed and although the developed recovery algorithms can deal with faults in more than one agent and one can reconfigure

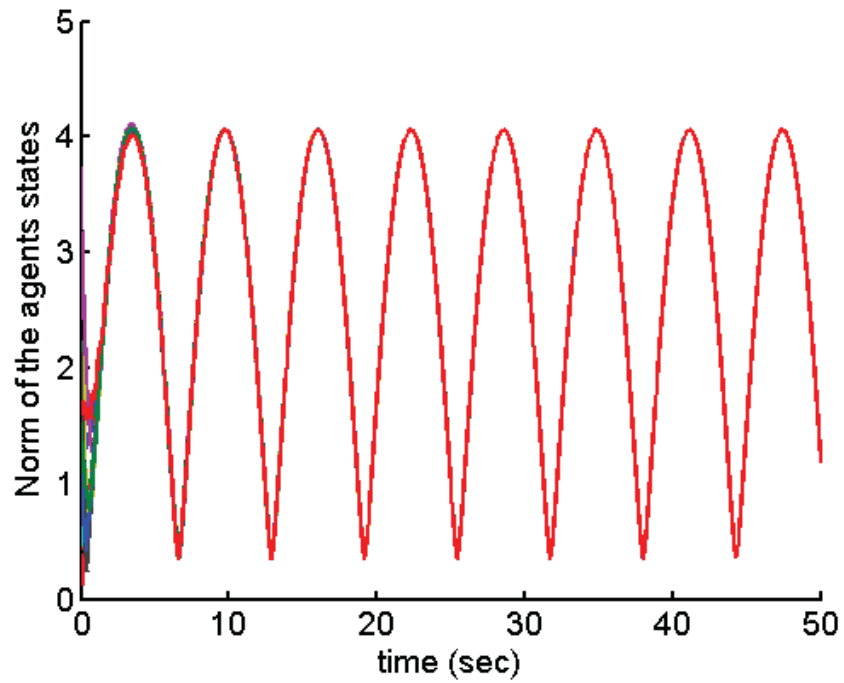


Figure 4.10: Norm of the agent states in presence of faults by invoking the reconfiguration strategy.

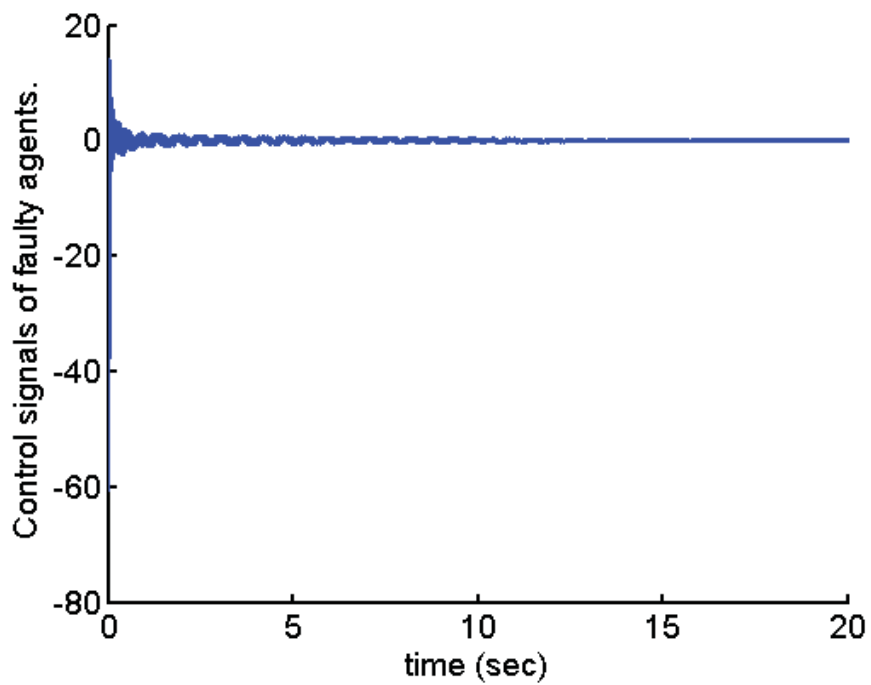


Figure 4.11: Control signals of the team in presence of faults (30% estimated accurately by the FDI module) by invoking the reconfiguration strategy.

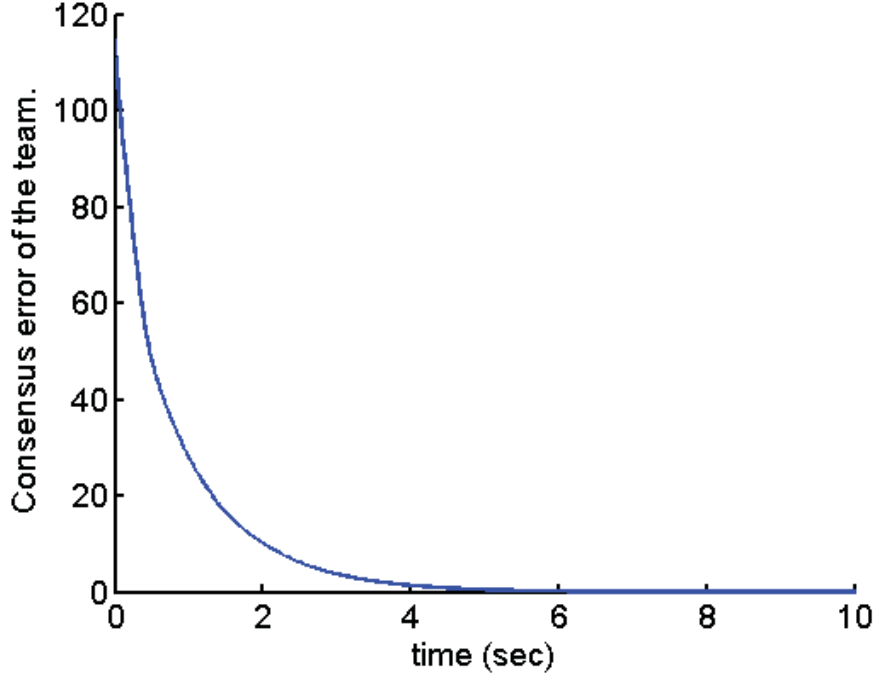


Figure 4.12: Consensus error of the team in presence of faults (30% estimated accurately by the FDI module) by invoking the centralized fault recovery approach developed in [44].

the controller gains based on the estimate of the fault severities, however the effects of inaccurate estimates in more than one agent was not investigated.

For comparison with the centralized approach it is assumed that all agents have access to the relative state measurements of all the other agents. In other words, the information flow graph is undirected and fully connected. In [44] following the fault occurrence and based on the estimate of fault severities the solution of an LMI optimization problem is obtained and a new set of controller gains is computed. Figures 4.12 and 4.13 show the consensus error and control signals of the team as a result of the application of this control strategy. The centralized fault recovery strategy yields an average of the team consensus error over 50sec of 1.3388.

For comparison with the decentralized fault recovery approach that is developed in [44], the topology of the information flow graph remains unchanged and only the controller gains are updated to reconfigure the consensus algorithm. In [44] the agents control gains are fully independent from each other

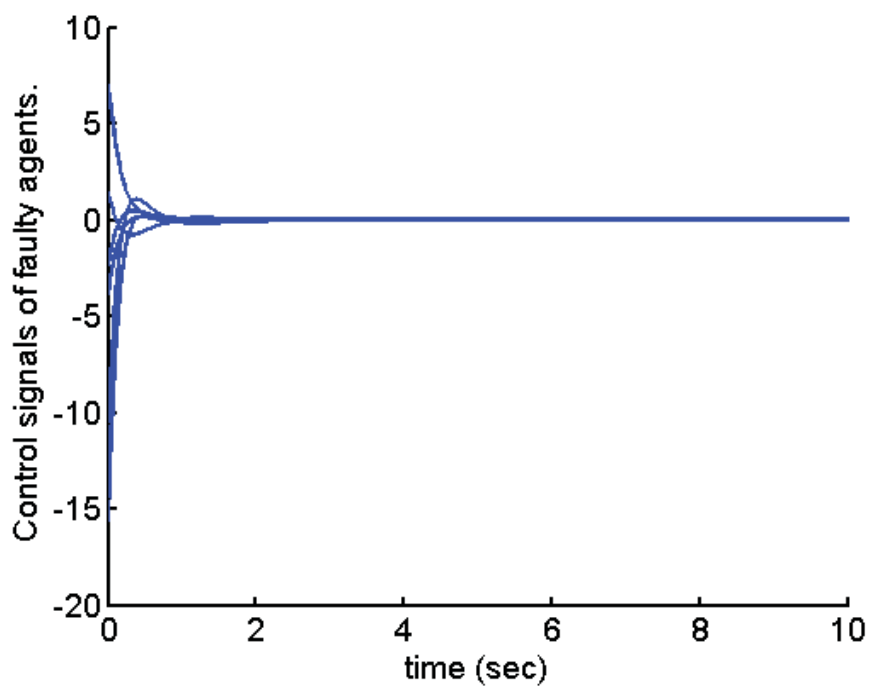


Figure 4.13: Control signals of the team in presence of faults (30% estimated accurately by the FDI module) by invoking the centralized fault recovery approach developed in [44].

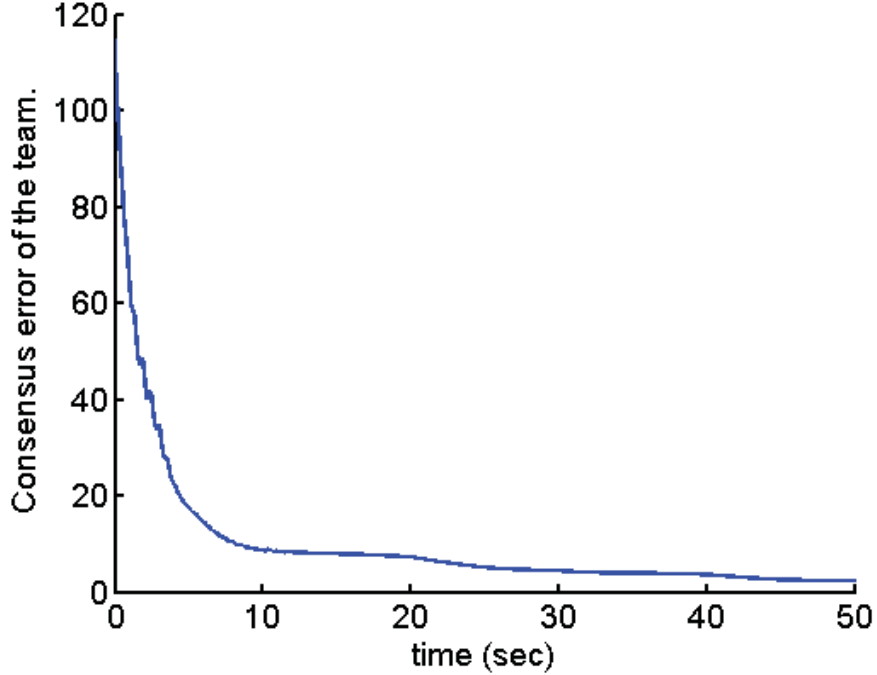


Figure 4.14: Consensus error of the team in presence of faults (30% estimated accurately by the FDI module) by invoking the decentralized fault recovery approach developed in [44].

and are obtained based on the solution of an LMI optimization problem. Figures 4.14 and 4.15 show the consensus error and control signals of the team as a result of the application of this control strategy. The average of the team consensus error over 50sec is 17.964 for the decentralized fault recovery strategy.

As can be observed from results in Figures 4.12 and 4.14 and the average team consensus error, the rate of convergence of the consensus error using our proposed method is significantly faster than the rate of convergence of the decentralized fault recovery method that is developed in [44]. Not surprisingly the performance of the centralized method is the best even when compared to the performance of the healthy team that uses only the ring communication network topology where the network is not fully connected. Notwithstanding the above benefit, due to communication limitations and constraints it is not always feasible to use the centralized method when the number of the agents is too high. Table 4.1 summarizes the above simulation results and

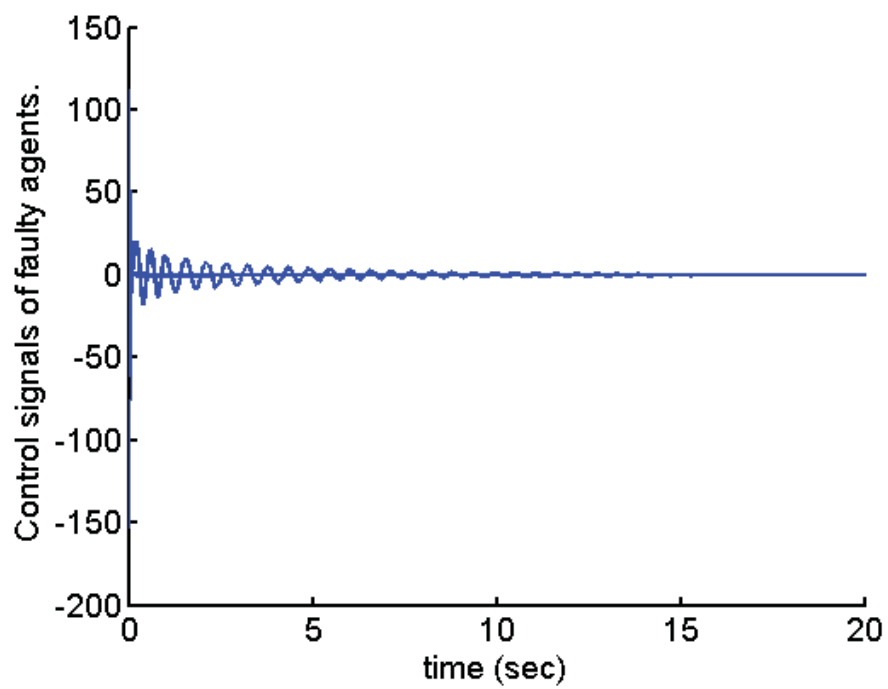


Figure 4.15: Control signals of the team in presence of faults (30% estimated accurately by the FDI module) by invoking the decentralized fault recovery approach developed in [44].

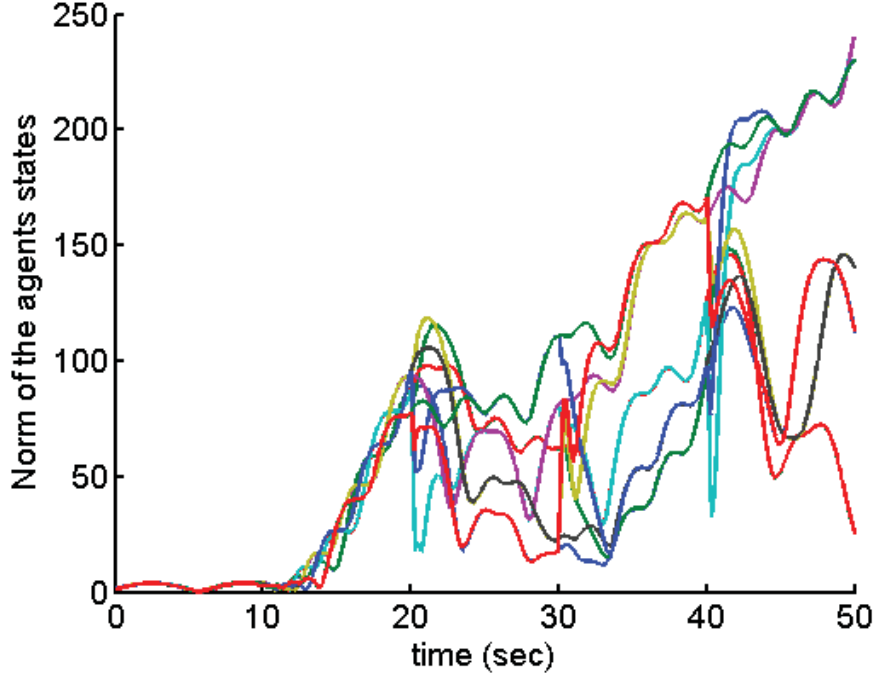


Figure 4.16: Norm of the agents states in presence of actuator saturation faults without using our proposed reconfiguration strategy.

presents quantitative comparisons between our proposed strategy and the one developed in [44].

Finally, to demonstrate the capabilities and effectiveness of our proposed method to deal with actuator saturation fault, next we consider the same multi-agent team and communication networks and assume that the actuators of 1^{th} , 3^{th} , 5^{th} , 7^{th} and 9^{th} agents are saturated and their associated saturation bounds is given by $[1 \ 1]^T$. By employing the same design parameters η , Q_H and Q_A and the same consensus algorithm numerical simulations for the team of multi-agents are conducted. The states of the agents and consensus errors are shown in Figures 4.16 and 4.17, respectively. As can be observed the multi-agent team cannot achieve consensus by using the recovery control strategy in [44] and as shown in Figure 4.18 actuators of faulty agents are saturated. To recover the multi-agent team, the vector C in the optimization problem (4.25) is set as per described in Section 4.2.3 to $[0.1422 \ 0 \ 0.1422 \ 0 \ 0.1422 \ 0 \ 0.1422 \ 0 \ 0.1422 \ 0]^T$. The solution to the optimization problem (4.25) is now computed and the resulting agent gains

Table 4.1: The comparison between our proposed method and the methods in [44].

	Control effort (max)	Control effort (L_2 norm)	Consensus error (RMS)	Settling time (sec)
Healthy team	60.57	9.04	8.317	6.29
Faulty team without using control reconfiguration strategy (95% estimated accurately)	60.57	10.67	8.32	6.4
Faulty team by invoking control reconfiguration strategy (95% estimated accurately)	60.57	9.942	8.321	6.35
Faulty team by invoking centralized method developed in [44] (95% estimated accurately)	25.2	4.33	8.745	6.53
Faulty team by invoking decentralized method developed in [44] (95% estimated accurately)	247.92	47.87	15.28	102.4
Faulty team without using control reconfiguration strategy (30% estimated accurately)	60.57	316.6	14.15	unstable
Faulty team by invoking control reconfiguration strategy (30% estimated accurately)	60.57	19.8	8.394	25.8
Faulty team by invoking centralized method developed in [44] (30% estimated accurately)	15.62	4.28	8.975	6.68
Faulty team by invoking decentralized method developed in [44] (30% estimated accurately)	153.12	56.87	16.83	143.58

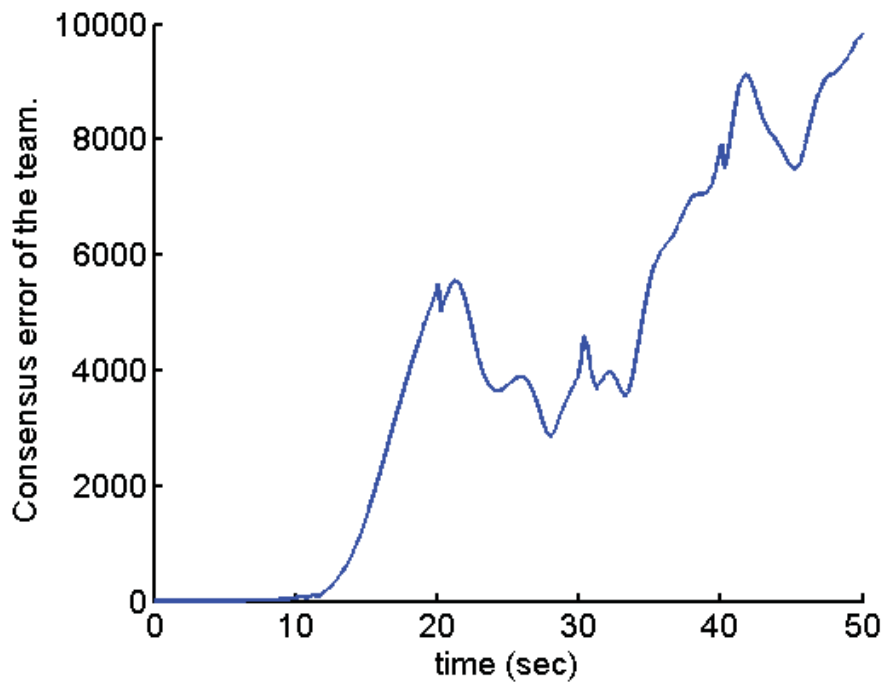


Figure 4.17: Consensus error of the team in presence of actuator saturation faults without using our proposed reconfiguration strategy.

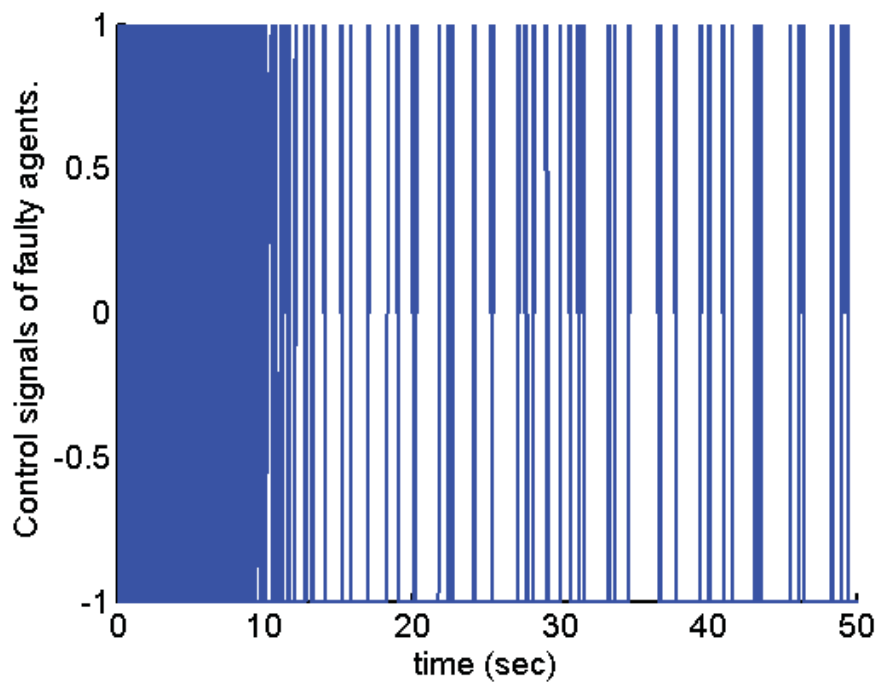


Figure 4.18: Control signals of the agents affected by actuator saturation faults without using our proposed reconfiguration strategy.

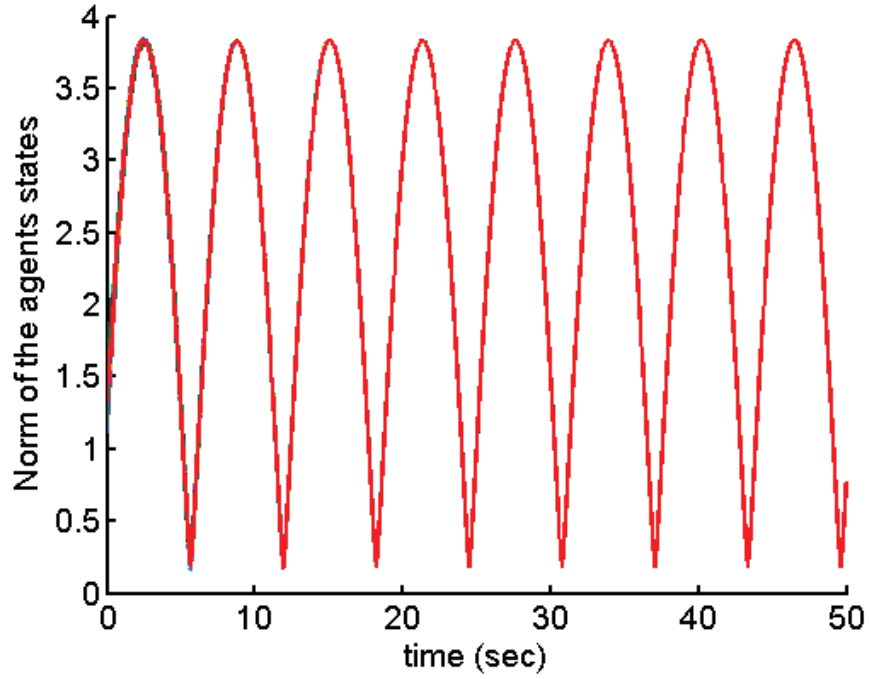


Figure 4.19: Norm of the agents states in presence of actuator saturation faults by invoking our proposed reconfiguration strategy.

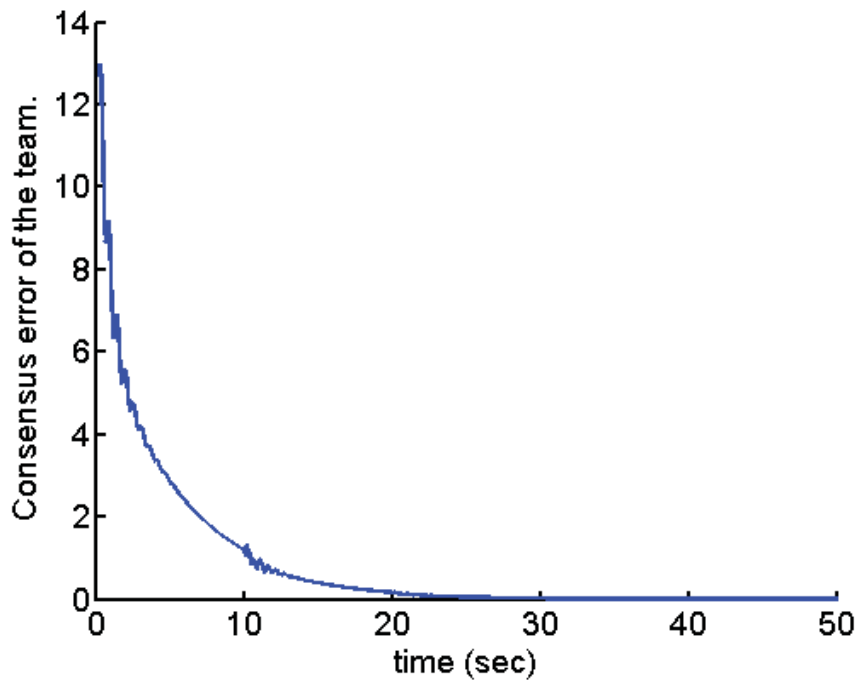


Figure 4.20: Consensus error of the team in presence of actuator saturation faults by invoking our proposed reconfiguration strategy.

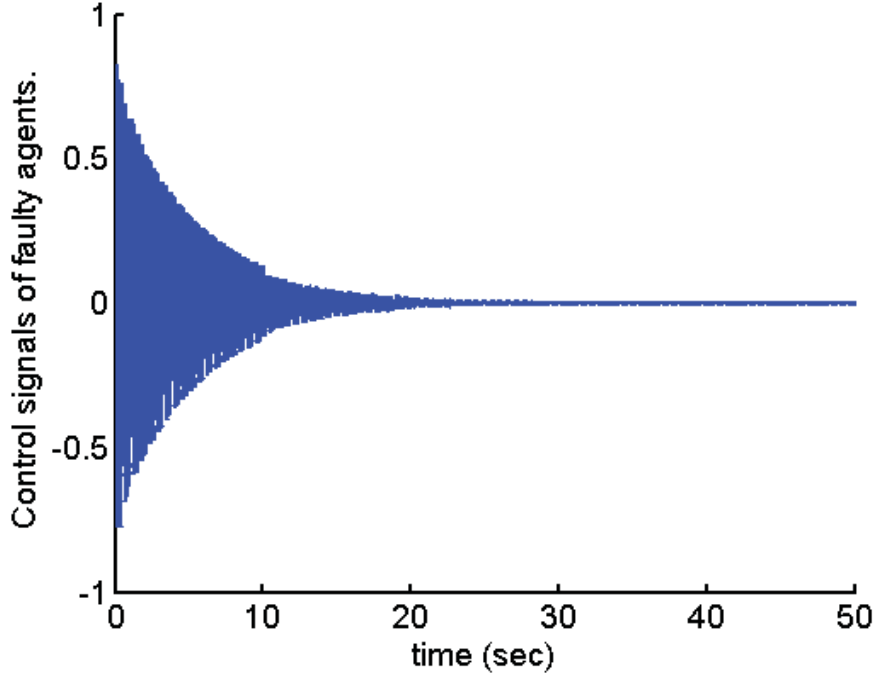


Figure 4.21: Control signals of the agents affected by actuator saturation faults by invoking our proposed reconfiguration strategy.

are obtained as 1.25, 5.27, 1.20, 2.57, 1.17, 5.08, 1.20, 5.01, 1.25, 5.21 for first to 10th agent, respectively. Figures 4.19, 4.20 and 4.21 show the simulation results of the recovered multi-agent team that confirms that the team achieves consensus and none of the actuators are saturated. Table 4.2 provides the comparative summary of the faulty multi-agent system with and without the control recovery implementation subject to saturation fault.

4.4 Summary

In this chapter, a fault tolerant consensus scheme for a team of LTI multi-agent systems is developed under switching topologies and directed communication network graph. A weighted consensus algorithm is proposed for consensus achievement of the multi-agent system based on an inaccurate estimate of the fault severities. Moreover, a control reconfiguration strategy is also proposed to improve the fault tolerance capabilities of our proposed consensus strategy. The faults can occur simultaneously in any number of agents and there is no

Table 4.2: The comparison between consensus performance of the team in presence of actuator saturations

	Without using control reconfiguration strategy	By invoking control reconfiguration strategy
Control effort of faulty agents (max)	1	0.8268
Control effort (L_2 norm)	unstable	10.28
Consensus error (RMS)	unstable	2.036
Settling time (sec)	unstable	21.7

need to have an accurate knowledge of the fault severities. Two kinds of faults are considered, namely a loss-of-effectiveness and a control saturation in the actuators. The stability of the overall closed-loop switched system is shown by using Lyapunov analysis. Finally, it is shown how to remedy the actuator faults and saturations in the multi-agent team and improve the consensus achievement performance by employing our proposed reconfiguration strategy. The effectiveness and capabilities of our proposed consensus algorithms are illustrated through numerical simulations to a team of ten multi-agent systems where the performance of our proposed methods is compared with the performance of centralized and decentralized fault recovery methods that are available in the literature.

In the next chapter we address the disturbance attenuation properties of consensus achievement algorithms for a multi-agent team with output measurement noise and teams of agents with model uncertainties including Lipschitz nonlinearity. Furthermore, we propose a cooperative-adaptive consensus algorithm for a team of multi-agent systems with unknown nonlinearity.

Chapter 5

Consensus Achievement of Multi-Agent Teams In Presence of Measurement Noise and Model Uncertainties

In this chapter, the disturbance attenuation properties of consensus achievement algorithms for a multi-agent team with output measurement noise and teams of agents with model uncertainties including Lipschitz nonlinearity are investigated. The communication network topology is assumed to be switching. The teams are homogeneous and the information flow graph is directed. The sufficient conditions to design observers and distributed controllers are presented. Based on the solution of two algebraic Riccati equations and without need to solve linear matrix inequalities (LMIs), design techniques are proposed. The stability of the proposed controllers are investigated based on Lyapunov stability analysis. The effectiveness of the proposed consensus algorithm is illustrated by performing numerical simulations.

Furthermore, a cooperative-adaptive consensus algorithm for a team of multi-agent systems with unknown non-linearity in presence of unknown disturbance signals is presented. In this proposed cooperative learning method each agent shares the knowledge learned about the non-linearity with its neighboring agents to improve the overall performance of the team.

5.1 Consensus Achievement in Presence of Measurement Noise

In this section we consider LTI multi-agent systems and assume that agents only have access to their measured outputs which is contaminated by noise. First, we present the problem statement of this section and based on a new variable that is presented we drive the overall dynamics of the team. Furthermore, the main result of this section is presented as a theorem and validity of our analytical results are verified by performing numerical simulations.

5.1.1 Problem Statement And The Main Result

To formally present the problem statement of this section we consider a multi-agent system with N agents where their dynamics is described by the following equations:

$$\begin{cases} \dot{x}_i = Ax_i + Bu_i + B_2\omega_i \\ y_i = Cx_i + \nu_i \end{cases} \quad (5.1)$$

where $A \in \mathbb{R}^{p \times p}$, $B \in \mathbb{R}^{p \times m}$, $C \in \mathbb{R}^{r \times p}$, $B_2 \in \mathbb{R}^{p \times q}$ denote real matrices, and $x_i \in \mathbb{R}^p$ and $u_i \in \mathbb{R}^m$, $y_i \in \mathbb{R}^r$, $\omega_i \in \mathbb{R}^q$, and $\nu_i \in \mathbb{R}^r$ denote state, control input, output, disturbance, and measurement noise of the i^{th} agent, respectively. We also assume that the dynamics of all agents satisfy the Assumption 5.1.

Assumption 5.1. *In this section it is assumed that the matrix A is not Hurwitz (see Remark 3.5), the pair (A, B) is controllable, and the pair (A, C) is observable.*

In the remainder of this section, our objective is to design a distributed cooperative control law u_i for the agent to ensure that the team while achieves output consensus as per Definition 5.1 and can reject effects of input disturbances and measurement noise as per Definition 5.2.

Definition 5.1. *The control input u_i solves the output-consensus problem if*

$$\|y_i - y_j\| \rightarrow 0 \text{ as } t \rightarrow \infty, \forall i, j \in \{1, \dots, n\} \quad (5.2)$$

Definition 5.2. *The multi-agent system (5.1) achieves H_∞ output consensus in presence of disturbance input and measurement noise with bounds γ_ρ and γ_n if*

- *it achieves output consensus as per Definition 5.1 when there is no disturbance, nor measurement noise,*
- *and there exists a positive constant ξ such that for any $T > 0$ in presence of disturbance input and measurement noise, the following inequality holds:*

$$\begin{aligned} \frac{1}{n} \left(\sum_{i=1}^n \sum_{j=i+1}^n \frac{1}{T} \int_0^T \|y_i - y_j\| dt \right) &\leq \gamma_\rho^2 \sum_{i=1}^n \frac{1}{T} \int_0^T \|\omega_i\|^2 dt \\ &+ \gamma_n^2 \sum_{i=1}^n \frac{1}{T} \int_0^T \|\nu_i\|^2 dt. \end{aligned}$$

Before we continue, let us define the relative state as $\Xi_i = \sum_{j \in \mathcal{N}_i} x_i - x_j$ and the relative output as $\mathcal{Y}_i = \sum_{j \in \mathcal{N}_i} y_i - y_j$ for the i^{th} agent.

To design the consensus algorithm, let us introduce the following augmented system which represents the dynamics of the entire multi-agent system

$$\begin{cases} \dot{\mathbf{x}} = (I \otimes A)\mathbf{x} + (I \otimes B)\mathbf{u} + (I \otimes B_2)\boldsymbol{\omega} \\ \mathbf{y} = (I \otimes C)\mathbf{x} + \boldsymbol{\nu} \end{cases} \quad (5.3)$$

where $\mathbf{x} = [x_1, \dots, x_n]^T$, $\mathbf{u}(\mathbf{x}) = [u_1, \dots, u_n]^T$, $\boldsymbol{\omega} = [\omega_1, \dots, \omega_n]^T$ and $\mathbf{y} = [y_1, \dots, y_n]^T$. Now let us introduce the relative state vector $\Xi = [\Xi_1^T, \dots, \Xi_n^T]^T$ and relative the output vector $\mathcal{Y} = [\mathcal{Y}_1^T, \dots, \mathcal{Y}_n^T]^T$. By replacing these vectors into equation (5.3) one can obtain:

$$\Xi = (L_\sigma \otimes I)\mathbf{x} \quad (5.4)$$

$$\mathcal{Y} = (L_\sigma \otimes I)\mathbf{y} = (I \otimes C)\Xi + (L_\sigma \otimes I)\boldsymbol{\nu}$$

where L_σ is the Laplacian matrix of the communication network as per Definition 3.8. From equation (5.3) we have:

$$\begin{aligned} \dot{\Xi} = (L_\sigma \otimes I)\dot{\mathbf{x}} &= (L_\sigma \otimes A)\mathbf{x} + (L_\sigma \otimes B)\mathbf{u} + (L_\sigma \otimes B_2)\boldsymbol{\omega} = (I \otimes A)\Xi + (L_\sigma \otimes B)\mathbf{u} + (L_\sigma \otimes B_2)\boldsymbol{\omega} \end{aligned} \quad (5.5)$$

In order to use the same framework which we developed in the Chapters 3 and 4 to design the consensus algorithm for the team, we need to estimate the relative states of the agents. Towards this end, the relative states of the team can be estimated by using the following observer:

$$\dot{\hat{\Xi}} = (I \otimes A)\hat{\Xi} + (L_\sigma \otimes B)\mathbf{u} + (I \otimes GC)\hat{\Xi} - (I \otimes G)\mathcal{Y} \quad (5.6)$$

where $\hat{\Xi}$ denotes the estimated relative state and the matrix G denotes the observer gain. Let us denote the estimation error by $\mathbf{e} = \hat{\Xi} - \Xi$. Therefore, we have:

$$\dot{\mathbf{e}} = I \otimes (A + GC)\mathbf{e} - (L_\sigma \otimes B_2)\omega - (L_\sigma \otimes G)\nu \quad (5.7)$$

Consider the following Lyapunov function candidate

$$V_o = \mathbf{e}^T (P_{H_\sigma} \otimes P_o)\mathbf{e} \quad (5.8)$$

The time derivative of (5.8) along the trajectories of equation (5.7) is given by:

$$\begin{aligned} \dot{V}_o &= \mathbf{e}^T (P_{H_\sigma} \otimes (P_o(A + GC) + (A + GC)^T P_o))\mathbf{e} - 2\mathbf{e}^T (P_{H_\sigma} L_\sigma \otimes P_o B_2)\omega \\ &\quad - 2\mathbf{e}^T (P_{H_\sigma} L_\sigma \otimes P_o G)\nu \end{aligned} \quad (5.9)$$

Knowing that for any positive definite matrices \mathcal{P}_1 and \mathcal{P}_2 , the vectors \mathbf{v}_1 and \mathbf{v}_2 , and a positive constant γ , the following inequality then holds:

$$0 \leq (\gamma \mathbf{v}_1^T (\mathcal{P}_1 \otimes \mathcal{P}_2) - \gamma^{-1} \mathbf{v}_2^T) (\gamma (\mathcal{P}_1^T \otimes \mathcal{P}_2^T) \mathbf{v}_1 - \gamma^{-1} \mathbf{v}_2)$$

One can verify that in view of the above the following inequality is now valid:

$$2\mathbf{v}_1^T (\mathcal{P}_1 \otimes \mathcal{P}_2) \mathbf{v}_2 \leq \gamma^2 \mathbf{v}_1^T (\mathcal{P}_1 \mathcal{P}_1^T \otimes \mathcal{P}_2 \mathcal{P}_2^T) \mathbf{v}_1 + \gamma^{-2} \mathbf{v}_2^T \mathbf{v}_2 \quad (5.10)$$

One can also verify that the following inequality holds for any positive constants γ_R by using the above inequality and by setting $\gamma = \gamma_R \sqrt{\lambda_{\min}(P_{H_\sigma})}$

:

$$\begin{aligned}
& 2\mathbf{e}^T(P_{H_\sigma}L_\sigma \otimes P_oB_2)\omega \\
& \leq \lambda_{\min}(P_{H_\sigma})^{-1}\gamma_R^{-2}\mathbf{e}^T(P_{H_\sigma}L_\sigma L_\sigma^T P_{H_\sigma} \otimes P_oB_2B_2^T P_o)\mathbf{e} + \lambda_{\min}(P_{H_\sigma})\gamma_R^2\omega^T\omega \\
& \leq \mu_\sigma\lambda_{\max}(L_\sigma^T L_\sigma)\gamma_R^{-2}\mathbf{e}^T(P_{H_\sigma} \otimes P_oB_2B_2^T P_o)\mathbf{e} + \lambda_{\min}(P_{H_\sigma})\gamma_R^2\omega^T\omega
\end{aligned} \tag{5.11}$$

Similarly, for any positive constant γ_ν by taking $\gamma = \gamma_\nu\sqrt{\frac{1}{2}\lambda_{\min}(P_{H_\sigma})}$ we have:

$$\begin{aligned}
& 2\mathbf{e}^T(P_{H_\sigma}L_\sigma \otimes P_oG)\nu \\
& \leq \frac{1}{2}\lambda_{\min}(P_{H_\sigma})^{-1}\gamma_\nu^{-2}\mathbf{e}^T(P_{H_\sigma}L_\sigma L_\sigma^T P_{H_\sigma} \otimes P_oGG^T P_o)\mathbf{e} + 2\lambda_{\min}(P_{H_\sigma})\gamma_\nu^2\nu^T\nu \\
& \leq \frac{1}{2}\mu_\sigma\lambda_{\max}(L_\sigma^T L_\sigma)\gamma_\nu^{-2}\mathbf{e}^T(P_{H_\sigma} \otimes P_oGG^T P_o)\mathbf{e} + 2\lambda_{\min}(P_{H_\sigma})\gamma_\nu^2\nu^T\nu
\end{aligned} \tag{5.12}$$

Using the above inequality one can verify that the following inequality holds for positive constants γ_R and γ_ν :

$$\begin{aligned}
\dot{V}_o & \leq \mathbf{e}^T(P_{H_\sigma} \otimes (P_o(A + GC) + (A + GC)^T P_o))\mathbf{e} \\
& \quad + \mu_\sigma\lambda_{\max}(L_\sigma^T L_\sigma)\gamma_R^{-2}\mathbf{e}^T(P_{H_\sigma} \otimes P_oB_2B_2^T P_o)\mathbf{e} + \lambda_{\min}(P_{H_\sigma})\gamma_R^2\omega^T\omega \\
& \quad + \frac{1}{2}\mu_\sigma\lambda_{\max}(L_\sigma^T L_\sigma)\gamma_\nu^{-2}\mathbf{e}^T(P_{H_\sigma} \otimes P_oGG^T P_o)\mathbf{e} + 2\lambda_{\min}(P_{H_\sigma})\gamma_\nu^2\nu^T\nu
\end{aligned} \tag{5.13}$$

Now, let P_A be a solution to the following algebraic Riccati equation

$$\begin{aligned}
-Q_o & = P_o(A + GC) + (A + GC)^T P_o + \delta P_o \\
& \quad + \mu_\sigma\lambda_{\max}(L_\sigma^T L_\sigma) \left(\frac{1}{2}\gamma_\nu^{-2}P_oGG^T P_o + \gamma_R^{-2}P_oB_2B_2^T P_o \right)
\end{aligned} \tag{5.14}$$

where Q_o denotes a positive definite matrix and δ denotes a positive constant. Therefore, we have:

$$\dot{V}_o \leq -\mathbf{e}^T(P_{H_\sigma} \otimes (Q_o + \delta P_o))\mathbf{e} + \lambda_{\min}(P_{H_\sigma})\gamma_R^2\|\omega\|^2 + 2\lambda_{\min}(P_{H_\sigma})\gamma_\nu^2\|\nu\|^2 \tag{5.15}$$

Let us propose our distributed consensus control algorithm as

$$\mathbf{u} = -\frac{1}{2\eta\alpha_\sigma}(I \otimes B^T P_A)\hat{\Xi} = -\frac{1}{2\eta\alpha_\sigma}(L_\sigma \otimes B^T P_A)\mathbf{x} - \frac{1}{2\eta\alpha_\sigma}(I \otimes B^T P_A)\mathbf{e} \tag{5.16}$$

where $0 < \eta < 1$ is a real constant, α_σ is a connectivity measure of the communication network and defined in Definition 4.2, and P_A is a positive definite matrix.

Lemma 5.1. *Consider the vectors $x_1, \dots, x_n, \bar{x} \in \mathfrak{R}^q$ and let us define $z_i = x_i - \bar{x}$ for $i = 1, \dots, n$, then the following inequality is satisfied:*

$$0 \leq \sum_{i=1}^n \sum_{j=i+1}^n \|x_i - x_j\|^2 \leq n \sum_{i=1}^n \|z_i\|^2 \quad (5.17)$$

Proof. We have:

$$\begin{aligned} \sum_{i=1}^n \sum_{j=i+1}^n \|x_i - x_j\|^2 &= \sum_{i=1}^n \sum_{j=i+1}^n \|z_i - z_j\|^2 = \\ &= (n-1) \sum_{i=1}^n \|z_i\|^2 - \sum_{i=1}^n \sum_{j=i+1}^n (z_i^T z_j + z_j^T z_i) \end{aligned} \quad (5.18)$$

and we know that

$$\begin{aligned} \left(\sum_{i=1}^n z_i \right)^T \left(\sum_{i=1}^n z_i \right) &= \sum_{i=1}^n \|z_i\|^2 \\ &+ \sum_{i=1}^n \sum_{j=i+1}^n z_i^T z_j + z_j^T z_i \geq 0 \end{aligned}$$

which concludes the proof of the lemma. ■

Remark 5.1. *Consider the multi-agent system (5.3) and assume that $\nu = 0$. Note that for any vector $\bar{x}(t)$, one can write*

$$\|y_i - y_j\| = \|Cx_i - Cx_j\| = \|Cx_i - C\bar{x} - Cx_j + C\bar{x}\| = \|Cz_i - Cz_j\| \leq \|Cz_i\| + \|Cz_j\|$$

where,

$$z_i = x_i - \bar{x}.$$

Therefore, if $z_i \rightarrow 0$ as $t \rightarrow \infty, \forall i \in \{1, \dots, n\}$ then the multi-agent system (5.3) achieves consensus.

Similar as in Chapter 4, let us introduce the virtual agent with the following

dynamics:

$$\dot{\bar{x}} = A\bar{x} - \frac{\Delta_\sigma}{n\eta\alpha_\sigma} BB^T P_A \sum_{j=1}^n (\bar{x} - x_j) \quad (5.19)$$

where Δ_σ is the maximum degree of the Laplacian matrix L_σ .

Now, let us define the vector $\mathbf{z} = [z_1, \dots, z_n]^T$. This implies that $\mathbf{z} = \mathbf{x} - \mathbf{1} \otimes \bar{x}$ where $\mathbf{1} = [1, \dots, 1]^T$. It can be verified that for any matrix $\mathcal{M} \in \mathfrak{R}^{p \times p}$ we have $\mathcal{M}z_i = \mathcal{M}x_i - \mathcal{M}\bar{x}$, therefore $I \otimes \mathcal{M}\mathbf{z} = I \otimes \mathcal{M}\mathbf{x} - (L_\sigma \mathbf{1}) \otimes \mathcal{M}\bar{x}$. Furthermore, one can verify that the following equation holds:

$$(L_\sigma \otimes \mathcal{M})\mathbf{z} = (L_\sigma \otimes \mathcal{M})\mathbf{x} - ((L_\sigma \mathbf{1}) \otimes \mathcal{M})\bar{x} = (L_\sigma \otimes \mathcal{M})\mathbf{x} \quad (5.20)$$

Using the above equation and dynamics of the augmented system (5.3) one can obtain:

$$\begin{aligned} \dot{\mathbf{z}} = & (I \otimes (A - \frac{1}{2}BB^T P_A))\mathbf{z} - \frac{1}{2\eta\alpha_\sigma} ((H_\sigma - \eta\alpha_\sigma I) \otimes BB^T P_A)\mathbf{z} \\ & - \frac{1}{2\eta\alpha_\sigma} (I \otimes BB^T P_A)\mathbf{e} + (I \otimes B_2)\omega \end{aligned} \quad (5.21)$$

where $\mathbf{z} = \mathbf{x} - \mathbf{1} \otimes \bar{x}$. The time derivative of the Lyapunov function candidate

$$V_A = \mathbf{z}^T (P_{H_\sigma} \otimes P_A)\mathbf{z} \quad (5.22)$$

along the trajectories of the equation (5.21) yields:

$$\begin{aligned} \dot{V}_A = & \mathbf{z}^T (P_{H_\sigma} \otimes (P_A A + A^T P_A - P_A BB^T P_A))\mathbf{z} - \frac{1}{2\eta\alpha_\sigma} \mathbf{z}^T (Q_{H_\sigma} \otimes P_A BB^T P_A)\mathbf{z} \\ & - \frac{1}{\eta\alpha_\sigma} \mathbf{z}^T (P_{H_\sigma} \otimes P_A BB^T P_A)\mathbf{e} + \mathbf{z}^T (P_{H_\sigma} \otimes P_A B_2)\omega \end{aligned} \quad (5.23)$$

Using the inequality (5.10) one gets:

$$\begin{aligned}
\dot{V}_A &\leq \mathbf{z}^T (P_{H_\sigma} \otimes (P_A A + A^T P_A - P_A B B^T P_A)) \mathbf{z} - \frac{1}{\eta \alpha_\sigma} \mathbf{z}^T (P_{H_\sigma} \otimes P_A B B^T P_A) \mathbf{e} \\
&+ \frac{\gamma_R^{-2}}{\lambda_{\min}(P_{H_\sigma})} \mathbf{z} (P_{H_\sigma}^2 \otimes P_A B_2 B_2^T P_A) \mathbf{z} + \lambda_{\min}(P_{H_\sigma}) \gamma_R^2 \|\omega\|^2 \\
&+ 2\lambda_{\min}(P_{H_\sigma}) \mathbf{z}^T (I \otimes C^T C) \mathbf{z} - 2\lambda_{\min}(P_{H_\sigma}) \mathbf{z}^T (I \otimes C^T C) \mathbf{z}
\end{aligned} \tag{5.24}$$

Assume that P_A is a solution to the algebraic Riccati equation (5.25)

$$P_A A + A^T P_A - P_A B B^T P_A + \mu_\sigma \gamma_R^{-2} P_A B_2 B_2^T P_A + 2C^T C = -Q_A \tag{5.25}$$

where Q_A is a positive definite matrix. We have:

$$\begin{aligned}
\dot{V}_A &\leq -\mathbf{z}^T (P_{H_\sigma} \otimes Q_A) \mathbf{z} - \frac{1}{\eta \alpha_\sigma} \mathbf{z}^T (P_{H_\sigma} \otimes P_A B B^T P_A) \mathbf{e} \\
&+ \lambda_{\min}(P_{H_\sigma}) (\gamma_R^2 \|\omega\|^2 - 2\mathbf{z}^T I \otimes C^T C \mathbf{z})
\end{aligned} \tag{5.26}$$

Now, let us consider the following piece-wise quadratic function as our Lyapunov function to analyze the consensus achievement of the overall team:

$$V_\sigma = V_\sigma(\mathbf{z}, \mathbf{e}) = \mathbf{z}^T (P_{H_\sigma} \otimes P_A) \mathbf{z} + \mathbf{e}^T (P_{H_\sigma} \otimes P_o) \mathbf{e} \tag{5.27}$$

Note that V_σ is the sum of piece-wise quadratic function V_o as per equation (5.8) and piece-wise quadratic function V_A as per equation (5.22). Therefore, one can use inequalities (5.15) and (5.26) to obtain the time derivative of the Lyapunov function (5.27) along the trajectories of the multi-agent system (5.1) and can verify that it satisfies the following inequality:

$$\begin{aligned}
\dot{V}_\sigma &= \dot{V}_A + \dot{V}_o \leq -\mathbf{z}^T (P_{H_\sigma} \otimes Q_A) \mathbf{z} - \frac{1}{\eta \alpha_\sigma} \mathbf{z}^T (P_{H_\sigma} \otimes P_A B B^T P_A) \mathbf{e} \\
&- \mathbf{e}^T (P_{H_\sigma} \otimes (Q_o + \delta P_o)) \mathbf{e} + 2\lambda_{\min}(P_{H_\sigma}) (\gamma_\nu^2 \|\nu\|^2 + \gamma_R^2 \|\omega\|^2 - \mathbf{z}^T I \otimes C^T C \mathbf{z})
\end{aligned} \tag{5.28}$$

Similar to results in Section 5.2, one can verify the integrity of the following inequality

$$\dot{V}_\sigma \leq -\delta V_\sigma + 2\lambda_{\min}(P_{H_\sigma}) (\gamma_\nu^2 \|\nu\|^2 + \gamma_R^2 \|\omega\|^2 - \mathbf{z}^T I \otimes C^T C \mathbf{z}) \tag{5.29}$$

if the following matrix is positive semi-definite:

$$\begin{bmatrix} Q_A - \delta P_A & \frac{1}{2\eta\alpha_\sigma} P_A B B^T P_A \\ \frac{1}{2\eta\alpha_\sigma} P_A B B^T P_A & Q_o \end{bmatrix} \geq 0 \quad (5.30)$$

Furthermore, from the Schur complement condition for positive semi-definiteness we know that a block matrix

$$\mathcal{X} = \begin{bmatrix} \mathcal{A} & \mathcal{B} \\ \mathcal{B}^T & \mathcal{C} \end{bmatrix}$$

is positive semi-definite if \mathcal{A} is positive definite and $\mathcal{C} - \mathcal{B}^T \mathcal{A}^{-1} \mathcal{B}$ is positive semi-definite. Therefore, δ should satisfies the inequality (5.31)

$$\delta < \frac{\lambda_{\min}(Q_A)}{\lambda_{\max}(P_A)} \quad (5.31)$$

and the following inequality should hold:

$$Q_o \geq \frac{\lambda_{\max}(P_A B B^T P_A)^2}{4\eta^2 \alpha_\sigma^2 \lambda_{\min}(Q_A - \delta P_A)} \quad (5.32)$$

To formally present the main result of this section, we propose the following theorem.

Theorem 5.1. *Consider the multi-agent system (5.1) which satisfies Assumption 5.1 and let the matrix G is the observer gain. Assume all the graphs \mathcal{G}_σ have directed spanning trees where $\sigma(t)$ be a piecewise constant switching signal with average dwell time τ_a and let μ_σ be defined as per equation (5.31). If the algebraic Riccati equation (5.25) has a unique positive definite solution P_A for a positive constant γ_R and positive definite matrix Q_A and positive definite matrix P_o is the solution to the algebraic Riccati equation (5.14) for a positive definite matrix Q_o that satisfies the inequality (5.32), then the distributed consensus control presented in (5.16) solves the H_∞ output consensus problem of the multi-agent team as per Definition 5.2 with bounds $\gamma_\rho = \gamma_R \sqrt{\mu}$ and $\gamma_n = \gamma_\nu \sqrt{\mu}$, where μ is defined as per equation (5.38).*

Proof. From (5.29) it is clear that the following inequality holds when $\omega = 0$

and $\nu = 0$:

$$\dot{V}_\sigma \leq -\delta V_\sigma \quad (5.33)$$

Furthermore, using (5.27) one can verify that V_σ satisfies the following inequalities

$$\alpha_1(\|\mathbf{z}\|^2 + \|\mathbf{e}\|^2) \leq V_\sigma \leq \alpha_2(\|\mathbf{z}\|^2 + \|\mathbf{e}\|^2) \quad (5.34)$$

where

$$\alpha_1 = \min_{\sigma} \{ \lambda_{\min}(P_{H_\sigma}) \lambda_{\min}(P_A), \lambda_{\min}(P_{H_\sigma}) \lambda_{\min}(P_o) \} \quad (5.35)$$

and

$$\alpha_2 = \max_{\sigma} \{ \lambda_{\max}(P_{H_\sigma}) \lambda_{\max}(P_A), \lambda_{\max}(P_{H_\sigma}) \lambda_{\max}(P_o) \} \quad (5.36)$$

Finally, the inequality (5.37) holds for any $t_1, t_2 \geq 0$, this is

$$V_\sigma(t_1) \leq \mu V_\sigma(t_2) \quad (5.37)$$

where

$$\mu = \frac{\alpha_2}{\alpha_1} \quad (5.38)$$

Noting that the Lyapunov function (5.27) satisfies conditions (5.33), (5.34), and (5.37) therefore, using Lemma 3.7 one can conclude that the vector \mathbf{z} exponentially converges to zero if the average dwell time $\tau_a \geq \frac{\ln(\mu)}{\delta}$.

To show the H_∞ output consensus of the multi-agent team, using Lemma 3.5 for any $T > 0$ and any given initial condition we have:

$$\frac{1}{T} \int_0^T \zeta(t) (\dot{V}_\sigma + \delta V_\sigma) dt + \frac{1}{T} V_\sigma(0) \geq 0 \quad (5.39)$$

where $\zeta(t) = e^{\delta_k(t-t_k)}$ and δ_k and t_k are defined in Lemma 3.5.

From (5.29) it is easy to verify that the following inequality holds:

$$\mathbf{z}^T (I \otimes C^T C) \mathbf{z} - \gamma_R^2 \boldsymbol{\omega}^T \boldsymbol{\omega} - \gamma_\nu \boldsymbol{\nu}^T \boldsymbol{\nu} + \frac{1}{2\lambda_{\min}(P_{H_\sigma})} (\dot{V}_\sigma + \delta V_\sigma) \leq 0 \quad (5.40)$$

Noting that $\zeta(t)$ is always positive gives us:

$$\begin{aligned} \frac{1}{T} \int_0^T \zeta(t) \mathbf{z}^T (I \otimes C^T C) \mathbf{z} - \frac{1}{T} \int_0^T \zeta(t) \gamma_R^2 \omega^T \omega - \frac{1}{T} \int_0^T \zeta(t) \gamma_\nu^2 \nu^T \nu \\ + \frac{1}{2\lambda_{\min}(P_{H_\sigma})T} \int_0^T \zeta(t) (\dot{V}_\sigma + \delta V_\sigma) \leq 0 \end{aligned} \quad (5.41)$$

Using the inequality (5.39) we have:

$$\begin{aligned} \frac{1}{T} \int_0^T \zeta(t) \mathbf{z}^T (I \otimes C^T C) \mathbf{z} - \frac{1}{T} \int_0^T \zeta(t) \gamma_R^2 \omega^T \omega - \frac{1}{T} \int_0^T \zeta(t) \gamma_\nu^2 \nu^T \nu \\ - \frac{1}{2\lambda_{\min}(P_{H_\sigma})T} V_\sigma(0) \leq 0 \end{aligned} \quad (5.42)$$

Using the fact that $1 \leq \zeta(t) < \mu$ for any $t \geq 0$ one can verify that:

$$\frac{1}{T} \int_0^T \mathbf{z}^T (I \otimes C^T C) \mathbf{z} \leq \frac{\mu \gamma_R^2}{T} \int_0^T \omega^T \omega + \frac{\mu \gamma_\nu^2}{T} \int_0^T \nu^T \nu + \frac{1}{\lambda_{\min}(P_{H_\sigma})T} V_\sigma(0) \quad (5.43)$$

Now, using the above inequality and Lemma 5.1, one concludes the proof of the theorem. ■

5.1.2 Simulation Results

The effectiveness of our proposed consensus algorithm design methodology is now demonstrated by performing the following numerical simulations. Towards this end, the diving consensus of a team of four unmanned underwater vehicles (UUV) similar to those studied in Chapter 3 is considered. The linearized diving dynamics of the UUVs can be represented as $\dot{x}_i = Ax_i + Bu_i + B_\omega \omega_i$, $y_i = Cx_i + \nu_i$, where:

$$A = \begin{bmatrix} -0.7 & -0.3 & 0 \\ 1 & 0 & 0 \\ 0 & u_0 & 0 \end{bmatrix}, B = \begin{bmatrix} 0.035 \\ 0 \\ 0 \end{bmatrix}, B_\omega = \begin{bmatrix} 0 \\ 0.01 \\ 0 \end{bmatrix} \quad (5.44)$$

and

$$C = \begin{bmatrix} 0 & 0 & 1 \end{bmatrix}$$

$x_i = [q_i, \theta_i, z_i]^T$, z_i denotes the depth, θ_i denotes the pitch angle and q_i denotes the pitch angular velocity, and u_0 denotes the nominal value of the surge linear velocity and is set to $0.3 \frac{m}{s}$. The control input u_i is the deflection of the control surface from the stern plane and ω_i is the external disturbance. Units of z_i, θ_i, q_i, u_0 and u_i are m, rad, rad/sec and deg, respectively. The digraphs associated with the communication networks of the team are shown in Figure 5.1. The values of α_σ are computed based on the network topologies shown in

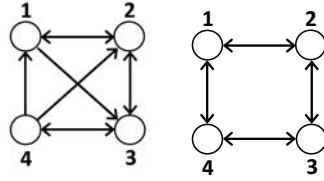


Figure 5.1: Communication networks digraphs.

Figure 5.1. For the graph in the left side it is equal to 1.25 and for the graph in the right side it is 1. Furthermore, the design parameters are selected as $Q_H = I$, $Q_A = 6I$, $\gamma_R = 0.6$, $\gamma_\nu = 230$ and $\eta = 0.5$. The poles of observers are set to $-0.9, -0.95$ and -1 . The resulting observer gain is $G = \begin{bmatrix} -1.41, & 3.07, & -2.17 \end{bmatrix}$ and the controller gain becomes $K_1 = \begin{bmatrix} -2.66, & -1.93, & 2.33 \end{bmatrix}$ and $K_2 = \begin{bmatrix} -3.33, & -2.41, & 2.92 \end{bmatrix}$. Figures 5.2 and 5.3 show the angular velocity and pitch angle of the agents, respectively. The depth of the agents, which is the output signal is shown in Figure 5.4. Figure 5.5 shows the feasibility of the resulting control signal. The disturbance signal ω_i is a combination of several sinusoidal signals with different frequencies where their phases and frequencies are selected randomly and with RMS of 1 and a pseudo-random signal with RMS of $= 0.1$ is used to simulate noise signal and these are applied to the agents to justify the H_∞ performance of our output-feedback distributed controller. The estimation errors are shown in Figure 5.6 to illustrate the performance of the presented observers.

One of the most recent works in the field of output-feedback consensus achievement for homogenous LTI multi-agent systems is presented in [143]. In this work, based on solution to an algebraic Riccati equation a distributed cooperative consensus controller with the disturbance rejection property is presented. However, in comparison to our proposed method, the method in [143]

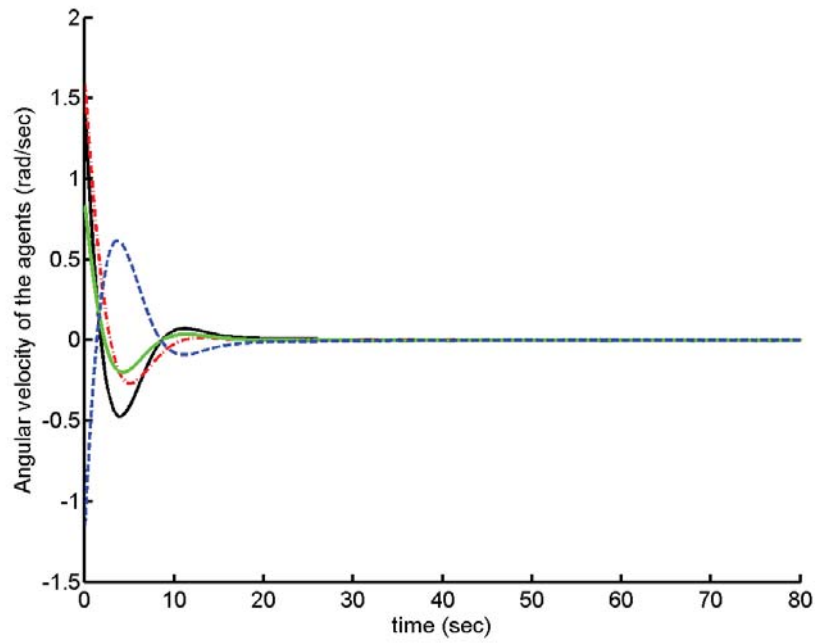


Figure 5.2: Angular velocity of the agents.

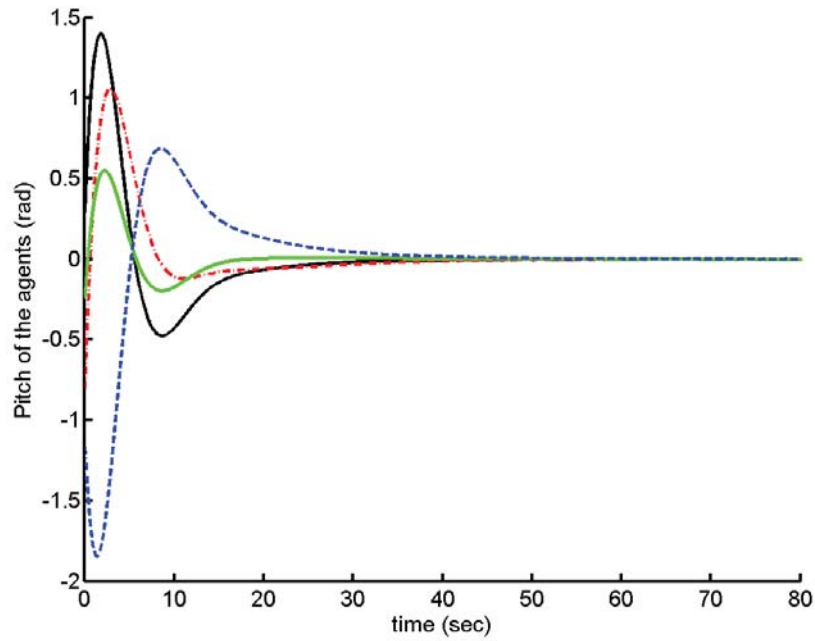


Figure 5.3: Pitch angle of the agents.

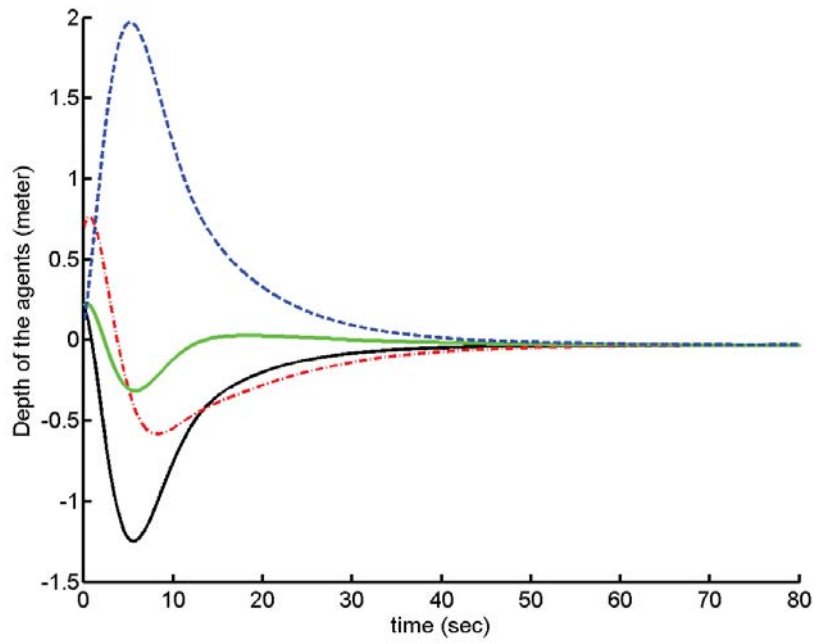


Figure 5.4: Depth (output signal) of the agents.

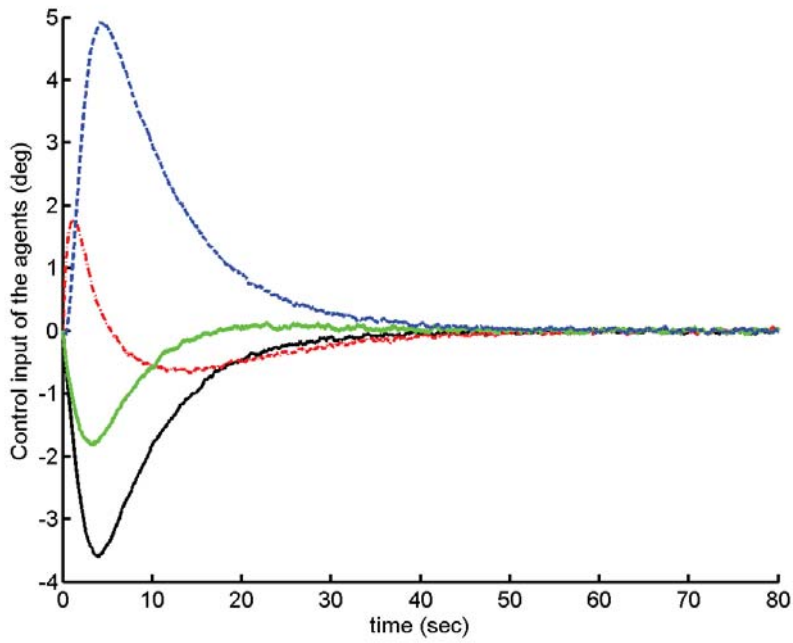


Figure 5.5: Control input of the agents.

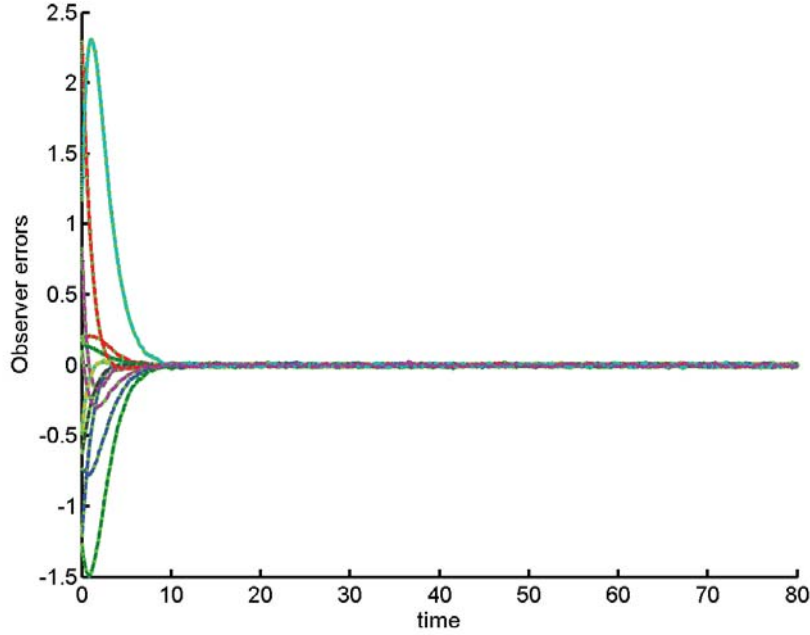


Figure 5.6: Observers estimation errors.

is limited to fixed communication topologies and does not consider the measurement noise. In order to compare the performance of our proposed method with their presented method, we consider the same numerical example presented in [143] and increase the disturbance coefficient D . The team consists of a leader and 4 follower agents having the following dynamics:

$$\begin{cases} \dot{x}_0 = Ax_0 \\ y_0 = Cx_0 \end{cases}, \quad \begin{cases} \dot{x}_i = Ax_i + Bu_i + D\omega_i \\ y_i = Cx_i \end{cases} \quad (5.45)$$

where x_0 is the state of the leader, y_0 is the output of the leader, x_i is the state of the i^{th} agent, y_i is its output, u_i is its control input, ω_i is its disturbance signal and matrices A, B, C, D are:

$$A = \begin{bmatrix} 0 & 1 \\ 1 & -1 \end{bmatrix}, B = I, C = \begin{bmatrix} 1 & 0.6 \end{bmatrix}, D = \begin{bmatrix} 0.01 \\ 0 \end{bmatrix}$$

Figure 5.7 shows the topology of the communication networks used by the agents to exchange information. We used the same design parameters

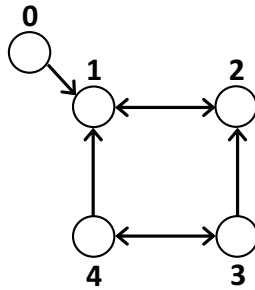


Figure 5.7: Communication network topology [143].

that are presented in [143] and performed the numerical simulations using a combination of several sinusoidal signals with different frequencies with RMS of 1 as the disturbance signal. Figures 5.8 and 5.9 depict the outputs and the control inputs of the agents by using the presented method in [143]. Since, matrix A is not stable, as can be seen in Figure 5.8, the output of the agents is increasing. We applied our proposed method to the same multi-agent system and used $Q_H = I$, $Q_A = 3.5I$, $\eta = 0.55$ and $\gamma_R = 1.3$ as design parameters and placed the observer poles at -1.58 . The resulting observer gain matrix obtained is $G = [-1.7602, -0.9383]$ and the controller gain matrix is given by:

$$K = \begin{bmatrix} -7.9491 & -3.2304 \\ -3.2304 & -4.6658 \end{bmatrix}$$

We used the same initial conditions and disturbance signals and repeated the numerical simulation by using our proposed method. The resulting agents outputs are shown in Figure 5.10 and the control inputs are depicted in Figure 5.11. Furthermore, in Table 5.1 a quantitative comparison between maximum of the control inputs, L_2 norm of the control inputs, RMS of the consensus error and the settling time of these two approaches are presented. As illustrated in these figures and the comparison table, the settling time of our approach is not significantly slower than their method. However, the control effort that is required by our method is less than the one in the method of [143] and RMS of the consensus error of our proposed method is also smaller.

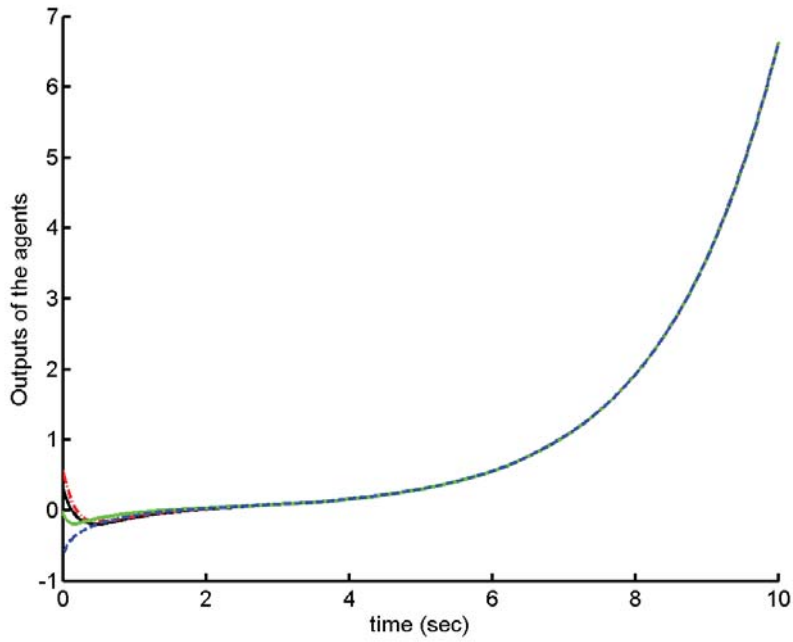


Figure 5.8: The outputs of the agents by using the method in [143].

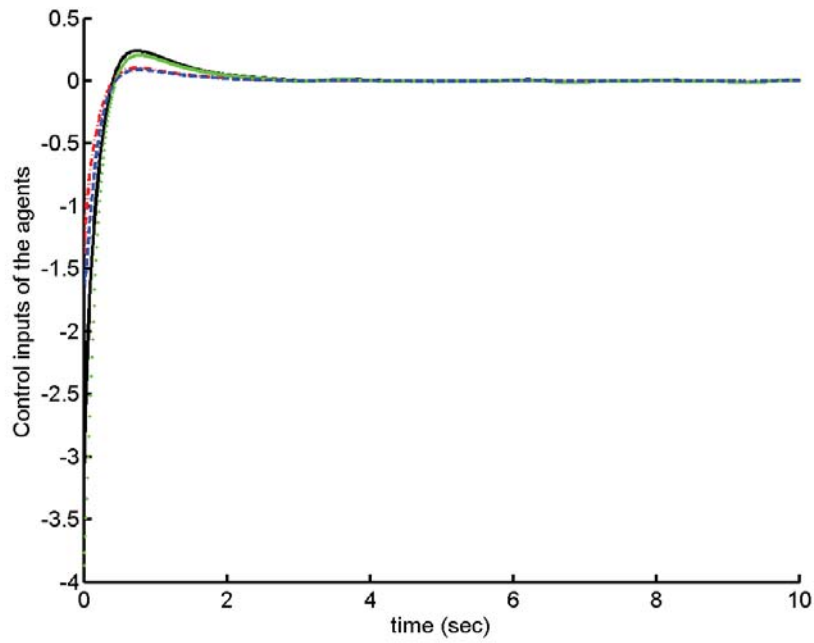


Figure 5.9: The control inputs of the agents by using the method in [143].

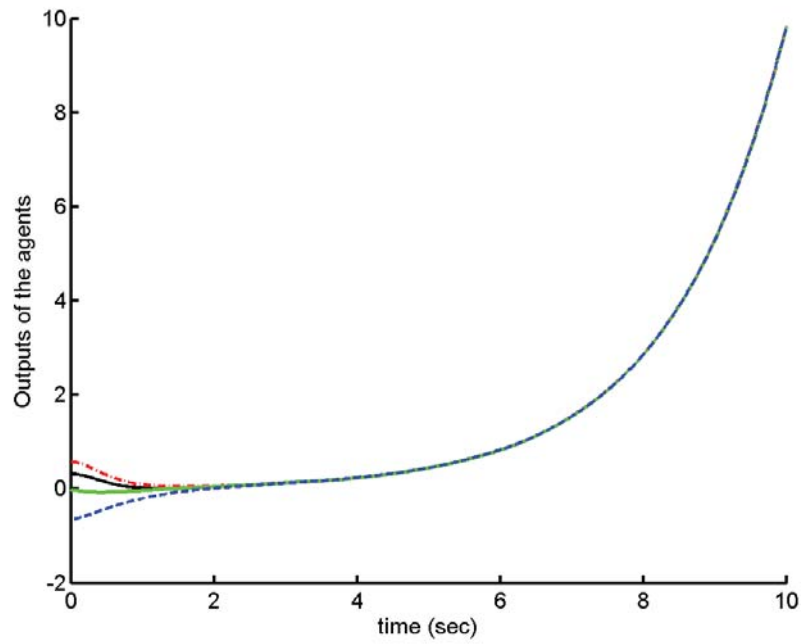


Figure 5.10: The outputs of the agents by using the method in [143].

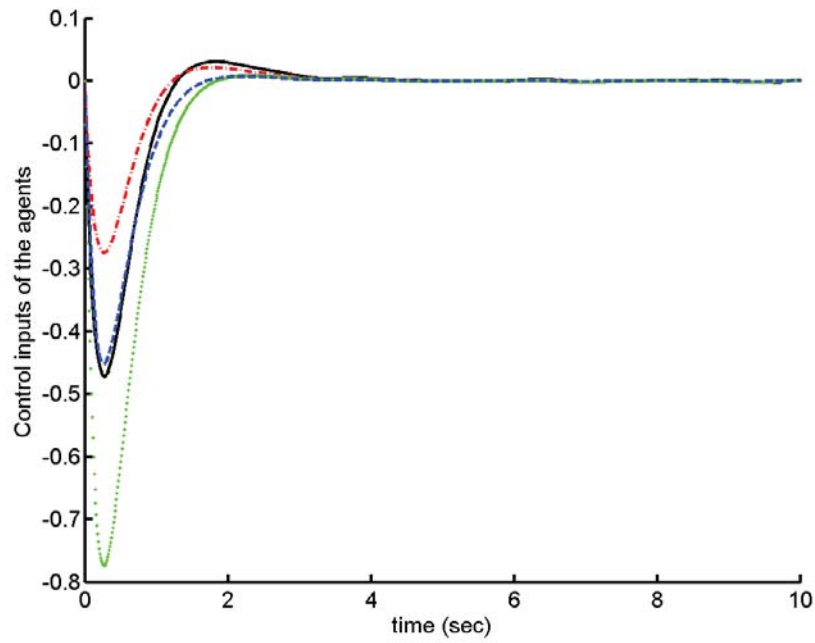


Figure 5.11: The control inputs of the agents by using the method in [143].

Table 5.1: The comparison between our proposed method and the method in [143].

	Control effort (max)	Control effort (L_2 norm)	Consensus error (RMS)	Settling time (sec)
Our proposed method	0.7742	9.71	4.81	1.8981
The method in [143]	3.8675	18.49	6.05	1.85814

5.2 Consensus Achievement In Presence of Model Uncertainties

In this section we study a team of multi-agents with model uncertainties including Lipschitz nonlinearities. In the first step, we propose a distributed consensus algorithm in absence of the measurement noise and in the next step we present an approach to tackle the consensus achievement problem of the team in presence of both model uncertainties and measurement noise. Finally, we performed numerical simulations to support our analytical results.

5.2.1 Problem Statement and Main Result

In this section we extend our proposed method to design a distributed consensus algorithm for a multi-agent team of N agents with model uncertainties, including Lipschitz nonlinearity, as presented in equation (5.46) to guarantee it achieves H_∞ consensus as per Definition stated next.

$$\dot{x}_i = (A + \Delta A(t))x_i + f(x_i) + Bu_i + B_2\omega_i \quad (5.46)$$

In the above equation, $A \in \mathbb{R}^{p \times p}$, $B \in \mathbb{R}^{p \times m}$, $B_2 \in \mathbb{R}^{p \times q}$ are known real matrices, time varying matrix $\Delta A(t) \in \mathbb{R}^{p \times p}$ represents unknown linear model uncertainties, the function $f : \mathbb{R}^p \rightarrow \mathbb{R}^p$ is unknown non-linearity and, $x_i \in \mathbb{R}^p$, $u_i \in \mathbb{R}^m$ and $\omega_i \in \mathbb{R}^q$ are state, control input and disturbance of the i^{th} agent, respectively.

Definition 5.3. *The multi-agent system (5.46) achieves H_∞ consensus with*

bound γ_ρ in presence of the disturbance if it achieves consensus when there is no disturbance and there exists a positive constant θ such that for any $T > 0$ in presence of disturbance the following inequality holds:

$$\frac{1}{n} \left(\sum_{i=1}^n \sum_{j=i+1}^n \frac{1}{T} \int_0^T \|x_i - x_j\| dt \right) \leq \gamma_\rho^2 \sum_{i=1}^n \frac{1}{T} \int_0^T \|\omega_i\|^2 dt + \frac{\theta}{T} V(x_1(0), \dots, x_n(0)) \quad (5.47)$$

where $V(\cdot)$ is a positive definite function and $x_1(0), \dots, x_n(0)$ are the initial states of the agents.

Assumption 5.2. In this chapter it is assumed that the matrix A is not Hurwitz (see Remark 3.5), and the pair (A, B) is controllable.

Assumption 5.3. The vector function $f : \mathfrak{R}^p \rightarrow \mathfrak{R}^p$ satisfies the following Lipschitz condition:

$$\|f(x_1) - f(x_2)\| \leq \gamma_L \|x_1 - x_2\| \quad (5.48)$$

Assumption 5.4. The model uncertainty matrix $\Delta A(t)$ can be represented as:

$$\Delta A(t) = E_L \Delta_A(t) E_R$$

where $E_L \in \mathfrak{R}^{p \times r}$ and $E_R \in \mathfrak{R}^{r \times p}$ are known constant matrices and the unknown matrix $\Delta_A(t) \in \mathfrak{R}^{r \times r}$ satisfies the following inequality for any $t \geq 0$:

$$\Delta_A(t) \Delta_A(t)^T \leq I \quad (5.49)$$

In the remainder of this section $\Delta_A(t)$ will be denoted by Δ_A .

To design the consensus algorithm, let us introduce the following augmented system which represents the dynamics of the entire multi-agent systems

$$\dot{\mathbf{x}} = I \otimes A \mathbf{x} + I \otimes (E_L \Delta_A E_R) \mathbf{x} + \mathbf{f}(\mathbf{x}) + I \otimes B \mathbf{u} + I \otimes B_2 \boldsymbol{\omega} \quad (5.50)$$

where $\mathbf{x} = [x_1, \dots, x_n]^T$, $\mathbf{f}(\mathbf{x}) = [f(x_1), \dots, f(x_n)]^T$, and $\boldsymbol{\omega} = [\omega_1, \dots, \omega_n]^T$.

The following equation gives our proposed consensus control law

$$u_i = -\frac{1}{2\eta\alpha_\sigma|\mathcal{N}_i|}B^T P_A \sum_{j \in \mathcal{N}_i} (x_i - x_j) \quad (5.51)$$

where \mathcal{N}_i is the set of neighboring agents, $0 < \eta < 1$ is a real constant, α_σ is a connectivity measure of communication network and defined in Definition 4.2, P_A is a positive definite matrix. As can be seen the overall structure of the above controller is the same as that of the previous ones. However, the way that we compute the matrix P_A , which determines the controller gains, is different and will be addressed in the remainder of this chapter and will let us deal with model uncertainties and nonlinearities.

To facilitate dealing with the Lyapunov stability analysis, similar to the previous chapters in the remainder of this section we will use augmented control law which is denoted by $\mathbf{u} = [u_1, \dots, u_n]^T$. Using the Laplacian matrix presented in Definition 3.8 one can obtain the following control law for the augmented system (5.50):

$$\mathbf{u} = -\frac{1}{2\eta\alpha_\sigma}L_\sigma \otimes B^T P_A \mathbf{x} \quad (5.52)$$

Furthermore, in order to evaluate the consensus achievement of the team using Lyapunov method, similar to Chapter 4, we use a virtual agent as a reference to measure the consensus error of the team and we will denote its state as \bar{x} . As stated in Remark 4.2, the dynamics of the virtual agent could be chosen arbitrarily and it is shown that if the resulting consensus error converges to zero, the team will achieve consensus. However, selecting the following dynamics for the virtual agent in the remainder of this section will help us achieve our goal, namely:

$$\dot{\bar{x}} = A\bar{x} + E_L \Delta_A E_R \bar{x} + f(\bar{x}) - \frac{\Delta_\sigma}{n\eta\alpha_\sigma} B B^T P_A \sum_{j=1}^n (\bar{x} - x_j) \quad (5.53)$$

Following along the same lines as in Section 5.1 and noting that:

$$(L_\sigma \otimes \mathcal{M})\mathbf{z} = (L_\sigma \otimes \mathcal{M})\mathbf{x} - (L_\sigma \mathbf{1}) \otimes \mathcal{M}\bar{x} = L_\sigma \otimes \mathcal{M}\mathbf{x}$$

By using the above virtual agent dynamics and the dynamics of the augmented system (5.50) one can obtain the following consensus error dynamic equation:

$$\begin{aligned}\dot{\mathbf{z}} = \dot{\mathbf{x}} - \mathbf{1} \otimes \dot{\bar{x}} &= I \otimes A\mathbf{x} + I \otimes E_L \Delta_A E_R \mathbf{x} - \frac{1}{2\eta\alpha_\sigma} L_\sigma \otimes B^T P_A \mathbf{z} + I \otimes B_2 \omega + \mathbf{f}(\mathbf{x}) \\ &\quad - \mathbf{1} \otimes A\bar{x} - \mathbf{1} \otimes E_L \Delta_A E_R \bar{x} - \frac{\Delta_\sigma}{n\eta\alpha_\sigma} \mathbf{1}\mathbf{1}^T \otimes B B^T P_A \mathbf{z} - \bar{\mathbf{f}}\end{aligned}\quad (5.54)$$

where $\bar{\mathbf{f}} = \mathbf{1} \otimes f(\bar{x})$. Using the matrix H_σ as defined in equation (4.7) and some algebraic manipulations we have:

$$\begin{aligned}\dot{\mathbf{z}} &= I \otimes A\mathbf{z} + I \otimes E_L \Delta_A E_R \mathbf{z} - \frac{1}{2\eta\alpha_\sigma} (L_\sigma + \frac{2\Delta_\sigma}{n} \mathbf{1}\mathbf{1}^T) \otimes B^T P_A \mathbf{z} + I \otimes B_2 \omega \\ &\quad + \mathbf{f}(\mathbf{x}) - \bar{\mathbf{f}} \\ &= I \otimes (A - \frac{1}{2} B B^T P_A) \mathbf{z} + I \otimes E_L \Delta_A E_R \mathbf{z} - \frac{1}{2\eta\alpha_\sigma} (H_\sigma - \eta\alpha_\sigma I) \otimes B^T P_A \mathbf{z} \\ &\quad + I \otimes B_2 \omega + \mathbf{f}(\mathbf{x}) - \bar{\mathbf{f}}\end{aligned}\quad (5.55)$$

Now, to guarantee that the team achieves consensus, we need to show that the above consensus error dynamics converges to zero. Towards this end, let us define the following Lyapunov candidate function:

$$V_\sigma = \mathbf{z}^T P_{H_\sigma} \otimes P_A \mathbf{z} \quad (5.56)$$

The time derivative of (5.56) along the trajectories of the dynamical system (5.55) is given by:

$$\begin{aligned}\dot{V}_\sigma &= \mathbf{z}^T P_{H_\sigma} \otimes (P_A A + A^T P_A - P_A B B^T P_A) \mathbf{z} - \frac{1}{2\eta\alpha_\sigma} \mathbf{z}^T Q_{H_\sigma} \otimes (P_A B B^T P_A) \mathbf{z} \\ &\quad + 2\mathbf{z}^T P_{H_\sigma} \otimes P_A B_2 \omega + 2\mathbf{z}^T (P_{H_\sigma} \otimes P_A) (\mathbf{f}(\mathbf{x}) - \bar{\mathbf{f}}) + \mathbf{z}^T P_{H_\sigma} \otimes P_A E_L \Delta_A E_R \mathbf{z} \\ &\quad + \mathbf{z}^T P_{H_\sigma} \otimes E_R^T \Delta_A^T E_L^T P_A \mathbf{z}\end{aligned}\quad (5.57)$$

One can determine that the following inequality holds for any positive definite matrices \mathcal{P}_1 and \mathcal{P}_2 and vectors \mathbf{v}_1 and \mathbf{v}_2 :

$$2\mathbf{v}_1^T \mathcal{P}_1 \otimes \mathcal{P}_2 \mathbf{v}_2 \leq \gamma \mathbf{v}_1^T (\mathcal{P}_1 \mathcal{P}_1^T \otimes \mathcal{P}_2 \mathcal{P}_2^T) \mathbf{v}_1 + \gamma^{-1} \mathbf{v}_2^T \mathbf{v}_2 \quad (5.58)$$

Using the inequality (5.58) one can verify that the following inequality holds:

$$\begin{aligned}
\dot{V}_\sigma &\leq \mathbf{z}^T P_{H_\sigma} \otimes (P_A A + A^T P_A - P_A B B^T P_A) \mathbf{z} \\
&+ \frac{\gamma_L^2}{\lambda_{\min}(P_{H_\sigma})} \mathbf{z}^T P_{H_\sigma}^2 \otimes P_A^2 \mathbf{z} + \frac{\lambda_{\min}(P_{H_\sigma})}{\gamma_L^2} \|\mathbf{f}(\mathbf{x}) - \bar{\mathbf{f}}\|^2 \\
&+ \frac{\gamma_\Delta^2}{\lambda_{\min}(P_{H_\sigma})} \mathbf{z}^T P_{H_\sigma}^2 \otimes P_A E_L \Delta_A \Delta_A^T E_L^T P_A \mathbf{z} + \frac{\lambda_{\min}(P_{H_\sigma})}{\gamma_\Delta^2} \mathbf{z}^T I \otimes E_R E_R^T \mathbf{z} \\
&+ \frac{\gamma_R^{-2}}{\lambda_{\min}(P_{H_\sigma})} \mathbf{z}^T P_{H_\sigma}^2 \otimes (P_A B_2 B_2^T P_A) \mathbf{z} + \lambda_{\min}(P_{H_\sigma}) \gamma_R^2 \|\omega\|^2
\end{aligned} \tag{5.59}$$

Now, using Assumptions 5.3 and 5.4 and after some algebraic manipulations one can get:

$$\begin{aligned}
\dot{V}_\sigma &\leq \mathbf{z}^T P_{H_\sigma} \otimes (P_A A + A^T P_A - P_A B B^T P_A) \mathbf{z} \\
&+ \mu_\sigma \gamma_L^2 \mathbf{z}^T P_{H_\sigma} \otimes P_A^2 \mathbf{z} + \lambda_{\min}(P_{H_\sigma}) \mathbf{z}^T \mathbf{z} \\
&+ \mu_\sigma \gamma_\Delta^2 \mathbf{z}^T P_{H_\sigma} \otimes P_A E_L E_L^T P_A \mathbf{z} + \gamma_\Delta^{-2} \mathbf{z}^T P_{H_\sigma} \otimes E_R E_R^T \mathbf{z} \\
&+ \mu_\sigma \gamma_R^{-2} \mathbf{z}^T P_{H_\sigma} \otimes (P_A B_2 B_2^T P_A) \mathbf{z} + \lambda_{\min}(P_{H_\sigma}) \gamma_R^2 \|\omega\|^2 \\
&- \lambda_{\min}(P_{H_\sigma}) \mathbf{z}^T \mathbf{z} + \lambda_{\min}(P_{H_\sigma}) \mathbf{z}^T \mathbf{z}
\end{aligned} \tag{5.60}$$

where δ is a positive constant, μ_σ is defined as follows

$$\mu_\sigma = \frac{\lambda_{\max}(P_{H_\sigma})}{\lambda_{\min}(P_{H_\sigma})}. \tag{5.61}$$

We require P_A to satisfy the following equation:

$$\begin{aligned}
P_A A + A^T P_A - P_A B B^T P_A + \mu_\sigma \gamma_L^2 P_A P_A + \mu_\sigma \gamma_R^{-2} P_A B_2 B_2 P_A \\
+ \mu_\sigma \gamma_\Delta^2 P_A E_L E_L^T P_A + \gamma_\Delta^{-2} E_R E_R^T + \delta P_A + 2I = -Q_A
\end{aligned} \tag{5.62}$$

where Q_A is a positive definite matrix. Now, we have the following inequality:

$$\dot{V}_\sigma \leq -\mathbf{z}^T P_{H_\sigma} \otimes Q_A \mathbf{z} - \delta \mathbf{z}^T P_{H_\sigma} \otimes P_A \mathbf{z} + \lambda_{\min}(P_{H_\sigma}) (\gamma_R^2 \|\omega\|^2 - \|\mathbf{z}\|^2) \tag{5.63}$$

The main result of this section can be formalized into the following theorem.

Theorem 5.2. *Consider the nonlinear multi-agent system (5.46) which satisfies Assumptions 5.2, 5.3 and 5.4. Assume that all the graphs \mathcal{G}_σ have directed*

spanning trees where $\sigma(t)$ is a piecewise constant switching signal with average dwell time τ_a and let μ_σ be defined in equation (5.61). If the algebraic Riccati equation (5.62) has a unique positive definite solution P_A for a positive constant γ_R and positive definite matrix Q_A , then the distributed consensus control presented in (5.51) solves the H_∞ consensus problem of Definition 5.3 for the multi-agent team with a bound $\gamma_\rho = \gamma_R\sqrt{\mu}$, where μ is defined in equation (5.69).

Proof. In the first step, we need to show the multi-agent system (5.46) achieves consensus in absence of disturbances i.e. $\mathbf{z} \rightarrow 0$ as $t \rightarrow \infty$. Consider the piecewise quadratic Lyapunov function (5.56). From (5.63) it follows that the following inequality holds when $\omega = 0$:

$$\dot{V}_\sigma \leq -\delta V_\sigma \quad (5.64)$$

Furthermore, using (5.56) one can verify that V_σ satisfies the following inequalities

$$\alpha_1 \|\mathbf{z}\|^2 \leq V_\sigma \leq \alpha_2 \|\mathbf{z}\|^2 \quad (5.65)$$

where

$$\alpha_1 = \min_{\sigma} \{ \lambda_{\min}(P_{H_\sigma}) \lambda_{\min}(P_A) \} \quad (5.66)$$

and

$$\alpha_2 = \max_{\sigma} \{ \lambda_{\max}(P_{H_\sigma}) \lambda_{\max}(P_A) \} \quad (5.67)$$

Finally, the inequality (5.68) holds for any $t_1, t_2 \geq 0$

$$V_\sigma(t_1) \leq \mu V_\sigma(t_2) \quad (5.68)$$

where

$$\mu = \frac{\alpha_2}{\alpha_1} \quad (5.69)$$

To show that inequality (5.47) in Definition 5.3 holds, one can use Lemma 5.1 and prove that the following inequality holds:

$$\frac{1}{T} \int_0^T \mathbf{z}^T \mathbf{z} dt \leq \gamma_\rho^2 \frac{1}{T} \int_0^T \omega^T \omega dt + \frac{\theta}{T} V(x_1(0), \dots, x_n(0)) \quad (5.70)$$

Using the function $\xi(t)$ and its properties as per defined in Lemma 3.5 and setting $\theta = \lambda_{\min}(P_{H_\sigma})^{-1}$, one can verify that the inequality (5.70) holds if the following inequality is valid:

$$\frac{1}{T}\lambda_{\min}(P_{H_\sigma}) \int_0^T \xi(t) (\mathbf{z}^T \mathbf{z} - \gamma_\rho^2 \omega^T \omega) dt - \frac{1}{T}\xi(t)V_0 \leq 0 \quad (5.71)$$

where $V_0 = V(x_1(0), \dots, x_n(0))$. Noting that the Lyapunov function (5.56) satisfies the conditions (5.64), (5.65), and (5.68) from Lemma 3.5 we have:

$$\frac{1}{T} \int_0^T \xi(t) (\dot{V}_\sigma + \delta V_\sigma) dt + \frac{1}{T}\xi(t)V_0 \geq \frac{1}{T} \int_0^T \xi(t) (\dot{V}_\sigma + \delta V_\sigma) dt + \frac{1}{T}V_0 \geq 0 \quad (5.72)$$

Therefore, one can show that the inequality (5.71) is valid if the following inequality is satisfied:

$$\begin{aligned} \frac{1}{T}\lambda_{\min}(P_{H_\sigma}) \int_0^T \xi(t) (\mathbf{z}^T \mathbf{z} - \gamma_\rho^2 \omega^T \omega) dt - \frac{1}{T}\xi(t)V_0 \\ \leq \frac{1}{T} \int_0^T \xi(t) \left(\lambda_{\min}(P_{H_\sigma}) \mathbf{z}^T \mathbf{z} - \gamma_\rho^2 \lambda_{\min}(P_{H_\sigma}) \omega^T \omega + \dot{V}_\sigma + \delta V_\sigma \right) dt \leq 0 \end{aligned} \quad (5.73)$$

This can be verified by using the inequality (5.63). Therefore, one can conclude proof of the theorem. ■

5.2.2 Output Consensus Achievement in Presence of Model Uncertainties and Measurement Noise

In this chapter, first we studied the output consensus problem for multi-agent systems in presence of measurement noise. Next, we proposed a distributed state-feedback cooperative consensus controller for multi-agent systems by considering the model uncertainties. Now, in order to show extendability of our proposed technique, we present the steps leading to design of an output-feedback consensus controller for the following multi-agent system in presence of measurement noise and model uncertainties, namely:

$$\begin{cases} \dot{x}_i = (A + \Delta A(t))x_i + f(x_i) + Bu_i + B_2\omega_i \\ y_i = Cx_i + \nu_i \end{cases} \quad (5.74)$$

In the above equation, $A \in \mathbb{R}^{p \times p}$, $B \in \mathbb{R}^{p \times m}$, $B_2 \in \mathbb{R}^{p \times q}$, $C \in \mathbb{R}^{r \times p}$ are known real matrices that satisfy the Assumption 5.1. The time varying matrix $\Delta A(t) \in \mathbb{R}^{p \times p}$ represents unknown linear model uncertainties that satisfy the Assumption 5.4. The function $f : \mathbb{R}^p \rightarrow \mathbb{R}^p$ is an unknown non-linearity and $x_i \in \mathbb{R}^p$ that satisfies the Assumption 5.3, and $y_i \in \mathbb{R}^r$, $u_i \in \mathbb{R}^m$, $\nu_i \in \mathbb{R}^r$ and $\omega_i \in \mathbb{R}^q$ are the state, output, control input, measurement noise and the disturbance of the i^{th} agent, respectively.

Similar to the last section, one can define an augmented system where its dynamics is governed by equation (5.50) and similar to Section 5.1 let the augmented measured output be denoted by \mathbf{y} and represented as follows:

$$\mathbf{y} = (I \otimes C)\mathbf{x} + \nu$$

By following along the same strategy as in Section 5.1 one can define the relative state vector Ξ as:

$$\Xi = (L_\sigma \otimes I)\mathbf{x} \quad (5.75)$$

where \mathbf{x} is the state of the augmented system. Let us use the same state observer that we designed in Section 5.1 and presented as equation (5.6) to estimate the relative state and denote it by $\hat{\Xi}$. By using the same virtual agent dynamics as presented in equation (5.53), the augmented system equation (5.50) and considering the equation (5.20), one can take the time derivative of Ξ and obtain:

$$\dot{\Xi} = (L_\sigma \otimes A)\mathbf{x} + (I \otimes (E_L \Delta_A E_R))\mathbf{z} + (L_\sigma \otimes I)\mathbf{f}(\mathbf{x}) + (L_\sigma \otimes B)\mathbf{u} + (L_\sigma \otimes B_2)\boldsymbol{\omega} \quad (5.76)$$

where \mathbf{u} is the augmented control law and is defined as follow:

$$\mathbf{u} = -\frac{1}{2\eta\alpha_\sigma}(I \otimes B^T P_A)\hat{\Xi} \quad (5.77)$$

where $0 < \eta < 1$ is a real constant, α_σ is a connectivity measure of the communication network, that is defined in Definition 4.2, and P_A is a positive definite matrix.

Now, if $\mathbf{e} = \hat{\Xi} - \Xi$ denotes the estimation error, one can obtain the following error dynamic equation:

$$\dot{\mathbf{e}} = (I \otimes (A + GC)) \mathbf{e} - (I \otimes (E_L \Delta_A E_R)) \mathbf{z} - (L_\sigma \otimes I)(\mathbf{f}(\mathbf{x}) - \bar{\mathbf{f}}) - (L_\sigma \otimes B_2) \omega - (L_\sigma \otimes G) \nu \quad (5.78)$$

To obtain the above equation we used the fact that:

$$(L_\sigma \otimes I) \bar{\mathbf{f}} = (L_\sigma \otimes I)(\mathbf{1} \otimes f(\bar{x})) = L_\sigma(\mathbf{1} \otimes f(\bar{x})) = 0$$

Consider the Lyapunov function candidate (5.8) where one can verify that its time derivative along the trajectories of the estimation error dynamics is as follows:

$$\begin{aligned} \dot{V}_o &= \mathbf{e}^T (P_{H_\sigma} \otimes (P_o(A + GC) + (A + GC)^T P_o)) \mathbf{e} - 2\mathbf{e}^T (P_{H_\sigma} L_\sigma \otimes P_o B_2) \omega \\ &\quad - 2\mathbf{e}^T (P_{H_\sigma} L_\sigma \otimes P_o G) \nu - 2\mathbf{e}^T (P_{H_\sigma} \otimes P_o (E_L \Delta_A E_R)) \mathbf{z} - 2\mathbf{e}^T (P_{H_\sigma} L_\sigma \otimes P_o) (\mathbf{f} - \bar{\mathbf{f}}) \end{aligned} \quad (5.79)$$

After some algebraic manipulations and using the inequality (5.10) one can verify that:

$$\begin{aligned} \dot{V}_o &\leq \mathbf{e}^T (P_{H_\sigma} \otimes (P_o(A + GC) + (A + GC)^T P_o)) \mathbf{e} \\ &\quad + \frac{\lambda_{\max}(L_\sigma^T L_\sigma) \gamma_R^{-2}}{\lambda_{\min}(P_{H_\sigma})} \mathbf{e}^T (P_{H_\sigma}^2 \otimes P_o B_2 B_2^T P_o) \mathbf{e} + 2 \frac{\lambda_{\min}(P_{H_\sigma}) \gamma_\nu^2}{\lambda_{\max}(L_\sigma^T L_\sigma)} \nu^T ((L_\sigma^T L_\sigma) \otimes I) \nu \\ &\quad + \frac{\lambda_{\min}(P_{H_\sigma}) \gamma_R^2}{\lambda_{\max}(L_\sigma^T L_\sigma)} \omega^T ((L_\sigma^T L_\sigma) \otimes I) \omega + \frac{\lambda_{\max}(L_\sigma^T L_\sigma) \gamma_\nu^{-2}}{2\lambda_{\min}(P_{H_\sigma})} \mathbf{e}^T (P_{H_\sigma}^2 \otimes P_o G G^T P_o) \mathbf{e} \\ &\quad + \frac{\gamma_\Delta^2 \lambda_{\max}(E_R E_R^T)}{\lambda_{\min}(P_{H_\sigma})} \mathbf{e}^T (P_{H_\sigma}^2 \otimes P_o E_L \Delta_A \Delta_A^T E_L^T P_o) \mathbf{e} + \frac{\lambda_{\min}(P_{H_\sigma})}{\gamma_\Delta^2 \lambda_{\max}(E_R E_R^T)} \mathbf{z}^T (I \otimes E_R E_R^T) \mathbf{z} \\ &\quad + \frac{\gamma_L^2 \lambda_{\max}(L_\sigma^T L_\sigma)}{\lambda_{\min}(P_{H_\sigma})} (\mathbf{e}^T P_{H_\sigma}^2 \otimes P_o^2) \mathbf{e} + \frac{\lambda_{\min}(P_{H_\sigma})}{\gamma_L^2} \|\mathbf{f}(\mathbf{x}) - \bar{\mathbf{f}}\|^2 \end{aligned} \quad (5.80)$$

Now, let P_A be a solution to the following algebraic Riccati equation

$$\begin{aligned} -Q_o &= P_o(A + GC) + (A + GC)^T P_o + \delta P_o + \mu_\sigma \gamma_\Delta^2 \lambda_{\max}(E_R E_R^T) P_o E_L^T E_L P_o \\ &\quad + \mu_\sigma \lambda_{\max}(L_\sigma^T L_\sigma) \left(\frac{1}{2} \gamma_\nu^{-2} P_o G G^T P_o + \gamma_R^{-2} P_o B_2 B_2^T P_o + \gamma_L^2 P_o P_o \right) \end{aligned} \quad (5.81)$$

where Q_o is a positive definite matrix and δ is a positive constant. Using the above Riccati equation one can verify that the following inequality holds:

$$\begin{aligned} \dot{V}_o \leq & -\mathbf{e}^T (P_{H_\sigma} \otimes (Q_o + \delta P_o)) \mathbf{e} + \lambda_{\min}(P_{H_\sigma})(1 + \gamma_{\Delta}^{-2}) \|\mathbf{z}\|^2 \\ & + \lambda_{\min}(P_{H_\sigma})\gamma_R^2 \|\omega\|^2 + 2\lambda_{\min}(P_{H_\sigma})\gamma_\nu^2 \|\nu\|^2 \end{aligned} \quad (5.82)$$

At this point one can follow along the same lines as presented for the observer-based consensus algorithm design presented in Section 5.1 and the controller design procedure for a team with model uncertainty in absence of measurement noise in Section 5.2.1 to design an observer-based distributed controller that guarantees H_∞ output consensus achievement of the multi-agent system in presence of measurement noise and model uncertainties.

5.2.3 Simulation Results

In this section we modified the case study that we selected to perform our numerical simulations in the previous section to show performance and effectiveness of our approach and also make it comparable with previous results that we obtained. In this section, our team consists of 4 agents with the following dynamics and we use the same communication network topology as in the previous section shown in Figure 5.1, namely.

$$\dot{x}_i = Ax_i + E_L \Delta E_R x_i + f(x_i) + Bu_i + B_\omega \omega_i$$

where $E_R = I$, $E_L = 0.001I$, matrices A , B , and B_ω are defined as in (5.44), the function $f(\cdot)$ and Δ are defined as follows:

$$\Delta = \begin{bmatrix} 0 & 0 & \sin(2t) \\ \sin(t) & 0 & 0 \\ 0 & \cos(t) & 0 \end{bmatrix}, \quad f(x) = 0.001 \begin{bmatrix} 0 \\ \frac{\sin(x_1)}{1+x_1^2} \\ \frac{x_2}{1+x_2^2} \end{bmatrix}$$

The design parameters are selected as $Q_H = I$, $Q_A = 14.5I$, $\gamma_R = 0.75$, $\gamma_L = 0.0013$, $\eta = 0.97$, and $\delta = 0.23$. The resulting agent controller gains become $K_1 = \begin{bmatrix} -32.90 & -26.74 & 35.61 \end{bmatrix}$ and $K_2 = \begin{bmatrix} -8.45 & -6.68 & 7.96 \end{bmatrix}$. Figures 5.12 and 5.13 depict the angular velocity and pitch angle of the agents,

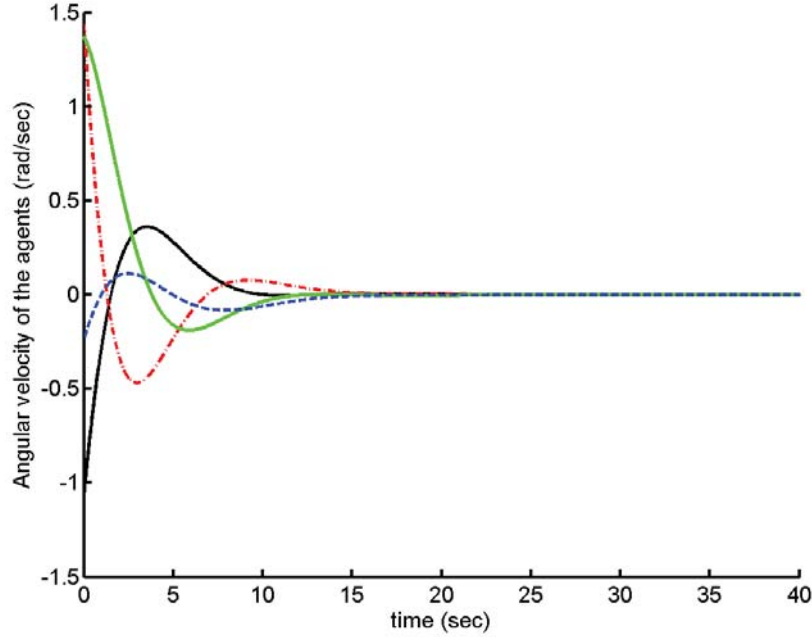


Figure 5.12: Angular velocity of the agents.

respectively. The depth of the agents is shown in Figure 5.14. Noting that the control input signal u_i is in fact the deflection of the control surface of the i^{th} agent which is measured in units of degrees, the resulting control signal depicted in Figure 5.15 is feasible. Similar to the previous section, disturbance signal is a combination of several sinusoidal signals with different frequencies where their phases and frequencies are selected randomly with an RMS of 1.

Furthermore, to compare the performance of our proposed distributed consensus algorithm design procedure with the work in the literature, we chose one of the most recent work in this field presented in [94]. Similar to our proposed approach, this work deals with consensus achievement of leaderless high-order multi-agent systems with Lipschitz nonlinearity and switching topology communication networks. However, their approach requires solving a set of computationally expensive LMIs and does not consider linear model uncertainties and disturbance signals. In contrast, our proposed method is based on the solution to an algebraic Riccati equation and can deal with linear model uncertainties and disturbance signals. We applied our method to

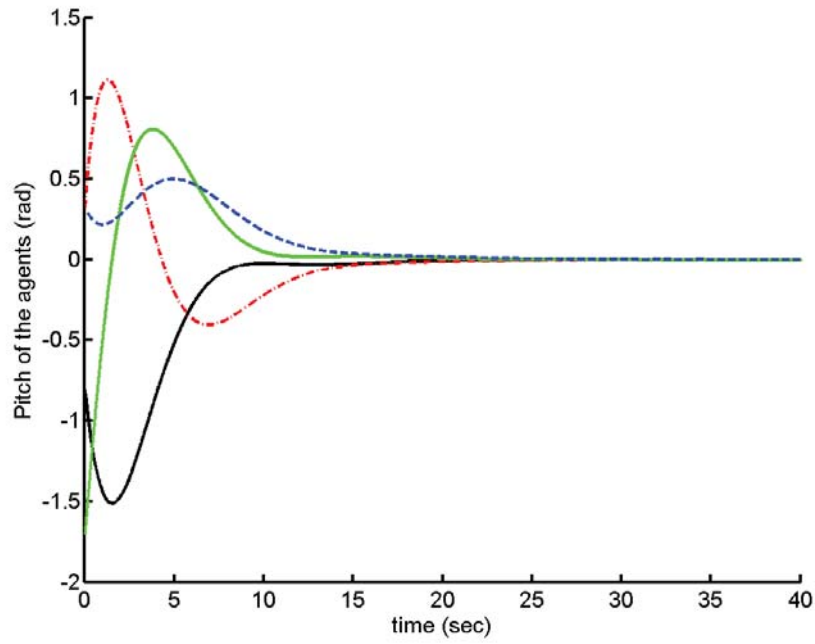


Figure 5.13: Pitch angle of the agents.

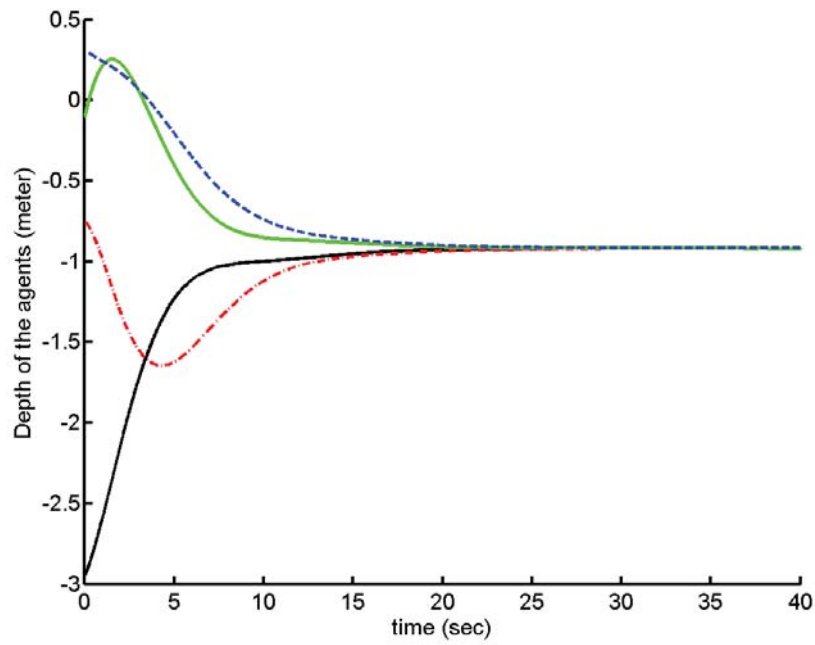


Figure 5.14: Depth (output signal) of the agents.

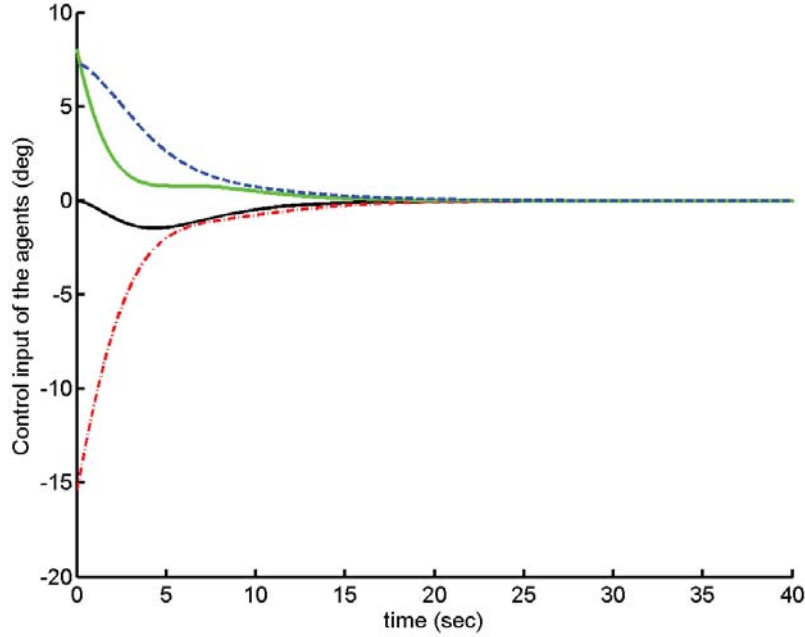


Figure 5.15: Control inputs of the agents.

the same numerical simulation example presented in [94]. In their work, the authors considered a team of 4 agents with following dynamics:

$$\dot{x}_i = Ax_i + Bu_i + f(x_i) \quad (5.83)$$

where

$$A = \begin{bmatrix} 0 & 1 \\ 0 & 0 \end{bmatrix}, B = \begin{bmatrix} 0 \\ 1 \end{bmatrix}, f(x_i) = \gamma_L \begin{bmatrix} 0 \\ \sin(x_{i2}) \end{bmatrix}, \quad (5.84)$$

where $\gamma_L = 0.05$. In [94], it is assumed that the communication network topology is selected among the graphs presented in Figure 5.16 and the piece-wise constant switching signal is illustrated in Figure 5.17. The agent controller gain that is calculated based on their proposed method is $K = [4.95461.1727]$. Figures 5.18 and 5.19 show the first and second states of the agents, respectively.

We have applied our proposed method to the same multi-agent system (5.84) with $\gamma_L = 0.075$ and used the same communication network and switching signal depicted in Figures 5.16 and 5.17, respectively. The controller gains

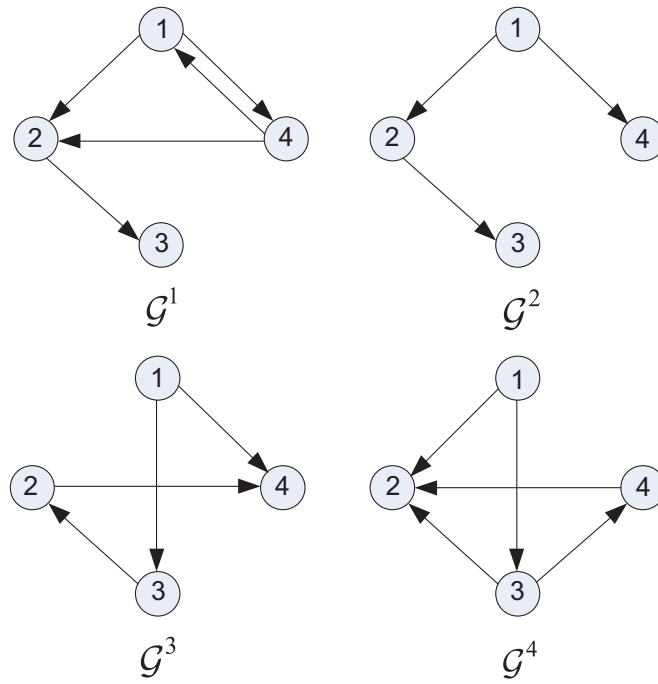


Figure 5.16: Communication network topologies that are used in [94].

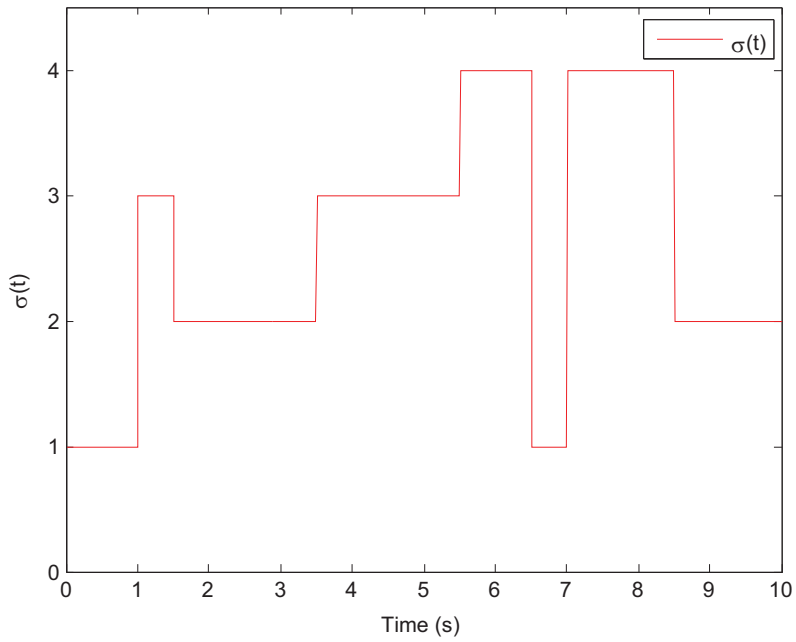


Figure 5.17: Switching signal that is used in [94].

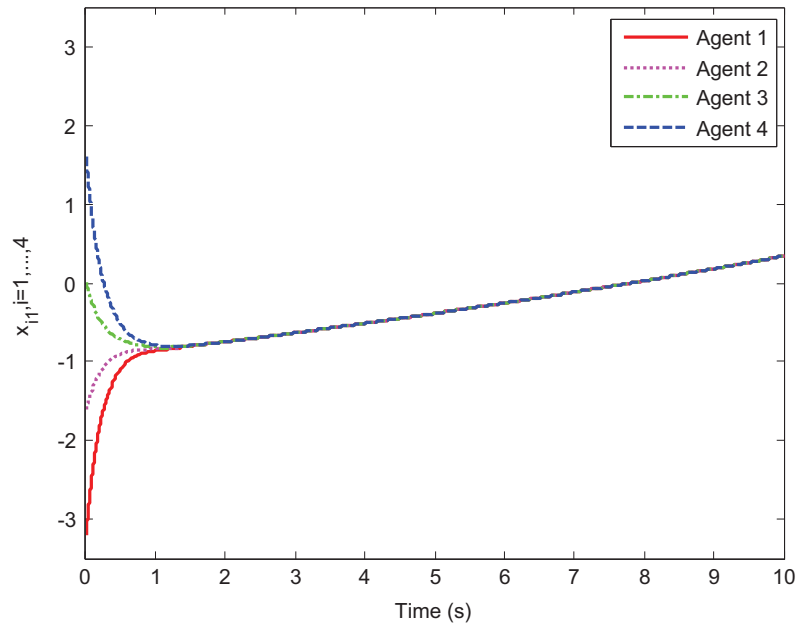


Figure 5.18: Trajectories of the first states in Example 1 of [94].

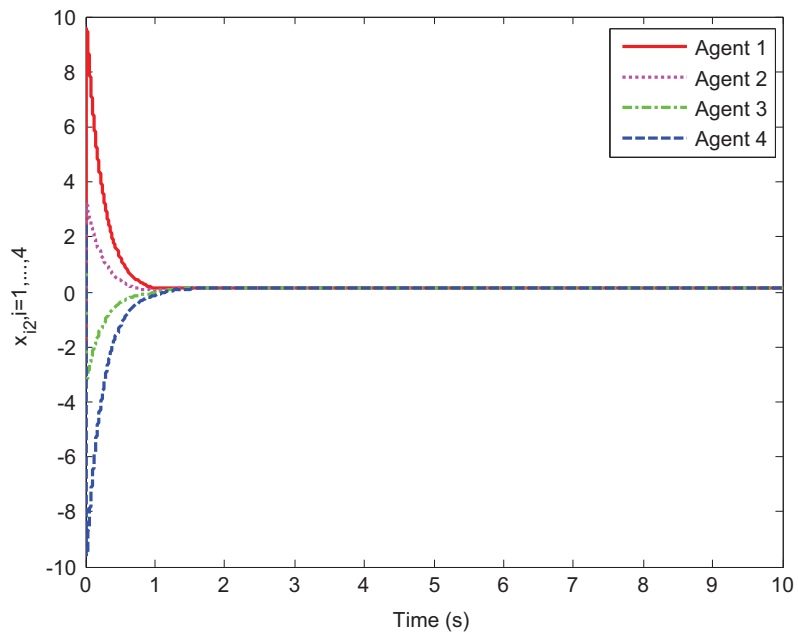


Figure 5.19: Trajectories of the second states in Example 1 of [94].

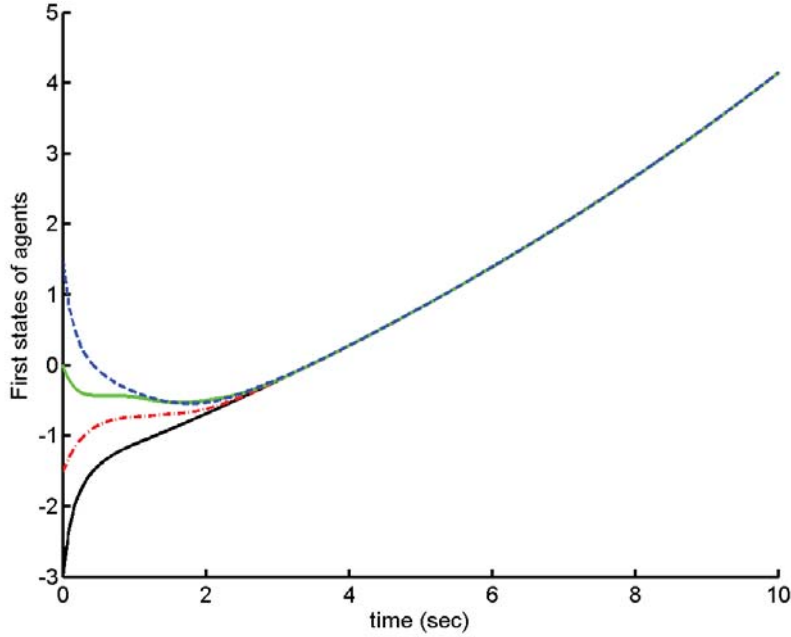


Figure 5.20: Trajectories of the first states of the agents using our proposed method.

obtained for different communication graphs \mathcal{G}_1 to \mathcal{G}_4 are $K_1 = [-3.9452 - 4.3882]$, $K_2 = [-4.3717 - 4.6469]$, $K_3 = [-4.8118 - 4.9099]$ and $K_4 = [-4.7976 - 4.9015]$, respectively. Figure 5.20 shows the trajectories of the first states of agents and in Figure 5.20 the second states of the team are illustrated.

Furthermore, the quantitative comparison between our proposed method and the method in [94] is presented in Table 5.2. As seen in these figures and Table 5.2, although the settling time of our proposed consensus algorithm is more than that of the method presented in [94], our proposed method can guarantee consensus achievement of the team with larger Lipschitz constants.

5.3 Cooperative Adaptive Consensus Achievement of Nonlinear Multi-Agent Systems

In this section we consider a more general class of nonlinear multi-agent systems and design a cooperative adaptive algorithm for online approximation of nonlinearity in dynamics of agents and based on that we will propose a

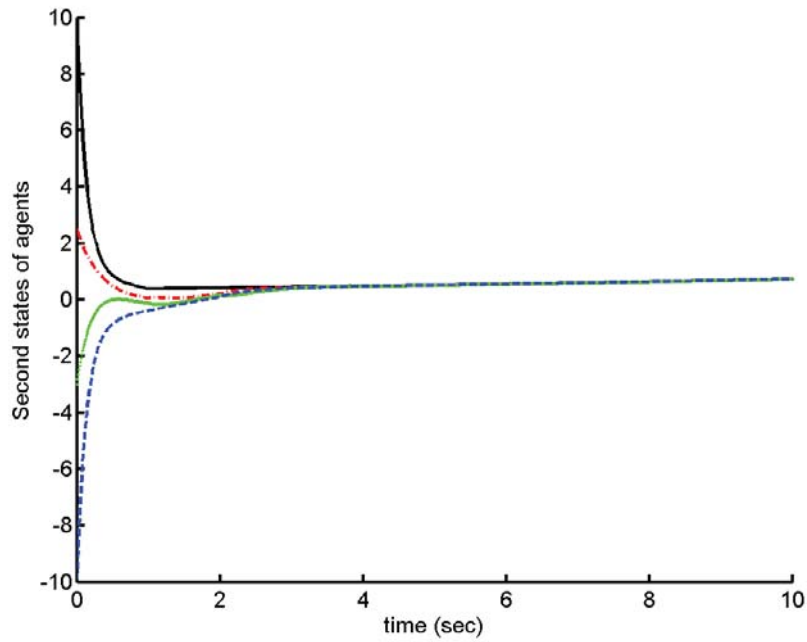


Figure 5.21: Trajectories of the second states of the agents using our proposed method.

Table 5.2: The comparison between our proposed method and the method in [94].

	Control effort (max)	Control effort (L_2 norm)	Consensus error (RMS)	Settling time (sec)
Our proposed method ($\gamma_L = 0.05$)	37.11	205.17	34.81	0.75
The method in [94] ($\gamma_L = 0.05$)	115.83	284.31	32.13	0.70
Our proposed method ($\gamma_L = 0.075$)	70.01	271.87	28.36	1.00
The method in [94] ($\gamma_L = 0.075$)	115.83	284.35	32.13	0.70

controller that guarantees uniformly ultimately bounded (UUB) consensus achievement of the team.

First, consider a multi-agent system consisting of N agents with the following dynamics:

$$\dot{x}_i = Ax_i + Bu_i + Bf_i(x_i) + B_2\omega_i \quad (5.85)$$

where $A \in \mathbb{R}^{p \times p}$, $B \in \mathbb{R}^{p \times m}$, $B_2 \in \mathbb{R}^{p \times q}$ are real matrices, $f_i : \mathbb{R}^p \rightarrow \mathbb{R}^m$ is an unknown nonlinear function, and $x_i \in \mathbb{R}^p$ and $u_i \in \mathbb{R}^m$, and $\omega_i \in \mathbb{R}^q$ are state, control input, and disturbance of the i^{th} agent, respectively. It is assumed that states of all agents are measurable and the pair (A, B) is controllable. The communication network among agents is considered to be undirected and connected. Furthermore, we consider a virtual leader with the following dynamics and assume its state is accessible to at least one of the agents and its dynamics is governed by the following equation:

$$\dot{x}_\ell = Ax_\ell \quad (5.86)$$

Therefore, all agents directly or through other agents can access the virtual leader information through the communication network. Now, let us define the consensus error of the i^{th} agent as follows:

$$e_i = \mathfrak{l}_i(x_i - x_\ell) + \sum_{j \in \mathcal{N}_i} (x_i - x_j) \quad (5.87)$$

where \mathcal{N}_i is the neighboring set of the i^{th} agent and \mathfrak{l}_i is equal to 1 when the agent has direct access to the virtual agent and it is zero otherwise. Using the above definition, the multi-agent team achieves consensus if e_i , for $i = 1, \dots, n$ converges to zero.

For the case of a known nonlinear function $f_i(\cdot)$, the controller design procedure is straightforward. Inspired by this fact, for the case of unknown function $f_i(\cdot)$, numerous methods are proposed in the literature to estimate the function and control the overall system. However, in most of these approaches only local information is used for function approximation despite the fact that in multi-agent systems each agent has access to information of its neighboring agents. To resolve this drawback, in this section we propose a cooperative learning algorithm for our function approximation phase. We assume that

the nonlinear function $f_i(\cdot)$ can be approximated by using a class of general function approximator that is formally formulated according to the following assumptions.

Assumption 5.5. *There exists a compact set $\Omega \subseteq \mathbb{R}^p$ and a smooth matrix function $\Phi : \Omega \rightarrow \mathbb{R}^{m \times l}$ where $l \geq 1$ known as the basis function, such that the unknown nonlinear function $f_i : \mathbb{R}^p \rightarrow \mathbb{R}^m$ satisfies the following equation for any $x \in \Omega$,*

$$f_i(x) = \Phi(x)W_i + \varepsilon_i(x) \quad (5.88)$$

where the vector $W_i \in \mathbb{R}^l$ represents the parameters of the approximator and $\varepsilon_i(x) \in \mathbb{R}^m$ denotes the approximation error.

Assumption 5.6. *For the nonlinear function $f_i(\cdot)$ and the general function approximator denoted by equation (5.88) in Assumption 5.5 there exists an optimal W_i^* which is defined as follows:*

$$W_i^* = \arg \min_{W_i \in \mathbb{R}^l} \left\{ \sup_{x \in \Omega} \|f_i(x) - \Phi(x)W_i\| \right\} \quad (5.89)$$

and the approximation error is bounded by ε_u^* , which is defined as

$$\varepsilon_u^* = \sup_{x \in \Omega} \|f_i(x) - \Phi(x)W_i^*\| \quad (5.90)$$

Assumption 5.7. *In the function approximation presented in Assumption 5.5, the approximation error bound ε_u^* defined in Assumption 5.6 can arbitrarily become small if the dimension of the basis function Φ denoted by l in Assumption 5.5 is sufficiently large.*

Remark 5.2. *In the remainder of this section we will use radial basis function (RBF) neural networks (NN) approach for the function approximation. However, we are not limited to RBF neural networks and many other function approximation techniques can be employed as long as they satisfy the assumptions presented in this section.*

For the RBF neural networks, the matrix function $\Phi(x) = [\Phi_1(x) \dots \Phi_l(x)]$ is defined as $\Phi_i(x) = \mathbf{e}_i \phi_i(x)$, where the constant vector $\mathbf{e}_i \in \mathbb{R}^p$ has a non-zero

element equal to 1 and the scalar function ϕ_i is a Gaussian function as follows

$$\phi_i(x) = e^{-\frac{\|x-\xi_i\|^2}{\eta_i}}.$$

and where ξ_i and η_i are the center and variance of the node, respectively.

Let us define $\mathbf{e} = [e_1^T, \dots, e_n^T]^T$, $\mathbf{x} = [x_1^T, \dots, x_n^T]^T$, $\mathbf{x}_\ell = [x_\ell^T, \dots, x_\ell^T]^T$, $\mathfrak{L}_\sigma = \text{diag}\{\iota_1, \dots, \iota_n\}$ and let L_σ be defined as per Definition 3.8. One can obtain:

$$\mathbf{e} = (L_\sigma \otimes I)\mathbf{x} + (\mathfrak{L}_\sigma \otimes I)(\mathbf{x} - \mathbf{x}_\ell)$$

Lemma 5.2. *Assume $L_\sigma \in \mathbb{R}^{n \times n}$ is a Laplacian matrix associated with a connected undirected graph and $\mathfrak{L}_\sigma \in \mathbb{R}^{n \times n}$ is a non-zero diagonal matrix with non-negative elements. The matrix $H_\sigma = L_\sigma + \mathfrak{L}_\sigma$ is symmetric and positive definite.*

Proof. Let the non-negative numbers ι_1, \dots, ι_n denote diagonal elements of the matrix \mathfrak{L}_σ and \mathcal{G} denotes the undirected graph associated with the Laplacian matrix L_σ . Now, let us construct the new digraph \mathcal{G}^* by adding a node to the graph \mathcal{G} and without loss of generality label it as the node $n + 1$. Let L^* be its corresponding Laplacian matrix that is defined as follows:

$$L^* = \begin{bmatrix} & & -\iota_1 \\ & L_\sigma + \mathfrak{L}_\sigma & \vdots \\ & & -\iota_n \\ 0 & \dots & 0 \end{bmatrix}$$

Note that the graph \mathcal{G} is undirected and connected and at least one of the real numbers ι_1, \dots, ι_n is positive. Therefore, the digraph \mathcal{G}^* has a directed spanning tree and node $n + 1$ is its root. Furthermore, the matrix H_σ is symmetric and its eigenvalues are real. Now, by using the Lemma 3.3 and knowing that the digraph \mathcal{G}^* has a directed spanning tree and all eigenvalues are the matrix H_σ are real, one can conclude the proof of the lemma. \blacksquare

Using the above lemma one can obtain the dynamics of the consensus error variables as follows:

$$\dot{\mathbf{e}} = (H_\sigma \otimes I)\dot{\mathbf{x}} - (\mathfrak{L}_\sigma \otimes I)\dot{\mathbf{x}}_\ell$$

Using Assumptions 5.5 and 5.6 and equations (5.85) and (5.86), one can verify the validity of the following dynamic equation:

$$\dot{\mathbf{e}} = (H_\sigma \otimes A)\mathbf{x} - (\mathfrak{L}_\sigma \otimes A)\mathbf{x}_\ell + (H_\sigma \otimes B)\Phi\mathbf{W}^* + (H_\sigma \otimes B)\boldsymbol{\varepsilon} + (H_\sigma \otimes B)\mathbf{u} + (H_\sigma \otimes B_2)\boldsymbol{\omega} \quad (5.91)$$

where $\mathbf{W}^* = [W_1^{*T}, \dots, W_n^{*T}]^T$ denotes the optimal approximator weights, $\boldsymbol{\varepsilon} = [\varepsilon_1^T, \dots, \varepsilon_n^T]^T$ denotes the optimal approximation errors, $\boldsymbol{\omega} = [\omega_1^T, \dots, \omega_n^T]^T$, $\mathbf{u} = [u_1^T, \dots, u_n^T]^T$, and the matrix Φ is defined as follows:

$$\Phi = \begin{bmatrix} \Phi_1(x_1) & 0 & \dots & 0 \\ 0 & \Phi_2(x_2) & \dots & 0 \\ \vdots & \ddots & & \vdots \\ 0 & \dots & 0 & \Phi_n(x_n) \end{bmatrix}$$

Now, let us consider the following controller:

$$u_i = -\frac{1}{2\epsilon_\sigma} B^T P_A e_i - \Phi(x_i) \hat{W}_i \quad (5.92)$$

where \hat{W}_i denotes the estimate of the optimal RBF neural networks weights that are used by the i^{th} agent, ϵ_σ is a positive number that satisfies the inequality $H_\sigma - \epsilon_\sigma I > 0$, and finally $P_A \in \mathfrak{R}^{p \times p}$ is a symmetric and positive definite solution to the following Riccati equation

$$P_A A + A^T P_A - P_A B B^T P_A + \mu_\sigma \gamma_\varepsilon^{-2} P_A B B^T P_A + \mu_\sigma \gamma_\omega^{-2} P_A B_2 B_2^T P_A = -Q_A \quad (5.93)$$

where Q_A is a symmetric positive definite matrix, γ_ε , and γ_ω are positive constants and $\mu_\sigma = \max_\sigma \frac{\lambda_{\max}(H_\sigma)}{\lambda_{\min}(H_\sigma)}$. By substituting equation (5.92) into equation (5.91), one obtains:

$$\begin{aligned} \dot{\mathbf{e}} = & (I \otimes A - \frac{1}{2} B B^T P_A) \mathbf{e} - \frac{1}{2\epsilon_\sigma} (H_\sigma - \epsilon_\sigma I \otimes B B^T P_A) \mathbf{e} \\ & - (H_\sigma \otimes B) \Phi \tilde{\mathbf{W}} + (H_\sigma \otimes B) \boldsymbol{\varepsilon} + (H_\sigma \otimes B_2) \boldsymbol{\omega} \end{aligned} \quad (5.94)$$

where $\tilde{W} = \hat{W} - W^*$ and $\hat{W} = [\hat{W}_1^T, \dots, \hat{W}_n^T]^T$. Now, let us present the following learning law:

$$\dot{\hat{W}} = \Gamma \left(\Phi^T (H_\sigma \otimes B^T P_A) \mathbf{e} - \eta \hat{W} \right) \quad (5.95)$$

where $\Gamma \in \mathfrak{R}^{nl \times nl}$ is a diagonal positive definite matrix and denotes the learning gain, η is a positive constant and denotes the learning factor.

Remark 5.3. *Whenever all the nonlinear functions $f_1(\cdot), \dots, f_n(x)$ are identical, the optimal approximator weights $W_1^{*T}, \dots, W_n^{*T}$ are the same and equal to W^* . Therefore, in principle all the estimated weights \hat{W}_i should converge to the same value. We can use this fact to our advantage and let the team share their learned knowledge by using the following cooperative learning law*

$$\dot{\hat{W}} = \Gamma \left(\Phi^T (H_\sigma \otimes B^T P_A) \mathbf{e} - \eta_c (L_\sigma \otimes I) \hat{W} - \eta \hat{W} \right) \quad (5.96)$$

where the positive constant η_c denotes the cooperative learning factor. Note that $\hat{W}_i - \hat{W}_j = \hat{W}_i - W^* + W^* - \hat{W}_j = \tilde{W}_i - \tilde{W}_j$. Therefore, one can verify the validity of the following equation:

$$(L_\sigma \otimes I) \hat{W} = (L_\sigma \otimes I) \tilde{W}$$

Remark 5.4. *In the remainder of this section, instead of using the learning law (5.95) we use the cooperative learning law (5.96) and set η_c to 0.*

Theorem 5.3. *The consensus error defined in (5.87) for the nonlinear multi-agent team (5.85) with the virtual leader (5.86) is uniformly ultimately bounded if the undirected switching topology communication network \mathcal{G}_σ is connected, the controller (5.92) and the learning rule (5.96) are employed, all the nonlinear functions $f_i(x)$ satisfies Assumptions 5.5- 5.7, the pair (A, B) is controllable, and the following inequality holds for all ω_i :*

$$\sup_t \{ \|\omega_i(t)\| \} \leq \varpi$$

where ϖ is a positive constant.

Proof. Consider the following Lyapunov function candidate:

$$V(\mathbf{e}, \tilde{\mathbf{W}}) = \frac{1}{2} \mathbf{e}^T (I \otimes P_A) \mathbf{e} + \frac{1}{2} \tilde{\mathbf{W}}^T \Gamma^{-1} \tilde{\mathbf{W}} \quad (5.97)$$

By taking the time derivative of the above Lyapunov function along the trajectories of the augmented equations (5.94) and (5.96), one can obtain:

$$\begin{aligned} \dot{V} &= \mathbf{e}^T (I \otimes P_A A + A^T P_A - P_A B B^T P_A) \mathbf{e} - \frac{1}{2\epsilon_\sigma} \mathbf{e}^T (H_\sigma - \epsilon_\sigma I \otimes P_A B B^T P_A) \mathbf{e} \\ &\quad - \mathbf{e}^T (H_\sigma \otimes P_A B) \Phi \tilde{\mathbf{W}} + \mathbf{e}^T (H_\sigma \otimes P_A B) \varepsilon + \mathbf{e}^T (H_\sigma \otimes P_A B_2) \omega \\ &\quad + \tilde{\mathbf{W}}^T \Phi^T (B^T P_A \otimes H_\sigma) \mathbf{e} - \eta_c \tilde{\mathbf{W}}^T (L_\sigma \otimes I) \tilde{\mathbf{W}} - \eta \tilde{\mathbf{W}}^T \hat{\mathbf{W}} \\ &\leq \mathbf{e}^T (I \otimes P_A A + A^T P_A - P_A B B^T P_A) \mathbf{e} + \mathbf{e}^T (H_\sigma \otimes P_A B) \varepsilon \\ &\quad + \mathbf{e}^T (H_\sigma \otimes P_A B_2) \omega - \eta_c \tilde{\mathbf{W}}^T (L_\sigma \otimes I) \tilde{\mathbf{W}} - \eta \tilde{\mathbf{W}}^T \hat{\mathbf{W}} \end{aligned} \quad (5.98)$$

Using the inequality (5.10), we have:

$$\begin{aligned} \dot{V} &\leq \mathbf{e}^T (I \otimes P_A A + A^T P_A - P_A B B^T P_A + \mu_\sigma \gamma_\epsilon^{-2} P_A B B^T P_A + \mu_\sigma \gamma_\omega^{-2} P_A B_2 B_2^T P_A) \mathbf{e} \\ &\quad + \gamma_\epsilon^2 \varepsilon^T \varepsilon + \gamma_\omega^2 \omega^T \omega - \eta_c \tilde{\mathbf{W}}^T (L_\sigma \otimes I) \tilde{\mathbf{W}} - \eta \tilde{\mathbf{W}}^T \hat{\mathbf{W}} \end{aligned} \quad (5.99)$$

After some algebraic manipulations one can verify that for any matrix \mathcal{M} the following inequality holds:

$$\begin{aligned} 2\tilde{\mathbf{W}}^T \mathcal{M} \hat{\mathbf{W}} &= 2(\hat{\mathbf{W}} - \mathbf{W}^*)^T \mathcal{M} \hat{\mathbf{W}} = 2\hat{\mathbf{W}}^T \mathcal{M} \hat{\mathbf{W}} - 2\mathbf{W}^{*T} \mathcal{M} \hat{\mathbf{W}} \\ &= 2\hat{\mathbf{W}}^T \mathcal{M} \hat{\mathbf{W}} - 2\mathbf{W}^{*T} \mathcal{M} \hat{\mathbf{W}} + \mathbf{W}^{*T} \mathcal{M} \mathbf{W}^* - \mathbf{W}^{*T} \mathcal{M} \mathbf{W}^* \\ &= \hat{\mathbf{W}}^T \mathcal{M} \hat{\mathbf{W}} + (\hat{\mathbf{W}} - \mathbf{W}^*)^T \mathcal{M} (\hat{\mathbf{W}} - \mathbf{W}^*) - \mathbf{W}^{*T} \mathcal{M} \mathbf{W}^* \quad (5.100) \\ &= \hat{\mathbf{W}}^T \mathcal{M} \hat{\mathbf{W}} + \tilde{\mathbf{W}}^T \mathcal{M} \tilde{\mathbf{W}} - \mathbf{W}^{*T} \mathcal{M} \mathbf{W}^* \\ &\geq \tilde{\mathbf{W}}^T \mathcal{M} \tilde{\mathbf{W}} - \mathbf{W}^{*T} \mathcal{M} \mathbf{W}^* \end{aligned}$$

Using the above inequality and substituting equation (5.93) into the inequality (5.99) one obtains:

$$\begin{aligned}
\dot{V} &\leq -\mathbf{e}^T(I \otimes Q_A)\mathbf{e} + \gamma_\varepsilon^2 \varepsilon^T \varepsilon + \gamma_\omega^2 \omega^T \omega - \eta_c \tilde{\mathbf{W}}^T (L_\sigma \otimes I) \tilde{\mathbf{W}} \\
&\quad - \frac{1}{2} \eta \tilde{\mathbf{W}}^T \tilde{\mathbf{W}} + \frac{1}{2} \eta \mathbf{W}^{*T} \mathbf{W}^* \\
&\leq -\mathbf{e}^T(I \otimes Q_A)\mathbf{e} - \eta_c \tilde{\mathbf{W}}^T (L_\sigma \otimes I) \tilde{\mathbf{W}} - \frac{1}{2} \eta \tilde{\mathbf{W}}^T \tilde{\mathbf{W}} \\
&\quad + \gamma_\varepsilon^2 \|\varepsilon\|^2 + \gamma_\omega^2 \|\omega\|^2 + \frac{1}{2} \eta \|\mathbf{W}^*\|^2
\end{aligned} \tag{5.101}$$

Using the above inequality one can verify that $\dot{V} < 0$ as long as the pair $(\mathbf{e}, \tilde{\mathbf{W}})$ is outside the compact set $\Theta = \Theta_e \cap \Theta_w$, where Θ_e and Θ_w are compact sets defined as follows:

$$\Theta_e = \left\{ (\mathbf{e}, \tilde{\mathbf{W}}) \mid \|\mathbf{e}\| \leq \sqrt{\frac{\mathcal{C}}{\lambda_{\min}(Q_A)}} \right\}, \quad \Theta_w = \left\{ (\mathbf{e}, \tilde{\mathbf{W}}) \mid \|\tilde{\mathbf{W}}\| \leq \sqrt{\frac{2}{\eta} \mathcal{C}} \right\} \tag{5.102}$$

where $\mathcal{C} = n\gamma_\varepsilon \varepsilon_u^{*2} + n\gamma_\omega^2 \varpi^2 + \frac{1}{2} \eta \|\mathbf{W}^*\|^2$. Therefore, the overall multi-agent system is uniformly ultimately bounded. Furthermore, one can verify that \dot{V} is negative definite outside the compact set Θ_e and therefore an attractive set. Therefore, the upper bound of $\|\mathbf{e}\|$ can be arbitrarily reduced as \mathcal{C} decreases or $\lambda_{\min}(Q_A)$ increases and this concludes the proof of the theorem. \blacksquare

Remark 5.5. *Although, our proposed cooperative learning based consensus algorithm guarantees that the estimation error of the RBF neural network weight remains bounded, however our method cannot guarantee that the upper bound of the estimation error of the NN weights can be arbitrarily reduced without invoking the persistent excitation (PE) condition [144].*

Simulation Results

To show the effectiveness of our proposed learning based consensus algorithm we performed numerical simulations for a team of four agents where their dynamics is governed by equation (5.85), with matrices A , B , and B_ω defined in (5.44). In our simulations, each agent uses an RBF neural network with 5 neurons to learn the nonlinear function $f(x)$. Figure 5.22 depicts the two undirected graph that are used by the agents to exchange information and the

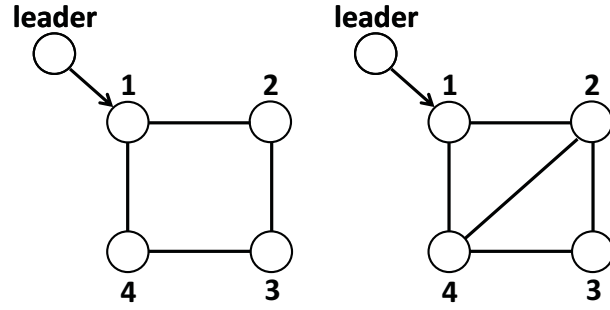


Figure 5.22: Communication networks topologies.

communication network topology of the team changes smoothly between these two networks every 30 seconds. The disturbance signals ω_i are combinations of a number of sinusoidal functions with different frequencies, amplitude of 1 and random phases. The matrix Γ in the learning rule (5.96) is set to $20I$, the learning constant $\eta = 0.0001$. Furthermore, in the algebraic Riccati equation (5.93) the constants γ_ε and γ_ω are set to 10 and the matrix $Q_A = 2I$. The resulting control gains $K_1 = \frac{1}{2\varepsilon_1}B^T P_{A_1}$ and $K_2 = \frac{1}{2\varepsilon_2}B^T P_{A_2}$ are as follows:

$$K_1 = \begin{bmatrix} -12.8491 & -9.0439 & 11.7027 \end{bmatrix}$$

$$K_2 = \begin{bmatrix} -16.9637 & -11.9357 & 15.4936 \end{bmatrix}$$

In our numerical simulation, the initial values for the RBF neural network weights and initial states of the leader and other agents are selected randomly.

To demonstrate that our proposed learning based consensus control algorithm capable of dealing with different nonlinear functions, in the first step we perform our numerical simulations on a team with the following different nonlinear functions:

$$f_1(x) = \begin{bmatrix} 0 \\ \frac{10(1-x_2^2)}{1+x_2^2} \\ 0 \end{bmatrix}, f_2(x) = -f_1(x), f_3(x) = \begin{bmatrix} 0 \\ \frac{5 \cos(x_2)}{1+x_2^2} \\ 0 \end{bmatrix}, f_4(x) = -f_3(x) \quad (5.103)$$

To make it easier to observe the effects of the neural network correction term in performance of the team, first we performed the simulations by ignoring the neural network output and by using $u_i = -\frac{1}{2\varepsilon_\sigma}B^T P_{A_i}e_i$ as the control

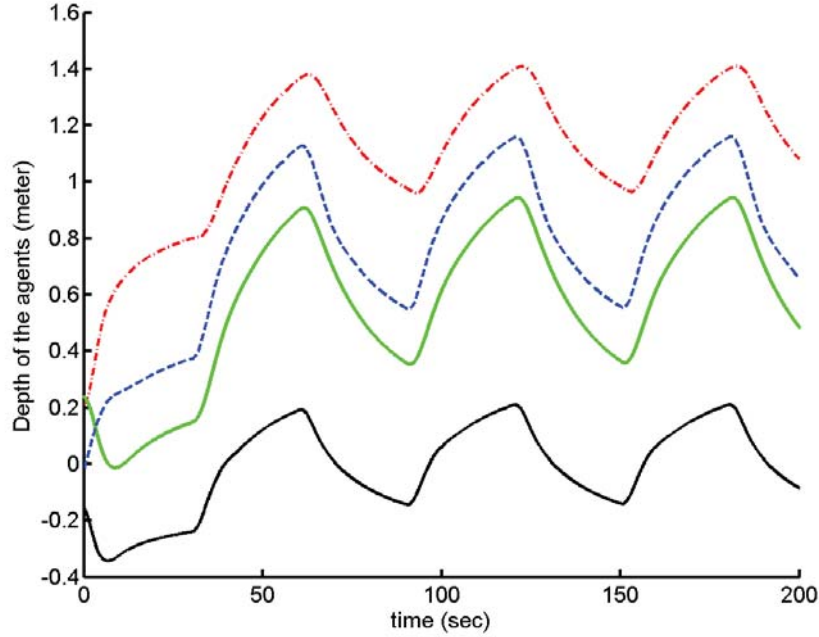


Figure 5.23: Depth of the agents with different nonlinearities and without using a neural network-based control approach.

law. Figure 5.23 shows the trajectories of the agents' depth where clearly the consensus is not achieved.

In comparison Figures 5.24, 5.25, 5.26 show different states of the agents and Figure 5.27 illustrates the consensus error signal by using the entire control law (5.92) with the neural network term and employing the learning law (5.95) with no cooperative learning term. As can be observed, the team achieves UUB consensus.

The control inputs of the agents is depicted in Figure 5.28 and finally Figure 5.29 shows the trajectories of the RBF neural network weights. In Table 5.3 the quantitative differences between these two scenarios are illustrated.

To show the importance and the performance improvement of the team by using the cooperative learning and make it easier to compare the non-cooperative learning-based and cooperative learning-based methods, in the next step we consider that the nonlinearity of all agents are identical and equal to the function $f_1(x)$ in equation (5.103). The depth of the agents and the neural network weights for the team with identical nonlinearities and

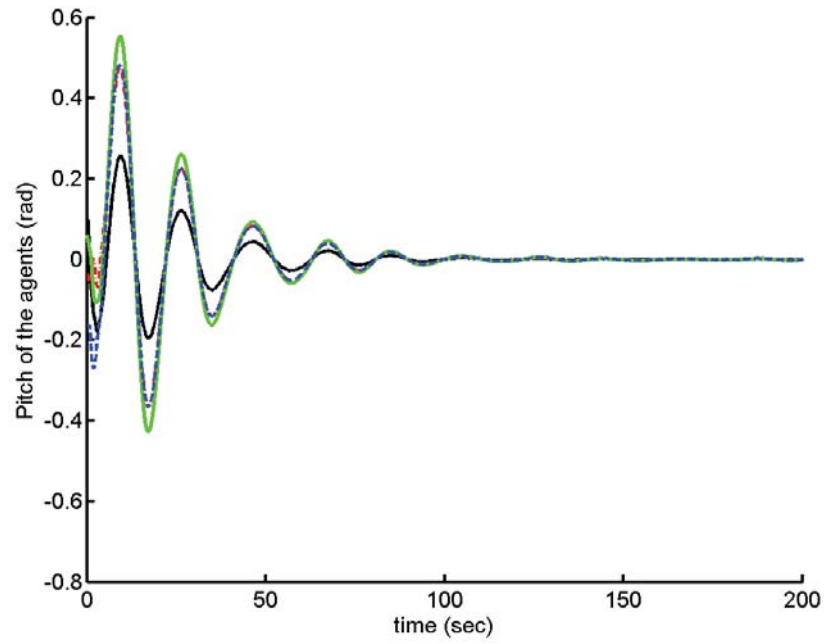


Figure 5.24: Pitch angle of the agents with different nonlinearities and by using a neural network-based control approach.

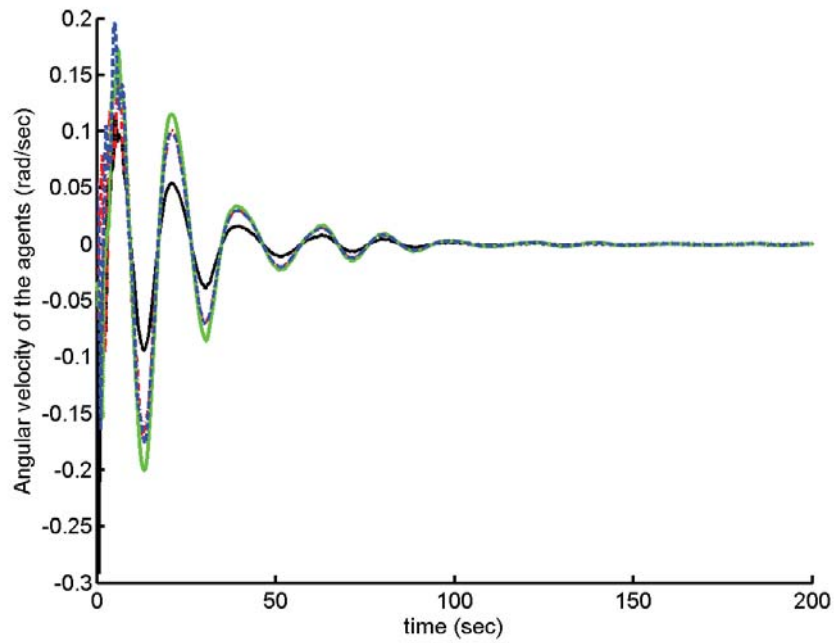


Figure 5.25: Angular velocity of the agents with different nonlinearities and by using a neural network-based control approach.

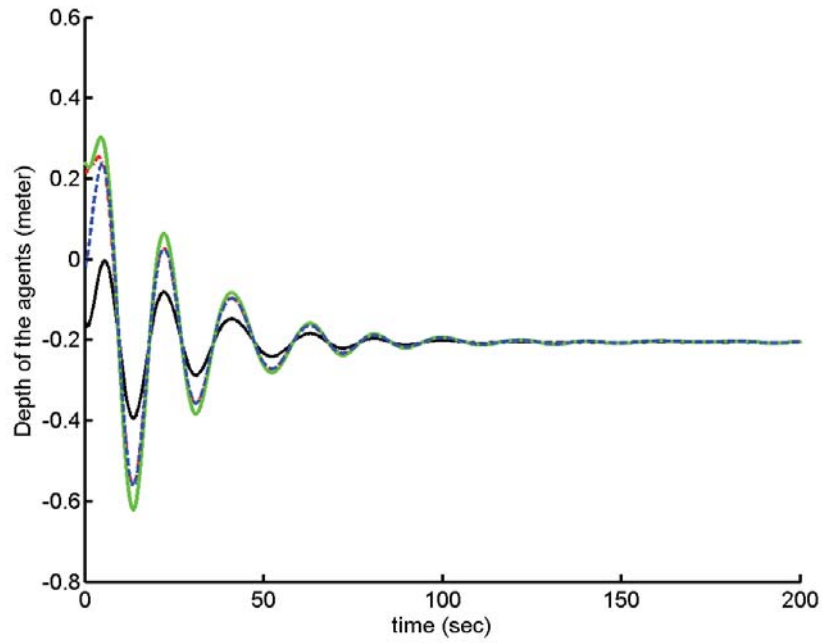


Figure 5.26: Depth of the agents with different nonlinearities and by using a neural network-based control approach.

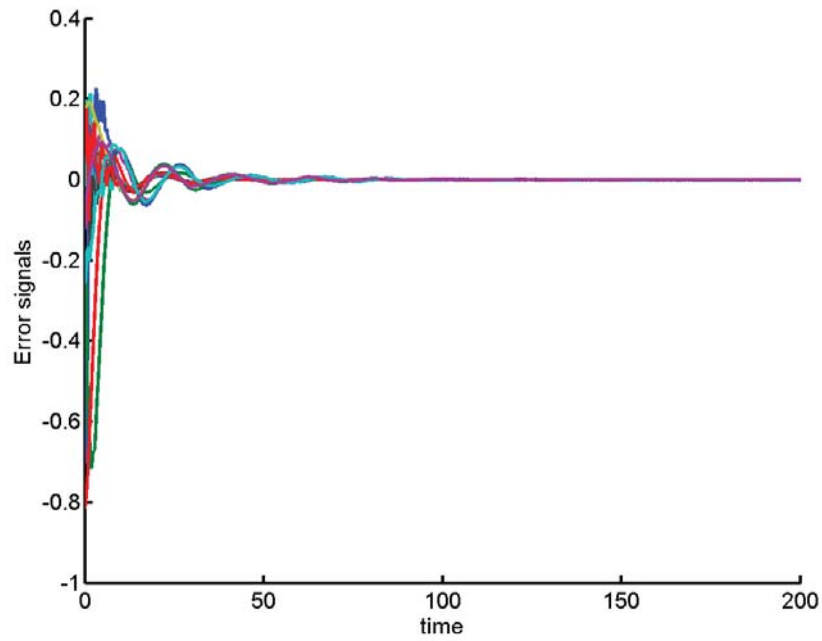


Figure 5.27: Consensus error of the team with different nonlinearities and by using a neural network-based control approach.

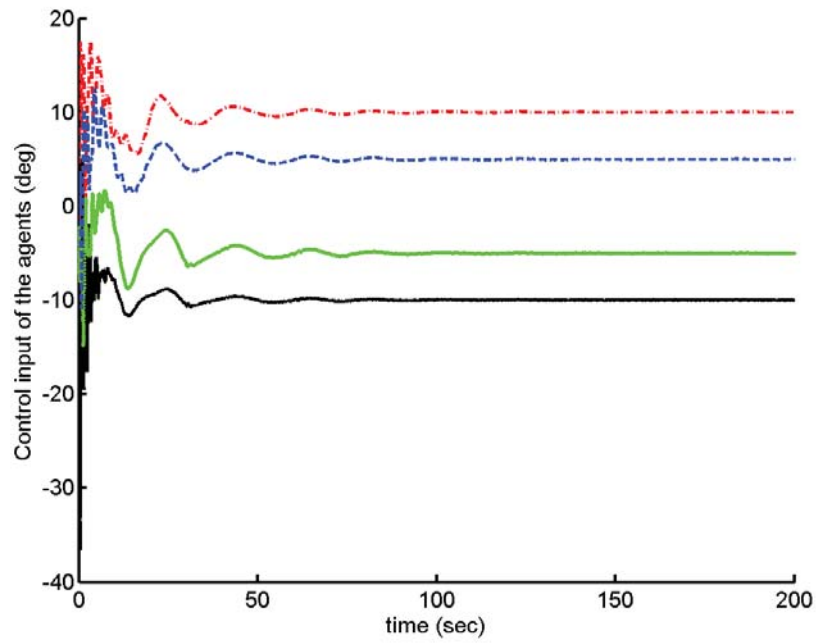


Figure 5.28: Control inputs of the agents with different nonlinearities and by using a neural network-based control approach.

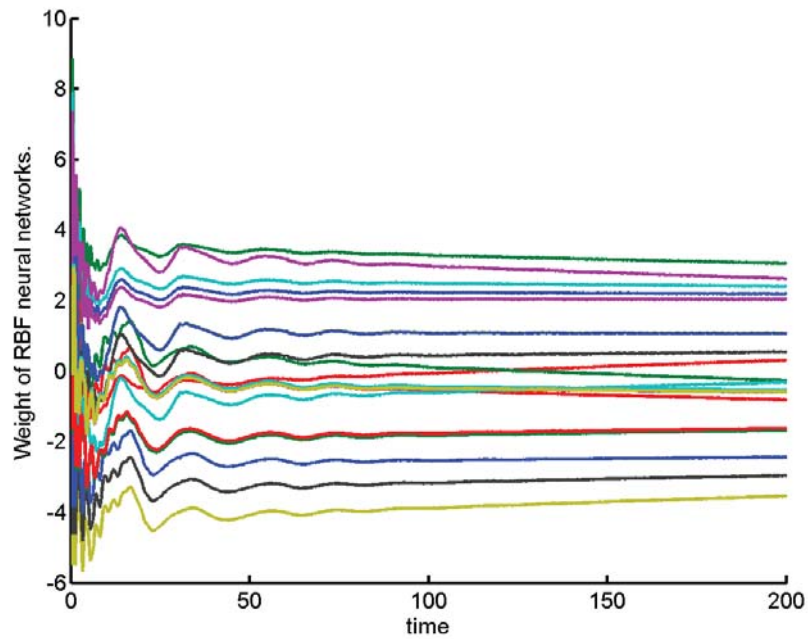


Figure 5.29: Neural network weights of the team with different nonlinearities.

Table 5.3: Quantitative comparison results for the team with different nonlinearities with and without using the neural network-based control approach.

	Settling time (sec)	Consensus error (L_2 norm)	Consensus error (steady state RMS)
The team by using the neural network-based control approach	27.09	19.60	0.0047
The team without using the neural network-based control approach	-	170.22	1.2048

without using the cooperative learning term are shown in Figures 5.30 and 5.31, respectively.

We now set the cooperative learning constant η_c to 0.1 and repeated our numerical simulation by using the cooperative learning law (5.96). In Figures 5.32, 5.33 and 5.34 the states of the agents are depicted, and the consensus error of the team is shown in Figure 5.35, and the control inputs are illustrated in Figure 5.36. As can be seen the team achieves consensus faster in comparison with the non-cooperative learning-based approach. Figure 5.37 depicts the neural network weights. It clearly shows how sharing the learned knowledge between the agents affects the trajectories of the estimated weights and causes the agents to reach a consensus on the neural network weights. Table 5.4 shows the quantitative comparison between the performances of the team with identical nonlinear functions under different control and learning laws. It can be observed that the settling time for the cooperative learning method is much faster in comparison with the non-cooperative learning method.

As stated earlier in this section, our proposed method is not limited to the RBF neural networks and is capable of dealing with different function approximation techniques. To demonstrate this, we assume that the structure of the nonlinear function is known and $f_i(x) = \kappa_i \Phi_i(x_i)$, where $\Phi_i(x) = \frac{1-x_2^2}{1+x_2^2}$, but the parameter κ_i is unknown and is required to be estimated. Let us denote the estimated values of the parameters by $\hat{\kappa}_1, \dots, \hat{\kappa}_4$. Using our proposed method, one can update the values of $\hat{\kappa} = [\hat{\kappa}_1, \dots, \hat{\kappa}_4]^T$ by employing the

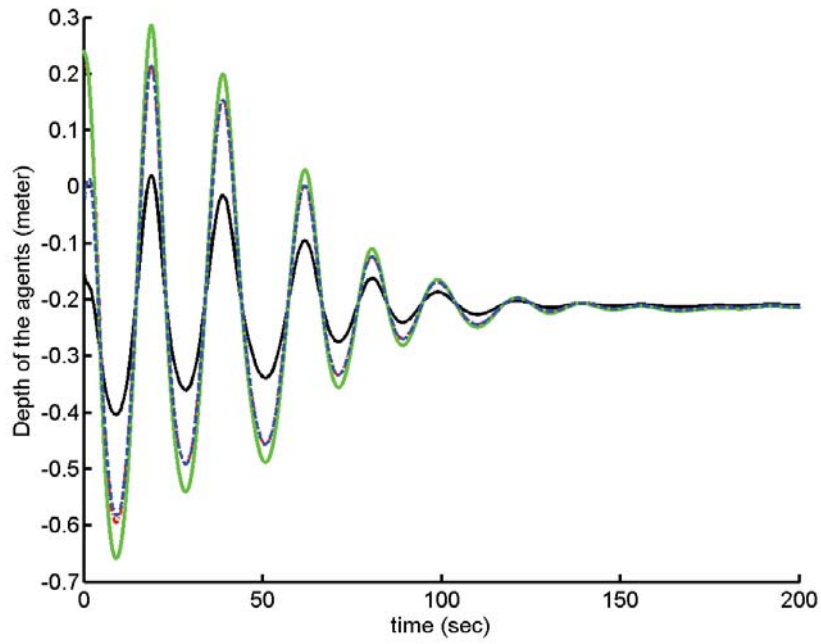


Figure 5.30: Depth of the agents with identical nonlinearities and without using the cooperative learning term.

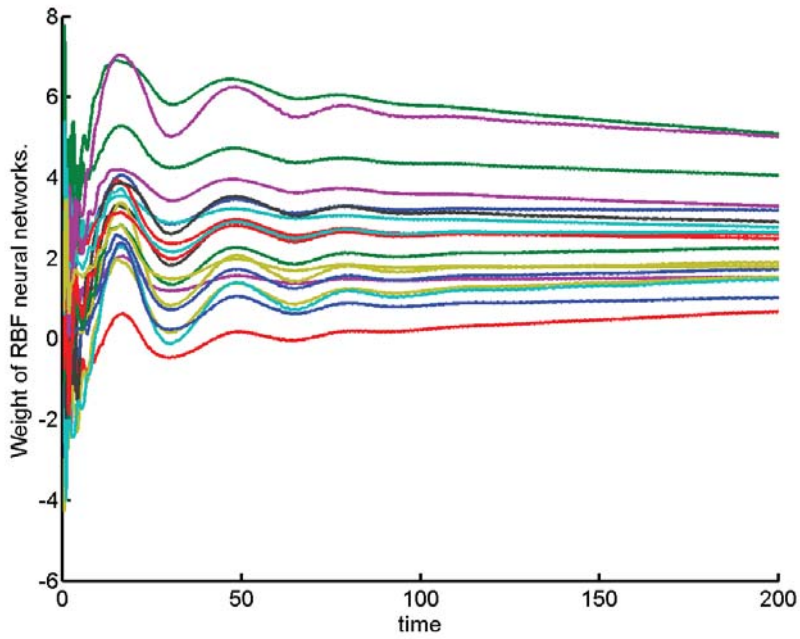


Figure 5.31: Neural network weights of the team with identical nonlinearities and without using the cooperative learning term.

Table 5.4: The simulation results for the team with identical nonlinearities.

	Settling time (sec)	Consensus error (L_2 norm)	Consensus error (steady state RMS)
The team without using the neural network-based control approach	-	191.840	1.6860
The team without using the cooperative learning method	29.998	19.632	0.0072
The team by using the cooperative learning method	9.819	18.121	0.0022

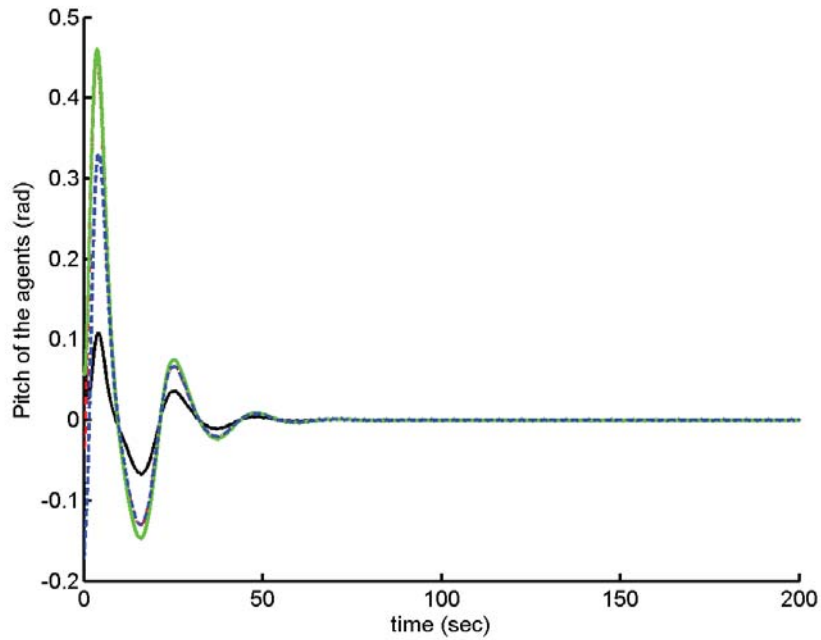


Figure 5.32: Pitch angle of the agents by using neural network and without employing the cooperative learning term.

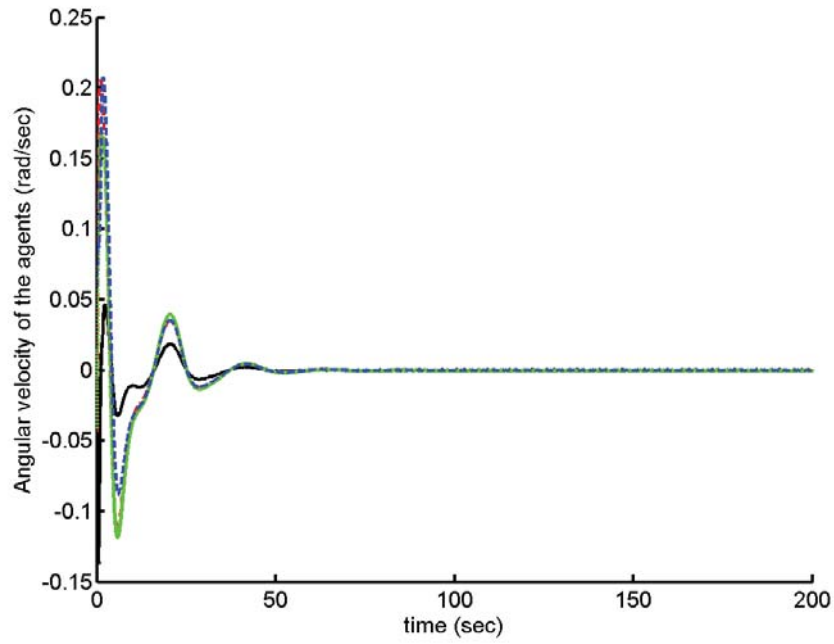


Figure 5.33: Angular velocity of the agents by using neural network and without employing the cooperative learning term.

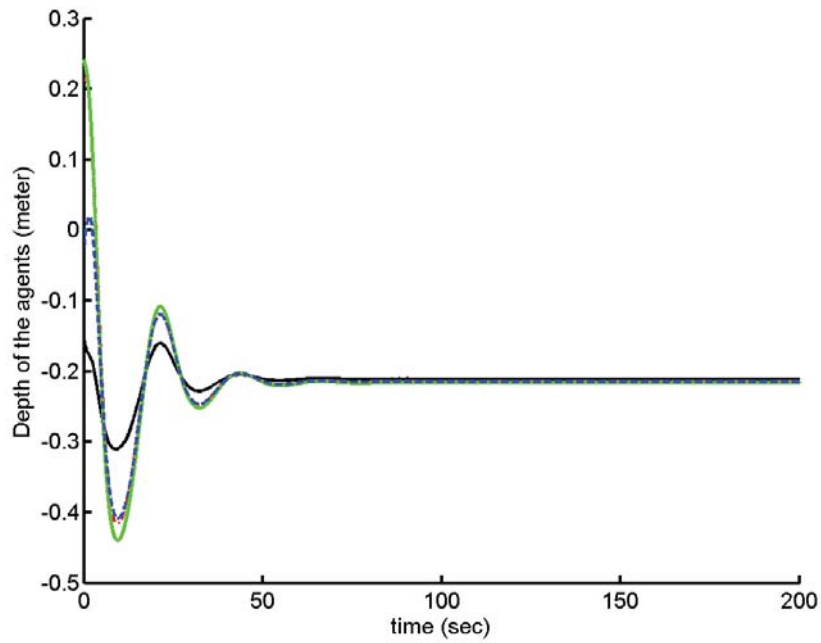


Figure 5.34: Depth of the agents without using neural network and without employing the cooperative learning term.

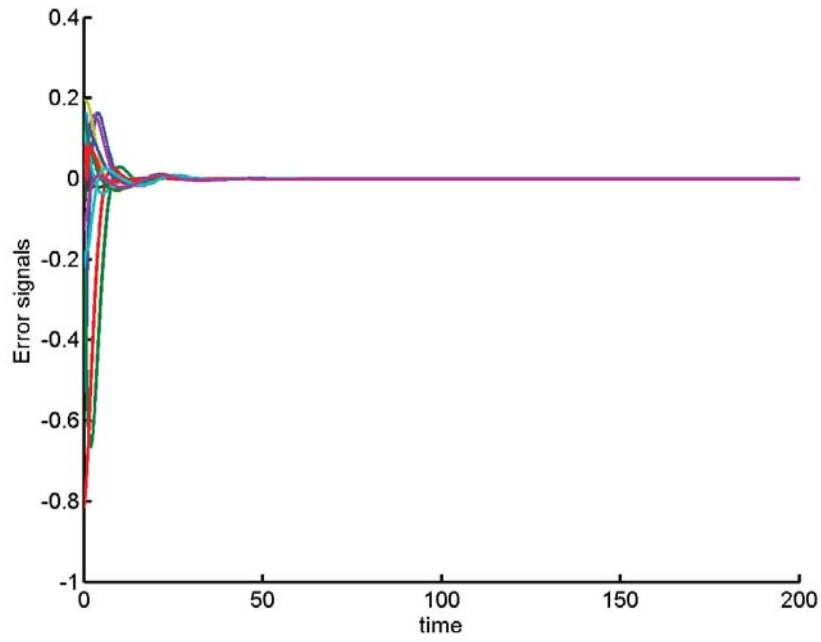


Figure 5.35: Consensus error of the team by using neural network and without employing the cooperative learning term.

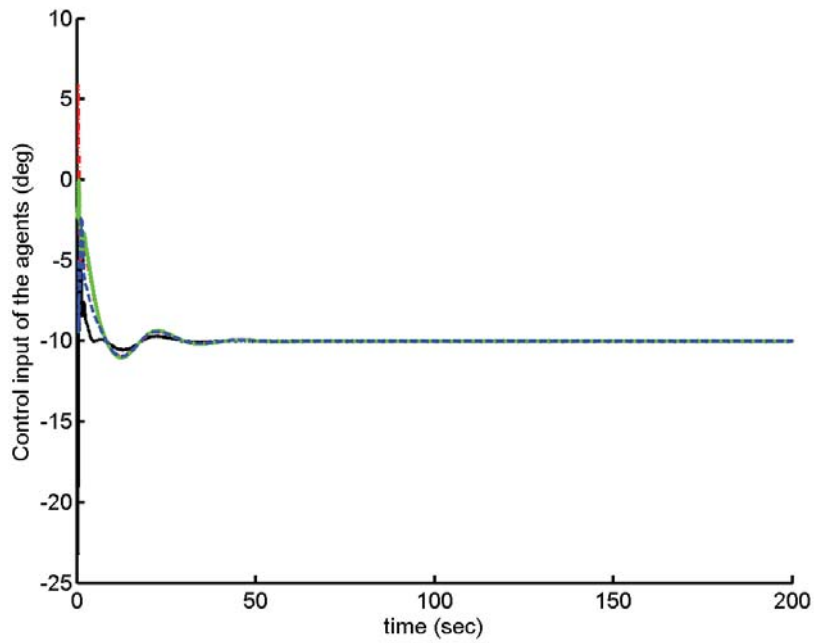


Figure 5.36: Control inputs of the agents by using neural network and without employing the cooperative learning term.

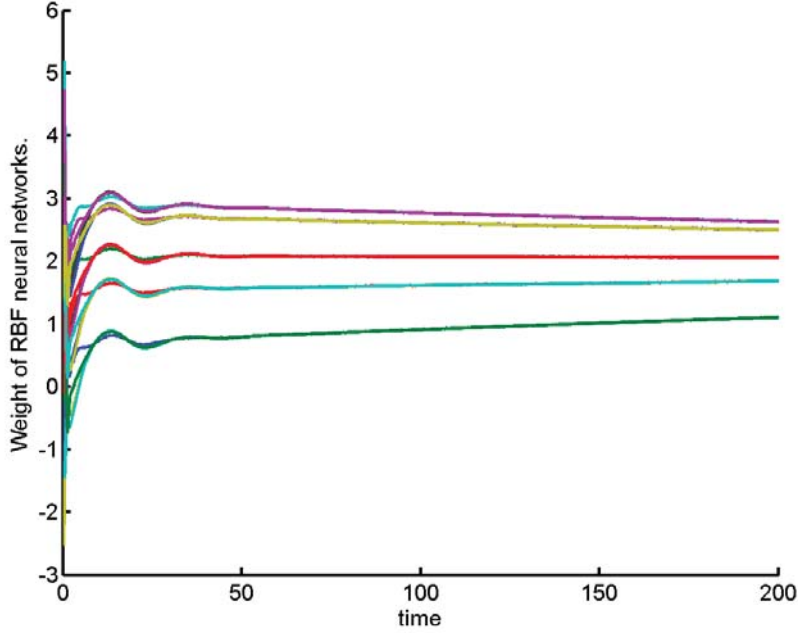


Figure 5.37: Neural network weights of the team and without employing the cooperative learning term.

following cooperative adaptive law:

$$\dot{\hat{\kappa}} = \Gamma \left(\Phi^T (H_\sigma \otimes B^T P_A) \mathbf{e} - \eta_c (L_\sigma \otimes I) \hat{\kappa} - \eta \hat{\kappa} \right) \quad (5.104)$$

In the above adaptation law, we used the same design parameters as those that are stated for the RBF neural network simulation scenarios to make comparison between the two approaches meaningful. The numerical simulations for both scenarios using non-cooperative adaptive and using cooperative adaptive laws are performed. For the first scenario, the depth trajectories of the agents are shown in Figure 5.38. Figure 5.39 illustrates the applied control signals. Finally, the estimated parameters for the four agents are shown in Figure 5.40.

In Figures 5.41, 5.42 and 5.43 the agents depth, control signals and estimated parameters for the second scenario are depicted, respectively.

Although, our approach cannot guarantee that persistent excitation condition is always satisfied, as can be seen in Figures 5.40 and 5.43, our proposed adaptive methods correctly estimate the unknown parameter values. Furthermore, the settling time, the L_2 norm of the consensus error, and the RMS value

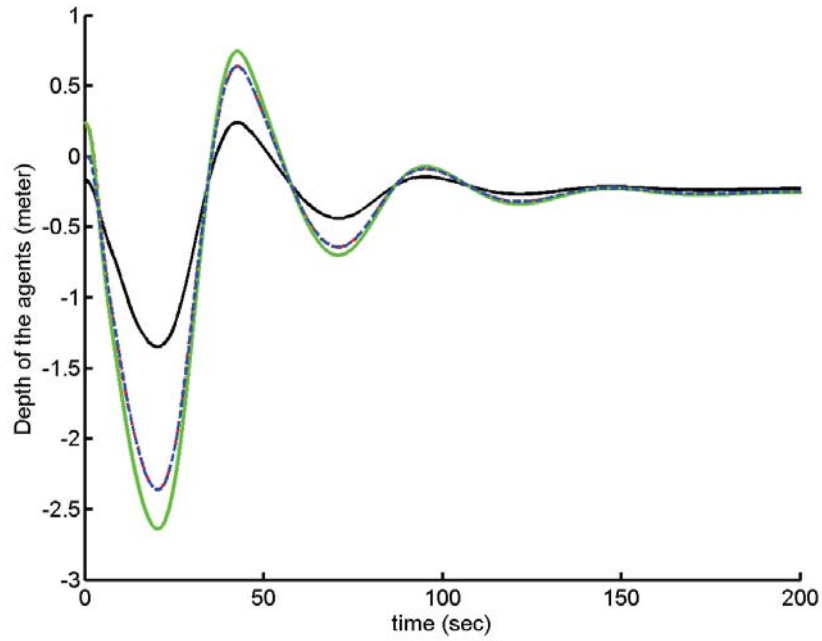


Figure 5.38: Depth of the agents by using the non-cooperative adaptive method.

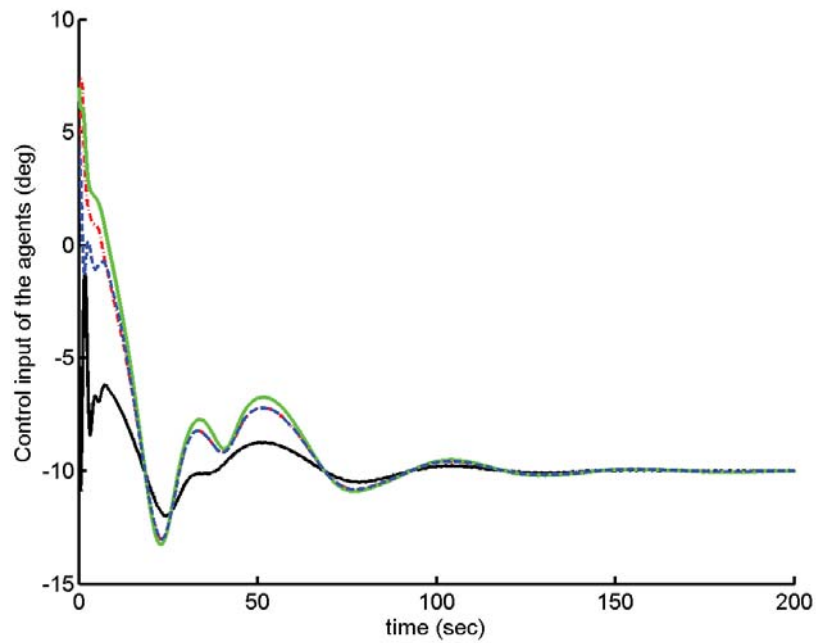


Figure 5.39: Control inputs of the agents by using the non-cooperative adaptive method.

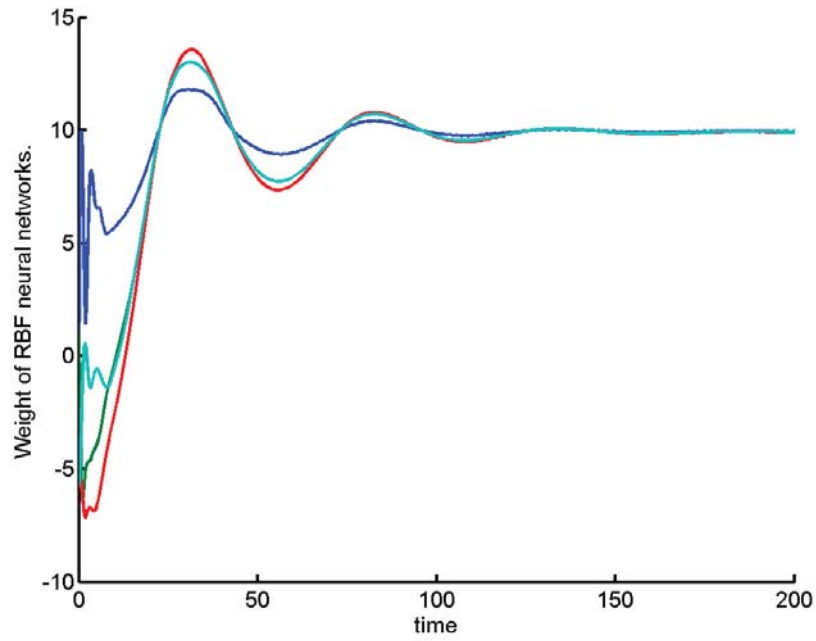


Figure 5.40: Estimated parameters by using the non-cooperative adaptive method.

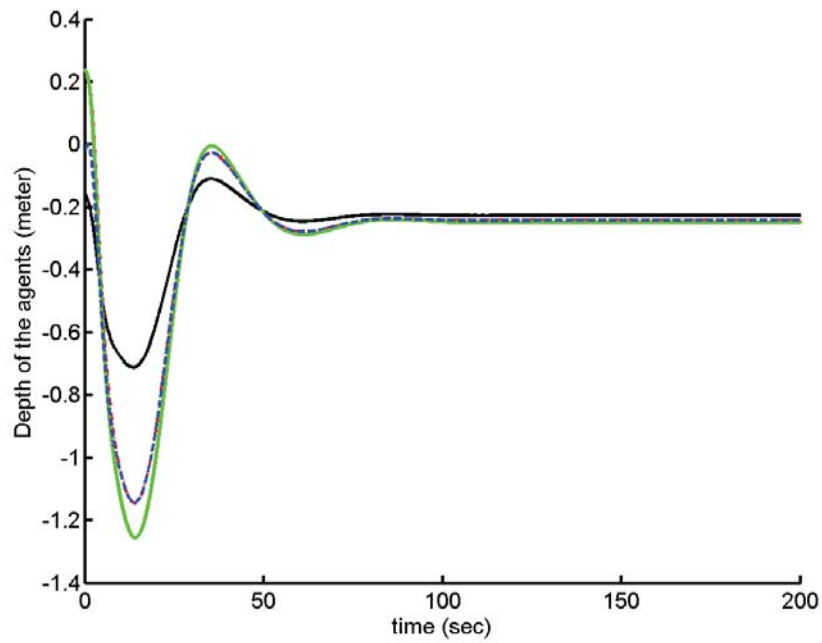


Figure 5.41: Depth of the agents by using the cooperative adaptive method.

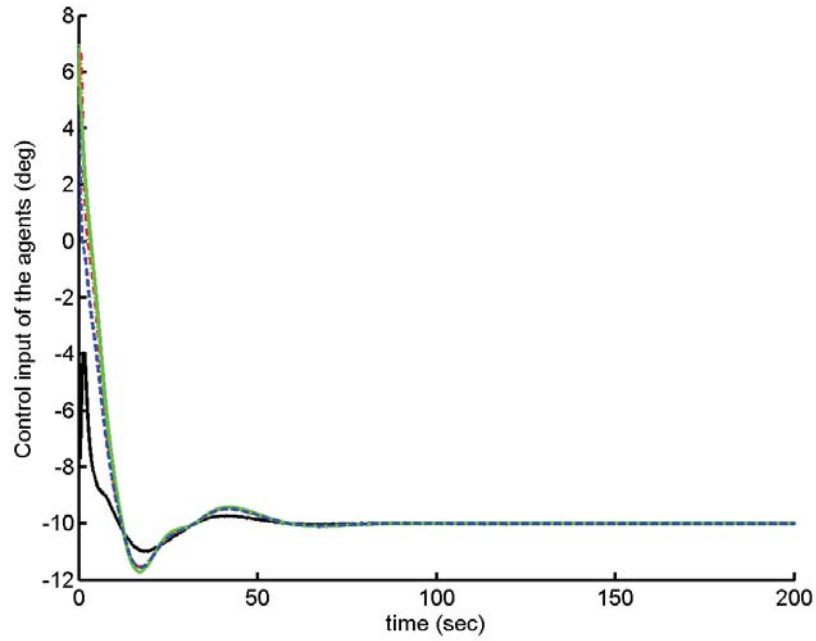


Figure 5.42: Control inputs of the agents by using the cooperative adaptive method.

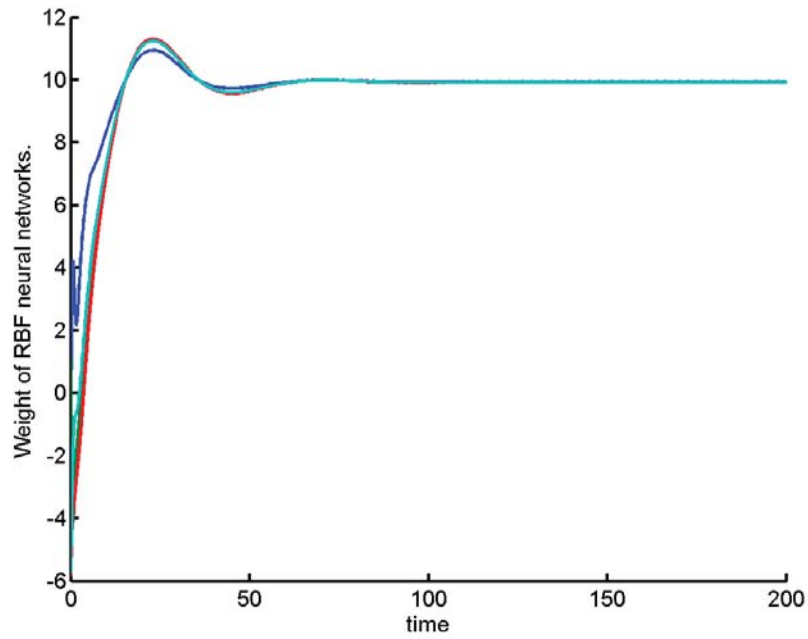


Figure 5.43: Estimated parameters by using the cooperative adaptive method.

Table 5.5: The comparison between cooperative and non-cooperative adaptive methods.

	Settling time (sec)	Consensus error (L_2 norm)	Consensus error (steady state RMS)
The non-cooperative adaptive method	80.89	27.56	0.0097
The cooperative adaptive method	24.11	18.07	0.0079

of the steady state consensus error for both adaptive approaches are presented in Table 5.5. It is shown that the settling time of the cooperative adaptive method is faster than that of the non-cooperative adaptive approach.

5.4 Summary

In this chapter effects of measurement noise and model uncertainties including Lipschitz nonlinearity on consensus achievement of multi-agent systems and their disturbance rejection capability was studied. In the first section, we proposed an observer based cooperative algorithm for output consensus of a team of LTI agents with a measurement noise. Next, consensus achievement problem for a homogenous team of multi-agent systems with unknown linear and Lipschitz nonlinearity model uncertainties is studied in the second section. Furthermore, an observer design procedure is proposed to show how one can deal with both model uncertainty and measurement noise at the same time. Finally, a novel cooperative-learning based consensus algorithm is presented and its shown that it guarantees UUB consensus achievement error for a class of nonlinear multi-agent systems with undirected and switching topology communication network. In this chapter, by using Lyapunov stability analysis and the method developed in Chapter 3 the disturbance rejection property of the overall team was also demonstrated.

Chapter 6

Conclusions and future work

In this thesis consensus based cooperative control of multi-agent system is addressed and its different aspects namely, consensus achievement in teams of LTI systems with directed and switching topology communication networks in presence of disturbances, fault-tolerant cooperative control and fault recovery of multi-agent systems for actuator saturation and loss-of-effectiveness fault, and observer based consensus achievement of multi-agent systems with measurement noise and a finally, cooperative control of team of agents with model uncertainties including nonlinear multi-agent systems are studied.

First, H_∞ and weighted H_∞ consensus problems for a team of homogenous LTI multi-agent systems subject to switching topology and directed communication network graphs were investigated. Then, we proposed a novel design procedure which is based on the solution of an algebraic Riccati equation. Sufficient conditions provided based on state feedback stabilizability of an LTI system and utilizing Lyapunov analysis the stability of the overall closed-loop switched system was asserted. Comparing to other existing methods in the literature, our proposed methodology proved to be more feasible in terms of computational complexity. The disturbance rejection property of the overall system was demonstrated by employing Lyapunov stability analysis and the proposed procedure.

We developed a fault tolerant consensus scheme for a team of LTI multi-agent systems under switching topologies and directed communication network graph. This is a weighted consensus algorithm for consensus achievement of

the multi-agent system based on an inaccurate estimate of the fault severities. Moreover, to improve the fault tolerance capabilities of our proposed consensus strategy a control reconfiguration strategy was proposed. The faults can occur simultaneously in any number of agents and there is no need to have an accurate knowledge of the fault severities. Two kinds of faults namely, a loss-of-effectiveness and a control saturation in the actuators were considered. The stability of the overall closed-loop switched system was shown by using Lyapunov analysis. Finally, it was shown how to remedy the actuator faults and saturation in the multi-agent team and improve the consensus achievement performance by employing our proposed reconfiguration strategy. The effectiveness and capabilities of our proposed consensus algorithms were illustrated through numerical simulations to a team of ten multi-agent systems where the performance of our proposed methods was compared with the performance of centralized and decentralized fault recovery methods that are available in the literature.

Finally, effects of measurement noise and model uncertainties including Lipschitz nonlinearity on consensus achievement of multi-agent systems and their disturbance rejection capability was studied. An observer based cooperative algorithm for output consensus of a team of LTI agents with a measurement noise is proposed and numerical simulation is performed to show its effectiveness. It is followed by, studying consensus achievement problem for a homogenous team of multi-agents with unknown linear and Lipschitz nonlinearity model uncertainties. Furthermore, an observer design procedure is proposed to show how one can deal with both model uncertainty and measurement noise at the same time. Finally, a novel cooperative-learning based consensus algorithm presented and its shown that it guarantees consensus achievement error of a class of nonlinear multi-agent systems with undirected and switching topology communication network is UUB.

6.1 Future work

Based on the work that has been done in this thesis and the obtained results, in the following some of the potential areas of study and suggestions for future

work and research directions are presented:

1. One of the fast growing research areas in consensus based cooperative control is event-driven consensus algorithms. In this thesis we developed a transformation and a stability analysis lemma to tackle H_∞ consensus problem of LTI multi-agent systems. Extending these results and make them suitable to design event-driven consensus algorithms in presence of disturbances will make them more capable to deal with real world practical scenarios.
2. Applying our algorithms to real multi-agent systems and addressing real-time issues.
3. We defined a fault index to quantify effects of the severities of agents actuator faults on stability of our proposed consensus controller and developed a framework to convert the fault tolerant cooperative control into an optimization problem and proposed a fault recovery strategy based on their solutions. However, it is an open problem to find the best numerical method to solve this or find a better approach to define a fault index or to formulate an optimization problem which has more efficient numerical solution.
4. Extend our results to address data-based FDI methods, fault detection delay, and also consider other types of actuator faults including the ones due to age and fatigue.
5. In this thesis, we used our proposed method to decouple communication network topology from agents dynamics and only use algebraic connectivity of the network and agents dynamics to design consensus algorithms to minimize the design procedure computational complexity. However, one may duplicate our results by employing classical pole placement techniques and make a comparison between the two to find out which one is less conservative.
6. Throughout this dissertation, we assumed that there is no delay in the communication network and furthermore we assumed that all the information that is sent to an agent is always received by it and no data loss is

considered. The effects of these two issues can be studied and addressed in future work.

7. Another interesting problem in multi-agent systems research domain that is not addressed in our work, is consensus achievement of non-homogeneous teams. In the first step, one can consider output consensus of non-homogenous LTI multi-agent systems and in the second step one can try to extend it to teams of nonlinear or time-varying systems.
8. In the literature, connectivity preserving and obstacle avoiding consensus algorithms are mainly addressed for single and second order multi-agent systems and extending these algorithms to teams of more general LTI systems is a step in generalizing multi-agent research area.
9. The cooperative adaptive consensus control is a new topic and in this work we only addressed a class of general function approximators including RBF neural networks. These results could be extended to other types of learning methods such as multilayer perceptron (MLP) networks.

Bibliography

- [1] F. Lewis, H. Zhang, K. Hengster-Movric, and A. Das, *Cooperative control of multi-agent systems; Optimal and adaptive design approaches*. Springer, 2014.
- [2] J. Yuan, Z.-H. Zhou, H. Mu, Y.-T. Sun, and L. Li, “Formation control of autonomous underwater vehicles based on finite-time consensus algorithms,” in *Proceedings of Chinese Intelligent Automation Conference*, pp. 1–8, Springer, 2013.
- [3] M. Davoodi, N. Meskin, and K. Khorasani, “Simultaneous fault detection and control design for a network of multi-agent systems,” in *European Control Conference*, pp. 575–581, June 2014.
- [4] Z. Gallehdari, N. Meskin, and K. Khorasani, “Cost performance based control reconfiguration in multi-agent systems,” in *American Control Conference*, pp. 509–516, IEEE, 2014.
- [5] O. Saif, I. Fantoni, and A. Zavala-Rio, “Flocking of multiple unmanned aerial vehicles by lqr control,” in *International Conference on Unmanned Aircraft Systems*, pp. 222–228, IEEE, 2014.
- [6] Y. F. Chen, N. K. Ure, G. Chowdhary, J. P. How, and J. Vian, “Planning for large-scale multiagent problems via hierarchical decomposition with applications to uav health management,” in *American Control Conference*, pp. 1279–1285, IEEE, 2014.
- [7] J. Leonard, A. Savvaris, and A. Tsourdos, “Energy management in swarm of unmanned aerial vehicles,” *Journal of Intelligent & Robotic Systems*, vol. 74, no. 1-2, pp. 233–250, 2014.

- [8] A. Souliman, A. Joukhadar, H. Alturbeh, and J. F. Whidborne, “Intelligent collision avoidance for multi agent mobile robots,” in *Intelligent Systems for Science and Information*, pp. 297–315, Springer, 2014.
- [9] S. Z. Khong, Y. Tan, C. Manzie, and D. Nešić, “Multi-agent source seeking via discrete-time extremum seeking control,” *Automatica*, 2014.
- [10] M. Guo, M. M. Zavlanos, and D. V. Dimarogonas, “Controlling the relative agent motion in multi-agent formation stabilization,” *IEEE Transaction on Automatic Control*, 2014.
- [11] P. Lin, W. Lu, and Y. Song, “Distributed nested rotating consensus problem of multi-agent systems,” in *The 26th Chinese Control and Decision Conference*, pp. 1785–1789, IEEE, 2014.
- [12] G. Wen, Z. Duan, W. Ren, and G. Chen, “Distributed consensus of multi-agent systems with general linear node dynamics and intermittent communications,” *International Journal of Robust and Nonlinear Control*, 2013.
- [13] C. Zhang, Y. Wang, and Y. Zhao, “Agent-based distributed simulation technology of satellite formation flying,” in *Fourth World Congress on Software Engineering*, pp. 13–16, IEEE, 2013.
- [14] A. Ryan, M. Zennaro, A. Howell, R. Sengupta, and J. K. Hedrick, “An overview of emerging results in cooperative uav control,” in *Proceedings of the 43rd IEEE Conference on Decision and Control*, pp. 602–607, 2004.
- [15] R. Olfati-Saber, J. A. Fax, and R. M. Murray, “Consensus and cooperation in networked multi-agent systems,” *Proceedings of the IEEE*, vol. 95, no. 1, pp. 215–233, 2007.
- [16] W. Ren, R. Beard, and E. Atkins, “A survey of consensus problems in multi-agent coordination,” in *Proceedings of the American Control Conference*, pp. 1859 – 1864 vol. 3, June 2005.

- [17] S. Feng and H. Zhang, “Formation control for wheeled mobile robots based on consensus protocol,” in *IEEE International Conference on Information and Automation*, pp. 696 –700, june 2011.
- [18] E. Semsar-Kazerooni and K. Khorasani, “Team consensus for a network of unmanned vehicles in presence of actuator faults,” *IEEE Transactions on Control Systems Technology*, vol. 18, no. 5, pp. 1155 – 1161, 2010.
- [19] S. M. Azizi and K. Khorasani, “Cooperative actuator fault accommodation of formation flying vehicles with absolute measurements,” in *49th IEEE Conference on Decision and Control*, pp. 6299–6304, 2010.
- [20] M. Joordens and M. Jamshidi, “Consensus control for a system of underwater swarm robots,” *IEEE Systems Journal*, vol. 4, pp. 65 – 73, March 2010.
- [21] J. liang Peng, X. xia Sun, F. Zhu, and X. qing Li, “Multi uavs cooperative task assignment using multi agent,” in *Chinese Control and Decision Conference*, pp. 4517 –4520, july 2008.
- [22] B. He and J. Wen, “Cooperative load transport: A formation-control perspective,” *IEEE Transactions on Robotics*, vol. 26, pp. 742 –750, aug. 2010.
- [23] D. Xu and K. Xia, “Role assignment, non-communicative multi-agent coordination in dynamic environments based on the situation calculus,” in *WRI Global Congress on Intelligent Systems*, vol. 1, pp. 89 –93, may 2009.
- [24] I. de Oliveira, F. Carvalho, J. B. Camargo, and L. M. Sato, “Multi-agent tools for air traffic management,” in *11th IEEE International Conference on Computational Science and Engineering Workshops*, pp. 355 –360, july 2008.
- [25] W. Ren and R. W. Beard, *Distributed Consensus in Multi-vehicle Cooperative Control; Theory and Applications*. Springer, 2008.

- [26] A. Jadbabaie, J. Lin, and A. S. Morse, “Coordination of groups of mobile autonomous agents using nearest neighbor rules,” *IEEE Transactions on Automatic Control*, vol. 48, pp. 988–1001, June 2003.
- [27] A. Jaimes B and M. Jamshidi, “Consensus-based and network control of uavs,” in *5th International Conference on System of Systems Engineering*, pp. 1–6, june 2010.
- [28] R. Olfati-saber and R. M. Murray, “Distributed cooperative control of multiple vehicle formations using structural potential functions,” in *IFAC World Congress*, 2002.
- [29] W. Ren, R. Beard, and E. Atkins, “Information consensus in multivehicle cooperative control,” *IEEE Control Systems*, vol. 27, no. 2, pp. 71–82, 2007.
- [30] D. Smallwood and L. Whitcomb, “Model-based dynamic positioning of underwater robotic vehicles: theory and experiment,” *IEEE Journal of Oceanic Engineering*, vol. 29, no. 1, pp. 169–186, 2004.
- [31] R. Olfati-Saber and J. Shamma, “Consensus filters for sensor networks and distributed sensor fusion,” in *44th IEEE Conference on Decision and Control and European Control Conference*, pp. 6698–6703, 2005.
- [32] U. Munz, A. Papachristodoulou, and F. Allgwer, “Consensus in multi-agent systems with coupling delays and switching topology,” *IEEE Transactions on Automatic Control*, vol. 26, pp. 2976–2982, December 2011.
- [33] A. Seuret, D. V. Dimarogonas, and K. H. Johansson, “Consensus under communication delays,” in *47th IEEE Conference on Decision and Control*, (Cancun, Mexico), pp. 4922–4927, December 2008.
- [34] A. Ajorlou, A. Momeni, and A. G. Aghdam, “A class of bounded distributed control strategies for connectivity preservation in multi-agent systems,” *IEEE Trans. on Automatic Control*, vol. 55, no. 12, pp. 2828–2833, 2010.

- [35] W. Ren and R. W. Beard, “Consensus seeking in multi-agent systems under dynamically changing interaction topologies,” *IEEE Transactions on Automatic Control*, vol. 50, pp. 655–661, May 2005.
- [36] W. Ren, “On consensus algorithms for double-integrator dynamics,” *IEEE Transactions on Automatic Control*, vol. 53, no. 6, pp. 1503–1509, 2008.
- [37] W. Yu, L. Zhou, X. Yu, J. Lu, and R. Lu, “Consensus in multi-agent systems with second-order dynamics and sampled data,” *IEEE Transactions on Industrial Informatics*, vol. 9, no. 4, pp. 2137–2146, 2013.
- [38] H. Li, X. Liao, and T. Huang, “Second-order locally dynamical consensus of multiagent systems with arbitrarily fast switching directed topologies,” *IEEE Transactions on Systems, Man, and Cybernetics: Systems*, vol. 43, no. 6, pp. 1343–1353, 2013.
- [39] S. Chen, J. Ji, and J. Zhou, “Second-order consensus of multiple non-identical agents with non-linear protocols,” *IET Control Theory Applications*, vol. 6, no. 9, pp. 1319–1324, 2012.
- [40] A. R. Mehrabian, S. Tafazoli, and K. Khorasani, “State synchronization of networked euler-lagrange systems with switching communication topologies subject to actuator faults,” in *Proceedings of the 8th IFAC World Congress*, (Milan, Italy), September 2011.
- [41] H. Tanner, A. Jadbabaie, and G. Pappas, “Stable flocking of mobile agents, part i: fixed topology,” in *42nd IEEE Conference on Decision and Control*, vol. 2, pp. 2010–2015 Vol.2, Dec 2003.
- [42] H. Tanner, A. Jadbabaie, and G. Pappas, “Stable flocking of mobile agents part i: dynamic topology,” in *42nd IEEE Conference on Decision and Control*, vol. 2, pp. 2016–2021 Vol.2, Dec 2003.
- [43] I. Saboori and K. Khorasani, “ h_∞ consensus problem of high-order lti multi-agent systems with directed fixed network,” in *Canadian Conference on Electrical and Computer Engineering*, 2012.

- [44] S. M. Azizi and K. Khorasani, “Cooperative actuator fault accomodation in formation flight of unmanned vehicles using relative measurements,” *International Journal of Control*, vol. 84, no. 5, pp. 876–894, 2011.
- [45] G. Guo, L. Ding, and Q.-L. Han, “A distributed event-triggered transmission strategy for sampled-data consensus of multi-agent systems,” *Automatica*, vol. 50, no. 5, pp. 1489 – 1496, 2014.
- [46] Y. Tan, J. Yue-Hui, W. Wei, and S. Ying-Jing, “Consensus of high-order continuous-time multi-agent systems with time-delays and switching topologies,” *Chin. Sys. B*, vol. 20, no. 2, pp. 020511–1–020511–6, 2011.
- [47] F. Jiang, L. Wang, and Y. Jia, “Consensus in leaderless networks of high-order-integrator agents,” in *American Control Conference*, (St. Louis, USA), pp. 4458–4463, 2009.
- [48] E. Semsar-Kazerooni and K. Khorasani, “Optimal consensus seeking in a network of multiagent systems: An lmi approach,” *IEEE Trans. on Systems, Man, and Cybernetics*, vol. 40, no. 20, pp. 540–547, 2010.
- [49] E. Semsar-Kazerooni and K. Khorasani, “Multi-agent team cooperation: A game theory approach,” *Automatica*, vol. 45, no. 10, pp. 2205–2213, 2009.
- [50] E. Semsar-Kazerooni and K. Khorasani, “An optimal cooperation in a team of agents subject to partial information,” *International Journal of Control*, vol. 82, no. 3, pp. 571–583, 2008.
- [51] Z. Li, Z. Duan, G. Chen, and L. Huang, “Consensus of multiagent systems and synchronization of complex networks: A unified viewpoint,” *IEEE Transactions on Circuits and Systems I: Regular Papers*, vol. 57, pp. 213 –224, jan. 2010.
- [52] S. Emre Tuna, “Conditions for synchronizability in arrays of coupled linear systems,” *ArXiv e-prints*, Nov. 2008.

- [53] S. Emre Tuna, “LQR-based coupling gain for synchronization of linear systems,” *ArXiv e-prints*, Jan. 2008.
- [54] L. Yang and J. Yingmin, “ h_∞ approach to the consensus problem of multi-agent systems,” in *29th Chinese Control Conference*, pp. 4542 – 4547, july 2010.
- [55] X. Jianxiang, C. Ning, and Z. Yisheng, “Consensus problems for high-order lti swarm systems,” in *29th Chinese Control Conference*, pp. 4483 –4487, july 2010.
- [56] X. Jianxiang, S. Zongying, and Z. Yisheng, “Consensus problems of high-order linear time-invariant swarm systems with time delays,” in *Proceedings of the 30th Chinese Control Conference*, (Yantai, China), pp. 4846–4851, July 2011.
- [57] F. Long, S. Fei, Z. Fu, S. Zheng, and W. Wei, “control and quadratic stabilization of switched linear systems with linear fractional uncertainties via output feedback,” *Nonlinear Analysis: Hybrid Systems*, vol. 2, no. 1, pp. 18 – 27, 2008.
- [58] Y. Cui and Y. Jia, “ $L_2 - L_\infty$ consensus control for high-order multi-agent systems with switching topologies and time-varying delays,” *IET Control Theory Applications*, vol. 6, no. 12, pp. 1933–1940, 2012.
- [59] X. Dong, J. Xi, Z. Shi, and Y. Zhong, “Practical consensus for high-order linear time-invariant swarm systems with interaction uncertainties, time-varying delays and external disturbances,” *International Journal of Systems Science*, vol. 44, no. 10, pp. 1843–1856, 2013.
- [60] Z. Li, Z. Duan, and G. Chen, “On H_∞ and H_2 performance regions of multi-agent systems,” *Automatica*, vol. 47, no. 4, pp. 797 – 803, 2011.
- [61] Y. Liu and Y. Jia, “ H_∞ consensus control of multi-agent systems with switching topology: A dynamic output feedback protocol,” *International Journal of Control*, vol. 83, no. 3, pp. 527–537, 2010.

- [62] L. Allerhand and U. Shaked, “Robust control of switched linear systems with dwell time,” in *26th Convention of Electrical and Electronics Engineers in Israel (IEEEI)*, pp. 000198 –000201, nov. 2010.
- [63] Y. Liu, Y. Jia, J. Du, and S. Yuan, “Dynamic output feedback control for consensus of multi-agent systems: An H_∞ approach,” in *American Control Conference*, pp. 4470 –4475, june 2009.
- [64] Z. Li, Z. Duan, and L. Huang, “ H_∞ control of networked multi-agent systems,” *Journal of Systems Science and Complexity*, vol. 22, pp. 35–48, 2009.
- [65] J. Hespanha, “Root-mean-square gains of switched linear systems,” *IEEE Transactions on Automatic Control*, vol. 48, pp. 2040 – 2045, nov. 2003.
- [66] L. Allerhand and U. Shaked, “Robust stability and stabilization of linear switched systems with dwell time,” *IEEE Transactions on Automatic Control*, vol. 56, pp. 381 –386, feb. 2011.
- [67] H. Kim, H. Shim, and J. H. Seo, “Output consensus of heterogeneous uncertain linear multi-agent systems,” *IEEE Transactions on Automatic Control*, vol. 56, no. 1, pp. 200–206, 2011.
- [68] H. Kim, H. Shim, J. Back, and J. H. Seo, “Consensus of output-coupled linear multi-agent systems under fast switching network: Averaging approach,” *Automatica*, vol. 49, no. 1, pp. 267 – 272, 2013.
- [69] T. Chen, J. Zhu, and Y. Shi, “Consensus of linear time-invariant multi-agent systems based on dynamic output feedback,” in *Control and Decision Conference*, pp. 4201–4205, 2009.
- [70] C. Godsil, *Algebraic Graph Theory*. Springer Graduate Texts in Mathematics, 2001.
- [71] B. F. Z. Lin, M. Brouke, “Local control strategies for groups of mobile autonomous agents,” *IEEE Transactions on Automatic Control*, vol. 49, pp. 622–629, April 2004.

- [72] M. Ji and M. Egerstedt, “Distributed coordination control of multiagent systems while preserving connectedness,” *IEEE Trans. on Robot.*, vol. 23, no. 4, pp. 693–703, 2007.
- [73] D. V. Dimarogonas and K. J. Kyriakopoulos, “On the rendezvous problem for multiple nonholonomic agents,” *IEEE Transactions on Automatic Control*, vol. 52, no. 5, pp. 916–922, 2007.
- [74] M. C. D. Gennaro and A. Jadbabaie, “Decentralized control of connectivity for multi-agent systems,” in *45th IEEE Conference on Decision and Control*, (San Diego, CA, USA), pp. 3628–3633, 2006.
- [75] D. V. Dimarogonas and K. H. Johansson, “Decentralized connectivity maintenance in mobile networks with bounded inputs,” in *IEEE International Conference on Robot and Automation*, (Pasadena, CA, USA), pp. 1507–1512, May 2008.
- [76] H. Su, X. Wang, and G. Chen, “Rendezvous of multiple mobile agents with preserved network connectivity,” *Systems and Control Letters*, vol. 59, pp. 313–322, 2010.
- [77] M. Zavlanos and G. Pappas, “Distributed connectivity control of mobile networks,” *IEEE Transactions on Robotics*, vol. 24, no. 6, pp. 1416–1428, 2008.
- [78] J. Li, “Distributed H_∞ consensus of high-order multi agents with nonlinear dynamics,” *Intelligent Control and Automation*, vol. 2, pp. 1–7, 2011.
- [79] M. SUN, Y. CHEN, L. CAO, and X.-F. WANG, “Adaptive third-order leader-following consensus of nonlinear multi-agent systems with perturbations,” *Chinese Physics Letters*, vol. 29, no. 2, pp. 020503 1–4, 2012.
- [80] Z. Qu, J. Chunyu, and J. Wang, “Nonlinear cooperative control for consensus of nonlinear and heterogeneous systems,” in *46th IEEE Conference on Decision and Control*, pp. 2301–2308, dec. 2007.

- [81] T. Lee and H.-S. Ahn, “Consensus of nonlinear system using feedback linearization,” in *International Conference on Mechatronics and Embedded Systems and Applications*, pp. 26–31, July 2010.
- [82] Z. Li, X. Liu, and M. Fu, “Global consensus control of Lipschitz nonlinear multi-agent systems,” in *18th IFAC World Congress*, pp. 10056–10061, September 2011.
- [83] Z. Li, W. Ren, X. Liu, and M. Fu, “Consensus of multi-agent systems with general linear and Lipschitz nonlinear dynamics using distributed adaptive protocols,” *CoRR*, vol. abs/1109.3799, 2011.
- [84] P. DeLellis, M. di Bernardo, and G. Russo, “On quad, Lipschitz, and contracting vector fields for consensus and synchronization of networks,” *IEEE Transactions on Circuits and Systems I: Regular Papers*, vol. 58, pp. 576–583, March 2011.
- [85] H. Du, Y. He, and Y. Cheng, “Finite-time synchronization of a class of second-order nonlinear multi-agent systems using output feedback control,” *IEEE Transactions on Circuits and Systems I: Regular Papers*, vol. 61, pp. 1778–1788, June 2014.
- [86] P. Wang and Y. Jia, “Brief paper - distributed containment control of second-order multi-agent systems with inherent non-linear dynamics,” *Control Theory Applications, IET*, vol. 8, pp. 277–287, March 2014.
- [87] B. Liu, W. Lu, and T. Chen, “Consensus in continuous-time multiagent systems under discontinuous nonlinear protocols,” *IEEE Transactions on Neural Networks and Learning Systems*, vol. 26, pp. 290–301, Feb 2015.
- [88] X. He, Q. Wang, and W. Yu, “Finite-time containment control for second-order multiagent systems under directed topology,” *IEEE Transactions on Circuits and Systems II: Express Briefs*, vol. 61, pp. 619–623, Aug 2014.

- [89] Y. Zhao, G. Wen, Z. Duan, and G. Chen, “Adaptive consensus for multiple nonidentical matching nonlinear systems: An edge-based framework,” *IEEE Transactions on Circuits and Systems II: Express Briefs*, vol. 62, pp. 85–89, Jan 2015.
- [90] W. Qin, Z. Liu, and Z. Chen, “Formation control for nonlinear multi-agent systems with linear extended state observer,” *IEEE/CAA Journal of Automatica Sinica*, vol. 1, pp. 171–179, April 2014.
- [91] G. Wen, Z. Duan, W. Yu, and G. Chen, “Consensus of multi-agent systems with nonlinear dynamics and sampled-data information: a delayed-input approach,” *International Journal of Robust and Nonlinear Control*, vol. 23, no. 6, pp. 602–619, 2013.
- [92] W. Chen, S. Hua, and S. S. Ge, “Consensus-based distributed cooperative learning control for a group of discrete-time nonlinear multi-agent systems using neural networks,” *Automatica*, vol. 50, no. 9, pp. 2254 – 2268, 2014.
- [93] W. Chen, S. Hua, and H. Zhang, “Consensus-based distributed cooperative learning from closed-loop neural control systems,” *IEEE Transactions on Neural Networks and Learning Systems*, vol. 26, pp. 331–345, Feb 2015.
- [94] W. Liu, S. Zhou, Y. Qi, and X. Wu, “Leaderless consensus of multi-agent systems with lipschitz nonlinear dynamics and switching topologies,” *Neurocomputing*, pp. –, 2015.
- [95] S. Bezzaoucha, B. Marx, D. Maquin, and J. Ragot, “Linear feedback control input under actuator saturation: A takagi-sugeno approach,” in *2nd International Conference on Systems and Control*, 2012.
- [96] A. Baniamerian and K. Khorasani, “Fault detection and isolation of dissipative parabolic pdes: Finite-dimensional geometric approach,” in *American Control Conference*, pp. 5894–5899, June 2012.

- [97] H. Wang and S. Daley, “Actuator fault diagnosis: an adaptive observer-based technique,” *IEEE Transactions on Automatic Control*, vol. 41, no. 7, pp. 1073–1078, 1996.
- [98] Q. Zhang, M. Basseville, and A. Benveniste, “Fault detection and isolation in nonlinear dynamic systems: A combined inputoutput and local approach,” *Automatica*, vol. 34, no. 11, pp. 1359 – 1373, 1998.
- [99] S. Stankovic, N. Ilic, Z. Djurovic, M. Stankovic, and K. Johansson, “Consensus based overlapping decentralized fault detection and isolation,” in *Conference on Control and Fault-Tolerant Systems (SysTol)*, pp. 570–575, 2010.
- [100] N. Meskin and K. Khorasani, “Actuator fault detection and isolation for a network of unmanned vehicles,” *IEEE Transactions on Automatic Control*, vol. 54, no. 4, pp. 835–840, 2009.
- [101] M. R. Davoodi, K. Khorasani, H. A. Talebi, and H. R. Momeni, “A robust semi-decentralized fault detection strategy for multi-agent systems: An application to a network of micro-air vehicles,” *International Journal of Intelligent Unmanned Systems*, vol. 1, pp. 21–35, 2013.
- [102] M. Davoodi, K. Khorasani, H. Talebi, and H. Momeni, “A novel distributed robust fault detection and isolation filter design for a network of nonhomogeneous multi-agent systems,” in *51st Annual Conference on Decision and Control*, pp. 592–599, 2012.
- [103] M. Davoodi, K. Khorasani, H. Talebi, and H. Momeni, “Distributed fault detection and isolation filter design for a network of heterogeneous multi-agent systems,” *IEEE Transactions on Control Systems Technology*, no. 99, 2013.
- [104] H. Dong, Z. Wang, and H. Gao, “Fault detection for markovian jump systems with sensor saturations and randomly varying nonlinearities,” *IEEE Transactions on Circuits and Systems I: Regular Papers*, vol. 59, pp. 2354–2362, Oct 2012.

- [105] P. TaeDong and P. Kiheon, “Kalman filter-based fault detection and isolation of direct current motor: Robustness and applications,” in *International Conference on Control, Automation and Systems*, pp. 933–936, 2008.
- [106] X.-G. Yan and C. Edwards, “Robust decentralized actuator fault detection and estimation for large-scale systems using a sliding mode observer,” *International Journal of Control*, vol. 81, no. 4, pp. 591–606, 2008.
- [107] X. He, Z. Wang, Y. Liu, and D. Zhou, “Least-squares fault detection and diagnosis for networked sensing systems using a direct state estimation approach,” *IEEE Transactions on Industrial Informatics*, vol. 9, pp. 1670–1679, Aug 2013.
- [108] S. M. Azizi and K. Khorasani, “A decentralized cooperative actuator fault accommodation of formation flying satellites in deep space,” in *3rd Annual IEEE Systems Conference*, pp. 230–235, 2009.
- [109] E. Semsar-Kazerooni and K. Khorasani, “Optimal performance of a modified leader-follower cooperative team with partial availability of the leader command and agents actuator faults,” in *46th IEEE Conference on Decision and Control*, pp. 2491–2497, 2007.
- [110] I. Saboori, H. Nayyeri, and K. Khorasani, “A distributed control strategy for connectivity preservation of multi-agent systems subject to actuator saturation,” in *American Control Conference*, pp. 4044–4049, 2013.
- [111] D. Vengertsev, H. Kim, J. H. Seo, and H. Shim, “Consensus of output-coupled high-order linear multi-agent systems under deterministic and markovian switching networks,” *International Journal of Systems Science*, vol. 46, no. 10, pp. 1790–1799, 2015.
- [112] S. M. Azizi and K. Khorasani, “Cooperative actuator fault accommodation in formation flight of unmanned vehicles using absolute measurements,” *IET Control Theory Applications*, vol. 6, pp. 2805–2819, Dec 2012.

- [113] S. M. Azizi and K. Khorasani, “A hierarchical architecture for cooperative actuator fault estimation and accommodation of formation flying satellites in deep space,” *IEEE Transactions on Aerospace and Electronic Systems*, vol. 48, pp. 1428–1450, APRIL 2012.
- [114] H. Li, X. Liao, T. Huang, W. Zhu, and Y. Liu, “Second-order global consensus in multiagent networks with random directional link failure,” *IEEE Transactions on Neural Networks and Learning Systems*, vol. 26, pp. 565–575, March 2015.
- [115] A. Nemirovski and P. Gahinet, “The projective method for solving linear matrix inequalities,” *American Control Conference*, pp. 840–844, 1994.
- [116] D. A. Bini, B. Iannazzo, and F. Poloni, “A fast newton’s method for a nonsymmetric algebraic riccati equation,” *SIAM Journal on Matrix Analysis and Applications*, vol. 30, no. 1, 2008.
- [117] D. R., *Graph Theory*. Springer-Verlag, 2000.
- [118] W. L. Brogan, *Modern control theory, 3rd*. Prentice Hall, 1991.
- [119] Z. Qu, *Cooperative control of dynamical systems*. Springer, 2009.
- [120] R. A. Horn and C. R. Johnson, *Matrix analysis*. Cambridge university press, 2012.
- [121] M. Fiedler, “Algebraic connectivity of graphs,” *Czechoslovak Mathematical Journal*, vol. 23, no. 2, pp. 298–305, 1973.
- [122] C. W. Wu, *Synchronization in complex networks of nonlinear dynamical systems*, vol. 76. World Scientific, 2007.
- [123] S. Kirkland, “A bound on the algebraic connectivity of a graph in terms of the number of cutpoints,” *Linear and Multilinear Algebra*, vol. 47, no. 1, pp. 93–103, 2000.
- [124] R. Merris, “A note on laplacian graph eigenvalues,” *Linear Algebra and its Applications*, vol. 285, no. 1, pp. 33–35, 1998.

- [125] C. W. Wu, “Algebraic connectivity of directed graphs,” *Linear and Multilinear Algebra*, vol. 53, no. 3, pp. 203–223, 2005.
- [126] C. W. Wu, “Synchronization in networks of nonlinear dynamical systems coupled via a directed graph,” *Nonlinearity*, vol. 18, no. 3, p. 1057, 2005.
- [127] W. N. Anderson Jr and T. D. Morley, “Eigenvalues of the laplacian of a graph,” *Linear and Multilinear Algebra*, vol. 18, no. 2, pp. 141–145, 1985.
- [128] B. Mohar and Y. Alavi, “The laplacian spectrum of graphs,” *Graph theory, combinatorics, and applications*, vol. 2, pp. 871–898, 1991.
- [129] R. A. Brualdi, *Combinatorial matrix classes*, vol. 13. Cambridge University Press, 2006.
- [130] Z. Qu, *Cooperative Control of Dynamical Systems; Applications to Autonomous Vehicles*. Springer, 2009.
- [131] W. Ren and R. W. Beard, *Distributed consensus in multi-vehicle cooperative control: Theory and applications*. Springer, 2008.
- [132] O. Taussky, “A recurring theorem on determinants,” *American Mathematical Monthly*, pp. 672–676, 1949.
- [133] D. Lee and M. W. Spong, “Stable flocking of multiple inertial agents on balanced graphs,” *IEEE Transactions on Automatic Control*, vol. 52, no. 8, pp. 1469–1475, 2007.
- [134] L. Moreau, “Stability of multiagent systems with time-dependent communication links,” *IEEE Transactions on Automatic Control*, vol. 50, no. 2, pp. 169–182, 2005.
- [135] Y. Shoham and K. Leyton-Brown, *Multiagent systems: Algorithmic, game-theoretic, and logical foundations*. Cambridge University Press, 2008.
- [136] W. Steeb and Y. Hardy, *Matrix Calculus and Kronecker Product: A Practical Approach to Linear and Multilinear Algebra*. World Scientific, 2011.

- [137] H. K. Khalil, *Nonlinear systems; Third Edition*. Prentice Hall, Englewood Cliffs, NJ, 2002.
- [138] L. Wu and J. Lam, “Weighted H_∞ filtering of switched systems with time-varying delay: Average dwell time approach,” *Circuits, Systems and Signal Processing Journal*, vol. 28, pp. 1017–1036, 2009.
- [139] V. Barbu, “ H_∞ boundary control with state feedback; the hyperbolic case,” *International Series of Numerical Mathematics*, vol. 107, pp. 141–148, 1992.
- [140] A. Healey and D. Lienard, “Multivariable sliding mode control for autonomous diving and steering of unmanned underwater vehicles,” *IEEE Journal of Oceanic Engineering*, vol. 18, pp. 327–339, jul 1993.
- [141] R. Olfati-Saber and R. Murray, “Consensus problems in networks of agents with switching topology and time-delays,” *IEEE Transactions on Automatic Control*, vol. 49, no. 9, pp. 1520–1533, 2004.
- [142] J. C. Lagarias, J. A. Reeds, M. H. Wright, and P. E. Wright, “Convergence properties of the nelder–mead simplex method in low dimensions,” *SIAM Journal on optimization*, vol. 9, no. 1, pp. 112–147, 1998.
- [143] K. Hengster-Movric, F. L. Lewis, and M. Sebek, “Distributed static output-feedback control for state synchronization in networks of identical {LTI} systems,” *Automatica*, vol. 53, pp. 282 – 290, 2015.
- [144] K. J. Åström and B. Wittenmark, *Adaptive control*. Courier Corporation, 2013.